

Removal of Perfluorinated Compounds in  
Drinking Water Treatment:  
A Study of Ion Exchange Resins and  
Magnetic Nanoparticles

by

Chuan Liu

A thesis  
presented to the University of Waterloo  
in fulfillment of the  
thesis requirement for the degree of  
Doctor of Philosophy  
in  
Civil Engineering

Waterloo, Ontario, Canada, 2017

©Chuan Liu 2017

## Examination Committee Membership

The following served on the examining committee for this thesis. The decision of the Examining Committee is by majority vote.

External Examiner	Dr. Madjid Mohseni Professor Department of Chemical & Biological Engineering University of British Columbia
Supervisors	Dr. Peter M. Huck Professor Department of Civil & Environmental Engineering University of Waterloo  Dr. Sigrid Peldszus Research Associate Professor Department of Civil & Environmental Engineering University of Waterloo
Internal Member	Dr. Nandita Basu Associate Professor Department of Civil & Environmental Engineering University of Waterloo
Internal-External Member	Dr. William A. Anderson Professor Department of Chemical Engineering University of Waterloo  Dr. Xianshe Feng Professor Department of Chemical Engineering University of Waterloo

## **Author's Declaration**

I hereby declare that I am the sole author of this thesis. This is a true copy of the thesis, including any required final revisions, as accepted by my examiners.

I understand that my thesis may be made electronically available to the public.

## Abstract

Perfluorinated compounds (PFCs) are emerging contaminants which have been detected in various environmental compartments, including drinking water sources. Because of their potential risks to human health, PFCs in drinking water systems have been studied at an increasing rate in recent years. Among all the PFCs, perfluoroalkyl carboxylic acids (PFCAs) and perfluoroalkyl sulfonic acids (PFSAs) are two common classes; while perfluorinated phosphonic acids (PFPAs) are a type of PFCs, which have only been detected in the environment in the past few years. As the two most commonly detected PFCs, perfluorooctanoic acid (PFOA) and perfluorooctanoic sulfonate (PFOS) have been included in USEPA's fourth Contaminant Candidate List (CCL4) recently. In terms of treatment, ion exchange batch studies showed promising results for PFC removal. Nanoparticles are novel and promising adsorbents due to their high specific surface areas and other properties.

The overall objective of this study is to investigate more efficient approaches to remove PFCs by ion exchange and adsorption processes in drinking water systems, including the application of anion exchange resins and nanoparticles, studying the influence of PFC characteristics on these processes, and the impact of water qualities, especially the effects of natural organic matter (NOM) and inorganic anions.

A liquid chromatography tandem mass spectrometry (LC-MS/MS) method was adapted for analyzing seven PFCAs, three PFSAs, and three PFPAs in water samples. Solid phase extraction (SPE) was applied to concentrate water samples and to reach lower detection limits. Both the LC parameters and the multiple reaction monitoring (MRM) conditions of the MS/MS were optimized to reach short retention times, good sensitivity, and nice peak shapes for the selected PFCs. The method detection limits (MDLs) for PFCAs and PFSAs ranged from 0.1 to 1.0 ng/L, while the MDLs for PFPAs were 5.0 to 5.1 ng/L. Four PFCAs and three PFSAs were then selected as target PFCs in subsequent removal studies.

Five commercially available anion exchange resins with different properties were chosen to test their PFCs removals in both ultrapure and Grand River water in batch studies. In ultrapure water, all resins had high removals of over 80% for all target PFCs. In Grand River

water, all resins had decreased PFC removals though they varied with different types of PFCs. PFSAAs had higher removals than PFCAs and short chain PFCs were less removed than long chain PFCs. Based on these results, TAN-1 and PFA444 were selected as target resins to study single compound isotherms in ultrapure water, PFC removal in Lake Erie water, and the effect of inorganic anions. These studies proved that the decrease of PFC removals in surface water was caused by competition from both NOM and inorganic anions. The existence of sulfate in water could decrease PFCs removal, especially short chain PFCAs.

Based on the PFC results above, TAN-1, PFA444 and A555 were selected as target anion exchange resins for regeneration batch studies. Regeneration conditions for selected anion exchange resins including regenerant types, cation types, and solvent types were tested in batch studies. The use of higher concentration of the regenerant salts,  $\text{Na}^+$  ions, and methanol can enhance the PFCs regeneration performance. Short chain PFCs had higher regeneration rates than long chain PFCs, and PFCAs had better regeneration performance compared to PFSAAs. A555 had the best regeneration performance among the three selected resins; thus it was chosen as target resin for column tests. In the column regeneration tests, the regeneration conditions of 5% NaCl and 10 ml/min flow rate had the best regeneration performance. In the anion exchange column experiment using Grand River water, the breakthrough of all PFCs gradually increased from 20% after 100000 BV, to 90% breakthrough after 220000 BV.

Magnetic nanoparticles with three different modified polymers were designed for PFC removal and synthesized. They were applied in PFC removal kinetic experiments in both ultrapure water and Grand River water. All magnetic nanoparticles achieved short equilibrium times of less than 10 hours in both waters. Magnetic nanoparticles modified with polymer p-DADMAC (N1) had the best PFC removal among all three nanoparticles in both waters. In Grand River water, the PFC removal of all three nanoparticles decreased substantially. NOM rather than inorganic anions was shown to be the main competitor for PFC removal by nanoparticles in surface water. The approach of using synthesized magnetic nanoparticles has potential to remove PFCs and should be further pursued.

## Acknowledgements

I would firstly like to thank my supervisors Dr. Sigrid Peldszus and Dr. Peter M. Huck, who have given me direction when I was lost, supported me when I was weak, encouraged me when I hesitated. Working with them gained me great research experience which will also guide me throughout the rest of my career.

I would also like to thank my committee Dr. William A. Anderson, Dr. Xianshe Feng and Dr. Nandita Basu for their valuable feedback and guidance. I would like to thank Dr. Madjid Mohseni for agreeing to be part of my examination committee.

I would like to express my warm thankfulness to Mohammad Feisal Rahman, Monica Tudorancea, Shinong Mao, Xuewen (Sharon) He, Jangchuk Tashi, Yanting (Helen) Liu, Guy Milton, Mark Sobon and Mark Merlau for providing their precious advice and help for my research and experiments. I would like to thank Ms. Dana Herriman for her valuable support. My appreciation also extends to Jie Yuan, Fei (Alex) Chen, Yulang (Michael) Wang, Ye (Zoe) Zhou, Silvia Vlad, Samia Aly, and other current and previous NSERC Chair group colleagues for their supports and help.

This research has been funded by the Natural Sciences and Engineering Research Council of Canada (NSERC) in the form of an Industrial Research Chair in Water Treatment at the University of Waterloo. Current Chair partners are listed at: <https://uwaterloo.ca/nserc-chair-water-treatment/partners>. The author was also funded by China Scholarship Council (CSC) as a PhD student for four years.

Finally, I would like to express my sincerest appreciation to my parents for their unconditional love and support. Also, I would like to thank my dear wife Bingjie Shi for her sincere support and love.

## Table of Contents

Examination Committee Membership.....	ii
Author’s Declaration .....	iii
Abstract .....	iv
Acknowledgements .....	vi
Table of Contents .....	vii
List of Figures .....	xi
List of Tables.....	xiv
List of Abbreviations.....	xvi
Chapter 1 Introduction.....	1
1.1 Problem Statement .....	1
1.2 Research Objectives and Scope.....	4
1.3 Research Approach and Thesis Organization.....	5
Chapter 2 Literature Review .....	8
2.1 PFCs in Environment .....	8
2.1.1 Definition and Classification of PFCs .....	8
2.1.2 Physicochemical Properties of PFCs.....	9
2.1.3 Toxicity and Occurrence of PFCs in the Environment.....	11
2.1.4 Sources and Pathways of PFCs Entering into the Environment.....	13
2.1.5 Analysis of PFCs .....	13
2.2 PFC Removal during Drinking Water Treatment.....	14
2.2.1 PFC Removal in Full-scale Water Treatment Plants.....	14
2.2.2 PFCs Removal in Bench-scale Treatment Studies .....	16
2.3 Conventional and New Adsorbents Used in Drinking Water Treatment .....	18
2.3.1 Adsorption Basics.....	18
2.3.2 Activated Carbon.....	19
2.3.3 Novel Adsorbents .....	20
2.3.4 Low Cost Adsorbents .....	22
2.3.5 Ion Exchange Resins .....	25
2.4 The Impact of NOM in Adsorption Process.....	26
2.4.1 Characterization of NOM .....	26
2.4.2 Competitive Adsorption between NOM and Contaminants .....	29

2.4.3 NOM Preloading on Adsorbents .....	29
2.5 Research Needs .....	30
Chapter 3 Quantitative Analysis of Perfluoroalkyl Acids in Water by LC-MS/MS .....	31
3.1 Introduction .....	31
3.2 Materials and Methods .....	33
3.2.1 Materials and Chemicals .....	33
3.2.2 Solid Phase Extraction.....	34
3.2.3 LC-MS/MS .....	36
3.2.4 Method Detection Limits (MDL), Limit of Quantity (LOQ), Reproducibility, Repeatability, and Calibration Curves .....	37
3.3 Results and Discussion.....	39
3.3.1 MRM Optimization Results .....	39
3.3.2 LC-MS/MS Results .....	42
3.3.3 Quality Assurance/Quality Control (QA/QC) .....	45
3.4 Method Summary .....	50
3.5 Conclusions .....	50
Chapter 4 PFCA and PFSA Removal during Drinking Water Treatment by Ion Exchange Resins: Removal Kinetics and Isotherms Studies .....	52
4.1 Introduction .....	53
4.2 Materials and Methods .....	55
4.2.1 Target Compounds and Water.....	55
4.2.2 Ion Exchange Resins .....	56
4.2.3 Kinetics and Isotherms Tests.....	57
4.2.4 Testing Effects of Inorganic Anions on Ion Exchange Performance .....	59
4.2.5 Analyses .....	60
4.3 Results and Discussion.....	63
4.3.1 Anion Exchange Resins Properties.....	63
4.3.2 Removal Kinetics and Capacities in Ultrapure Water.....	64
4.3.3 PFCs Removal Kinetics in Surface Water.....	86
4.3.4 Effect of Natural Organic Matter on PFC Removal by Anion Exchange Resins.....	96
4.3.5 Effect of Inorganic Anion Competition on PFCs Removal by Anion Exchange Resins.....	99
4.4 Conclusions .....	105



Chapter 5 PFCAs and PFSA removal during drinking water treatment by ion exchange resins:	
column tests and regeneration .....	107
5.1 Introduction .....	107
5.2 Materials and Methods .....	110
5.2.1 Target Compounds, Water, and Anion Exchange Resins.....	110
5.2.2 Regeneration Batch Tests .....	111
5.2.3 Design of Anion Exchange Column Set-up and Operating Parameters .....	113
5.2.4 Regeneration Column Tests.....	116
5.2.5 Analyses .....	117
5.3 Results and Discussion.....	118
5.3.1 Anion Exchange Resins Regeneration Batch Experiments .....	118
5.3.2 Anion Exchange Column Tests.....	122
5.3.3 Anion Exchange Resins Regeneration Method Optimization in Column Experiments....	127
5.3.4 Anion Exchange Resins Regeneration Column Experiments Using Surface Water .....	129
5.4 Conclusions .....	134
Chapter 6 PFCAs and PFSA removal during drinking water treatment by magnetic nanoparticles	135
6.1 Introduction .....	136
6.2 Materials and Methods .....	138
6.2.1 Magnetic Nanoparticles.....	138
6.2.2 Target Compounds and Water.....	141
6.2.3 Kinetic Tests.....	142
6.2.4 Analyses .....	143
6.3 Results and Discussion.....	143
6.3.1 Nano Adsorbents Properties .....	143
6.3.2 Adsorption Kinetics and Capacities in Ultrapure Water .....	146
6.3.3 Adsorption Kinetics and Capacities in Surface Water .....	152
6.3.4 Factors Affecting PFC Removal by Magnetic Nanoparticles .....	157
6.4 Conclusions .....	164
Chapter 7 Conclusions and recommendations.....	166
7.1 Summaries and Conclusions.....	166
7.1.1 Development of an LC-MS/MS Analytical Method for Target PFCs.....	167
7.1.2 PFCs Removal Performance of Selected Anion Exchange Resins .....	167

7.1.3 Anion Exchange Resins Regeneration Performance for PFCs Removal and Column Experiments.....	169
7.1.4 PFCs Removal Performance of Synthesized Magnetic Nanoparticles.....	170
7.1.5 Contributions to Knowledge.....	170
7.2 Recommendations for Future Research.....	171
References .....	174
Appendix A LC-MS/MS Method Repeatability for PFCs Analysis .....	190
Appendix B Adsorption Kinetics Using GAC (F400) and Purolite A502p Resin for PFCs Removal .....	191
Appendix C PFCs Isotherms Using GAC (F400) and A502p Resin.....	196
Appendix D Application of the Pseudo-Second-Order Model to the Adsorption Data of All Target PFCs onto TAN-1 Resin in Different Surface Waters .....	201
Appendix E Pore Size Distribution Results for Anion Exchange Resins.....	202
Appendix F The Effect of Magnetic Separation for Nanoparticles.....	205
Appendix G Pseudo-Second-Order Model for N2 and N3.....	206
Appendix H LC-OCD Results of Grand River Raw Water and after 24 Hours Treatment Using N2 and N3 .....	208
Appendix I Supporting Documents for Column Experiments .....	209

## List of Figures

Figure 1.1 Thesis chapters and thesis structure.....	7
Figure 2.1 Classification of PFCs.....	8
Figure 2.2 Typical LC-OCD chromatograms of a surface water sample.....	28
Figure 3.1 Flow chart of SPE process for PFCs analysis.....	36
Figure 3.2 LC-MS/MS chromatograms for PFCAs.....	43
Figure 3.3 LC-MS/MS chromatograms for PFSAs.....	44
Figure 3.4 LC-MS/MS chromatograms for PFPAs.....	44
Figure 3.5 LC-MS/MS chromatograms for internal standards.....	45
Figure 3.6 LC-MS/MS chromatogram of all target PFCs and internal standards.....	45
Figure 3.7 Representative calibration curves of PFCAs.....	46
Figure 3.8 Calibration curves of PFSAs.....	46
Figure 3.9 Calibration curves of PFPAs.....	47
Figure 3.10 Peak areas of internal standards during calibration curves.....	47
Figure 4.1 PFCs adsorption kinetics of all five anion exchange resins in ultrapure water.....	65
Figure 4.2 Application of the pseudo-second-order model to the adsorption data of all target PFCs onto TAN-1 resin in ultrapure water.....	69
Figure 4.3 Freundlich isotherms of PFCs adsorption in ultrapure water.....	74
Figure 4.4 95% joint confidence regions (JCRs) and point estimates for the Freundlich parameters of isotherms generated with TAN-1 and PFA444 resins in ultrapure water.....	76
Figure 4.5 Freundlich isotherms of TAN-1 and PFA444 resins in ultrapure water.....	81
Figure 4.6 Comparison of maximum percentage removals for PFOA and PFOS among all selected resins in ultrapure water.....	83
Figure 4.7 Comparison of calculated equilibrium aqueous concentrations ( $q_e$ ) and maximum percentage removals among all target PFCs in TAN-1 resin in ultrapure water.....	84

Figure 4.8 Freundlich isotherms of different PFCs using TAN-1 resins in ultrapure water.....	85
Figure 4.9 PFCs adsorption kinetics of all five anion exchange resins in Grand River water.....	86
Figure 4.10 PFCs kinetics using TAN-1 and PFA444 resins in ultrapure water, Grand River water (GRW), and Lake Erie water (LEW).....	93
Figure 4.11 Removal kinetics results of different PFCs using TAN-1 resin in Lake Erie water.....	96
Figure 4.12 DOC removals by different anion exchange resins in Grand River water.....	97
Figure 4.13 LC-OCD results after 48-hour treatment by anion exchange resins in Grand River water.....	98
Figure 4.14 LC-OCD results by TAN-1 resin in different adsorption times in Grand River water.....	99
Figure 4.15 Inorganic anions concentrations after treatment by TAN-1 and PFA444 resins in Grand River water.....	101
Figure 4.16 Sulfate competitions with PFCs in ultrapure water using both PFA444 and TAN-1 resins.....	103
Figure 4.17 Nitrate competitions with PFCs in ultrapure water using both PFA444 and TAN-1 resins.....	104
Figure 5.1 Schematic diagram of the general experimental procedure of the study in Chapter 5.....	110
Figure 5.2 Column test setup for ion exchange resins: A) schematic diagram; B) real setup.....	115
Figure 5.3 Regeneration efficiencies of target PFCs after regeneration with different methods.....	119
Figure 5.4 Breakthrough curves of PFCs in anion exchange column tests using Grand River water.....	123
Figure 5.5 SEM images of unused A555 resin and its surface.....	125
Figure 5.6 SEM images of A5555 resin and its surface after treating PFCs in ultrapure water.....	126
Figure 5.7 SEM images of A5555 resin and its surface after treated with PFCs in Grand River water.....	126
Figure 5.8 PFCs breakthrough curves for regeneration method optimization.....	127

Figure 5.9 Regeneration efficiencies of target PFCs when using different regeneration operation conditions in ultrapure water.....	129
Figure 5.10 DOC loading curve.....	130
Figure 5.11 Inorganic anions loading curves.....	131
Figure 5.12 Regeneration loading curves using Grand River water.....	132
Figure 5.13 Anion exchange resins column regeneration elution curves using PFCs spiked Grand River water.....	133
Figure 6.1 Schematic of the synthesized nanoparticles.....	139
Figure 6.2 Structures of three selected polymers modified on the magnetic nanoparticles.....	140
Figure 6.3 TEM images of synthesized nanoparticles.....	144
Figure 6.4 Zeta potential variations during the nanoparticle coating procedure.....	145
Figure 6.5 Dynamic light scattering results of nanoparticles before and after LbL deposition.....	145
Figure 6.6 PFCs adsorption kinetics of all three nanoparticles in ultrapure water.....	147
Figure 6.7 Application of the pseudo-second-order model to the adsorption data of all target PFCs onto N1 particle in ultrapure water.....	148
Figure 6.8 PFCs adsorption kinetics of all three nanoparticles in Grand River water.....	153
Figure 6.9 Application of the pseudo-second-order model to the adsorption data of all target PFCs onto N1 particle in Grand River water.....	157
Figure 6.10 Adsorption results of different PFCs using N1 particle in ultrapure water.....	158
Figure 6.11 Results of $q_e$ of different PFCs using all three nanoparticles in ultrapure water.....	159
Figure 6.12 Results of $q_e$ of different PFCs using all three nanoparticles in Grand River water.....	160
Figure 6.13 LC-OCD results of raw water and after 48 hours using N1.....	161
Figure 6.14 NOM results for three magnetic nanoparticles N1, N2 and N3 in Grand River water....	162
Figure 6.15 Anion concentrations using N2 in Grand River water.....	163

## List of Tables

Table 2-1 Structure and physicochemical properties of common PFAAs.....	9
Table 2-2 Recommended tolerable intake levels of PFAAs by regulatory bodies.....	12
Table 2-3 Waste materials for making low cost adsorbents.....	22
Table 2.4 Summary of adsorbent materials.....	24
Table 3-1 Peak area comparison of different ionization modes for selected PFCs.....	40
Table 3-2 MS parameters for the MRM quantitation of target PFCs.....	41
Table 3-3 MDLs and LOQs for target PFCs.....	48
Table 3-4 Percentage recoveries of PFCs.....	49
Table 4-1 Target PFCs selected in the ion exchange experiments.....	55
Table 4-2 Grand River and Lake Erie water quality parameters.....	56
Table 4-3 Anion exchange resin properties.....	62
Table 4-4 Pseudo-second-order model parameters of all target PFCs for all anion exchange resins in ultrapure water.....	70
Table 4-5 Freundlich isotherm parameters for TAN-1 and PFA444 resins in ultrapure water.....	79
Table 4-6 Pseudo-second-order model parameters of all target PFCs for all anion exchange resins in Grand River water.....	88
Table 4-7 Pseudo-second-order model parameters of all target PFCs for TAN-1 and PFA444 resins in Lake Erie water.....	91
Table 5-1 Grand River water quality parameters.....	111
Table 5-2 Two-level factors for regenerants.....	112
Table 5-3 Regeneration methods.....	113
Table 5-4 Anion exchange column tests parameters.....	115
Table 5-5 Operational conditions need to be optimized for the regeneration column studies.....	116

Table 6-1 Grand River water quality parameters.....	141
Table 6-2 Pseudo-second-order model parameters of all target PFCs for all nanoparticles in ultrapure water.....	149
Table 6-3 Pseudo-second-order model parameters of all target PFCs for all nanoparticles in Grand River water.....	155

## List of Abbreviations

APCI	Atmospheric-Pressure Chemical Ionization
BV	Bed Volume
CE	Collision Energy
CID	Collision Induced Dissociation
CCL	Contaminant Candidate List
CMBR	Completely Mixed Batch Reactor
CSA	Controlled Superparamagnetic Iron Oxide Nanoparticle Aggregate
DFT	Density Functional Theory
DOC	Dissolved Organic Carbon
EBCT	Empty Bed Contact Time
ESI	Electrospray Ionization
FEEM	Fluorescence Excitation Emission Matrices
GAC	Granular Activated Carbon
GC/MS	Gas Chromatography/Mass Spectrometry
GRW	Grand River Water
IC	Ion Chromatography
LbL	Layer-by-layer
LC-MS/MS	Liquid Chromatography Coupled to Tandem Mass Spectrometry
LC-OCD	Liquid Chromatography – Organic Carbon Detector
LEW	Lake Erie Water
LOAEL	Lowest Observed Adverse Effect Levels
LOD	Limit of Detection
LOQ	Limit of Quantitation
MAC	Maximum Acceptable Concentration
MDL	Method Detection Limit
MIB	2-Methylisoborneol
MIEX	Magnetic Ion Exchange



NF	Nanofiltration
NOM	Natural Organic Matter
pAA-co-DADMAC	poly (Acrylamide-co-Diallyl Dimethyl Ammonium Chloride) (N3)
PAC	Powdered Activated Carbon
PES	Polyethersulfone
pDADMAC	poly (Dimethyl Diallyl Ammonium Chloride) (N1)
PFAAs	Perfluoroalkyl Acids
PFASs	Perfluoroalkyl and Polyfluoroalkyl S ubstances
PFBA	Perfluorobutanoic Acid (C4)
PFBS	Perfluorobutanoic Sulfonate
PFCs	Perfluorinated Compounds
PFCAs	Perfluoroalkyl Carboxylic Acids
PFDA	Perfluorodecanoic Acid (C10)
PFDPA	Perfluorodecanoic Phosphonic Acid
PFHpA	Perfluoroheptanoic Acid (C7)
PFHxA	Perfluorohexanoic Acid (C6)
PFHxPA	Perfluorohexanoic Phosphonic Acid
PFHxS	Perfluorohexanoic Sulfonate
PFNA	Perfluorononanoic Acid (C9)
PFOA	Perfluorooctanoic Acid (C8)
PFOPA	Perfluorooctanoic Phosphonic Acid
PFOS	Perfluorooctanoic Sulfonate
PFPA	Perfluorinated Phosphonic Acids
PFPeA	Perfluoropentanoic Acid (C5)
PFR	Plug Flow Reactor
PFSAs	Perfluoroalkyl Sulfonic Acids
pHpzc	Point of Zero Charge
polyBEP	poly [Bis (2-Chloroethyl) Ether-Alt-1,3-Bis [3-(Dimethyl Amino)

	Propyl] Urea] Quaternized (N2)
PSS	Poly (Sodium 4-Styrenesulfonate)
QA/QC	Quality Assurance and Quality Control
RO	Reverse Osmosis
RSD	Relative Standard Deviation
SEC	Size Exclusion Chromatography
SPE	Solid Phase Extraction
SPION	Superparamagnetic Iron Oxide Nanoparticle
SUVA	Specific UV-absorbance
TEM	Transmission Electron Microscopy
TOC	Total Organic Carbon
UCMR3	Unregulated Contaminants Monitoring Rule 3
USEPA	US Environmental Protection Agency
WAX	Weak Anion Exchange

# Chapter 1

## Introduction

### 1.1 Problem Statement

Over the last decade, perfluorinated compounds (PFCs) have emerged as a group of contaminants of concern. Due to their strong carbon-fluorine bonds, their relatively high polarity, and their low vapor pressure, PFCs are of high thermal and chemical stability. As a result, PFCs have been widely applied in manufacturing of common household items and industrial products such as non-stick pots and pans, flame-resistant and water-proof clothing, fast food containers, alkaline cleaners, and personal care products (Brooke et al., 2004). Some of the most frequently detected PFCs are perfluoroalkyl carboxylic acids (PFCAs) and perfluoroalkyl sulfonic acids (PFSAs). Perfluorinated phosphonic acids (PFPAs), which have similar structures but a different functional group compared to PFCAs and PFSAs, have only been recently been in the environment, although they have been used in industry for many years (Guo et al., 2012; Esparza et al., 2011). The high stability of PFCs leads to a high persistence in the environment. Under typical environmental conditions, PFCs are difficult to hydrolyze, photolyse, or biodegrade (USEPA, 2013). Furthermore, these compounds bioaccumulate in animal organs and biomagnify in wildlife (USEPA, 2013). Some toxicological studies on animals (mostly mouse) have shown that the ingestion of PFC contaminated water could lead to adverse health effects with lowest observed adverse effect levels (LOAEL) of 5000 ng/L in drinking water (White et al., 2011; Post et al., 2012). The presence of PFCs in human blood serum was proved to be associated with some adverse endpoints in some epidemiological studies for both the general population and populations exposed to contaminated water in the workplace (Alexander et al., 2003; Eriksen et al., 2009). Some of the PFCs, for example perfluorooctanoic acid (PFOA) and perfluorooctanoic sulfonate (PFOS) have

been detected in surface waters at concentrations in the ng/L ranges (e.g. Zareitalabad et al., 2013). Hence, due to potential risks to human health, PFOA and PFOS have been included in USEPA's third Contaminant Candidate List (CCL3) and also in the newly released CCL4 for further study and potential regulation (USEPA, 2009; USEPA, 2016c). Both of these two compounds as well as four other PFCs have been listed in the unregulated contaminants monitoring rule 3 (UCMR3) and mandatory surveys to community water systems are under way for the unregulated contaminants based on UCMR3 (USEPA, 2011). Recently, USEPA (2016a; 2016b) has issued drinking water health advisories of 70 ng/L for both PFOA and PFOS. In 2016, Health Canada purposed drinking water guideline for PFOA of 0.2 µg/L as a maximum acceptable concentration (MAC) (Health Canada, 2016a); guideline for PFOS was purposed as well with an MAC of 0.6 µg/L (Health Canada, 2016b). Therefore, the presence of PFCs in drinking water systems warrants further study.

In order to study the removal of PFCs in drinking water systems, some full-scale surveys have been assessing different treatment technologies including coagulation, sand filtration, adsorption, advanced oxidation, and membranes (Flores et al., 2013; Eschauzier et al., 2012; Takagi et al., 2011). These studies along with some bench-scale studies suggest that both activated carbon filters and high pressure membranes (mainly reverse osmosis) can be effective for PFC removal at concentration levels typically detected in drinking water; however, other conventional water treatment options such as coagulation/ flocculation/ sedimentation, sand filtration, chlorination and advanced oxidation will only achieve relatively low PFC removals (Rahman et al., 2014). Compared with high pressure membranes, GAC filters have lower operating costs and are more widely used in water treatment. Although GAC can remove PFCs efficiently, the capacity of the GAC can be exhausted after it has been applied for only a few months, and short chain PFCs break through earlier compared to long chain ones (Takagi et al., 2011). As a result, new adsorbents, which have high adsorption capacity, can adsorb short chain PFCs

effectively, and have high resistance to fouling by natural organic matter (NOM), are required.

Although ion exchange has rarely been applied for organic contaminants, it seems to be a promising treatment method for PFCs removal (Deng et al., 2010). Anion exchange resins are considered capable of removing perfluoroalkyl carboxylic acids (PFCAs) and perfluoroalkyl sulfonic acids (PFSAs), because these compounds hydrolyze into anions at pH values typical for ground or surface water.

In addition to activated carbons and ion exchange resins, some new types of adsorbents, including nanomaterials, agriculture wastes, and some other low cost adsorbents have been studied for their potential in removing PFCs in water and wastewater (Yu et al., 2011; Chen et al., 2011; Deng et al., 2012); however, the PFC concentrations in these studies were usually much higher compared to those observed in drinking water (Ochoa-Herrera et al., 2008). Some of these adsorbents were shown to be effective to remove PFCs at high concentrations: for example, Chen et al. (2011) reported that single-walled carbon nanotubes and maize straw-origin ash showed high adsorption capacities of over 700 mg/g. Nanoparticles have been regarded as novel and promising adsorbents particularly due to their high specific surface areas. Magnetic nanoparticles are an interesting option as they can be designed to be magnetically separated from water treatment systems (Linley et al., 2013). Overall, the adsorption capacity, adsorption rate, and selectivity of promising novel adsorbents for removing PFCs needs to be established at the low concentrations they are encountered at in surface waters.

The presence of NOM in natural water can dramatically decrease the adsorption performance of adsorbents for PFCs due to both the NOM preloading and NOM competitive adsorption (Li et al., 2003; Ridder et al., 2011; Matsui et al., 2003). Because of the diversity and complexity of the NOM, the influence of the NOM characteristics on adsorption and ion exchange performance should be systematically investigated. In anion exchange process inorganic anions may compete with PFCs for

anion exchange sites. Among all the anions, sulfate and nitrate are two frequently detected anions with relative high concentrations (i.e. mg/L) in surface water, which are likely to compete with PFCs. As a result, the influence of the inorganic anions on the removal of PFCs with different properties also needs to be investigated in the anion exchange process.

## **1.2 Research Objectives and Scope**

The primary objective of this research was to investigate more efficient approaches to remove PFCs by ion exchange and adsorption processes in drinking water treatment. The influence of the characteristics of the PFCs, water quality and properties of anion exchange resins and nanoparticles on adsorption and anion exchange processes was thoroughly studied. To reach better removal efficiencies, anion exchange resins and magnetic nanoparticles were tested for PFC adsorption and compared to GAC. The NOM effects in both adsorption and ion exchange processes, as well as the competition of the anions in the ion exchange process were also considered important factors likely influencing efficient PFC removal.

The specific objectives of this investigation were to:

(1) Select appropriate perfluorinated compounds (PFCAs, PFSAAs or PFPAs) as target trace contaminants based on criteria to be established in this research. Set up and optimize an analytical method for the selected target compounds using LC-MS/MS.

(2) Investigate the effects of different physical and chemical properties of the target compounds on the adsorption and ion exchange processes and fundamentally interpret the results based on these properties.

(3) Examine the effects of the characteristics of selected anion exchange resins and custom designed nanoparticles on PFC removal in both ultrapure water and natural water.

(4) Examine the feasibility of applying ion exchange resins and magnetic nanoparticles to remove target PFCs in ultrapure and natural water. Compare the adsorption performance of the selected anion exchange resins and magnetic nanoparticles with that of a conventional adsorbent. In all cases, provide a fundamental interpretation of results based on adsorbents and PFC properties.

(5) Investigate and interpret the impacts of NOM fouling on PFC adsorption. Study the influence of NOM fraction characteristics on competitive adsorption between PFCs and NOM for both ion exchange resins and nanoparticles.

(6) Investigate the influence of the inorganic anions commonly found in surface water on the ion exchange process, especially the competition between inorganic anions and PFCs with different carbon chain lengths and functional groups.

(7) Evaluate the ion exchange resins regeneration performance and select appropriate regeneration conditions after PFCs treatment. Investigate the factors impacting ion exchange regeneration after PFC treatment.

### **1.3 Research Approach and Thesis Organization**

This thesis is consisted of seven chapters, with Chapter 3, 4, 5 and 6 prepared in journal article format. Chapter 1 is the overall introduction, which presents the motivation, objectives, context and structure of the thesis. Chapter 2 introduces PFCs, provides a literature review about PFCs removal in drinking water treatment, and identifies knowledge gaps where further research is needed. Chapter 3 developed a

quantitative analytical method for PFCs in water by LC-MS/MS. The analysis method was established for seven PFCAs, three PFSAs, and three PFPAs. This method was used in the subsequent treatment chapters to analyze PFCAs and PFSAs. Chapter 4 describes the characterization results of selected ion exchange resins, as well as the performance of PFCs removal using ion exchange resins. The results include ion exchange resin isotherms and kinetics in ultrapure water and kinetics performance in natural water. The influence of both adsorbents and PFCs properties on PFC removal has been thoroughly studied. The impacts of the existence of NOM and inorganic anions for PFCs removal in the ion exchange process have also been analyzed and discussed. In Chapter 5, an ion exchange column test was conducted to evaluate the PFCs removal performance for a selected anion exchange resin, and to identify the adsorption and regeneration conditions for pilot and full-scale design. The ion exchange regeneration conditions have been optimized in both batch and column experiments and factors impacting regeneration have been investigated in this chapter. Chapter 6 focuses on PFC treatment using custom designed magnetic nanoparticles. The design and characterization of magnetic nanoparticles, the PFCs kinetics performance in both ultrapure and natural water, and factors impacting adsorption including both the properties of the selected PFCs and the modified functional groups of the nanoparticles are discussed in this chapter. In Chapter 4, 5 and 6, the feasibility of using anion exchange resins and magnetic nanoparticles for PFCs removal has been thoroughly analyzed and investigated, and the results are compared with those of a commonly used GAC. The last chapter, Chapter 7, summarizes the main outcomes and contributions of this research, and provides recommendations for future studies pertaining to PFC removal in water treatment. Figure 1.1 shows the thesis structure and the sequence of the chapters.



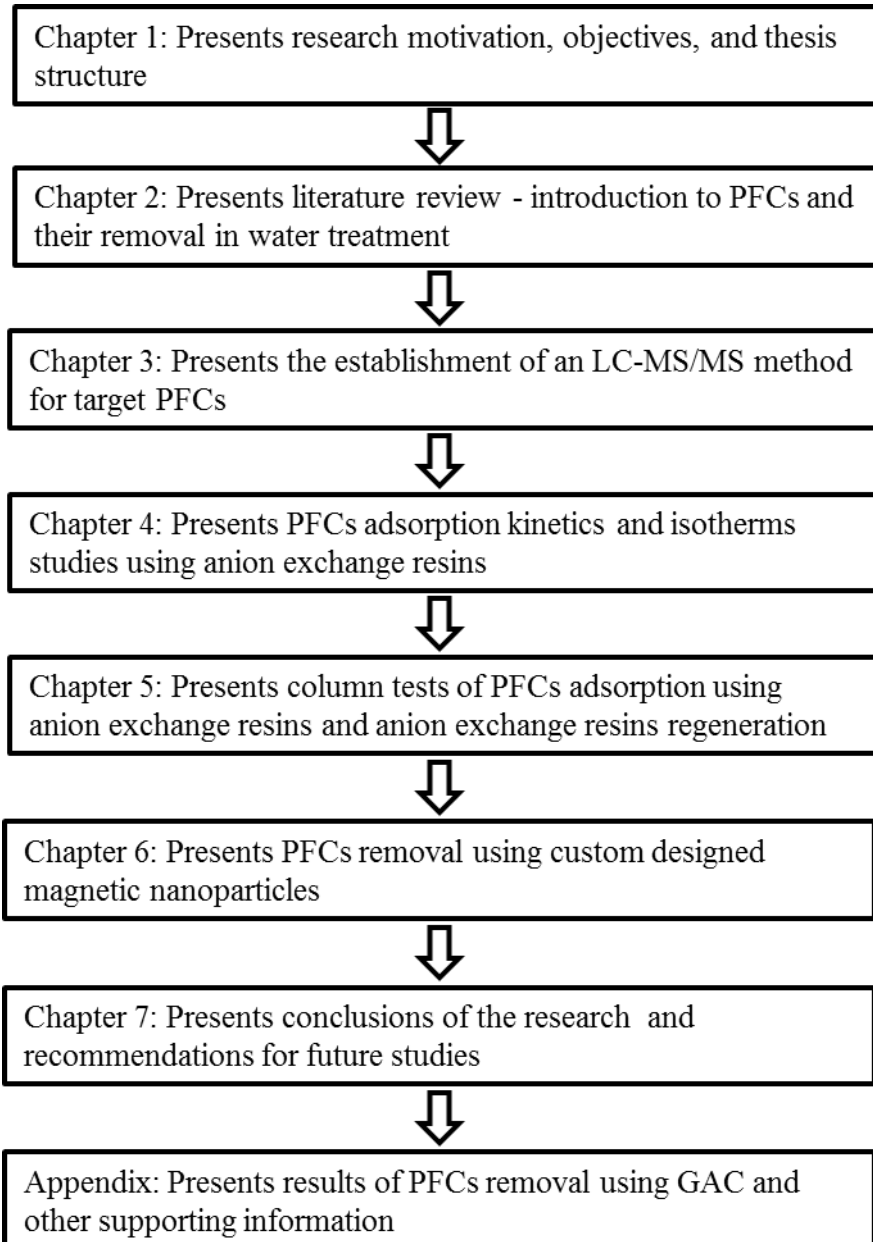


**Figure 1.1 Thesis chapters and thesis structure**

## Chapter 2

### Literature Review

#### 2.1 PFCs in Environment

##### 2.1.1 Definition and Classification of PFCs

PFCs are a class of human-made organic compounds which have been fully fluorinated. The term perfluoroalkyl and polyfluoroalkyl substances (PFASs) is also been used to present these compounds. As shown in figure 2.1, PFCs can be separated into perfluoroalkyl substances (all the hydrogen atoms in the carbon chain have been replaced by fluorine) and polyfluoroalkyl substances (not all of the hydrogen atoms in the carbon chain have been replaced by fluorine). Perfluoroalkyl carboxylic acids (PFCAs) and perfluoroalkane sulfonic acids (PFSAAs) are two main classes of perfluoroalkyl acids (PFAAs) applied in industry and detected in the environment; however, perfluorinated phosphonic acids (PFPAs) have only been recently detected. Perfluorooctanoic acid (PFOA) is the PFCA with 8 carbons and perfluorooctane sulfonic acid (PFOS) is the PFSA with 8 carbons. Among all the PFASs, PFOA and PFOS have attracted most attention because they are the most commonly detected ones in the environment and in biological samples (Rumsby et al., 2009).

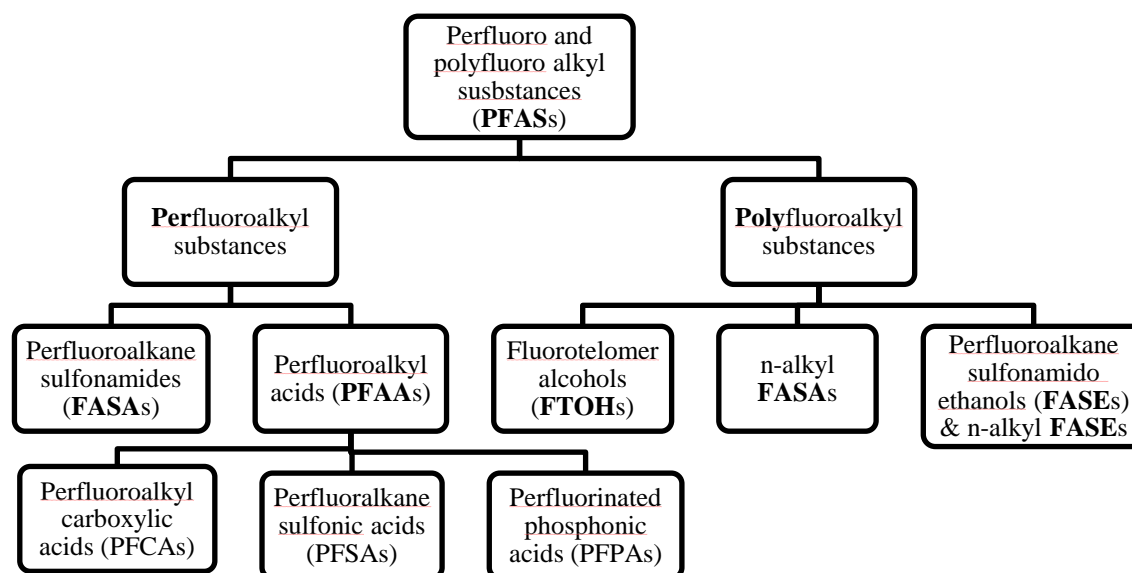
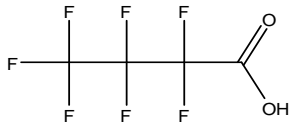
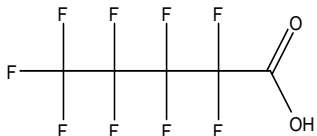
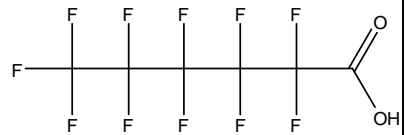


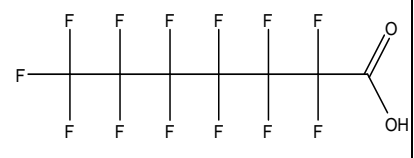
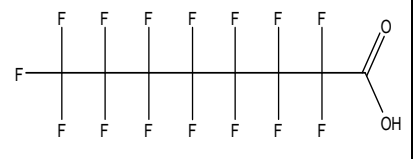
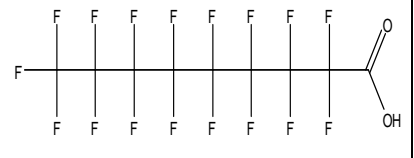
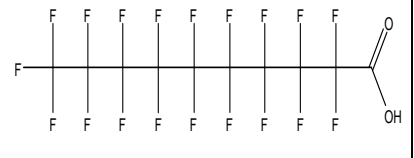
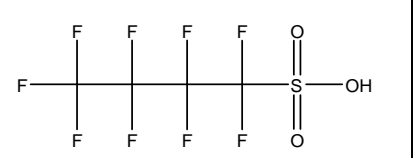
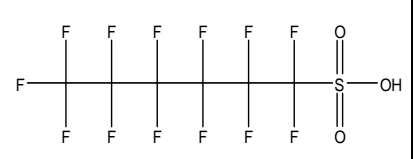
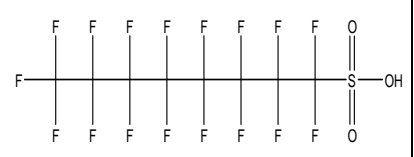
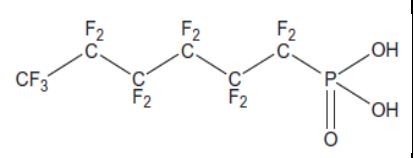
Figure 2.1 Classification of PFCs

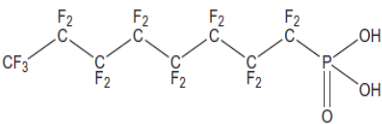
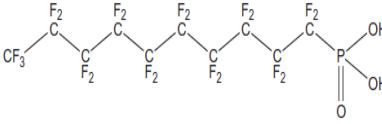
## 2.1.2 Physicochemical Properties of PFCs

Different carbon chain lengths and functional groups will influence the molecular size, hydrophobicity, and pKa values of the PFCs. Table 2-1 summarizes the structure and physicochemical properties of the main PFAAs. With the increase in carbon chain length, PFAAs have larger molecular weights and, as indicated by their log D values, become more hydrophobic. For example, as a PFAA with eight carbons, PFOA with a logD value of 1.58 is more hydrophilic than PFOS with a log D value of 3.05. PFOA and PFOS have high solubility and long half lives in water at 25°C of 41 and 92 years respectively (USEPA, 2013). The m/z notation is used as mass to charge ratio in mass spectrometry, where m refers to the molecular mass and z refers to the charge number of the ion. Since PFCs have the same charge number of the ion, the m/z value for each compound is related to its molecular weight as shown in Table 2-1.

**Table 2-1 Structure and physicochemical properties of common PFAAs (Kaiser et al., 2006; Awad et al., 2011; Jensen et al., 2008; Stock et al., 2009; Esparza et al., 2011; Rahman, 2014b).**

Compound Name & CAS Registry #	Structure	MW	m/z	Log Kow	Log D at pH 7	pKa	Solubility (mg/L)
Perfluoroalkyl Carboxylic Acids (PFCAs)							
Perfluorobutanoic Acid (PFBA) [375-22-4]		214.1	213	2.31	-1.22	1.07	N/A
Perfluoropentanoic Acid (PFPeA) [2706-90-3]		264.1	263	N/A	N/A	N/A	N/A
Perfluorohexanoic Acid (PFHxA) [307-24-4]		314.1	313	3.71	0.18	-0.78	N/A

Perfluoroheptanoic Acid (PFHpA) [375-85-9]		364.1	363	N/A	N/A	N/A	118,000 (21.6 °C)
Perfluorooctanoic Acid (PFOA) [335-67-1]		414.1	413	5.11	1.58	-4.2	4340 (24.1 °C)
Perfluorononanoic Acid (PFNA) [375-95-1]		464.1	463	5.81	2.28	-6.51	N/A
Perfluorodecanoic Acid (PFDA) [335-76-2]		514.1	513	N/A	2.37	N/A	260 (22.4 °C)
<b>Perfluoroalkyl Sulfonic Acids (PFSAs)</b>							
Perfluorobutanoic sulfonate (PFBS) [375-73-5]		300.1	299	2.63	0.25	-3.31	510
Perfluorohexanoic sulfonate (PFHxS) [355-46-4]		400.1	399	4.03	1.65	-3.32	N/A
Perfluorooctanoic sulfonate (PFOS) [1763-23-1]		500.1	499	5.43	3.05	-3.32	570
<b>Perfluoroalkyl phosphonic Acids (PFPAs)</b>							
Perfluorohexanoic phosphonic acid (PFHxPA)		400.03	399	N/A	N/A	N/A	N/A

Perfluorooctanoic phosphonic acid (PFOPA)		500.05	499	N/A	N/A	N/A	N/A
Perfluorodecanoic phosphonic acid (PFDPA)		600.06	599	N/A	N/A	N/A	N/A

### 2.1.3 Toxicity and Occurrence of PFCs in the Environment

PFCs have been detected in all kinds of environmental bodies, such as surface waters, wastewater, air, dust and soil. Among all the PFCAs and PFSAs, PFOA and PFOS are the most commonly detected ones in the environment and in biological samples (Rumsby et al., 2009). PFOA and PFOS have been detected in surface water at wide concentration ranges from several ng/L to hundreds of ng/L (ATSDR, 2009). Other PFCs detected in natural water, such as PFBA, PFHxA, PFHpA, PFNA, PFDA, PFBS, and PFHxS, have relatively lower concentrations at pg/L or low ng/L ranges (ATSDR, 2009). Compared with PFCAs and PFSAs, PFPAs have been detected in the environment and attracted research concern only in recent years. D' Eon et al. (2009) have been the first in demonstrating the presence of PFPAs in surface water and waste water treatment plant effluents in Canada with concentrations ranging from 0.026 to 3.4 ng/L in surface water and 0.33 to 6.5 ng/L in wastewater. PFOPA is the predominant PFPAs in surface water. PFOPA was found at 1 ng/L in one Dutch surface water sample and PFOS concentrations in surface water ranged from 3.3 ng/L to 25.4 ng/L (Esparza et al., Talanta, 2011). PFPAs were detected in lake trout from Lake Ontario, Lake Erie, and Lake Huron with concentration ranging from non-detect to 0.032 ng/g (Guo et al., 2012). PFPAs were also detected in indoor dust with a concentration of 2.3 ng/g (Silva et al., 2012). The toxicity of PFPAs is still not clear; however, owing to the similar structures between PFPAs and PFCAs, the potential risks of PFPAs to human health and the environment need to be considered.

Studies have found PFOS and PFOA in concentrations of around 0.3-30 ng/mL in umbilical cord blood samples and similar concentrations of PFOS and PFOA in children’s serum, indicating that exposure to the chemicals is widespread (ATSDR, 2009). Data indicate that PFOS and PFOA serum concentrations are higher in workers and individuals living near fluorochemical facilities than those reported for the general population (ATSDR, 2009). Several animal studies have shown a certain relationship between PFAA treatment and hormone levels; however, the existing epidemiological studies did not find that there was a significant association between the concentration of PFAAs and human DNA damage (Lau, 2012). Studies also illustrate that prolonged exposure to PFCs in drinking water may lead to adverse effects on human health (Post et al. 2012). As a result, the USEPA has taken regulating PFCs in drinking water into consideration.

PFOA and PFOS have been included in USEPA 3rd Contaminant Candidate List (CCL3), and also in the newly issued CCL4 for further study and potential regulation (USEPA, 2009; USEPA 2016c). Recently, USEPA (2016a; 2016b) has issued health advisories for both PFOA and PFOS. Both of these two compounds as well as four other PFASs have been listed in the unregulated contaminants monitoring rule 3 (UCMR3) (USEPA, 2011b). Some recommended tolerable intake levels of PFAAs are provided in table 2-2.

**Table 2-2 Recommended tolerable intake levels of PFAAs by regulatory bodies (Lau, 2012)**

	<b>PFOA</b>	<b>PFOS</b>
US Environmental Protection Agency (drinking water)	0.4µg/L	0.2µg/L
Minnesota Department of Health (drinking water)	0.3µg/L	0.3µg/L
New Jersey Department of Environmental Protection (drinking water)	0.04µg/L	-
Drinking Water Commission of German Ministry of	100 ng/kg BW	100 ng/kg BW

---

Health (drinking water)

European Food Safety Authority (food)	1.5 µg/kg BW	150 ng/kg BW
UK Committee on Toxicity in Food, Consumer Products and the Environment (food)	3 µg/kg BW	300 ng/kg BW
German Federal Institute for Risk Assessment (food)	100 ng/kg BW	100 ng/kg BW

BW= body weight

#### **2.1.4 Sources and Pathways of PFCs Entering into the Environment**

PFCs have been widely applied in making common household and industrial products such as non-stick pots and pans, flame-resistant and water-proof clothing, fast food containers, alkaline cleaners, and personal care products (Brooke et al., 2004). PFCs are released and also degraded and released into the water, air and soil during the processes of industry production, storage, transportation and usage. About 98% of the environmental release is to water (Rumsby et al., 2009). PFCs (reported at concentrations of around 50 to 1000 ng/L for PFOA and 3 to 70 ng/L for PFOS) would enter wastewater treatment plants and were only partially removed during wastewater treatment. PFCs present in treated wastewater treatment plant effluent are considered to be one of the main sources of PFCs in surface waters (Sinclair & Kannan, 2006). Due to the properties of extreme persistence, bioaccumulation and biomagnification, the background concentration of PFCs in the environment and in the trophic chain will gradually increase.

#### **2.1.5 Analysis of PFCs**

Both liquid chromatography mass spectrometry (LC/MS) and gas chromatography mass spectrometry (GC/MS) can be used to analyze the precursors of PFOAs (EFSA, 2008); however, LC-MS/MS is the most commonly used instrumentation because a wide range of PFCs can be analyzed by this method. USEPA established a standard

LC-MS/MS method for the determination of PFAAs in drinking water (USEPA, 2009). PFPAs, as a more recently detected type of PFAAs, have not been included in the USEPA method. An ultra-high performance liquid chromatography coupled to tandem mass spectrometry (UHPLC-MS/MS) has also been used to detect PFCs especially in recent years (Lacina et al., 2011). UHPLC operates at extremely high pressures using separation columns with smaller particle sizes, which enhances the separation speed, resolution and sensitivity (Anumol et al., 2013). Because the concentration of PFCs in drinking water system is very low (around ng/L range), solid phase extraction (SPE) is usually needed to concentrate the water sample before applying LC/MS or GC/MS. Taniyasu (2005) investigated SPE conditions in detail for both PFCAs and PFSAs . In his study, weak anion exchange (WAX) cartridges were proven to be effective as the extraction media. However, the SPE conditions need to be consolidated with those for PFPAs..

## **2.2 PFC Removal during Drinking Water Treatment**

Due to the potential risk of PFCs in drinking water system, studies have started to focus on different treatment technologies to remove PFCs.

### **2.2.1 PFC Removal in Full-scale Water Treatment Plants**

Treatment methods used in full-scale drinking water treatment plants include coagulation/flocculation/sedimentation, granular media filtration, GAC filtration, advanced oxidation, and high pressure membrane. PFCAs and PFSAs have been monitored at full-scale drinking water treatment plants but there are no full-scale data available for PFPAs.

#### (1) Adsorption

The GAC filter (adsorption process) is an effective treatment method for PFC removal. Takagi et al. (2011) reported that new GAC could reach up to nearly 100%



PFOA and PFOS removal. Other studies show that the treatment efficiency of GAC filters for PFOA and PFOS with a low influent concentration of around 5ng/L is about 50% (Eschauzier et al., 2012; Flores et al., 2013). After GAC has been used for more than one year, it cannot effectively remove PFOA and PFOS (Takagi et al., 2011). Compared to long carbon chain PFCAs and PFSAs, short chain ones have lower removal efficiency in GAC filters, and the PFC removal efficiency also decreases in natural water because of the NOM preloading effects (Takagi et al., 2011) which is the major drawback for GAC adsorption.

### (2) High pressure membranes

Another promising technology for PFC removal are high pressure membranes including nanofiltration (NF) and reverse osmosis (RO). RO can completely remove PFOA and PFOS at low concentration of 2ng/L (Flores et al., 2013). In general, high pressure membrane processes are not widely used for the treatment of drinking water other than dealing with specific contaminants, softening, and desalination, because of the high costs.

### (3) Other treatments.

Other conventional drinking water treatment processes are not effective for PFC removal. Coagulation/flocculation/sedimentation is not useful to remove PFOA and PFOS (Eschauzier et al., 2012). Sand filtration can only remove about 10% PFAAs (Flores et al., 2013). Ozonation as well as chlorination are not effective to remove PFAAs (Flores et al., 2013; Takagi et al., 2011).

As a result, GAC filtration could be the most promising method for PFC removal among all the common water treatment methods in drinking water treatment plants.

### 2.2.2 PFCs Removal in Bench-scale Treatment Studies

Since GAC adsorption is an effective method for PFC removal, the PFC adsorption process in bench-scale has been studied. In addition to adsorption, ion exchange also shows good treatment efficiency for PFCs.

#### (1) Adsorption

The majority of studies about PFC removal are looking at activated carbon adsorption. F400 was reported among the most effective activated carbons due to its surface chemistry (Ochoa-Herrera & Sierra-Alvarez, 2008). The adsorption capacity of F400 to remove PFCAs was proved to be excellent and the time to equilibrium in this process was approximately 21 days (Rahman, 2014). Powdered activated carbon (PAC) exhibited better adsorption performance on PFCs compared to GAC (Hansen et al., 2010). The presence of NOM significantly reduced the adsorption capacities and rates of PFCs (Yu et al., 2012).

The carbon chain length and functional groups of PFCs are two important factors that influence the molecular size, hydrophobicity, and pKa values of the target PFCs and all of these can impact the adsorption performance. The Freundlich adsorption coefficients value increased with increasing chain length for the PFC for both GAC and PAC (Hansen et al., 2010; Ochoa-Herrera & Sierra-Alvarez, 2008). PFSAAs were found to be more strongly adsorbed compared to their PFCA counterparts. It is speculated that the higher hydrophobicity of PFSAAs compared to that of PFCA counterparts may lead to the higher adsorption performance of PFSAAs (Hansen et al., 2010; Ochoa-Herrera & Sierra-Alvarez, 2008). The higher sorption capacity of PFOS on the GAC and PAC may be related to the more hydrophobic PFOS (Yu et al., 2009). Different from PFCAs and PFSAAs, adsorption performance for PFPAs has not been studied yet.

In addition to activated carbon, some other adsorbents, such as carbon nanotubes, functional groups modified hexagonal mesoporous silica, maize straw origin ash,

zeolites and chars, are also studied for their potential to remove of PFCs (Deng et al., 2012; Punyapalakul et al., 2013; Chen et al., 2011). Among these new materials, carbon nanotubes and maize straw origin ash showed high adsorption capacity of over 700mg/g (Deng et al., 2012); however, the concentrations of PFCs in these studies are around 100 mg/L which are much higher than PFC concentrations detected in surface water.

## (2) Ion exchange

Due to their low pKa values PFAAs such as PFOS and PFOA become anionic in water, and are thus removable by anion exchange resins. Some studies investigated the influence of polymer matrix, porosity, and functional group on PFOS removal (Deng et al., 2010). They revealed that anion exchange resins can be effective for PFOS removal and it was postulated that the hydrophilic matrix lead to faster sorption and higher sorption capacity of polyacrylic resins compared to polystyrenic resins. The adsorption and regeneration performance of ion exchange resins can change a lot according to the type of the resins. The recovery of PFBS from Amberlite IRA-458 ion exchange resin is only 4%, which indicated that PFSAs adsorbed by the resin was irreversible using a conventional regeneration method (Carter & Farrell, 2010); while in another study, PFA300 anion exchange resins reached the high PFOS adsorption capacity of 455mg/g and the regeneration efficiency of more than 99% (Chularueangakorn et al., 2013). Rahman (2014) used two anion exchange resins, A500 and A860, to test their performance on removing PFCAs in ultrapure and natural water. His results showed that the removal efficiency of A860 resin significantly decreased in natural water compared to that of A500. In general, the effects of ion exchange on removing PFPAs and short chain PFAAs need to be investigated, and effective regeneration methods for target ion exchange resins need to be developed.

## 2.3 Conventional and New Adsorbents Used in Drinking Water Treatment

### 2.3.1 Adsorption Basics

#### (1) Adsorption Isotherms

Adsorption isotherms describe the capacity of the adsorbent, or the amount of adsorbate which is adsorbed on the adsorbent at equilibrium and at a constant temperature. The mass balance at equilibrium is shown in Equation 2.1 (Chowdhury et al., 2013):

$$q_e = (C_0 - C_e) V/m \quad (\text{Equation 2.1})$$

$q_e$  = loading weight of adsorbate per unit weight of adsorbent at equilibrium (g/kg)

$C_0$  = initial adsorbate concentration (g/m<sup>3</sup>)

$C_e$  = equilibrium adsorbate concentration (g/m<sup>3</sup>)

$V$  = volume of solution (m<sup>3</sup>)

$m$  = weight of adsorbent (kg)

The Langmuir and Freundlich isotherm equations are the two most commonly used models for single solute adsorption equilibrium. The Langmuir isotherm equation is shown below (Suffet & McGuire, 1980):

$$q_e = \frac{Q_M b C_e}{1 + b C_e} \quad (\text{Equation 2.2})$$

in which  $Q_M$  is the saturation loading weight of adsorbate per unit weight of adsorbent forming a complete monolayer on the surface, and  $b$  is the Langmuir adsorption constant.

The Freundlich isotherm equation is shown in Equation 2.3:

$$q_e = K_f C_e^{1/n} \quad (\text{Equation 2.3})$$

in which  $K_f$  is the Freundlich adsorption capacity parameter, and  $1/n$  is the Freundlich adsorption intensity parameter (Suffet & McGuire, 1980).

## (2) Adsorption Kinetics

The kinetics of adsorption can be defined as the rate of approach to equilibrium. The adsorption rate is limited by mass transfer and influenced by the adsorbent and adsorbate. The whole adsorption process can be divided into three steps: external mass transfer or film diffusion, internal mass transfer or pore diffusion, and adsorption. The external mass transfer or film diffusion step is rate limiting in low turbulence, for example, in continuous flow beds; while, the internal mass transfer or pore diffusion step is rate limiting in batch reactors (Chowdhury et al., 2013). The adsorption step is too fast to be rate limiting. The time to equilibrium is influenced by the size of the adsorbent, diffusion coefficient of the adsorbate, initial concentration, and degree of shear or mixing (Chowdhury et al., 2013).

### **2.3.2 Activated Carbon**

Activated carbon is a carbon based material which is commonly used as adsorbent in drinking water treatment to adsorb contaminants from water. Raw materials often used to produce activated carbon include wood, coal, coconut shell, lignite and peat (López and Guijarro, 2010). There are two types of activated carbons: GAC and PAC.

#### (1) Granular Activated Carbon Adsorption

GAC is a kind of activated carbon with the particle size typically ranging from 0.5 to 3 mm (MWH, 2005). GAC is widely used as a good adsorbent because its superior adsorption capacity and chemical stability. In application, it is usually used in a fixed bed or as a layer of the media in a filter (Chowdhury et al., 2013). When water flows through the GAC filter, both the trace contaminants and the dissolved organic compounds in the water can be adsorbed on the adsorbents. After treatment, a backwash process is used to clean the GAC filter of particulate material. When GAC

is exhausted, it can be take out from the filter and regenerated through thermal methods. Because it is more economical on a large-scale or for continuous applications, GAC is widely used in water treatment applications.

#### (2) Powdered Activated Carbon Adsorption.

PAC is a kind of activated carbon with the particle size smaller than 100  $\mu\text{m}$  (MWH, 2005). Compared to GAC, PAC has a higher operational cost if it is continuously used. As a result, PAC is usually applied occasionally or seasonally (MWH, 2005). For example, this adsorbent can be used to remove geosmin and MIB which are two main compounds causing taste and odor, and are commonly produced in summer when algae blooms. PAC is usually added in front of the treatment train prior to or during coagulation /flocculation /sedimentation or filtration, so it can be removed by these treatments after adsorption. Although it is expensive, PAC has its advantage when dealing with the low concentration compounds in water and seasonally occurring contaminants.

### **2.3.3 Novel Adsorbents**

#### (1) Nanoadsorbents

In recent adsorption applications, nanoparticles have been a kind of novel and promising adsorbents due to their excellent adsorption performance. Nanoparticles can be defined as particles with a size typically ranging from 1 to 100 nm (Banfield and Zhang, 2001). According to the material and component, nanoparticles can be classified into metallic and metal oxide nanoparticles, silica nanoparticles, carbon nanoparticles and some other miscellaneous nanoparticles (Kaur and Gupta, 2009). Among all innovative adsorbents in drinking water treatment, nanoparticles are the most impressive ones. Due to the advantages of high specific surface area, rapid intraparticle diffusion and various modification possibilities, nanoparticles are a kind of promising adsorbents in water and wastewater treatment (Qu et al., 2012).

Some metal oxide nanoadsorbents and carbon nanotubes can be used to adsorb organic contaminants such as naphthalene, benzene, atrazine, trichloroethylene and other trace contaminants (Kaur and Gupta, 2009). Cyanobacterial toxins, e.g. microcystins, are reported to be removed by carbon nanotubes (Upadhyayula et al., 2009) and iron oxide nanoparticles (Lee and Walker, 2010) through adsorption process. The adsorption of arsenic and heavy metal ions using nanoparticles as adsorbents is applied in water treatment (Vunain et al., 2013; Recillas et al., 2010; Singh et al., 2011; Hua et al., 2012). Titanium dioxide nanoparticles with mesoporous hollow sphere structures were synthesized as photocatalysts initially, and then were found to have good dye adsorption capacity (Leshuk et al., 2012; Linley et al., 2013).

In some cases, the adsorption effect of nanoadsorbents is as remarkable as or even better than that of conventional adsorbents (Upadhyayula et al., 2009). The excellent adsorption performance is attributed to the huge specific surface area and active physical and chemical properties of nanoparticles (Kaur & Gupta, 2009). The good adsorption effects provide possibility for nanoadsorbents to substitute conventional adsorbents. It should be noticed that most of the studies on nanoadsorbents are experiments in deionized water or ultrapure water, and further tests in natural water are still required. The restrictive factors of high costs, potential risk to human health, regeneration and separation should be carefully studied in the future.

## (2) Surface modified adsorbents

Adsorbents can be modified to make them more selective. Some nano materials are used as modification to add more surface area and pores to the base adsorbents. The functional groups modified on the adsorbents will lead to more chemical adsorption which is more stable, rapid and selective. If the modification can be well designed according to the relationship between surface characteristics and adsorption capacity, the direct contaminants adsorption can be controlled.

Carbon based adsorbents can be modified on the surface using physical or chemical method to make the adsorbents more selective (Rivera-Utrilla et al., 2011). The modification methods include acidic treatment, base treatment, oxidation, impregnation and some miscellaneous methods (Bhatnagar et al., 2013). The purpose of modification is to introduce new functional groups to make the adsorbents more selective, or to change the pore structure to have better adsorption capacity.

### **2.3.4 Low Cost Adsorbents**

In order to reduce the cost of adsorption treatment, many low cost adsorbent materials are experimented with the intention to substitute activated carbon. Table 2-3 shows different types of waste materials for producing low cost adsorbents applied mainly in wastewater treatment, such as agricultural wastes, industrial wastes, soil and so on.

**Table 2-3 Waste materials for making low cost adsorbents (Ali et al., 2012)**

---

#### **1. House hold waste**

(1)Fruits waste (2)Coconut shell (3)Scrap tires

#### **2. Agricultural products**

(1)Bark and other tannin-rich materials (2)Sawdust and other wood type materials  
(3)Rice husk (4)Other agricultural waste

#### **3. Industrial wastes**

(1)Petroleum wastes (2)Fertilizer wastes (3)Fly ash (4)Sugar industry wastes (5)Blast furnace slag

#### **4. Sea materials**

(1)Chitosan and seafood processing wastes (2)Seaweed and algae (3)Peat moss

#### **5. Soil and ore materials**

(1)Clays (2)Red mud (3)Zeolites (4)Sediment and soil (5)Ore minerals

#### **6. Metal oxides and hydroxides**

---



---

## 7. Miscellaneous waste

---

Among all the low cost adsorbents, agricultural wastes are the most impressive ones. Agricultural wastes are carbon based materials with large surface area and special porous structure which can also be used to make activated carbon (Demirbas, 2009). As a result, they are considered to be excellent adsorbents in wastewater treatment (Ali et al., 2012). Several kinds of agricultural wastes are used as adsorbents to treat wastewater in batch scales. For example, bark and sawdust are both solid wastes produced in the timber industry. These two timber wastes are tested as adsorbents to treat dye wastewater and have good performance. The adsorption capacity could reach 100 mg dye/g of wood (Demirbas, 2009). Besides bark and sawdust, rice husk, raw wheat residues and other agricultural wastes are also studied as new adsorbents to treat dyes or other organic pollutants in wastewater (Ali et al., 2012; Demirbas, 2008). In addition to agricultural wastes, other low-cost materials are also studied for potential adsorption applications. Biochar was verified to be not effective to remove PFCs and NOM in water treatment (Rahman, 2014).

Using agricultural wastes or other low-cost materials as new adsorbents in water treatment provides a lot of advantages. Applying these new materials can dramatically drop the price of adsorbents, make sure the source of materials is sufficient, and provide a market for the agricultural wastes. As a result, agricultural wastes or other low-cost materials are considered to be used as adsorbents to remove either contaminants or NOM in water treatment. However, there are still several shortcomings for this innovative application. The adsorption performance of different low-cost adsorbents varies widely. The management and disposal of the exhausted adsorbents and the adsorbed contaminants is another issue. The performance of the low-cost adsorbents on removing target pollutants at low concentrations needs to be studied, because most studies of low-cost adsorbents were conducted at high

concentration around mg/ml ranges. To sum up, as their price superiority, agricultural wastes and other low cost adsorbents are potential adsorbents to be used in real applications; while, they should be improved to acquire better performance in adsorption application.

Adsorption properties of some adsorbent materials described above are summarized in Table 2-4.

**Table 2.4 Summary of adsorbent materials (Lian et al., 2009; Upadhyayula et al., 2009; Demirbas, 2008; Leshuk et al., 2012)**

<b>Adsorbents</b>	<b>Adsorption capacity</b>	<b>Regeneration</b>	<b>Structure</b>
<b>GAC (F400)</b>	1mmol methylene blue /g; iodine number: 998 mg/g	Thermal regeneration can be used	Large specific surface area (400-1000 m <sup>2</sup> /g ) and a wide range of pore sizes
<b>Carbon nanotubes</b>	~1-100 mg/g, a higher adsorption capacity toward organic pollutants and metal ions	Can be used in filters and regenerated as GAC	Aggregated pores due to the entanglement of tubes adhered to each other, large surface area(250 m <sup>2</sup> /g )
<b>Agricultural wastes</b>	100 mg dye/g of wood	Not economical	Three main structural components: hemicelluloses, cellulose and lignin.
<b>Mesoporous Hollow Sphere TiO<sub>2</sub></b>	High dye adsorption capacity	Can be magnetically separated	Hollow spheres with large surface area (~300 m <sup>2</sup> /g)

### 2.3.5 Ion Exchange Resins

In drinking water treatment, ion exchange is mainly used for softening, demineralization and metal removal. The exchange capacity and selectivity are two important properties for ion exchange resins. Ion exchange resins usually can be classified into four main groups (Barbaro & Liguori, 2009):

Cation exchanger (with anionic functionalities and positively charged ions)

1. Strong acid exchange: e.g., containing sulfonic acid groups or the corresponding salts;
2. Weak acid exchange: e.g., containing carboxylic acid groups or the corresponding salts;

Anion exchanger (with cationic functionalities)

3. Strong base exchange: e.g., containing quaternary ammonium groups;
4. Weak base exchange: e.g., containing ammonium groups.

Ion exchange resins are also used for NOM removals. The strong basic A860 resin was proved to have better NOM removal performance compared with the weak basic A847 resin in surface water, and the mechanism of the strong basic resin for NOM removal was dominated by ion exchange (Bazri et al., 2016a). Among the NOM fractions characterized by LC-OCD, the humic substances are the main fraction removed by ion exchange resins (Bazri et al., 2016b). An important finding from Rahmani and Mohseni's research (2017) is that the hydrophobic adsorption is the dominant mechanism for the uptake of organic compounds by ion exchange resins. They also found that the adding sulfate could decrease the impact of electrostatic interaction, so that the hydrophobic adsorption effects between anion exchange resins and organic compounds can be enhanced.

For removing PFCs such as PFCAs and PFSAs, strong basic anion exchange resins were proved to be effective for PFCs removal (Zaggia et al., 2016; Rahman et al., 2014). In the ion exchange process for PFCs removal, both the ion exchange and hydrophobic interactions exist (Gao et al., 2017), and the hydrophobicity of the resins plays an important role (Schuricht et al., 2017; Zaggia et al., 2016).

## **2.4 The Impact of NOM in Adsorption Process**

NOM is a complex heterogeneous mixture of compounds which originates from decomposition of microbial and plant materials in the environment. In adsorption, there are two mechanisms by which NOM can foul adsorbents: (1) NOM will compete with micropollutants for adsorption sites. This process is more important for PAC applications; (2) NOM will occupy or block pores in activated carbon. This process is more important for GAC applications. Two main mechanisms for NOM fouling are: (1) pore blockage mechanism; (2) direct site competition mechanism (Li et al., 2003). Adsorbents fouling by NOM can significantly reduce adsorption performance (Yu et al., 2012).

### **2.4.1 Characterization of NOM**

The molecular size or molecular weight, hydrophobicity, charge, structure and functional groups are considered to be characteristics of NOM influencing activated carbon fouling (Ridder et al., 2011). The effects of structure and functional groups of NOM have not been thoroughly studied, probably because NOM is complex and which makes their characterization and analysis challenging.

#### (1) Molecular size:

The influence of molecular size on fouling has been deeply studied, in particular size related mechanisms and the relation with activated carbon pore size (Velten et al.,

2011; Li et al., 2003; Matsui et al., 2002). Direct site competition is the main mechanism for small molecules of NOM with sizes similar to that of the target contaminants which would explain the decrease of adsorption capacity (Ding et al., 2008). Larger NOM molecules adsorb in large pores and reduce the effective pore diameter, thus, decreasing the rate of adsorption of smaller molecules that must pass through these pores to reach smaller pores (Ding et al., 2008). Low molecular weight organic contaminants can be adsorbed in the micropores of the adsorbents because of the size exclusion mechanism, while the high molecular weight part of the NOM is mainly adsorbed on adsorbent surface structures (Upadhyayula et al., 2009; Newcombe et al., 2002). Molecular size of NOM will influence the mechanism of fouling: pore blockage mechanism for large NOM constituents and direct site competition mechanism for small NOM constituents (Pelekani and Snoeyink, 1999).

LC-OCD uses size exclusion chromatography (SEC) coupled to an organic carbon detector. It is a fractionation method based on the molecular size. Compared to other SEC (for example, SEC with UV detectors), with LC-OCD it is possible to evaluate the content of high molecular weight polysaccharides and biopolymers in the sample (Matilainen et al., 2011). As shown in figure 2.2, LC-OCD can separate NOM into biopolymers, humic substances, building blocks, low molecular weight acids, and low molecular weight neutrals. Some studies using LC-OCD show that high molecular weight biopolymers were not retained by activated carbons (Velten et al., 2011). In contrast, humic substances and LMW organics were well and irreversibly removed (Velten et al., 2011). Poor removal of biopolymers was likely a result of their comparatively large size that prevented access to the internal pore structure of the GACs.

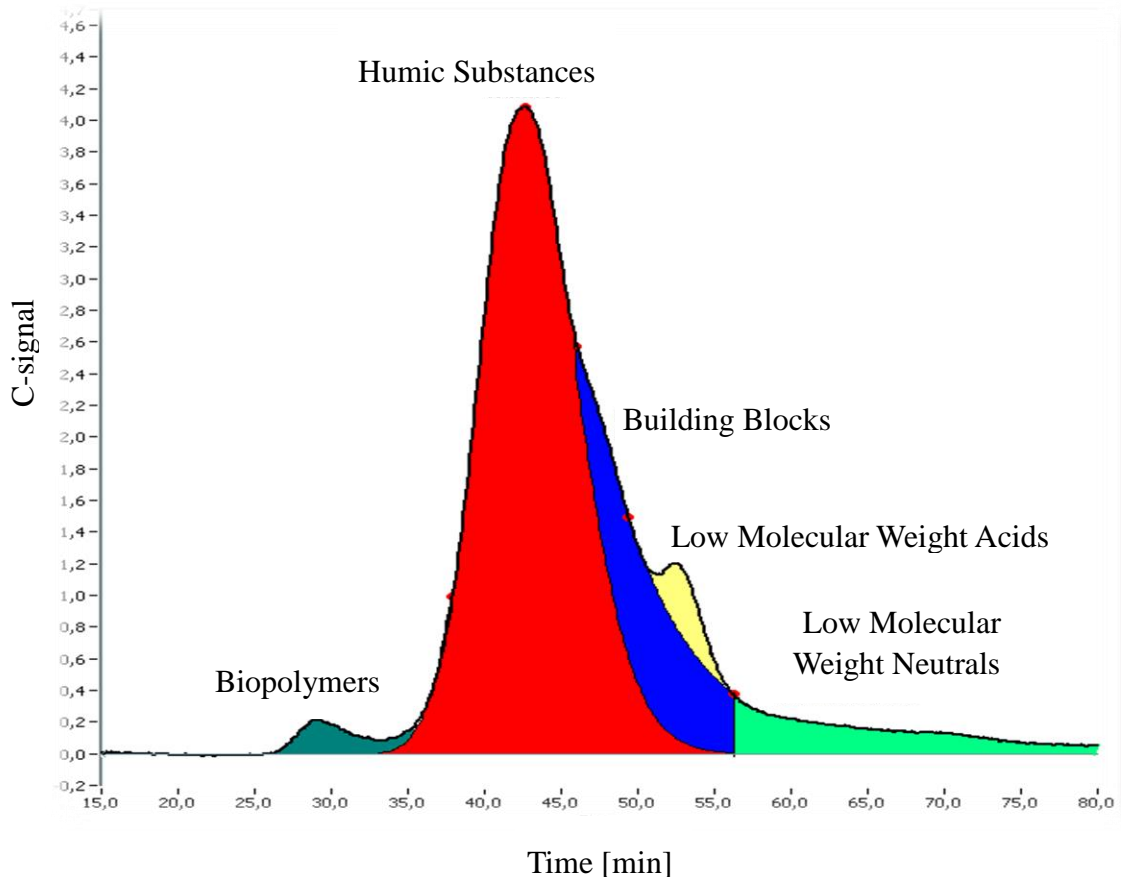


**Figure 2.2 Typical LC-OCD chromatograms of a surface water sample.**

**(Figure source: DOC-Labor Dr. Huber, [www.doc-labor.de](http://www.doc-labor.de))**

(2) Charge

GAC preloaded with NOM was postulated to be negatively charged, which influenced removal of charged pharmaceuticals significantly (Ridder et al., 2011). The authors postulated that the negative charge of the NOM preloaded adsorbents could repel negatively charged contaminants and attract positive charged ones.

(3) Hydrophobicity

Higher hydrophobicity of NOM will lead to lower pharmaceutical removal (Ridder et al., 2011). NOM competition was more severe for hydrophilic organic compounds than hydrophobic compounds (Zhang et al., 2011).

Specific UV-absorbance (SUVA) describes the nature of NOM in terms of aromaticity and hydrophobicity. In SUVA studies of natural water, some results showed that the more aromatic and hydrophobic components of NOM are preferentially adsorbed by GAC (Cheng et al., 2005).

#### **2.4.2 Competitive Adsorption between NOM and Contaminants**

The competitive adsorption between NOM and contaminants is significant in PAC and nano adsorbents adsorption process. The main mechanism of competitive adsorption between contaminants and NOM is a direct site competition mechanism (Matsui et al., 2003). The capacity of carbon for adsorbing the micropollutant in the presence of NOM is, among other factors, a function of the initial concentration of the micropollutant (Ding et al., 2008). The lower the initial concentration of micropollutant in natural water is, the lower the observed adsorptive capacity (Najm et al., 1991; Ding et al., 2008). Because of competition adsorption, NOM can significantly influence adsorption capacity of adsorbents (Lee and Walker, 2010). The presence of NOM will decrease the adsorption performance of adsorbents (Gutierrez et al., 2009). Some studies reported that direct competition with NOM can also lead to decreased adsorption capacity and kinetics of activated carbon for PFC removal (Zhao et al., 2011; Dudley, 2007).

#### **2.4.3 NOM Preloading on Adsorbents**

The process of NOM preloading on adsorbents is important and common for GAC filter adsorbents. The main mechanism of NOM preloading is pore blockage mechanism (Li et al., 2003). Ridder et al. (2011) studied the adsorption performance using 21 pharmaceuticals in both NOM preloading and NOM competition systems. The NOM preloading will change the surface characteristics of the adsorbents, such as hydrophobicity, charge, and pores size distribution. The NOM molecules with molecular weight between 200 and 700 Dalton appeared to be responsible for the pore blockage effect and preloading (Li et al., 2003). The NOM preloading will decrease

the adsorption capacity of GAC and shorten the breakthrough time (Corwin and Summers, 2010). The performance of GAC for PFC removal decreased in water with dissolved organic carbon (DOC) compared to that in low DOC water (Appleman et al., 2013).

## **2.5 Research Needs**

A suitable analytical method including SPE enrichment for not only PFCAs and PFSAAs but also PFPAs needs to be established and verified. Which new adsorbents or ion exchange resins are more suitable for PFCs removal and which are more suitable for short carbon chain PFCs needs to be studied. And only few studies have investigated the adsorption performance of ion exchange resins and nanoparticles for PFCs at low concentrations. The effect of functional groups and carbon chain lengths of PFCs and NOM characteristics on PFC removal in ion exchange processes, as well as the proper regeneration methods for selected ion exchange resins, need further investigations. The influence of some characteristics of NOM fractions on fouling of ion exchange resins and nanoparticles needs to be studied. How fouling of adsorbents and resins by different NOM fractions will influence adsorption of target contaminants is still not clear. Overall, more efficient approaches to remove PFCs by ion exchange and adsorption processes in drinking water treatment need to be thoroughly investigated.



## **Chapter 3**

### **Quantitative Analysis of Perfluoroalkyl Acids in Water by LC-MS/MS**

#### **Summary**

To simultaneously determine PFCs with three different functional groups (PFCAs, PFSAs, and PFPAs) in both ultrapure and surface water samples, a liquid chromatography tandem mass spectrometry (LC-MS/MS) analytical method has been developed. Seven PFCAs (C4-C10), three PFSAs (PFBS, PFHxS, and PFOS), and three PFPAs (PFHxPA, PFOPA, and PFDPA) were selected to be quantified in this method. A solid phase extraction (SPE) process was operated to reach a lower detection limit and was modified to be suitable for all selected PFCs. Both the LC parameters and the multiple reaction monitoring (MRM) conditions of the MS/MS were optimized to reach short retention times (1.2 min - 5.5 min), good sensitivity, and nice peak shapes for the selected PFCs. The method detection limits of the PFCs ranged from 0.1 to 5.0 ng/L. The results of method recoveries of target PFCs confirmed the method reliability. Calibration curves for the target PFCs were established with nine concentration points ranging from 10 to 3000 ng/L.

#### **3.1 Introduction**

As a type of frequently used chemical, perfluorinated compounds have been detected in a variety of environmental samples, including drinking waters and their sources (Rumsby et al., 2009; ATSDR, 2009). PFCAs and PFSAs are the two main types of PFCs applied in the industry and detected in the environment (Brooke et al., 2004). Among all PFCs, PFOA and PFOS are the two most ubiquitous ones detected in the environment, including in a range of water sources and drinking water systems

(Zareitalabad et al., 2013). Both compounds have been included in the USEPA's third Contaminant Candidate List (CCL3) (USEPA, 2009a). In the new finalized USEPA CCL4, PFOA and PFOAS are also included as two of the 97 chemicals of interest (USEPA, 2016c). In 2016, MAC values of 0.2 µg/L for PFOA and of 0.6 µg/L for PFOS were proposed by Health Canada (Health Canada, 2016a; 2016b) but have yet to be adopted into the Federal Drinking Water Guidelines. PFPAs have been detected in the environment only in recent years, although they have been used in industry for many years (Guo et al., 2012; Esparza et al., 2011). This may be largely due to the recent development of analytical methods specifically targeting PFPAs. More studies are needed to establish analytical methods which analyze different types of PFCs together in one method including the more recently detected PFPAs.

The most commonly used analytical method for PFCs is LC-MS/MS after sample extraction using solid phase extraction (SPE). The USEPA had promulgated method 537 (USEPA, 2009b) which suggested a LC-MS/MS method for determining PFASs including some PFCAs and PFSAAs in drinking water. The single laboratory lowest concentration minimum reporting levels (LCMRL) for tested PFCs in the USEPA method were in the range of 2.9-14 ng/L when using SPE to concentrate the analytes. Other studies reported analytical methods for PFCs using GC-MS. Rahman (2014) established a method using GC-MS to determining PFCAs with low MDLs. Another advantage for GC-MS was that it is less influenced by matrix effects compared to LC-MS (Fujii et al., 2012). However, GC-MS methods cannot be used for PFSAAs and PFPAs, and are not applicable to short chain PFCAs. Thus, LC-MS/MS is still the prevailing instrument for PFC analysis.

Due to the low concentration range of PFCs in the environment, the health advisory values for both PFOA and PFOS (70 ng/L) by USEPA (USEPA, 2016a; 2016b), and also the MAC values for PFOA (0.2 µg/L) and PFOS (0.6 µg/L) proposed by Health Canada, analytical methods for PFCs need to be applicable to such low

concentrations in order to provide accurate results. Thus, the SPE process was needed to concentrate the PFCs in water samples and enhance the sensitivity of PFC detection. The WAX and HLB cartridges are commonly used in the SPE process to concentrate target compounds from water. Both WAX and HLB cartridges can reach high recoveries for most of the PFCs; however, the WAX cartridge had better extraction performance for short chain PFCAs (Taniyasu et al., 2005). Recently, the on-line SPE coupled to LC-MS/MS was introduced, which largely decreased the processing time and reduced manual operation (Bartolome et al., 2016).

The objective of this study was to establish a suitable analytical method using LC-MS/MS for PFASs with different carbon chain lengths and functional groups and to include the only more recently detected PFPAs. The method had to be sensitive enough to detect all target PFCAs at low concentrations in typical drinking water samples. SPE was used to concentrate samples in order to achieve the required high sensitivity.

## **3.2 Materials and Methods**

### **3.2.1 Materials and Chemicals**

Seven PFCAs and three PFSAs including perfluorobutanoic acid (PFBA, purity  $\geq 99.5\%$ ), perfluoropentanoic acid (PFPeA, purity  $\geq 97\%$ ), perfluorohexanoic acid (PFHxA, purity  $\geq 97.0\%$ ), perfluoroheptanoic acid (PFHpA, purity  $\geq 99\%$ ), perfluorooctanoic acid (PFOA, purity  $\geq 99.2\%$ ), perfluorononanoic acid (PFNA, purity  $\geq 97\%$ ), perfluorodecanoic acid (PFDA, purity  $\geq 98\%$ ), perfluorobutanoic sulfonate acid (PFBS, purity  $\geq 97\%$ ), perfluorohexane sulfonate potassium salt (PFHxS, purity  $\geq 98\%$ ), and perfluorooctane sulfonate potassium salt (PFOS, purity  $\geq 98\%$ ) were purchased from Sigma-Aldrich (WI, USA). Three PFPAs including perfluorohexanoic phosphonic acid (PFHxPA,  $50 \pm 2.5 \mu\text{g/mL}$  in methanol), perfluorooctanoic

phosphonic acid (PFOPA,  $50 \pm 2.5$   $\mu\text{g/mL}$  in methanol), and perfluorodecanoic phosphonic acid (PFDDPA,  $50 \pm 2.5$   $\mu\text{g/mL}$  in methanol) were purchased from Wellington Laboratories (ON, Canada). Perfluoro-n- $^{13}\text{C}_8$ octanoic acid (M8PFOA,  $50 \pm 2.5$   $\mu\text{g/mL}$  in methanol) and sodium perfluoro-1- $^{13}\text{C}_8$ octane sulfonate (M8PFOS,  $50 \pm 2.5$   $\mu\text{g/mL}$  in methanol) were also purchased from Wellington Laboratories (ON, Canada), and both were used as internal standards.

HPLC grade methanol and ammonium acetate were acquired from Sigma-Aldrich (WI, USA). Any other solvents or chemicals used in the experiments were also HPLC grade. Ultrapure water was obtained from a Millipore Milli-Q<sup>®</sup> UV PLUS water system (MA, USA). Surface water was obtained from the Grand River, Ontario and filtered using  $0.45 \mu\text{m}$  polyethersulfone (PES) filters (Pall Corporation, NY, USA) before using. Oasis WAX cartridges (6 cc, 150 mg sorbent per cartridge,  $60 \mu\text{m}$  particle size) (Water Corporation, MA, USA) were used in the SPE process. 15 mL polypropylene conical vials (VWR, PA, USA) were used to collect elutes from the SPE. To reduce the adsorption of PFCs on the glassware, polypropylene containers were used for preparation and storage of the PFCs samples.

### 3.2.2 Solid Phase Extraction

The SPE process was conducted to reach a lower detection limit and help analyze PFCs in low concentrations. The SPE process in this research was established and optimized based on the study of Taniyasu et al. (2005). The SPE method was adjusted to accommodate not only PFCAs and PFSAs, but also PFPAs in the current research. Preliminary experiments were conducted to optimize some of the operational conditions. The volume of the water sample was selected to be 500 mL instead of 100 mL to reach a larger enrichment factor of 100. Oasis WAX 6 cc cartridges with 150 mg sorbent per cartridge were used in the SPE process.  $^{13}\text{C}_8$ -PFOA and  $^{13}\text{C}_8$ -PFOS were selected to be internal standards. The detailed SPE process is shown in Figure 3.1, which included conditioning, loading, washing, and eluting. In conditioning

process, 4 mL 0.1% NH<sub>4</sub>OH in methanol, 4mL methanol, and 4mL Milli-Q<sup>®</sup> water were passed successively at rate of about 2 to 3 drops per second through the WAX cartridges. Before the loading process, all 500 mL water samples were spiked with 100 µL of 1.0 mg/L internal standard solutions of both <sup>13</sup>C<sub>8</sub>-PFOA and <sup>13</sup>C<sub>8</sub>-PFOS, which is corresponded to a final concentration of 200 ng/L in the water sample. The spiked water samples were then passed through the preconditioned WAX cartridges at a speed of 1 to 2 drops per second in the loading process. After water samples were loaded, 4 mL of 25 mM acetate buffer (pH=4) was then passed through WAX cartridges at a rate of about 2 to 3 drops per second to wash away the impurities from the cartridges. In the eluting process, 4mL methanol and 4 mL 0.1% NH<sub>4</sub>OH in methanol were passed through cartridges in succession to elute the targeted PFCs. Both eluent solutions were gathered in 15 mL polypropylene vials then concentrated under a gentle stream of nitrogen at room temperature to slightly below 5mL. Methanol was then added to the solution to reach a volume of 5 mL in each sample, so that the elution volume could be controlled. The methanol solution was then be injected in the LC-MS/MS to detect and quantify the PFCs.

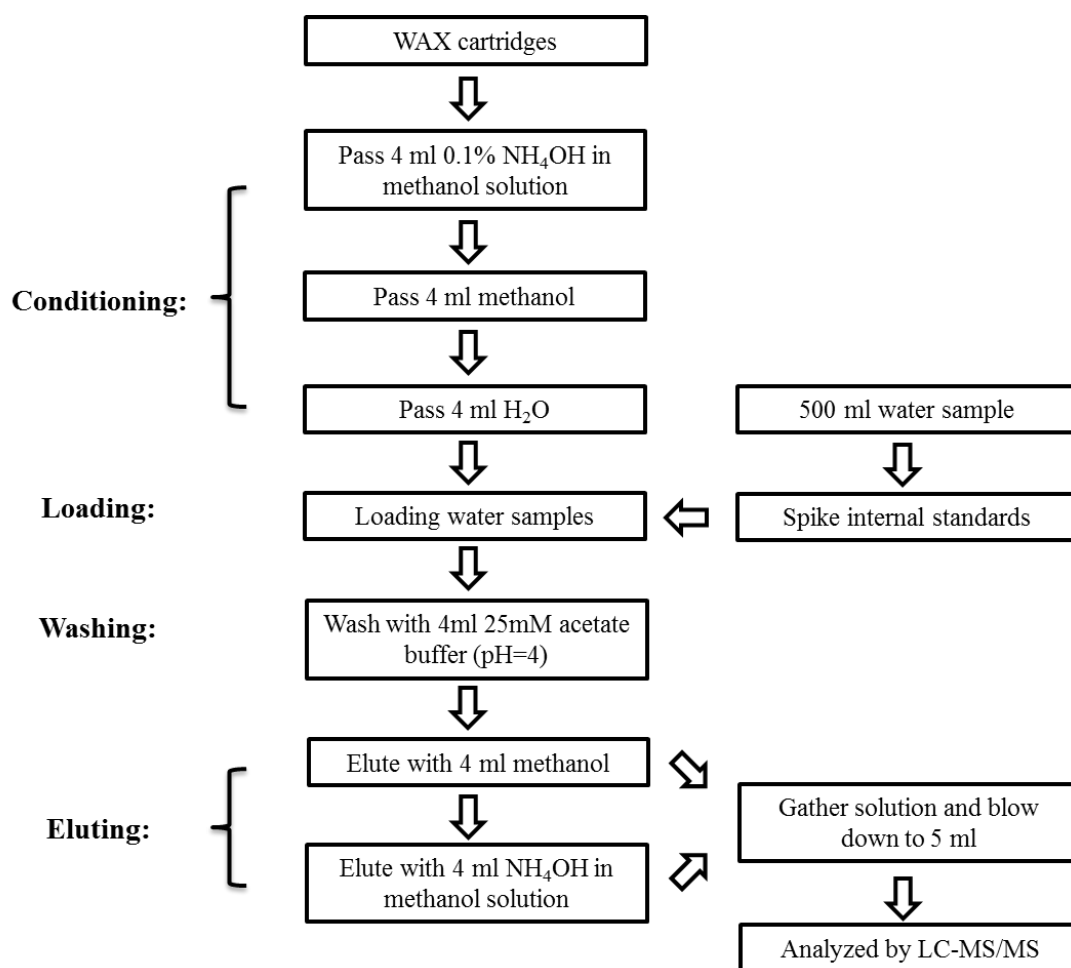


**Figure 3.1** Flow chart of SPE process for PFCs analysis

### 3.2.3 LC-MS/MS

After SPE process, PFC extracts were analyzed using a Shimadzu 8030 liquid chromatography tandem mass spectrometry (LC-MS/MS). A Poroshell SB C18 column (50 mm × 2.1 mm internal diameter, 1.8 μm packing) (Agilent, CA, USA) was used for separation of the PFCs.

Mobile phases were (A) 5 mM ammonium acetate in Milli-Q water, and (B) methanol. The following gradient was used: 0-0.5 min: 40% B; 0.5-4.5 min: steadily increase to 80% B; 4.5-6 min: 80% B; 6-6.5min: steadily decrease to 40% B; 6.5-10 min: 40% B. The LC was operated with a flow rate of 0.5 ml/min and the maximum

pump pressure was set to 3500 psi. Column temperature was kept at 30 °C. Nebulizing gas flow rate was 2 L/min. Drying gas flow rate was 15 L/min. Both nebulizing gas and drying gas were high purity nitrogen provided by a nitrogen dewar (99.998%, 230 psi) from Praxair (CT, USA). Desolvation line temperature was kept at 250 °C. Heat block temperature was 400 °C. Collision induced dissociation (CID) gas was argon gas provided by an argon cylinder (99.995%, 2000 psi) (Praxair, CT, USA), and the CID pressure was 230 kPa. A rinsing program was set up for the autosampler to clean the needle before each injection. The rinsing volume was set to be 50 µL. Rinsing speed was 35 µL/sec, and sampling speed was 5 µL/sec. The tubing purge time was 2 minutes. The cooler temperature of the autosampler was kept as 15 °C.

Multiple reaction monitoring (MRM) conditions were optimized including ionization mode, product ions and collision energy (CE) using the Shimadzu LabSolutions (version 5.60 SP2) analysis software. The electrospray ionization (ESI) in negative ionization mode was then applied for analyzing all target PFCs.

To solve the problem of retention time variability for some PFCs, especially long chain PFCs, a number of LC conditions were modified including column types, mobile phases, gradient conditions, pump mixer with different volume, and so on. Instead of the Restek Pinnacle DB C18 column, the Agilent Poroshell SB C18 column showed more stable retention times for all target PFCs. With the selected Poroshell column, the mobile phases and gradient conditions were modified to the conditions as described previously. A 100 µL pump mixer was proved to be good enough for mixing the mobile phase solutions. Increasing the volume of the pump mixer to 200 µL did not show obvious improvement for retention time stability.

#### **3.2.4 Method Detection Limits (MDL), Limit of Quantity (LOQ), Reproducibility, Repeatability, and Calibration Curves**

To calculate the MDLs of target PFCs, seven replicates of PFCs standard solution were processed, measured and quantified. The standard concentrations of PFCAs and

PFSAs were 1 ng/L, and the concentrations of PFPAs were 10 ng/L. The standard deviation of seven replicates was calculated at the 99% confidence interval (APHA, 2012). The MDLs were calculated as per eq. 3.1. The LOQs were calculated by multiplying the standard deviation by 10 (APHA, 2012).

$$MDL = SD \times 3.14 \quad (\text{Equation 3.1})$$

$$LOQ = SD \times 10 \quad (\text{Equation 3.2})$$

SD is the standard deviation of seven replicates, with recoveries of  $100 \pm 50\%$  and less than 20% RSD.

As shown in formula 3.3, the recoveries of the whole method were established by comparing the difference in measured concentrations between a spiked sample and an unspiked sample to that of the known concentration added to the spiked sample (Harris, 2007). The concentrations of PFCs spiked in the samples for method recovery were 100 ng/L for each compound in both ultrapure and surface water. Spiked and unspiked samples were processed through the entire analytical method including SPE as were all standards used to establish the calibration curves against which spiked and unspiked samples were evaluated.

$$Recovery = \frac{C_{spiked\ sample} - C_{unspiked\ sample}}{C_{added}} \quad (\text{Equation 3.3})$$

$C_{spiked\ sample}$  = concentration determined in a spiked sample

$C_{unspiked\ sample}$  = concentration determined in an unspiked sample

$C_{added}$  = target concentration added in an spiked sample

Method repeatability was calculated by determining the relative standard deviation (% RSD) of seven independent samples with same PFC concentrations. The method repeatability revealed the precision of the whole analytical method processes including the SPE process, the instrument detection, and other experimental operations. The concentrations of PFCs in the samples for method repeatability were 100 ng/L. The method repeatability results are shown in Appendix A.



Standards for the calibration curves were processed through the entire analytical method including SPE. Calibration curves were built by plotting the ratio of peak area of target compound to the peak area of internal standard against the concentration of target compound to the concentration of the internal standard. The M8PFOA was applied as an internal standard for PFCAs when calculating calibration curves; while the M8PFOS was applied for PFSAs and PFPAs. Nine point calibration curves with concentration levels ranging from 10 ng/L to 3000 ng/L in ultrapure water were established for PFCAs and PFSAs. Seven point calibration curves with concentrations ranging from 20 ng/L to 1000 ng/L were applied for PFPAs. The concentrations of internal standards used for calibration curves were 50 ng/L.

### **3.3 Results and Discussion**

#### **3.3.1 MRM Optimization Results**

MRM conditions including ionization mode, product ions, and collision energy (CE) were optimized for selected compounds.

##### **3.3.1.1 Ionization mode**

Both negative and positive single ion monitoring (SIM) modes were tested first for all the PFCs by directly injecting 10  $\mu$ L of PFCs standard solution via the autosampler into the instrument without a column. In the positive mode, there were many interfering signals and no parent ions of the target compounds could be found. However, in the negative mode, the parent ions of the target compounds were clearly detected with less interfering signals. Due to their low pKa values PFCs are dissociated into anions in water. As a result the negative ionization mode was more suitable and was selected.

The electrospray ionization (ESI) and atmospheric pressure chemical ionization (APCI) are two atmospheric pressure ionization methods interfacing the LC with the

MS/MS. To select the suitable ionization mode for the selected PFCs, tests were conducted for all compounds using three ionization modes of ESI, APCI and both ESI and APCI together. Peak area results are shown in Table 3-1 in the form of area ratio.

**Table 3-1 Peak area comparison of different ionization modes for selected PFCs**

PFCs	Name	Carbon	Ionization Mode (peak area ratio)			
			ESI	APCI	Both	Note
PFCAs	PFBA	4	1.00	1.06	1	
	PFPeA	5	0.91	1.11	1	
	PFHxA	6	0.95	1.10	1	
	PFHpA	7	0.91	1.19	1	
	PFOA	8	0.91	1.21	1	
	PFNA	9	0.92	1.29	1	
	PFDA	10	0.98	0.90	1	
PFSAAs	PFBS	4	1.00	1.13	1	APCI peak has bad shape
	PFHxS	6	0.93	0.95	1	
	PFOS	8	1.22	1.23	1	
PFPAAs	PFHxPA	6	1.11	0.64	1	APCI peak has bad shape
	PFOPA	8	1.06	1.44	1	
	PFDPa	10	0.96	1.53	1	

The ionization mode optimization results in Table 3-1 showed that there were no significant differences among the three modes for most of the compounds. In ESI mode, peak areas were -9% to 22% different from those using both ESI and APCI mode, which revealed that ESI could be a steady, reliable, and relatively sensitive mode for most of the PFCs. PFOPA and PFDPA showed much higher response in APCI mode compared to the other modes. PFHxPA had an irregular bad peak shape with low response in the APCI mode. PFBS showed similar response in all three modes; however, PFBS in the APCI mode also showed a bad peak shape. To sum up,

APCI mode was not suitable for some of the low carbon compounds, especially PFBS and PFHxPA. Thus, negative ESI mode was selected.

### 3.3.1.2 Product ions and collision energy (CE)

The optimization of the MS parameters was conducted by directly injecting 10  $\mu$ L PFCs standard solution to the MS/MS detector without the column. The product ions as well as corresponding collision energy of all target PFCs shown in table 3-2 were all obtained using LabSolutions' integrated MRM event optimization program (Shimadzu). The results for the parent and product ions of the target PFCs are in agreement with the ones reported in the literature, and the CE values reported here have also similar trends as shown in the analytical method papers (Gosetti et al., 2010; Lacina et al., 2011; Lankova et al., 2013; Onghena et al., 2012).

**Table 3-2 MS parameters for the MRM quantitation of target PFCs**

PFCs	Name	Carbon	Parent ion	Product ion 1		Product ion 2	
			(m/z)	(m/z)	CE (eV)	(m/z)	CE (eV)
<b>PFCAs</b>	PFBA	4	213	169	10	19	19
	PFPeA	5	263	219	10	19	25
	PFHxA	6	313	269	11	119	22
	PFHpA	7	363	319	11	169	18
	PFOA	8	413	369	11	169	18
	PFNA	9	463	419	12	169	20
	PFDA	10	513	469	13	219	19
<b>PFSAs</b>	PFBS	4	299	80	34	99	32
	PFHxS	6	399	80	45	99	40
	PFOS	8	499	80	55	99	45
<b>PFPAs</b>	PFHxPA	6	399	79	33		
	PFOPA	8	499	79	39		
	PFDPa	10	599	79	49		
<b>Internal Standards</b>	M8PFOA	8	421	376	11	172	21
	M8PFOS	8	507	80	52	99	46

### 3.3.2 LC-MS/MS Results

As shown in Figure 3.2, PFCAs with different carbon chain lengths (4-10) could be well separated without interference with each other in six minutes. PFSAs and PFPAs could also be well separated within their respective group, which is shown in Figure 3.3 and 3.4. For PFCs with the same functional group, short chain PFCs eluted earlier than long chain PFCs. Long chain PFCs are more hydrophobic than short chain PFCs. When PFCs solutions enter the column, the hydrophobic column material as stationary phase can retain the long chain PFCs longer time compared to short chain PFCs; thus, the less hydrophobic short chain PFCs tend to be eluted earlier with the mobile phase. For PFCs with the same carbon chain length but with different functional groups, the sequence of elution was PFPAs first followed by PFCAs and then PFSAs last. Although peaks of PFCs with the same functional group but the different carbon chain length could be well separated in the chromatograms, compounds with different functional groups may have similar retention times, and need to be quantified based on their MS information i.e. their characteristic parent and product ions. For example, the PFNA (nine-carbon PFCA) and PFOS (eight-carbon PFSAs) had similar retention time around 5.1 minutes. In the chromatograms of PFHxS and PFOS, there were some small peaks eluting right before the largest peaks, which was caused by the different isomers existing in the standards. The larger peaks should be linear isomers and the smaller peaks were believed to be related branched isomers (Berger et al., 2011). The total peak areas of all isomers were calculated when determining the calibration curves. From all the chromatograms, it could be observed that the peak of PFBA was the first one appearing at a retention time of 1.19 minutes among all the PFCs, and all selected target PFCs were eluted before 6 minutes when methanol concentration was kept as 80%. After 6.5 minutes, the concentration of methanol returned to 40% for 3.5 min, so that the system could be stabilized during the remainder of the run, and be ready for the next injection. An LC-MS

chromatogram including all target PFCs and internal standards was shown in Figure 3.6.

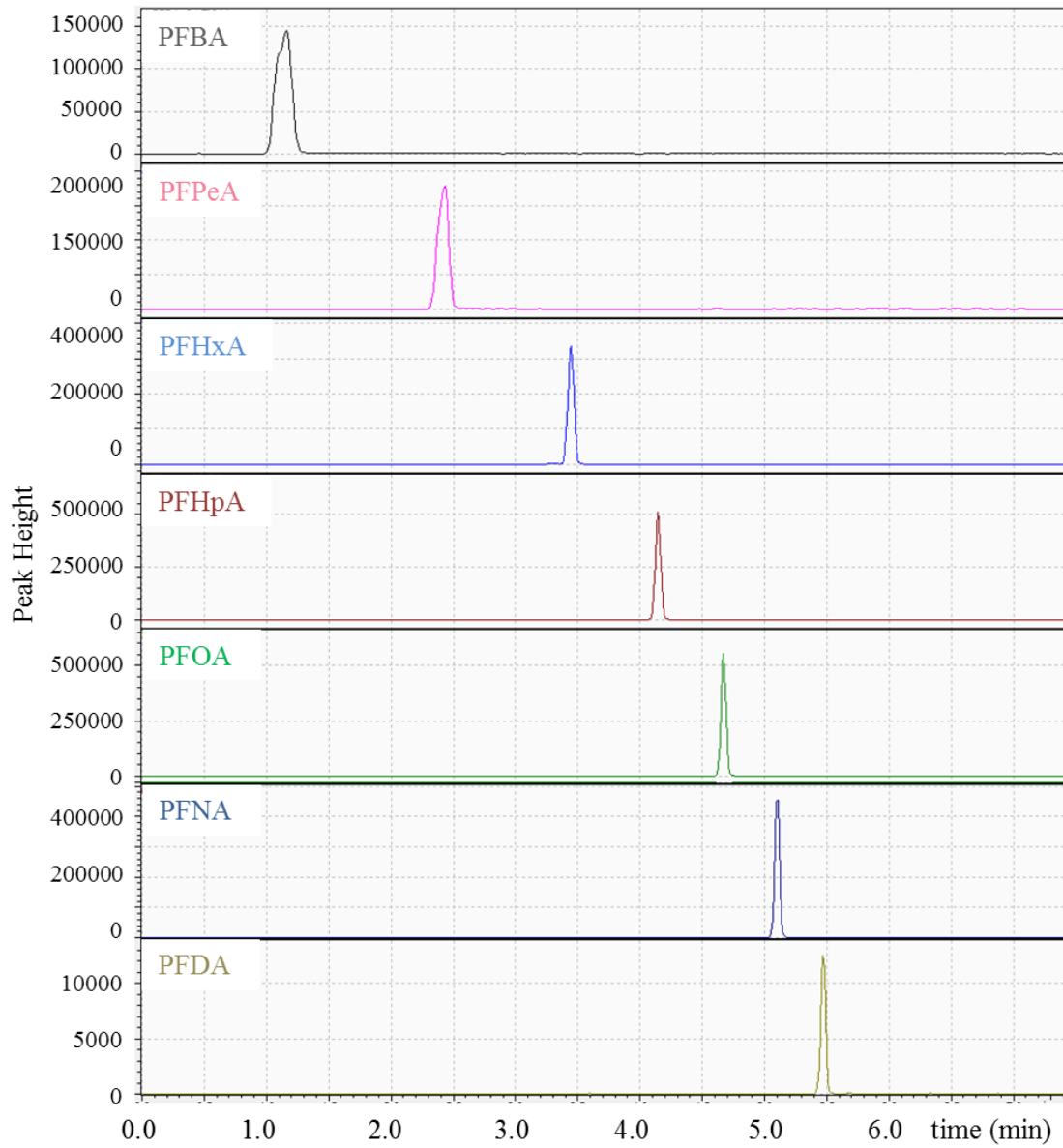


**Figure 3.2 LC-MS/MS chromatograms for PFCAs**

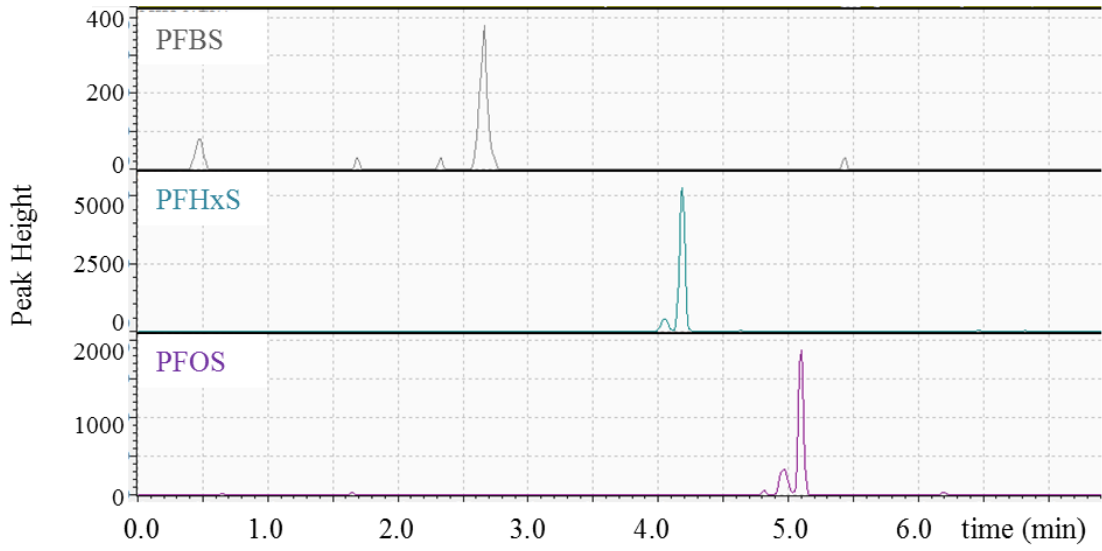


**Figure 3.3 LC-MS/MS chromatograms for PFSAs**

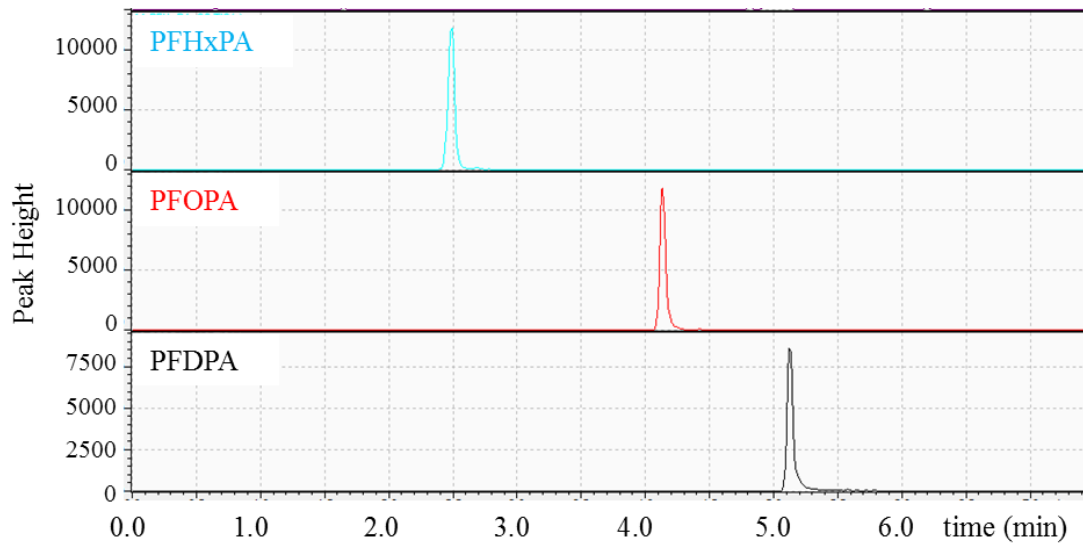


**Figure 3.4 LC-MS/MS chromatograms for PFPA**

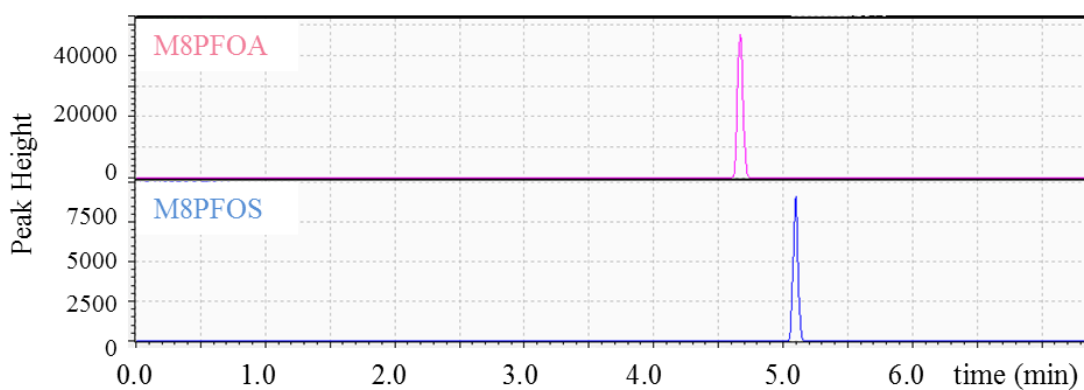


**Figure 3.5 LC-MS/MS chromatograms for internal standards**

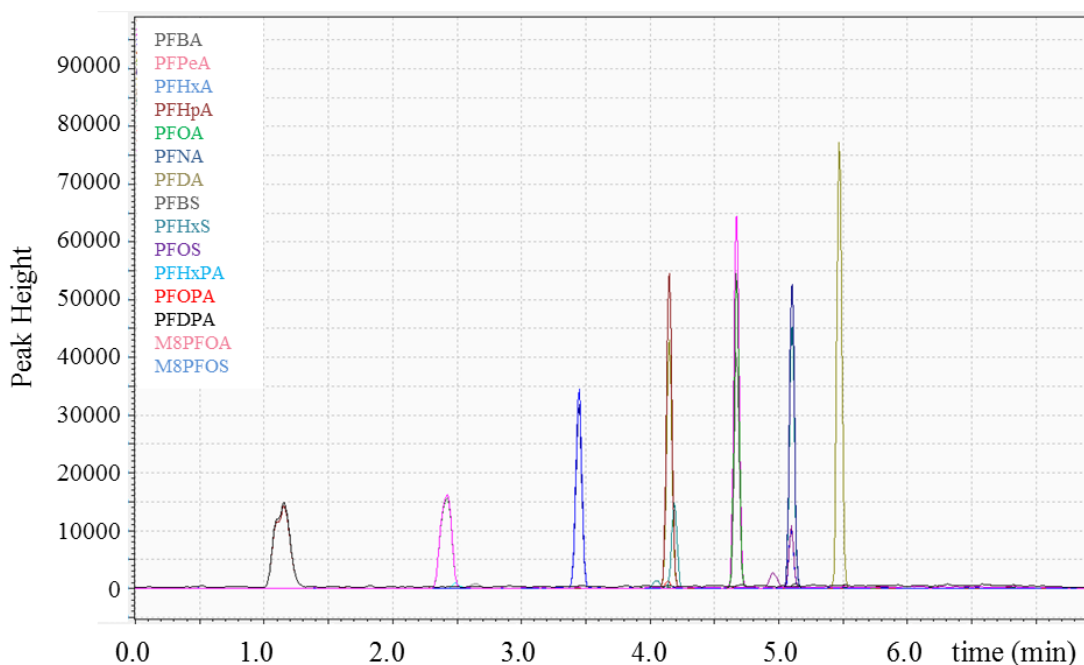


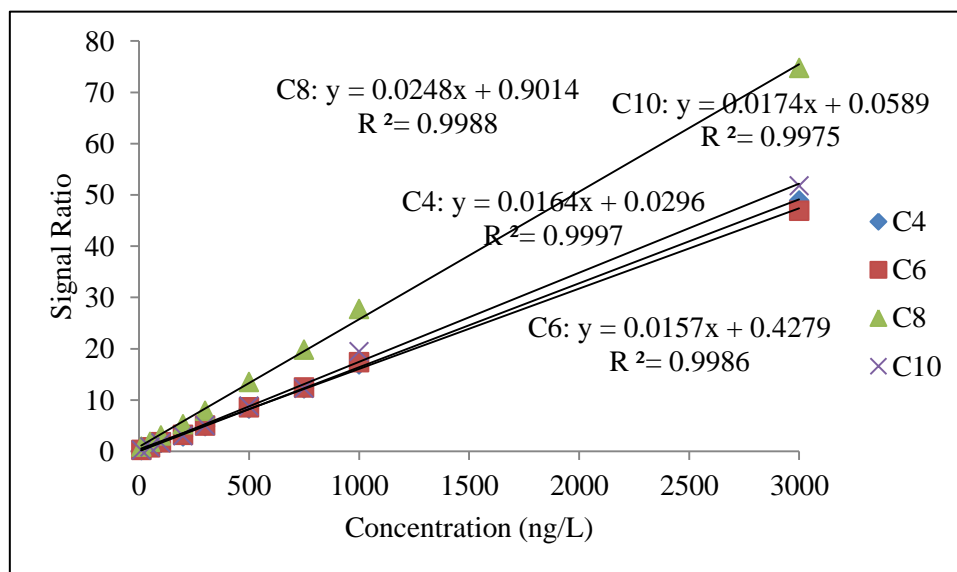
**Figure 3.6 LC-MS/MS chromatogram of all target PFCs and internal standards**

### 3.3.3 Quality Assurance/Quality Control (QA/QC)

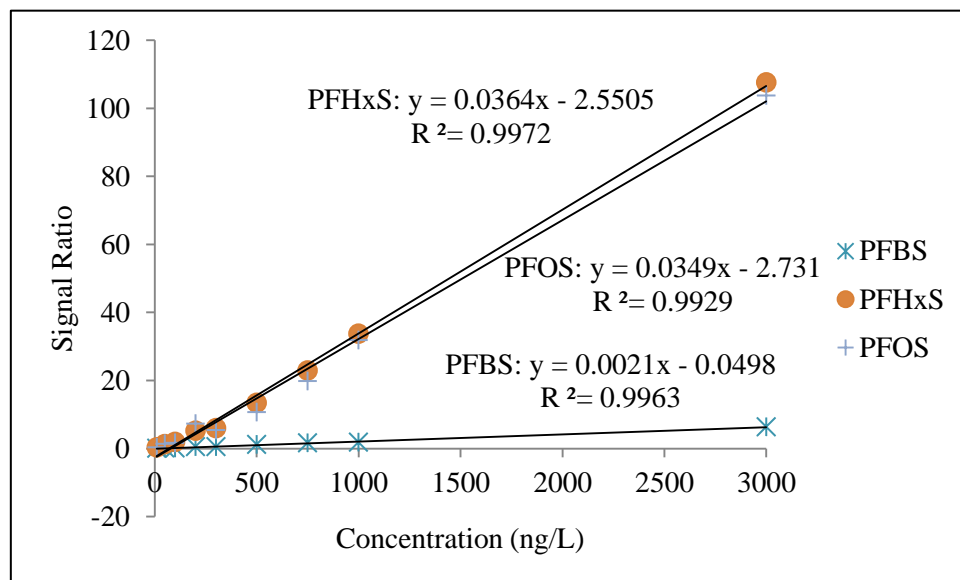
#### 3.3.3.1 Calibration curves

Figure 3.7, 3.8, and 3.9 show representative calibration curves of PFCAs, PFSAs, and PFPAs. The coefficients of determination ( $R^2$ ) for all compounds were larger than

0.99, which proved that the observed outcomes were replicated well by the linear regression model. Except for PFBS, PFCs with same functional group showed similar trend of calibration curves; however, PFBS had much lower peak area or signal ratio compared to the other PFSA. Figure 3.10 showed the peak area responses of eight replicates of the two internal standards. The results indicated that the two internal standards had good reproducibility especially for the M8PFOS.



**Figure 3.7 Representative calibration curves of PFCAs**



**Figure 3.8 Calibration curves of PFSA**



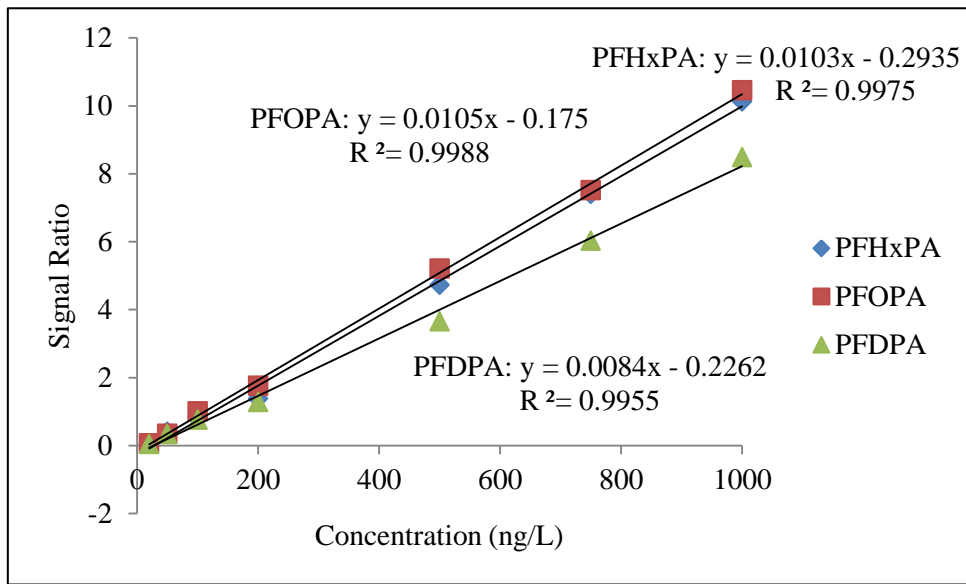


Figure 3.9 Calibration curves of PFPAs

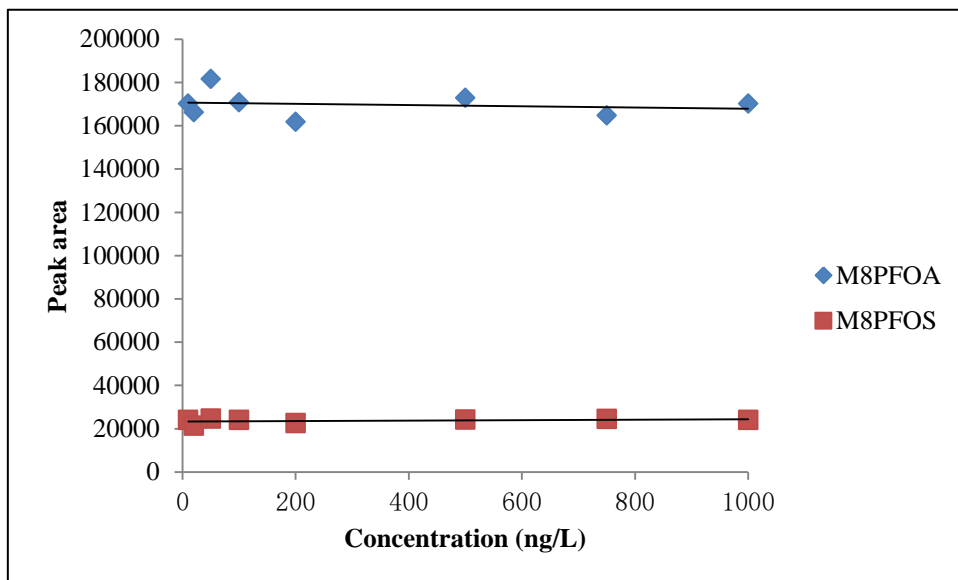


Figure 3.10 Peak areas of internal standards during calibration curves

### 3.3.3.2 MDLs and LOQs

The MDLs and LOQs of selected PFCs are shown in Table 3-3. All PFCs showed low MDLs. Three PFPAs had similar MDLs which are around 5 ng/L. Compared to PFPAs, PFCAs and PFSAs had even lower MDLs around 1 ng/L or less. The short chain PFCs like PFBA and PFBS had relative higher MDLs compared to long chain

PFCs. The low MDLs and LOQs demonstrate successful method development in that the target PFCs can be quantified in trace concentrations.

**Table 3-3 MDLs and LOQs for target PFCs**

<b>PFCs</b>	<b>MDL (ng/L)</b>	<b>LOQ (ng/L)</b>
<b>PFBA</b>	0.8	2.6
<b>PFPeA</b>	0.8	2.4
<b>PFHxA</b>	0.1	0.3
<b>PFCAs</b> <b>PFHpA</b>	0.1	0.3
<b>PFOA</b>	0.1	0.2
<b>PFNA</b>	0.1	0.2
<b>PFDA</b>	0.1	0.4
<b>PFBS</b>	1.0	3.3
<b>PFSAs</b> <b>PFHxS</b>	0.1	0.3
<b>PFOS</b>	0.1	0.3
<b>PFHxPA</b>	5.0	16
<b>PFPAs</b> <b>PFOPA</b>	5.1	16
<b>PFDPA</b>	5.1	16

### 3.3.3.3 Method recovery

Before the method recoveries were detected, the recoveries of the SPE process were tested in the preliminary experiments. The results of the preliminary experiments revealed that all target PFCAs and PFSAs had percentage recoveries from 98.6% to 99.9% during the SPE process. It revealed that the Oasis WAX cartridges had satisfied extraction performance for all target PFCs and the results further confirmed the recovery data presented by Taniyasu et al. (2005).

The method recovery results for target PFCs are summarized in Table 3-4. In ultrapure water, the percentage recoveries ranged from 95.3% to 106.1%; while it

ranged from 92.0% to 106.8% in surface water. The results between ultrapure water and surface water were quite similar and all showed satisfactory recovery results. The relative standard deviations for PFCAs were relatively low compared to PFSA and PFPAs. PFPAs had RSDs higher than 10% which were consistent with the MDL and repeatability results. The PFBS also showed poor recovery and high RSD compared to the other PFCs. The repeatability results shown in Appendix A Table A-1 also verified the practicability and reliability.

**Table 3-4 Percentage recoveries of PFCs (c = 100 ng/L, n = 7)**

PFCs	Ultrapure water		Surface water		
	% Recovery	% RSD	% Recovery	% RSD	
<b>PFCAs</b>	<b>PFBA</b>	95.7%	6.3%	98.5%	6.4%
	<b>PFPeA</b>	102.5%	4.7%	92.7%	8.2%
	<b>PFHxA</b>	101.8%	5.3%	98.9%	3.5%
	<b>PFHpA</b>	100.2%	7.5%	94.5%	6.2%
	<b>PFOA</b>	97.0%	2.5%	92.8%	7.6%
	<b>PFNA</b>	102.2%	5.8%	93.5%	8.5%
	<b>PFDA</b>	105.5%	6.0%	96.3%	6.2%
<b>PFSA</b>	<b>PFBS</b>	106.1%	10.5%	105.3%	10.2%
	<b>PFHxS</b>	96.5%	8.9%	95.8%	8.1%
	<b>PFOS</b>	104.0%	4.9%	100.8%	10.1%
<b>PFPAs</b>	<b>PFHxPA</b>	98.8%	11.6%	92.0%	11.5%
	<b>PFOPA</b>	95.3%	13.9%	98.3%	12.1%
	<b>PFDPA</b>	105.3%	13.1%	106.8%	14.6%

### **3.4 Method Summary**

The analytical method for target PFCs were thoroughly established in this chapter. This method was applied throughout the entire research project to determine the concentrations of target PFCs in both ultrapure and surface water. To briefly summarize the method: as internal standards, 200 ng/L M8PFOA and M8PFOS were added to 500 ml water sample. Oasis WAX cartridges (150 mg adsorbent per cartridge) were used in the SPE process. Through the conditioning, loading, washing, and eluting processes, the 500 ml water sample was concentrated to a 5 ml methanol sample. The sample was then introduced to the Shimadzu 8030 LC-MS/MS. Poroshell SB C18 column was used to separate the PFCs with the mobile phases of 5 mM ammonium acetate in Milli-Q water and methanol.

It was reported that glass was able to irreversibly adsorb PFCs (Martin et al., 2004). Therefore, polypropylene containers or labwares were used for all PFC solutions or samples whenever it was possible. Teflon based labware was avoided throughout the entire study to prevent potential contamination. New PFCs standard solutions were prepared every 6 month, and were stored in polypropylene bottles in the fridge at 4 °C in darkness. PFCs samples were processed immediately, or were preserved by storing them in polypropylene bottles or vials in the fridge at 4 °C in darkness for no more than 10 days and were then processed and detected. The internal standards were applied throughout all PFCs analyses.

### **3.5 Conclusions**

An LC-MS/MS analytical method using SPE has been successfully established to determine 13 PFASs with three different functional groups in water at trace concentrations. The main findings are summarized as follows:

(1) The target PFCs can be analyzed in both ultrapure and surface water using the developed LC-MS/MS method at trace concentrations (low ng/L to µg/L).

(2) Both LC conditions and MRM parameters were optimized to accommodate the detection and quantification of all target PFCs. The method separates most target PFCs with nice peak shapes, has stable the retention times, and achieves high sensitivities.

(3) The method reached low MDLs for all three types of PFCs. PFCAs and PFSAAs had MDLs of 1 ng/L or less; while the MDLs for PFPAs were around 5 ng/L. The recoveries of PFCs, the repeatability results, and the calibration curves proved and validated the reliability of the method.

(4) Compared to PFCAs and PFSAAs, PFPAs had both higher MDLs and higher relative standard deviations of the method reproducibility. Considering this, as well as some other reasons, such as the relatively low concentrations of PFPAs in the environment and the unavailability of pure PFPAs without organic solutions, PFPAs were not selected as target compounds in the ion exchange and adsorption studies in the following chapters.

The method has been applied to study the removal of PFCAs and PFSAAs in drinking water treatment using both ion exchange and adsorption processes.

## Chapter 4

# PFCAs and PFSA Removal during Drinking Water Treatment by Ion Exchange Resins: Removal Kinetics and Isotherms Studies

### Summary

The removal potentials of PFCAs and PFSAs from both ultrapure water and surface water were evaluated using five anion exchange resins. Bottle point method was applied for both adsorption kinetics and isotherms experiments. PFC concentrations were determined using LC-MS/MS with the method developed in Chapter 3. Pseudo-second-order model was applied to calculate relevant kinetics parameters. Freundlich model was used to predict isotherms parameters for anion exchange resins. The impact factors of PFCs adsorption by anion exchange resins including anion exchange resins properties, PFC chain length, and PFC functional groups were investigated based on the experimental data. The effect of natural organic matters in PFCs adsorption by anion exchange resins was studied using LC-OCD and other analysis. The effect of inorganic anions, especially sulfate and nitrate, in PFCs adsorption was investigated by adding different amounts of inorganic anions in anion exchange resin adsorption samples. The results showed that commercially available anion exchange resins had good removal efficiency for all selected PFCs in ultrapure water. In surface water, the PFC removal efficiency decreased. PFSAs showed higher removal compared to PFCAs. The reduction of PFC removal in surface water is likely influenced by competition with NOM and inorganic anions. The existence of the inorganic ions, especially sulfate, could decrease the removal of short chain PFCAs when using ion exchange resins.

## 4.1 Introduction

As a type of commonly used chemicals, perfluorinated compounds have been detected in all kinds of environmental samples, including drinking waters and their sources (Rumsby et al., 2009; ATSDR, 2009). PFCAs and PFSAAs are the two main types of PFCs applied in industry and detected in the environment (Brooke et al., 2004). Among all the PFCs, PFOA and PFOS are the two most ubiquitous ones detected in the environment, especially in water sources and drinking water systems (Zareitalabad et al., 2013). Both of them have been included in the USEPA's third Contaminant Candidate List (CCL3) (USEPA, 2009a). In the new finalized USEPA CCL4, they have also been included as two of the 97 chemicals of interest (USEPA, 2016c). As strong acids, target PFCs including both PFCAs and PFSAAs were present in the form of anions in neutral pH or in the pH range of both ultrapure and natural water (Wang et al., 2011; Ahrens et al., 2012).

Due to the potential risk of PFCs in drinking water system, studies have started to focus on different treatment technologies to remove PFCs. The GAC filter is an effective treatment method for PFC removal. Takagi et al. (2011) reported that fresh new GAC could reach up to nearly 100% PFOA and PFOS removal. Other studies have shown that the treatment efficiency of GAC filters for PFOA and PFOS with a low influent concentration of around 5 ng/L is about 50% (Eschauzier et al., 2012; Flores et al., 2013). Another promising method for PFC removal are high pressure membranes including nanofiltration (NF) and reverse osmosis (RO). RO can completely remove PFOA and PFOS including low concentration of 2 ng/L (Flores et al., 2013). Other conventional drinking water treatment processes are not really effective for PFC removal. Coagulation/flocculation/sedimentation is not useful to remove PFOA and PFOS (Eschauzier et al., 2012). Sand filtration can only remove about 10% PFAAs (Flores et al., 2013). Ozonation as well as chlorination are not effective to remove PFAAs (Flores et al., 2013; Takagi et al., 2011).

Due to their low pKa values PFCs such as PFOS and PFOA become anionic at pH values typical for drinking water and its sources, and are thus removable by anion exchange resins. Some studies investigated the influence of polymer matrix, porosity, and functional groups on PFOS removal (Deng et al., 2010). It revealed that anion exchange resins can be effective for PFC removal and it was postulated that the hydrophilic matrix lead to faster sorption. The adsorption and regeneration performance of ion exchange resins varies a lot depending on the type of the resins. The removal of PFBS and PFOS by Amberlite IRA-458 ion exchange resins reached equilibrium much faster compared to GAC, and the uptake of the PFCs was influenced by both hydrophobic adsorption and ion exchange effects (Carter & Farrell, 2010). In another study, PFA300 anion exchange resins reached the high PFOS adsorption capacity of 455 mg/g (Chularueangksorn et al., 2013). IRA67 anion exchange resin was applied for PFOA and PFOS removal with short equilibrium time (2 h) and high removal efficiencies (> 98%) at mg/L level (Yao et al., 2014). Rahman (2014) used two anion exchange resins, A500 and A860, to test their performance on removing PFCAs in ultrapure and natural water. His results showed that the removal efficiency of A860 resin significantly decreased in natural water compared to that of A500. The mechanisms of both ion exchange and hydrophobicity adsorption are involved in the PFCs removal by anion exchange resins (Gao et al., 2017; Schuricht et al., 2017; Zaggia et al., 2016). In general, ion exchange could be a satisfied treatment method for PFCs removal.

To investigate the effects and the impact factors of the anion exchange resins on PFCs removal, five commercially available anion exchange resins with different properties were chosen to test their removal performance of four PFCAs and three PFSAs. Firstly, the PFC removal kinetics of all five resins in both ultrapure water and Grand River water in batch were studied using bottle point method. Based on the kinetics results, TAN-1 and PFA444 were selected as target anion exchange resins in the removal kinetics study in Lake Erie water, the isotherms study in ultrapure water,



and the study of inorganic anions effects. During these experiments, the effects of different physical and chemical properties of target PFCs, as well as the effects of the characteristics of selected anion exchange resins were examined. The influence of the NOM fouling and the impacts of inorganic anions on PFCs removal in the anion exchange process were also examined.

## 4.2 Materials and Methods

### 4.2.1 Target Compounds and Water

Four PFCAs and three PFSA s including PFBA, PFH<sub>x</sub>A, PFOA, PFDA, PFBS, PFH<sub>x</sub>S, and PFOS were purchased from Sigma-Aldrich (WI, USA). Their purity and carbon chain length information are listed in Table 4-1. More detailed information about physical and chemical properties of the selected PFCs was provided in Table 2-2 in Chapter 2. Amount of 30 mg of each target PFC was weighed out and all seven PFCs were dissolved in 1 L of high purity water to make mixture PFCs stock solutions. New stock solutions were prepared every 6 month, and were preserved in polypropylene bottles in fridge at 4 °C. The concentration of each target PFC spiked in samples was 3.0 µg/L in all tests in this chapter.

**Table 4-1 Target PFCs selected in the ion exchange experiments**

<b>PFCs with different functional groups</b>	<b>Name</b>	<b>Carbon</b>	<b>Purity (no less than, % )</b>
<b>PFCAs (Perfluoroalkyl carboxylic acids)</b>	PFBA (C4)	4	99.5
	PFH <sub>x</sub> A (C6)	6	97
	PFOA (C8)	8	99.2
	PFDA (C10)	10	98
<b>PFSA s (Perfluoralkane sulfonic acids)</b>	PFBS	4	97
	PFH <sub>x</sub> S	6	98
	PFOS	8	98

Ultrapure water was generated from a Millipore Milli-Q<sup>®</sup> UV PLUS water system (MA, USA). Surface water samples from two sources, Grand River and Lake Erie, were used in this study. Grand River water (GRW) was collected from the raw water intake of Mannheim Water Treatment Plant (Region of Waterloo, ON, Canada) on October 7, 2015. Lake Erie water (LEW) was collected from the raw water intake of Elgin Area Water Treatment Plant (Elgin, ON, Canada) on July 10, 2016. Surface water was filtered using 0.45 µm PES filters (Pall Corporation, NY, USA) before using to remove suspended solids. Table 4-2 lists the water quality parameters of Grand River and Lake Erie water prior to filtration. No pH adjustment was done for all water samples in the study.

**Table 4-2 Grand River and Lake Erie water quality parameters**

	<b>pH</b>	<b>Turbidity (NTU)</b>	<b>DOC (mg C/L)</b>	<b>Cl<sup>-</sup> (mg /L)</b>	<b>SO<sub>4</sub><sup>-</sup> (mg/L)</b>	<b>NO<sub>3</sub><sup>-</sup> (mg/L)</b>
GRW	<b>7.8</b>	4.6	5.6	66.1	27.2	8.0
LEW	<b>7.8</b>	0.5	2.4	24.2	11.4	3.5

#### **4.2.2 Ion Exchange Resins**

Five anion exchange resins including Purolite<sup>®</sup> A444, A500plus, A555, A502p, and Purofine<sup>®</sup> PFA444 were obtained directly from Purolite Corporation (PA, USA). Anion exchange resin DOWEX<sup>®</sup> TAN-1 was purchased from Dow Chemical (MI, USA). The properties of all the resins are listed in Table 4-3. A GAC commonly used in filtration studies Filtrasorb 400<sup>®</sup> (F400) was acquired from Calgon Carbon (PA, USA) and was compared to the anion exchange resins.

To determine the moisture retention of the resins, around 1000 mg resin of each type was measured and dried in oven at 105 °C for 24 hours. The moisture retention was calculated through the following equation:

$$\text{Moisture Retention} = \frac{M_0 - M_{\text{dry}}}{M_0} \times 100\% \quad (\text{Equation 4.1})$$

Where  $M_0$  is the initial weight of the resin;  $M_{\text{dry}}$  is the weight of the resin after drying.

The pore size characterization of all anion exchange resins was examined by Autosorb<sup>TM</sup> iQ automated gas sorption analyzer (Quantachrome, FL, USA). The data of the specific surface area, the pore size distribution and pore volume were provided by the iQWin software, which were calculated based on the Brunauer-Emmett-Teller (BET) adsorption model and the density functional theory (DFT).

The point of zero charge ( $\text{pH}_{\text{pzc}}$ ) of all the resins was determined based on the method established by Summers (1986). The pH values of a series of 20 mL of 0.1 M sodium chloride were adjusted in sealed Erlenmeyer flasks with 0.1 M hydrochloric acid or 0.1 M sodium hydroxide to different pH values between 2 and 12. After measuring the initial pH, 100 mg (dry weight) of ion exchange resins were added to each of the flasks. The flasks were placed on orbital shakers at 120 rpm at room temperature for 24 hours. The final pH values were then measured. The final pH of the solutions was plotted against the initial pH. The crossing point of the resulting curve and the line of the initial pH is equal to the final pH was measured as the point of zero charge, and the  $\text{pH}_{\text{pzc}}$  was determined as the pH of the crossing point.

#### **4.2.3 Kinetics and Isotherms Tests**

The bottle point technique was used for both adsorption kinetics and isotherms of anion exchange resins. Briefly, polypropylene opaque bottles (VWR, PA, USA) filled with 1 L PFC samples and anion exchange resins were placed on an orbital shaker with a speed of 150 rotations per minute at room temperature. Single or mixture PFCs were spiked at a concentration of 3.0  $\mu\text{g/L}$  for each PFC in each sample. A separate bottle was needed for each data point i.e. for each contact time or adsorbent dose.

After the preset contact time, the bottle was taken off the shaker and the sample was then analyzed using SPE and LC-MS/MS as described in Chapter 3.

To ensure that the PFC concentrations and the pH were uniform in all bottles of the same batch, a large polypropylene container was used to prepare a spiked batch before dispensing aliquots into the sample bottles. Ultrapure water or filtered natural water which was enough for a whole batch of experiments was filled in the large container. The calculated amount of single or mixture PFCs were then spiked in the large water batch to reach the PFC concentration of 3.0  $\mu\text{g/L}$  for each solute. After the PFC containing solution was stirred and well-mixed, the accurate initial concentrations of the PFCs in this batch sample were analyzed and quantified. Ultrapure or surface water blanks, PFCs spiked ultrapure or surface water without anion exchange resins, and ultrapure or surface water containing only anion exchange resins were also prepared and processed with the other samples in the experiments. The concentrations of PFCs spiked ultrapure or surface water without anion exchange resins were monitored as reference.

For adsorption kinetics experiments, a screening study of 5 anion exchange resins (A444, A500+, A555, PFA444, and TAN-1) was conducted in both ultrapure water and Grand River water to test their PFC adsorption performance. Anion exchange resins with good PFCs performance were selected and applied in further studies. The PFA444 and TAN-1 resins were then applied in the adsorption kinetics experiments in Lake Erie water. In all anion exchange resins kinetics experiments, an aliquot of resins equivalent to 50 mg dry weight was added to each of the 1 L bottles (i.e. one bottle per contact time). Seven target PFCs were spiked as a mixture at concentration of 3.0  $\mu\text{g/L}$  for each PFC in each sample. The samples were taken off and analyzed at corresponding contact times until the equilibrium was reached.

For adsorption isotherm experiments, PFA444 and TAN-1 resins were selected based on the results of the kinetics screening study. Isotherm resin dosages ranged

from 5mg/L to 80mg/L (dry weight). Four PFCs including PFBA, PFOS, PFBS, and PFOS were selected as target PFCs and spiked separately as single solute in each sample with the initial concentration of 3.0 µg/L in adsorption isotherms experiments. Samples were placed on the shaker until the equilibrium time which was determined in the kinetics experiments (48 hours for anion exchange resins in this study). PFC concentrations of the samples after equilibrium time with different resin doses were quantified to determine the adsorption isotherms.

Besides the adsorption experiments of the 5 anion exchange resins (A444, A500+, A555, PFA444, and TAN-1), a GAC (F400) often used in research studies and a new anion exchange resin replacement product (A502p) were also tested in both kinetics and isotherms studies to compare with the other 5 resins. The methods and the results of F400 and A502p are listed in Appendix B and C.

#### **4.2.4 Testing Effects of Inorganic Anions on Ion Exchange Performance**

The influence of inorganic anions on PFC removal in the anion exchange process was studied. As two major inorganic anions existing in surface water, sulfate and nitrate were selected as research focus in this study. The bottle point method used for adsorption kinetics was applied for the inorganic anions influence tests. According to the concentrations of sulfate and nitrate in surface water, different amounts of sodium sulfate and sodium nitrate were added into separate 1 L plastic bottles filled with ultrapure water. The concentrations of sulfate were controlled to be 0, 10, and 30 mg/L (calculated as  $SO_4^{2-}$ ) respectively; and the concentrations of nitrate were 0, 5, and 10 mg/L (calculated as  $NO_3^-$ ). PFCs were spiked in 1 L ultrapure water sample as a mixture with the initial concentration of 3.0 µg/L for each compound. TAN-1 and PFA444 resins were selected based on their superior PFC removal performance in adsorption kinetics experiments, and the resin doses were kept as 50 mg/L (calculated as dry weight) throughout the entire tests. After resins were added to the 1 L bottles

with ultrapure water containing target PFCs and certain amount of sulfate or nitrate, the bottles were placed on a shaker at a speed of 150 rotations per minute. The contact times for each set were 0, 6, 24, and 48 hours. One single bottle had to be prepared for each data point i.e. each contact time.

#### 4.2.5 Analyses

All target PFCs were analyzed with a Shimadzu 8030 LC-MS/MS. An SPE process was conducted before the LC-MS/MS analysis. The established analytical method was described in detail in Chapter 3. Three injections were analyzed by LC-MS for each PFC sample. A typical example showing the average and the standard deviation of 3 repeat injections is shown in Fig. 4.1(F). Otherwise, average values are reported in all the results. Error associated with the duplication of an experiment is illustrated in Fig. 4.1(G).

The concentrations of the anions including chloride, sulfate and nitrate in natural water were analyzed by Dionex ICS-1100 ion chromatography (IC) system (Thermo Scientific, MA, USA). The Dionex IonPax<sup>TM</sup> AS4A-SC analytical column (4 × 250 mm) was applied with the eluents of 1.8 mM Na<sub>2</sub>CO<sub>3</sub> and 1.7 mM NaHCO<sub>3</sub>. The Dionex anion self-regeneration suppressor (Dionex ASRSTM 300) was used for electrolytically regenerated suppression.

Dissolved organic carbon (DOC) was determined with Aurora 1030 TOC analyzer (OI Analytical, TX, USA). DOC samples were filtered using 0.45 μm PES filters (Pall Corporation, NY, USA). Turbidity of all water samples was measured by Hach 2100P Turbidimeter (CO, USA). Water sample pH was monitored using ORION Benchtop 420A pH meter (MA, USA).

The natural organic matter (NOM) composition was analyzed using a liquid chromatography – organic carbon detector (LC-OCD) (DOC-Labor Dr. Huber,

Karlsruhe, Germany). LC-OCD is a size exclusion instrument which separates NOM into different fractions including biopolymers, humic substances, building blocks, low molecular weight (LMW) acids, and LMW neutrals (Huber et al., 2011).

**Table 4-3 Anion exchange resin properties**

Resin	Polymer Structure (polystyrene) *	Functional Group (Type of Quaternary Ammonium) *	Total Capacity (eq/l) *	Moisture Retention (%) **	pHpzc	Particle Size ( $\mu\text{m}$ ) *	BET Surface Area ( $\text{m}^2/\text{g}$ )	Pore Volume ( $\times 10^{-3} \text{ cm}^3/\text{g}$ )	Pore size distribution ( $\times 10^{-3} \text{ cm}^3/\text{g}$ )		
									< 0.8 nm	0.8-2 nm	> 2 nm
<b>PFA444</b>	Gel	Type I	1.1	55.8	6.3	$570 \pm 50$	0.423	2.71	0	0	2.71
<b>A444</b>	Gel	Type I	1.1	53.4	7.8	300-1200	0.158	0.09	0.034	0.029	0.027
<b>A555</b>	Macroporous	Type III	1.1	51.6	7.5	300-1200	2.402	5.04	0	0.03	5.01
<b>A500+</b>	Macroporous	Type I	1.15	61.8	7.2	300-1200	11.980	17.47	0.19	2.16	15.12
<b>TAN-1</b>	Macroporous	Type I	0.7	66.9	7.4	300-1200	0.975	0.38	0.06	0.28	0.04
<b>A502p</b>	Macroporous	Type I	0.85	65.0	7.5	300-1200	5.443	8.30	0.52	0.20	7.58

\* Data were provided by the manufacturers; \*\* moisture content was determined by drying anion exchange resins in oven at 105 °C for 24 h.



## 4.3 Results and Discussion

### 4.3.1 Anion Exchange Resins Properties

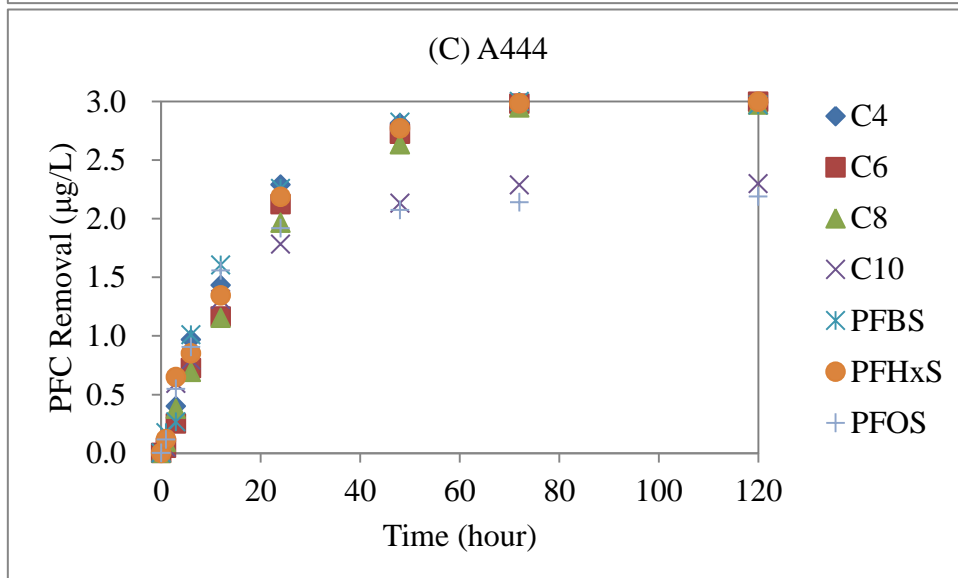
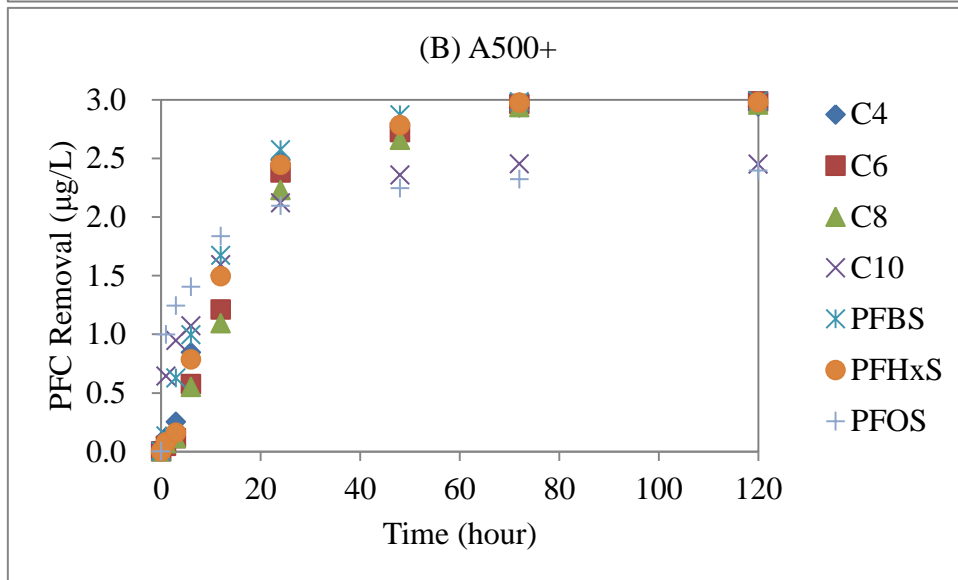
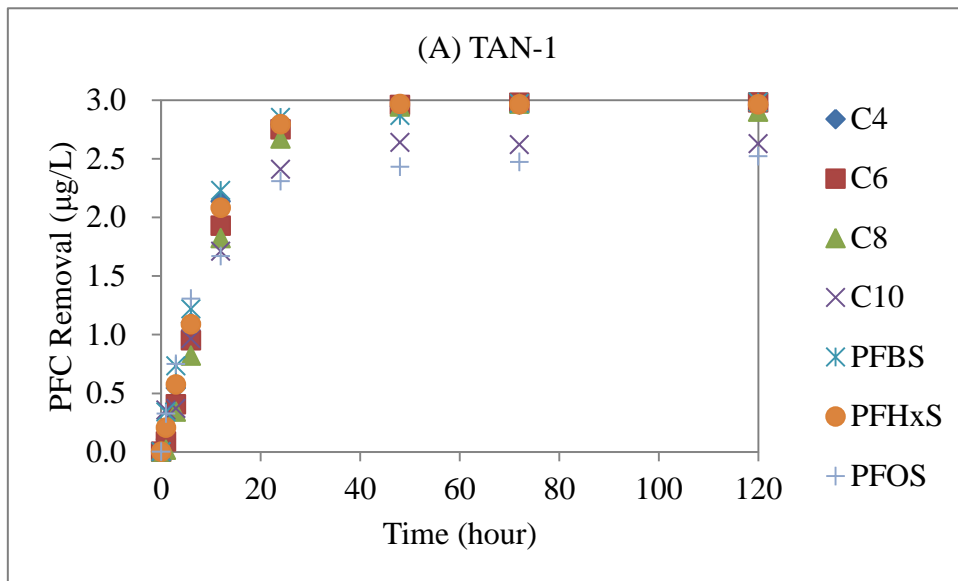
Properties of the selected anion exchange resins including polymer structure, functional groups, total capacity, moisture retention, point of zero charge, particle size, surface area and pore size distribution are presented in Table 4-3. For polymer structure, PFA444 and A444 were selected as gel resins which have irregular pores between the polymer chains; while all the other resins were macroporous resins which are fabricated with discrete macro pores in the beads. The structures of all selected resins are cross-linked polystyrene with quaternary ammonium functional groups, because a previous study has shown that polystyrene resins had better PFCs adsorption performance compared with polyacrylic resins (Rahman, 2014). Different from all the other resins, A555 is the only resin with Type III quaternary ammonium functional group. Type III resins are composed with water based acrylic and water based epoxy dispersion; while type I resins are liquid epoxy resins with water based amine. Compared to type I resins, type III resins are designed to reach a higher regeneration performance. Total capacities of the PFA444, A444, and A555 resins are all 1.1 eq/l. A500+ resin has the largest capacity of 1.15 eq/l, and the TAN-1 resin has the lowest capacity of 0.7 eq/l. Moisture retention of the resins ranges from 51.6% to 66.9%, and pH<sub>pzc</sub> ranges from 6.3 to 7.8. All resins have the same particle size in the range of 300-1200  $\mu\text{m}$  with the only exception of the PFA444 resin which has more uniform particle size of  $570 \pm 50 \mu\text{m}$ .

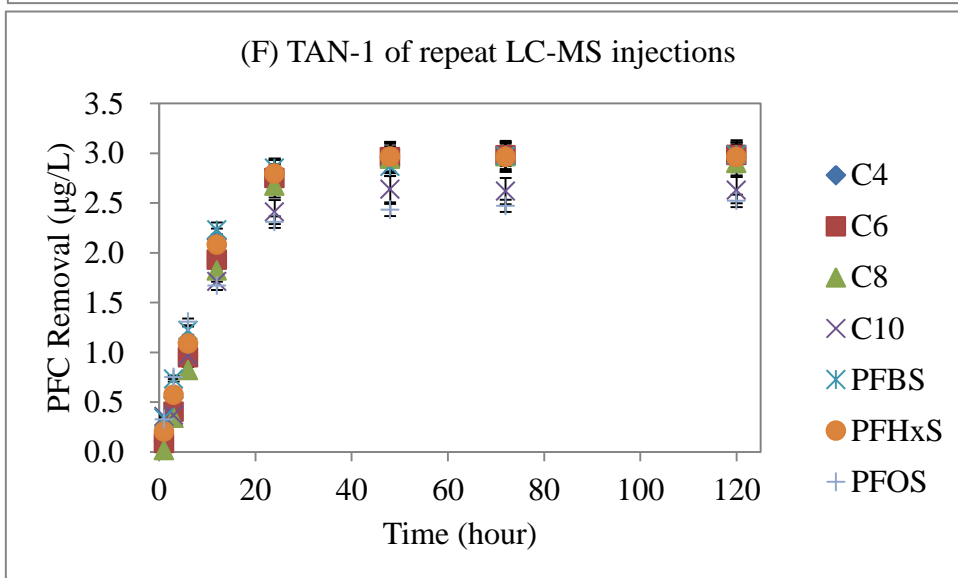
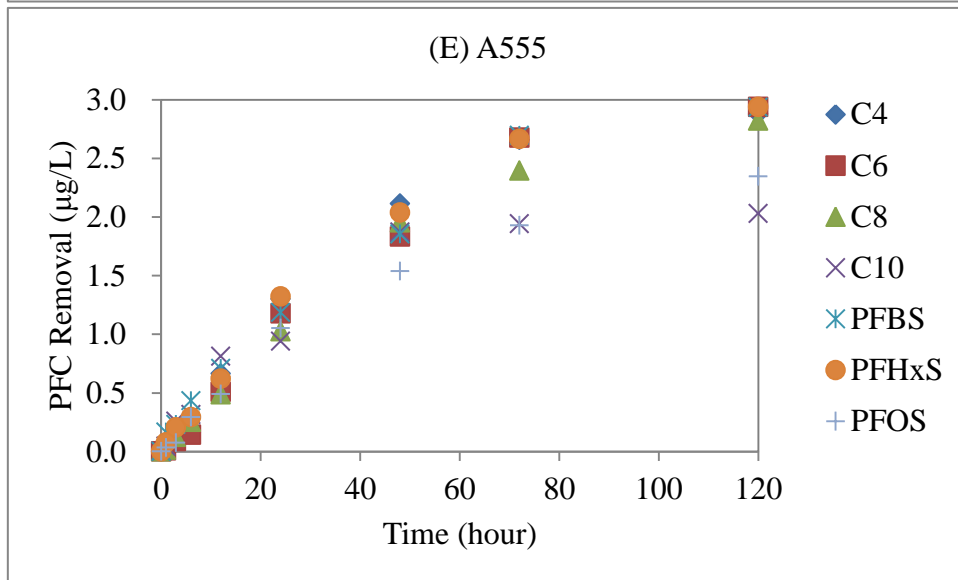
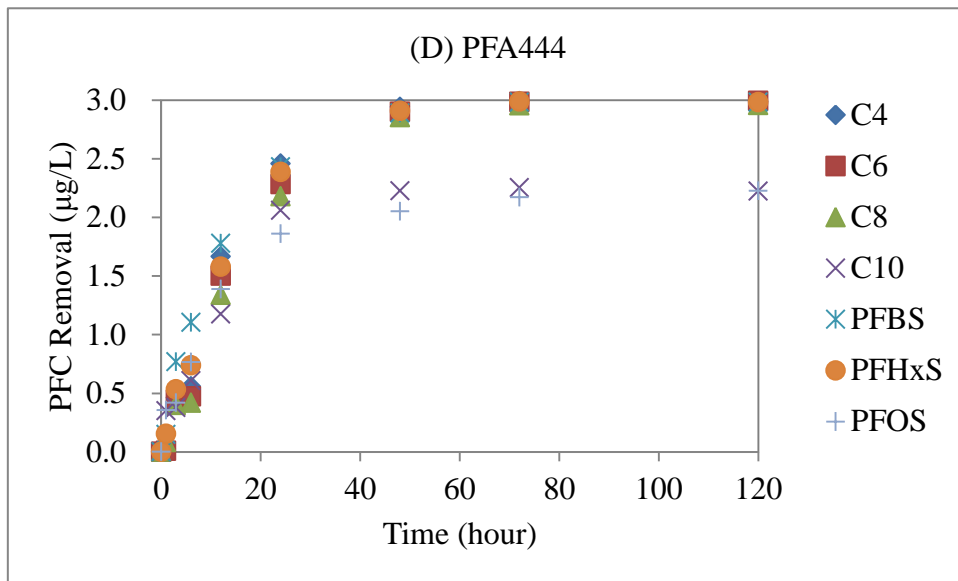
The BET surface area and pore size distribution results demonstrate the structures of the resins which also imply the adsorption performance. The external surface area of anion exchange resin can be calculated to be  $0.01 \text{ m}^2/\text{g}$  if  $600 \mu\text{m}$  is used as the diameter of the resin. The BET surface areas of all target anion exchange resins were much larger than the estimated external surface areas of the resins. From all the selected resins, A500+ has both the largest BET surface area ( $11.980 \text{ m}^2/\text{g}$ ) and the

largest pore volume ( $17.47 \times 10^{-3} \text{ cm}^3/\text{g}$ ). PFA444, A444, and TAN-1 resins present low pore volumes as well as surface areas which are lower than  $1 \text{ m}^2/\text{g}$ . Two gel resins have relative lower surface areas and pore volumes. Between the two gel resins, the PFA444 resin which has more uniform particle size did not show any micropores (pore size  $< 2 \text{ nm}$ ); while the pore size of the A444 resin equally distributes in the ranges of primary micropores ( $< 0.8 \text{ nm}$ , Rouquerol et al., 1994), secondary micropores (0.8-2 nm), and mesopores (2-50 nm). For the macroporous resins, A555, A500+, and A502p resins have more than 85% pores in the range of mesopores and macropores ( $> 50 \text{ nm}$ ). Although TAN-1 resin has low BET surface area of  $0.975 \text{ m}^2/\text{g}$  and low pore volume of  $3.8 \times 10^{-4} \text{ cm}^3/\text{g}$ , it has around 74% pores in the range of secondary micropores. The molecular sizes of PFCAs and PFSA were calculated to be in the range of  $6.2 \text{ \AA}$  and  $8.0 \text{ \AA}$ , using the Molinspiration interactive services (Molinspiration Cheminformatics, Slovak). The estimate molecular sizes of PFCs indicate that pores in the secondary micropore range (0.8-2 nm) and mesopore range would fit the PFC molecules well. Pores in the higher primary micropore range might also be relevant for adsorption of some of the smaller PFCs. As a common type of GAC, F400 has a large surface area of  $963 \text{ m}^2/\text{g}$  and pore volume of  $0.5 \text{ cm}^3/\text{g}$  (Vlad, 2015). Compared to F400, the surface areas and pore volumes of anion exchange resins are several orders of magnitude smaller. More detailed results of the pore size distribution are shown in Appendix E.

### **4.3.2 Removal Kinetics and Capacities in Ultrapure Water**

#### **4.3.2.1 Adsorption kinetics in ultrapure water**





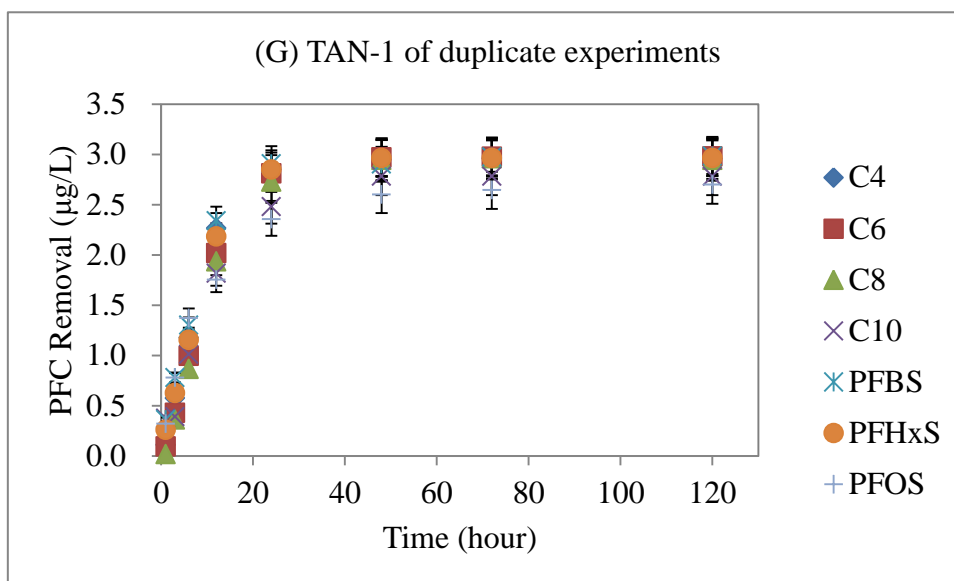


**Figure 4.1 PFCs adsorption kinetics of all five anion exchange resins in ultrapure water (initial PFC concentrations were 3 µg/L for each compound; resin doses were 50 mg/L as dry weight): (A) TAN-1; (B) A500+; (C) A444; (D) PFA444; (E) A555; (F) TAN-1 of repeat LC-MS injections (the error bars represent the standard deviations of three LC-MS injections); (G) TAN-1 of duplicate experiments (the error bars represent the high and low values of duplicate experiments).**

The results of PFCs adsorption kinetics of all five anion exchange resins in ultrapure water shown in Figure 4.1 indicated that all the anion exchange resins could reach very high removal of PFCs in ultrapure water. As long chain PFCs, PFDA (C10) and PFOS could reach maximum removals around 70%-90% for all the resins; while all the other PFCs could reach extremely high removals of more than 95%. A555 had the longest equilibrium time of more than 120 hours among all the anion exchange resins. Except for A555, all the other resins reached the equilibrium after 48 hours to 72 hours. Among all resins, TAN-1 had the best adsorption performance in ultrapure water with shortest equilibrium time of 48 hours and excellent PFC removal. All the resins showed good and similar maximum PFC percentage removal.

A pseudo-second order model has previously been used to describe the kinetics of activated carbon adsorption of a wide range of compounds (Ho & McKay, 1999).

While this type of adsorption model is effectively empirical (Worch, 2012), it can provide useful kinetic descriptors for comparatively evaluating different adsorbents. As per Ho and McKay (1999), the rate of adsorption in a batch process can be modeled as:

$$\frac{dq_t}{dt} = k_2(q_e - q_t)^2 \quad (\text{Equation 4.2})$$

where  $t$  is the number of days or hours elapsed,  $q_t$  ( $\mu\text{g}/\text{mg}$ ) is the amount of solute adsorbed at time  $t$ ,  $k_2$  is the rate constant of adsorption and  $q_e$  is the total amount of solute adsorbed at equilibrium.

Equation above can be integrated over time ( $t$ ) and amount adsorbed ( $q_t$ ) to yield:

$$q_t = \frac{q_e^2 k_2 t}{(1 + q_e k_2 t)} \quad (\text{Equation 4.3})$$

The above equation can be rearranged into a linear form as follows:

$$\frac{t}{q_t} = \frac{1}{k_2 q_e^2} + \frac{1}{q_e} t \quad (\text{Equation 4.4})$$

The kinetic data are plotted in this form and exhibit excellent linearity for all datasets as shown in Figure 4.2 as an example and similar figures in the Appendix D; furthermore, the model fits all results in  $R^2$  values greater than 0.95, indicating the pseudo-second order model described the data well as shown in Table 4-4. It should be noted that although the  $R^2$  values are high, there appears to be systematic errors observed from the trends in Figure 4.2 which indicates that the underlying mechanism implied by the pseudo-second order model is not completely representative of the adsorption system as observed in this study. To apply the best kinetics model for PFCs adsorption process, pseudo-first order model was also attempted. The  $R^2$  values calculated using pseudo-first order model were much lower compared to pseudo-second order model, which indicated pseudo-first order model could not fit the data well. Nevertheless, it is possible to use the parameters of the pseudo-second order model to provide a good approximate description which can be used to compare the kinetic behaviour of the different anion exchange resins in adsorbing PFCs.

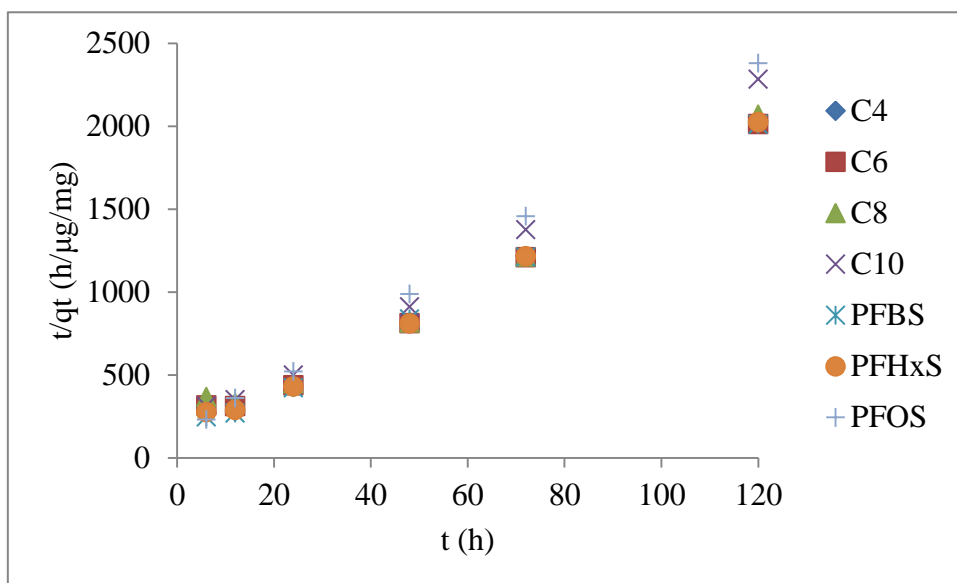


**Figure 4.2 Application of the pseudo-second-order model to the adsorption data of all target PFCs onto TAN-1 resin in ultrapure water (initial PFC concentrations were 3  $\mu\text{g/L}$  for each compound; resin doses were 50 mg/L as dry weight)**

Based on the Equation 4-4,  $t/q_t$  and  $t$  have a linear relation. Thus kinetics parameters  $k_2$  and  $q_e$  can be calculated by plotting  $t/q_t$  with  $t$ , and the  $R^2$  can be used to determine if the data fit the pseudo-second order model. Figure 4.2 showed the plotting of the pseudo-second-order model application of using TAN-1 resin for PFCs removal in ultrapure water. The plotting showed good linear relation of the kinetics parameters for all target PFCs, which signified that the PFCs adsorption kinetics data fit the pseudo-second-order model well. The kinetics data plotted for all target PFCs were quite close and could not be well separated, which indicated that all PFCs had similar pseudo-second-order model parameters. The application of pseudo-second-order model to the PFCs adsorption data for all the other anion exchange resins showed similar trends as TAN-1 resin. The detailed Pseudo-second-order model parameters for all anion exchange resins in ultrapure water were listed in Table 4-4. Linear regression was used to calculate the pseudo-second-order model parameters in this study; however, linear regression involves fitting a transformation of the original data. Since this transformation distorts

the variance structure of the original data, the parameter estimates may be less reliable than those obtained with non-linear regression of the original data. Because the purpose of calculating the kinetics parameters is to estimate relative PFC removal performance with the different resins, the limitations of using linear regression can be neglected in this case.

**Table 4-4 Pseudo-second-order model parameters of all target PFCs for all anion exchange resins in ultrapure water**

<b>Resins</b>	<b><math>k_2</math> (mg/<math>\mu</math>g/h)</b>	<b><math>q_e</math> (ng/mg)</b>	<b><math>q_{e, \text{exp}}</math> (ng/mg) *</b>	<b>Maximum removal (%)</b>	<b><math>R^2</math></b>
<b>PFBA</b>					
<b>TAN-1</b>	2.56	63.3	59.1	98.6	0.995
<b>A500+</b>	1.18	66.7	58.8	98.1	0.992
<b>A555</b>	0.18	90.1	57.6	96.0	0.964
<b>A444</b>	1.10	68.1	59.8	99.7	0.995
<b>PFA444</b>	1.20	67.8	59.7	99.5	0.989
<b>PFHxA</b>					
<b>TAN-1</b>	1.84	65.2	59.6	99.4	0.992
<b>A500+</b>	0.62	73.5	59.7	99.5	0.971
<b>A555</b>	0.08	118	58.8	98.0	0.866
<b>A444</b>	0.67	72.7	59.9	99.9	0.988
<b>PFA444</b>	0.97	69.4	59.9	99.8	0.990
<b>PFOA</b>					
<b>TAN-1</b>	1.63	64.6	58.0	96.7	0.986
<b>A500+</b>	0.53	74.7	59.1	98.6	0.970
<b>A555</b>	0.08	114	56.4	94.0	0.889
<b>A444</b>	0.61	72.9	59.4	99.0	0.990
<b>PFA444</b>	0.81	70.3	59.1	98.6	0.987



<b>PFDA</b>					
<b>TAN-1</b>	2.45	56.8	52.6	87.6	0.995
<b>A500+</b>	2.77	52.5	49.0	81.6	0.999
<b>A555</b>	0.66	52.0	40.6	67.6	0.956
<b>A444</b>	1.79	51.0	45.9	76.5	0.998
<b>PFA444</b>	1.85	50.1	44.5	74.1	0.987
<b>PFBS</b>					
<b>TAN-1</b>	2.84	63.1	59.7	99.4	0.997
<b>A500+</b>	1.49	66.2	59.8	99.7	0.995
<b>A555</b>	0.15	95.4	58.7	97.9	0.964
<b>A444</b>	1.29	66.7	59.4	99.0	0.996
<b>PFA444</b>	1.83	64.9	59.7	99.4	0.998
<b>PFHxS</b>					
<b>TAN-1</b>	2.45	63.6	59.3	98.8	0.995
<b>A500+</b>	1.03	68.5	59.6	99.4	0.990
<b>A555</b>	0.15	96.5	58.8	97.9	0.952
<b>A444</b>	0.89	69.8	59.9	99.9	0.994
<b>PFA444</b>	1.24	67.3	59.6	99.4	0.994
<b>PFOS</b>					
<b>TAN-1</b>	3.48	53.0	50.4	84.0	0.999
<b>A500+</b>	4.41	49.6	47.9	79.9	1.000
<b>A555</b>	0.19	75.6	46.9	78.2	0.976
<b>A444</b>	3.23	46.5	43.8	72.9	0.999
<b>PFA444</b>	1.99	48.9	44.5	74.2	0.997

\* Because A555 resin did not reach the equilibrium in the PFCs kinetics experiments,  $q_t$  ( $t=120$  hours) values were applied in Table 4-4 as  $q_{e, \text{exp}}$  values of A555 resins, with the assumption that PFCs removed by A555 resin were close to the equilibrium at 120 hours.

Table 4-4 showed Pseudo-second-order model parameters of all target PFCs for all anion exchange resins in ultrapure water. In Table 4-4, Pseudo-second-order model parameters including  $k_2$ ,  $q_e$ , and  $R^2$  were summarized as well as the experimental  $q_e$  ( $q_{e,exp}$ ) and maximum percentage removal.

The adsorption kinetics of PFHxA and PFOA using A555 resin had relative low  $R^2$  values less than 0.9. All the other adsorption kinetics reached high  $R^2$  values greater than 0.95, which meant that most adsorption kinetics data fit the pseudo-second-order model well. Among all the anion exchange resins, TAN-1 resin had high  $k_2$  (1.63-3.48 mg/ $\mu$ g/h) values for all target PFCs. The high  $k_2$  and  $v$  values revealed that TAN-1 resin had higher adsorption rates and shorter equilibrium times for all target PFCs compared to the other resins, which was also evident in Figure 4.1. Compared to TAN-1 resin, A500+ resin had lower  $k_2$  and  $v$  values for short chain PFCs, but had even higher  $k_2$  (2.77 mg/ $\mu$ g/h for PFDA and 4.41 mg/ $\mu$ g/h for PFOS) values for target PFCs with longer carbon chains. It indicated that A500+ resin had superior adsorption rate for long chain PFCs. Both PFA444 and A444 resins presented  $k_2$  and  $v$  values in the middle range, and PFA444 resin had slightly higher  $k_2$  and  $v$  values than A444 resin. A555 resin showed lowest  $k_2$  values for all target PFCs, which reflected that it had longest equilibrium times for all target PFCs. All resins showed similar high  $q_e$  and  $q_{e,exp}$  values for target PFCs. The  $q_e$  and  $q_{e,exp}$  values for most resins were close, which explained that the adsorption kinetics data were well simulated by the model. Among all the  $q_e$  data, only A555 resin had about 10% larger  $q_e$  values for short chain PFCs, compared to both the  $q_{e,exp}$  values of A555 and the  $q_e$  values of the other resins. These abnormally high  $q_e$  values could be related to the simulation errors caused by the low adsorption rate and long equilibrium time of the A555 resin. It can be observed in Figure 4.1 that different from all the other resin, the PFCs adsorption using A555 resin did not reached the equilibrium before 120 hours; thus, the exact equilibrium times for A555 resin could not be determined through the existing experimental data. As a result, some of the calculated  $q_e$  values of A555 resin based

on the pseudo-second-order model were exaggerated compared to the other resins. Except for PFDA and PFOS, all the other PFCs reached high maximum percentage removals of more than 95% for all selected anion exchange resins. PFDA and PFOS, which are long chain PFCs, had lower maximum percentage removals in the range of around 70% to 80%. Overall these results showed that anion exchange resins had equilibrium times ranging from 48 hours to more than 120 hours but were very similar among the different compounds for a particular resin. However, larger maximum removals were observed for short chain PFCs rather than long chain ones in ultrapure water for all resins. The reason that short chain PFCs had better removals in ultrapure water may be that the ion exchange mechanism dominated the removal process when there was no competition from NOM or inorganic ions in ultrapure water; thus, the short chain PFCs with lower mass/charge ratios were preferentially removed.

Lampert et al. (2007) reported very high PFOS and PFOA adsorption capacities of 23.5 mg/g and 45.7 mg/L by GAC; however, the results were from wastewater experiments with high PFC concentration of up to 53 mg/L. Hansen et al. (2010) reported PFOA adsorption capacities of 20 ng/mg by PAC and 1.1 ng/mg by GAC in contaminated groundwater, which were relatively lower than the adsorption capacities detected in this study.

#### **4.3.2.2 Adsorption isotherms in ultrapure water**

The empirically-derived Freundlich model is generally found to best represent experimental data for adsorption in aqueous solutions, particularly for heterogeneous adsorbents such as activated carbon (Crittenden et al. 2012); its recurring use in water treatment studies has established it as a kind of standard (Worch, 2012). The Freundlich equation is expressed as follows:

$$q_e = K_F C_e^{1/n} \quad \text{(Equation 4.5)}$$

where  $K_F$  and  $n$  are model parameters, indicating adsorption strength and energetic heterogeneity of the adsorbent surface, respectively (Worch, 2012). The Freundlich parameters were calculated by the non-linear squares regression analysis using the MATLAB<sup>®</sup> curve fitting toolbox (Mathworks, 2016).

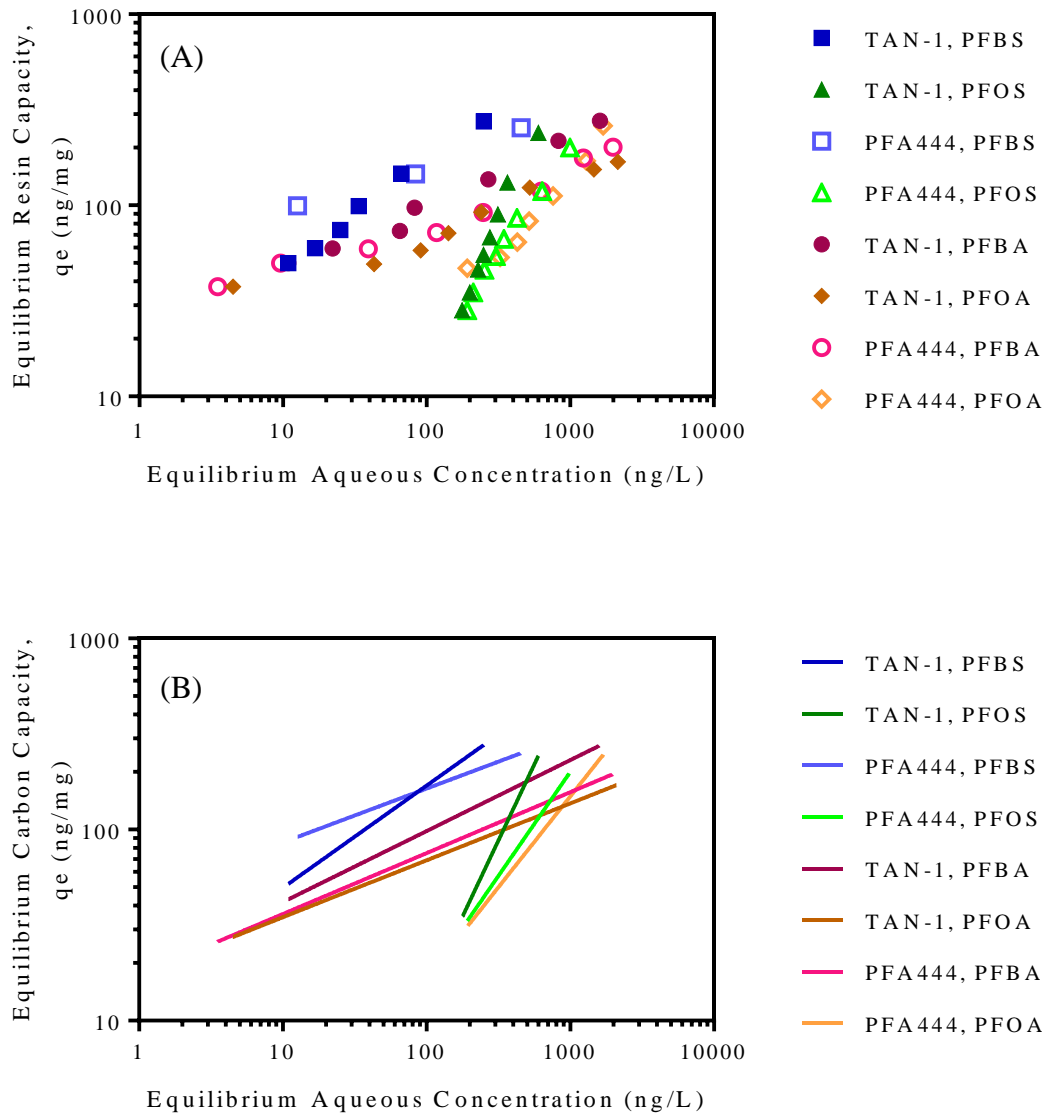


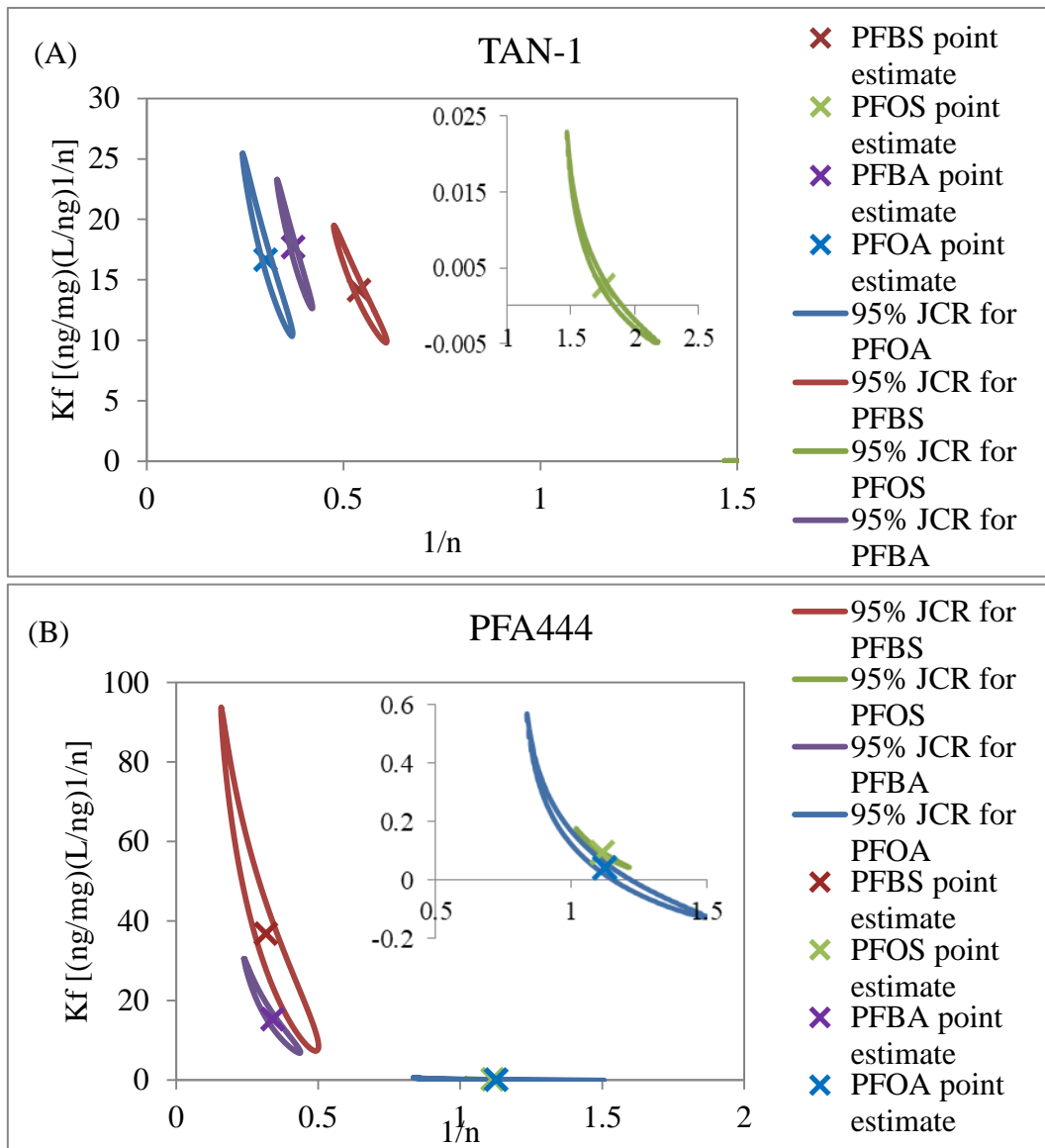
**Figure 4.3** Freundlich isotherms of PFCs adsorption in ultrapure water (resin doses were 50 mg/L, and the contact time was 48 hours): (A) experimental data of Freundlich isotherms; (B) trend lines of isotherms.

From the previous removal kinetics results in ultrapure water, TAN-1 had shortest equilibrium times for all PFCs among all target resins. The later study of removal kinetics in Grand River water proved that PFA444 resin had best PFCs removal in surface water. As a result, TAN-1 and PFA444 resins were selected as target PFCs in the studies of isotherm, removal kinetics in Lake Erie water, and effects of inorganic anions. To simplify the lab work, two PFCAs (PFBA and PFOA) and two PFSAs (PFBS and PFOS) were selected as target PFCs in the isotherms studies. Figure 4.3 showed all isotherms results of two anion exchange resins and four PFCs, as well as their trends. The PFOS adsorption using both TAN-1 and PFA444 resins had equilibrium aqueous concentrations in the range of 100 to 1000 ng/L. Data of PFOA adsorption using TAN-1 resin had a somewhat wider range of equilibrium aqueous concentrations. The PFBA and PFBS adsorption isotherms had larger equilibrium aqueous concentrations of 2 to 2000 ng/L. With different equilibrium aqueous concentration ranges, adsorption isotherms of both resins and all target PFCs had similar equilibrium resin capacity ranges of 20 to 300 ng/mg.

The isotherms results are comparable with the kinetics results. Taking TAN-1 resin and PFBA as an example, the kinetics results showed that the  $q_e$  value for PFBA when using TAN-1 resin was around 60 ng/mg at PFBA concentration of 16 ng/L as shown in Figure 4.1 and Table 4-4. The data could well fit the isotherm curve shown in Figure 4.3. The other isotherm data also confirmed the reliability of the kinetics results.

As shown in the Freundlich model (Equation 4.5), the two parameters ( $K_f$  and  $1/n$ ) are closely linked, which implies that the estimate of one parameter may influence the value of the other parameter. As a result, confidence intervals for individual parameters can hardly present the relationship between the two parameters. To better understand the correlation between the two Freundlich parameters and their estimates, joint confidence regions (JCRs) of  $K_f$  and  $1/n$  were calculated for each PFC and each

resin at a 95% confidence level. The results of 95% JCRs and point estimates for the Freundlich parameters are shown in Figure 4.4.



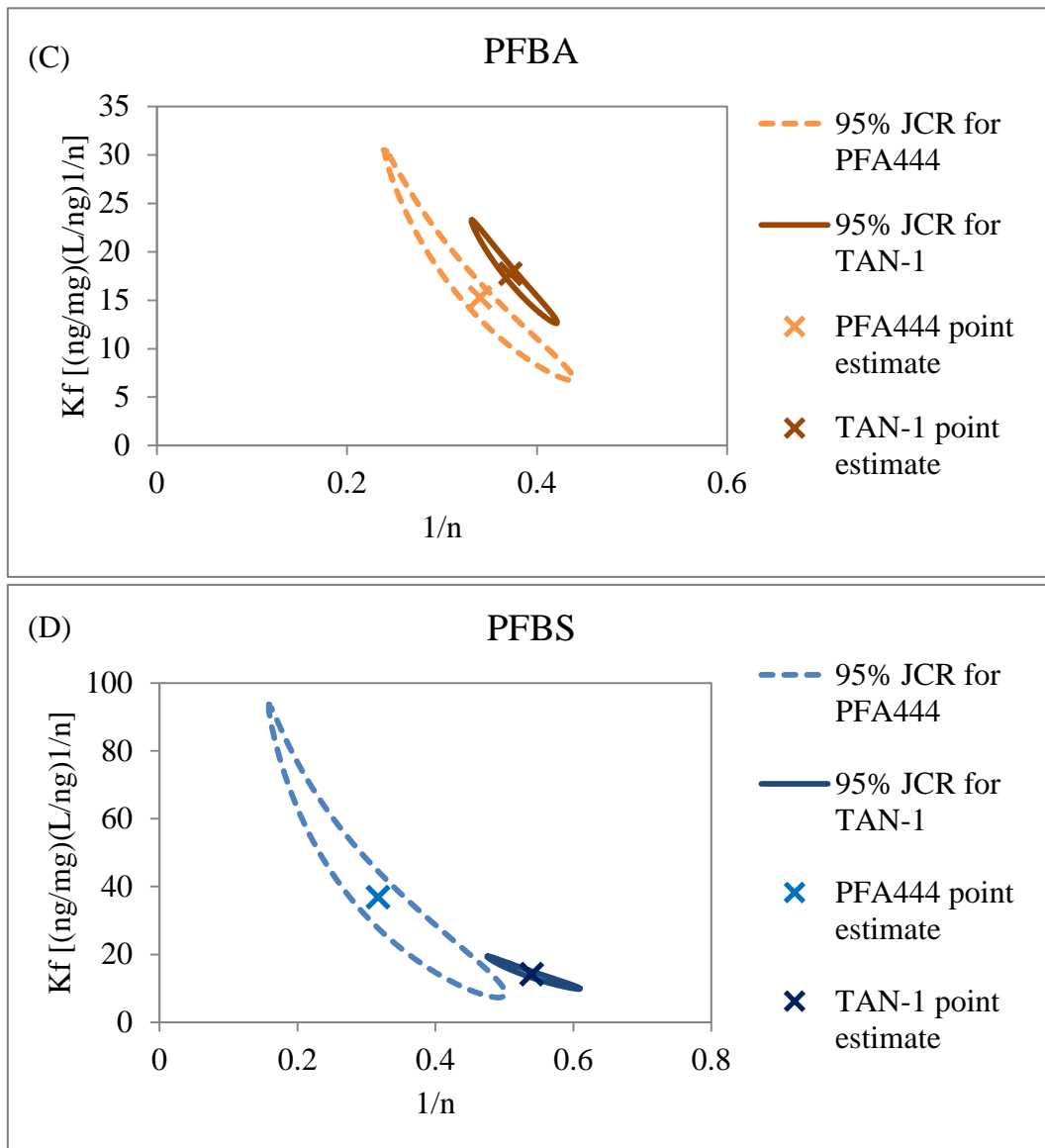


**Figure 4.4 95% joint confidence regions (JCRs) and point estimates for the Freundlich parameters of isotherms generated with TAN-1 and PFA444 resins in ultrapure water: (A) JCRs for TAN-1 resin of all four target PFCs; (B) JCRs for PFA444 resin of all four target PFCs; (C) JCRs for both TAN-1 and PFA444 of PFBA; (D) JCRs for both resins of PFBS.**

As shown in Figure 4.4, the 95% joint confidence regions (JCRs) for the Freundlich parameters of isotherms generated with TAN-1 and PFA444 resins in ultrapure water have the shape of narrow ellipses. This reflects that the two Freundlich parameters  $K_f$  and  $1/n$  were not independent. PFA444 had a larger joint confidence region compared

to TAN-1, which indicated that the Freundlich parameters of PFA444 resin had greater uncertainty. The 95% joint confidence regions of TAN-1 resin showed that PFBS, PFOA, and PFBA had same  $K_f$  range of 10-25 (ng/mg)(L/ng)<sup>1/n</sup> with different 1/n values; while PFOS had much lower  $K_f$  value of 0.0025 (ng/mg)(L/ng)<sup>1/n</sup>. From the Figure 4.4, it can be observed that the JCRs for individual isotherms did not overlap from each other, which illustrated that the Freundlich parameters for individual isotherms were statistically different from each other.

Freundlich isotherm parameters including  $K_f$  and 1/n as well as  $R^2$  and number of data points used for the calculations are listed in Table 4-5. When higher doses of PFA444 were applied, the equilibrium aqueous concentrations of PFBS were below the detection limit; thus, the PFBS isotherms adsorbed by PFA444 resin had only 3 available data points, which made the data with more uncertainty. It could be verified by the results of 95% joint confidence regions in Figure 4.4. Different from the other PFCs, PFOS had extremely low  $K_f$  values and higher 1/n values when using both TAN-1 and PFA444 resins. It implied that the equilibrium resin capacity for PFOS would have significant change with the change of equilibrium aqueous concentration.

The Freundlich isotherms results also verified the relevant research in the literature. Rahman reported that PFOA had 1/n value of 0.3 and  $K_f$  value of 60 (ng/mg) (ng/L)<sup>-1/n</sup> when using F400 GAC, and had 1/n value of 0.33 and  $K_f$  value of 108 (ng/mg) (ng/L)<sup>-1/n</sup> when using A502P anion exchange resins (Rahman, 2014). The  $K_f$  values of PFOA using GAC and anaerobic sludge reported by Ochoa-Herrera and Sierra-Alvarez (2008) were 26 and 0.6 (ng/mg) (ng/L)<sup>-1/n</sup> respectively (reverting to the same unit as in this study). Chularueangaksorn et al. also acquired the  $K_f$  value of 18 (mg/g) (g/L)<sup>-1/n</sup> and 1/n value of 0.73 for PFOA adsorption when using XAD4 ion exchange resins. Comparing to the reported Freundlich isotherm parameters for PFCs removal, the TAN-1 resin had similar results; while, the PFA444 resin showed lower  $K_f$  value for PFOA removal.



**Table 4-5 Freundlich isotherm parameters for TAN-1 and PFA444 resins in ultrapure water**

Resin	PFCs	Number of data points	Freundlich capacity factor, $K_f$ (ng/mg) (ng/L) <sup>-1/n</sup>	Freundlich intensity factor, 1/n (dimensionless)	R <sup>2</sup>
TAN-1	PFBS	6	12.9 (9.8-19.5)	0.56 (0.48-0.61)	0.992
	PFOS	8	0.0025 (0-0.022)	1.81 (1.47-2.18)	0.983
	PFBA	7	19.8 (12.7-23.3)	0.35 (0.33-0.42)	0.985
	PFOA	8	20.8 (10.6-25.5)	0.26 (0.24-0.37)	0.946
PFA444	PFBS	3	49.6 (7.7-93.7)	0.26 (0.16-0.50)	0.981
	PFOS	8	0.077 (0.04-0.18)	1.14 (1.02-1.21)	0.989
	PFBA	8	25.1 (7.2-30.5)	0.27 (0.24-0.44)	0.956
	PFOA	7	0.55 (0-0.57)	0.81 (0.80-1.50)	0.960

Figure 4.5 provided a comparison of PFCs adsorption capacities at different equilibrium aqueous PFCs concentrations between TAN-1 and PFA444 resins. Taking PFBS as an example, it can be calculated that TAN-1 had a higher resin loading ( $q_e$ ) of 170 ng/mg at 0.1 µg/L aqueous concentration and had a lower  $q_e$  of 620 ng/mg at 1.0 µg/L aqueous concentration, compared to PFA444 resin. At concentrations of 0.1 and 1.0 µg/L, PFA444 resin had the  $q_e$  values of 170 and 300 ng/mg. For PFOA, the two resins showed opposite trend compared to PFBS. For PFOA and PFBA, TAN-1

resin had higher resin loadings at most aqueous concentrations. As can be seen, the aqueous adsorbate concentration can be a critical factor in selecting the optimal carbon, due to the different  $1/n$  values of the Freundlich isotherms.

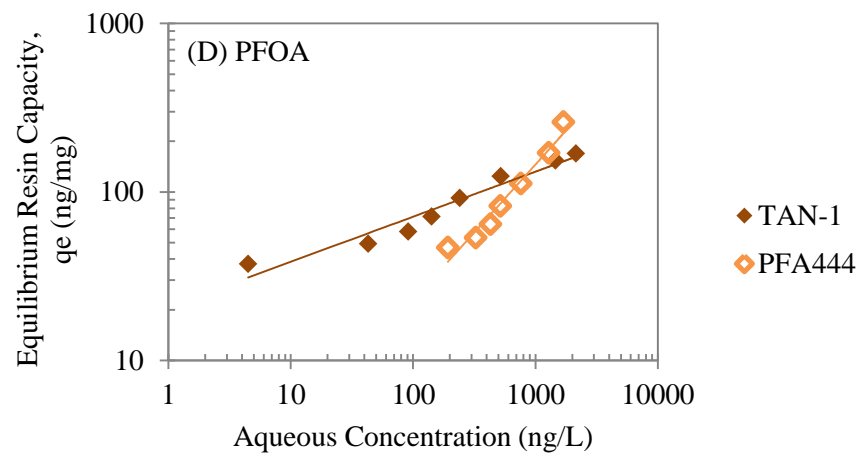
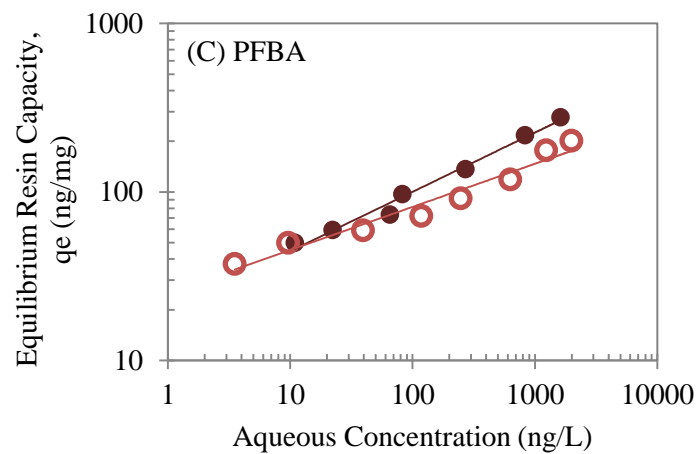
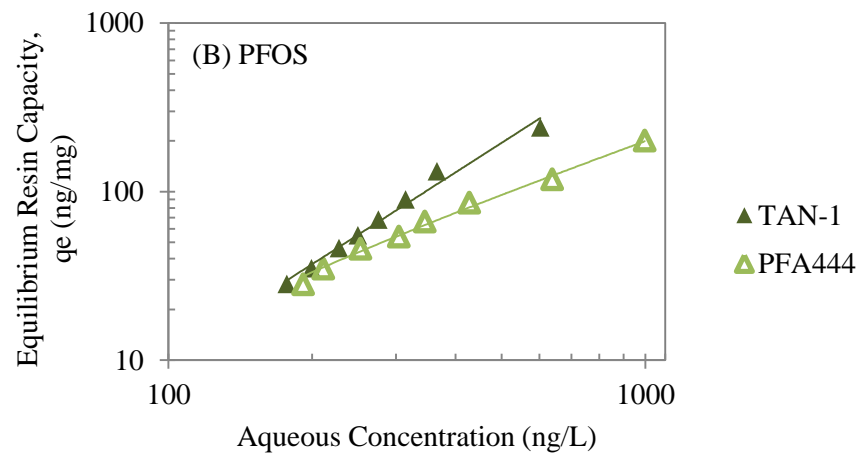
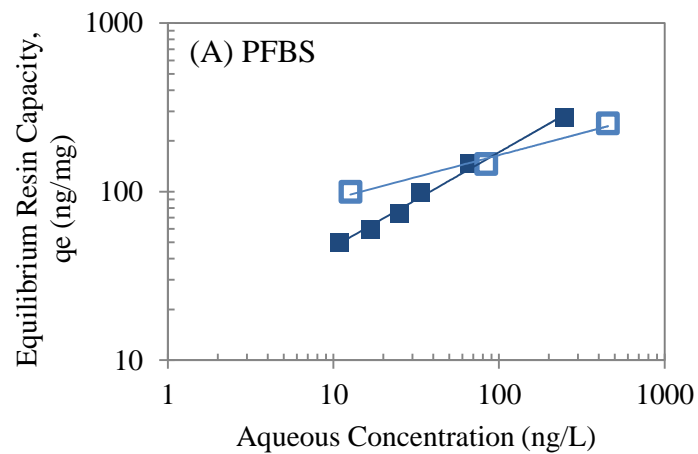


**Figure 4.5** Freundlich isotherms of TAN-1 and PFA444 resins in ultrapure water (resin doses were 50 mg/L, and the contact time was 48 hours): (A) PFBS; (B) PFOS; (C) PFBA; (D) PFOA.

### 4.3.2.3 Effect of anion exchange resins properties

#### (1) Pore size distribution

Among all the selected resins, A500+ has both the largest BET surface area of 11.980 m<sup>2</sup>/g and the largest pore volume of 17.47 ×10<sup>-3</sup> cm<sup>3</sup>/g as shown in Table 4-3. The pore size distribution results in Table 4-3 and Appendix E showed that more than 99% pores of A555 resin were mesopores, especially in the range of 2 to 10 nm. The large mesopore volume of A500+ did not distinguish it from the other resins in the adsorption of short chain PFCs in ultrapure water, but it did have high adsorption rates and k<sub>2</sub> values for PFDA and PFOS which are long chain PFCs. It can be assumed that long chain PFCs with large molecular size (the molecular sizes of PFCAs and PFSAs were calculated to be in the range of 6.2 Å and 8.0 Å) would be restricted by the primary micropores (< 0.8 nm); thus, large volume of secondary micropores and mesopores would ensure the intraparticle diffusion for long chain PFCs, so that the adsorption rates increased. If 600 μm is used as the diameter of the resin as discussed in section 4.3.1 assuming the resin is a sphere, the external surface area of anion exchange resin can be calculated to be 0.01 m<sup>2</sup>/g. The BET surface areas of all target anion exchange resins were much larger than the estimated external surface areas of the resins. Although the BET surface areas of anion exchange resins were much lower than activated carbons, the pore sizes and volumes could still be important factors that influence the PFCs removal performance.

#### (2) Polymer structure (macroporous and gel resins)

As gel resins, PFA444 and A444 resins did not show obvious difference from the macroporous resins on PFCs adsorption kinetics in ultrapure water. As shown in Figure 4.6, the two gel resins (PFA444 and A444) showed similar PFOA removals and slightly lower PFOS removals compared to the three macroporous resins (TAN-1, A500+, A555). The adsorption rates, capacities, and maximum PFC removals of both gel and macroporous resins were in the same range. It could be concluded from the

results that the polymer structure of macroporous or gel was not a prominent and crucial factor in PFCs adsorption in ultrapure water.

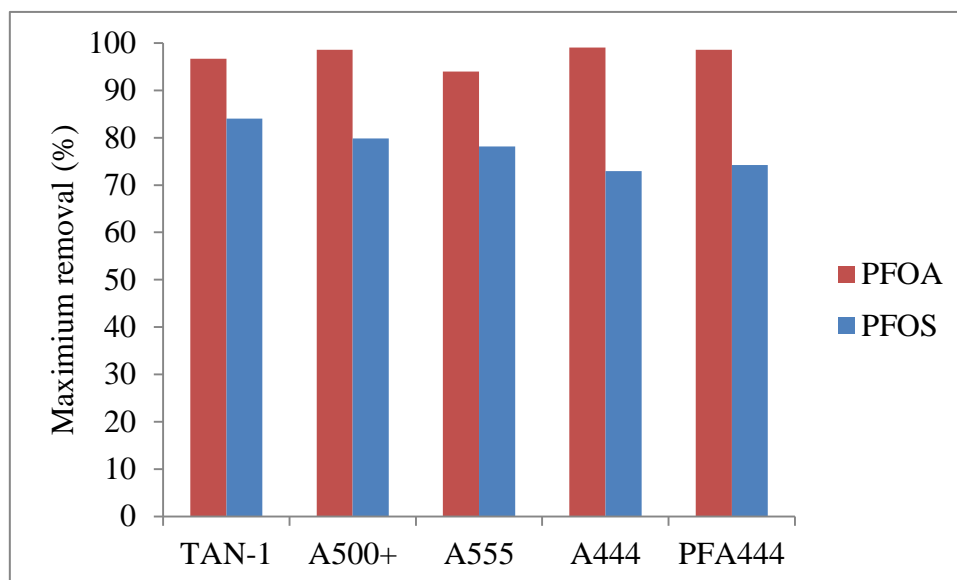


**Figure 4.6 Comparison of maximum percentage removals for PFOA and PFOS among all selected resins in ultrapure water**

### (3) Functional Group

A555 was the only anion exchange resin with Type III quaternary ammonium functional group which was designed to reach high regeneration performance. All the other resins were traditional Type I quaternary ammonium resins. Type I resins showed higher adsorption rates compared to the Type III resin A555 as shown in Table 4-4. Since A555 resin did not show obvious low surface area and pore volume, the low adsorption rates and long equilibrium times for target PFCs when using A555 resin were expected to be caused by its Type III quaternary ammonium functional group.

The other resin properties did not show obvious significant impacts on PFCs adsorption in ultrapure water.

#### 4.3.2.4 Effect of PFC properties on PFCs removal

The PFC properties are mainly influenced by the carbon chain length and functional groups. As shown in Table 2-1, long carbon chain length would lead to high hydrophobicity and large particle size. The functional groups will influence the pKa, solubility, and ion exchange ability. The  $q_e$  values and maximum percentage removals of all target PFCs using TAN-1 resin in ultrapure water were compared in Figure 4.7. It can be observed that long carbon chain PFCs such as PFDA and PFOS had lower  $q_e$  values and maximum percentage removals compared to the short chain PFCs in ultrapure water. This trend was not obvious when the carbon chain length was smaller than 8 carbons. The PFCAs and PFSA with same carbon chain length did not show obvious difference. The other resins had similar PFCs removal performance as TAN-1 resin.

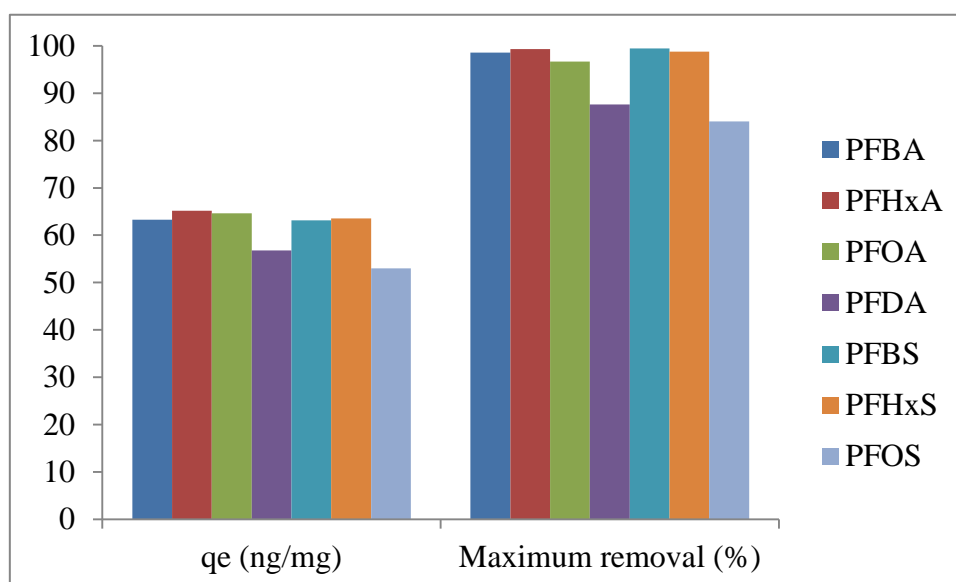


**Figure 4.7 Comparison of calculated equilibrium aqueous concentrations ( $q_e$ ) and maximum percentage removals among all target PFCs in TAN-1 resin in ultrapure water**

Figure 4.8 shows the Freundlich isotherms of all target PFCs using TAN-1 resin in ultrapure water. To compare the short chain PFCs with the long chain PFCs, it can be seen that the Freundlich isotherms curve of PFBS was above the curve of PFOS, which indicated that at the same equilibrium aqueous concentration, more PFBS

would be adsorbed on the resin compared to PFOS. The same trend was shown for PFBA and PFOA. The isotherms data confirmed the results of kinetics that short chain PFCs had higher percentage removals. For the effect of functional groups, it can be observed that the slopes of the linear regression curves of PFSA's were larger compared to PFCAs. It implied that the equilibrium carbon capacity for PFSA's would have significant change with the change of equilibrium aqueous concentration, and PFSA's would reach higher equilibrium carbon capacities in high equilibrium aqueous concentrations. Different from the results observed for activated carbons, the short chain PFCs (more hydrophilic compounds) had higher maximum removal and  $q_e$  values. One hypothesis to explain this phenomenon is that the ion exchange process is not determined by a single mechanism. It is controlled by both the adsorption mechanism and the ion exchange mechanism. In ultrapure water, the ion exchange mechanism seems to be more dominant which leads to the higher removal of short chain PFCs.

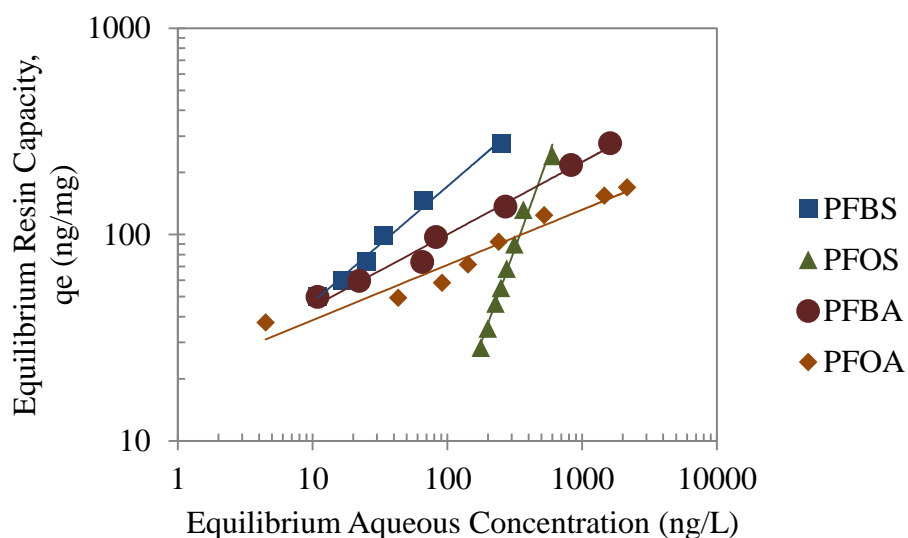
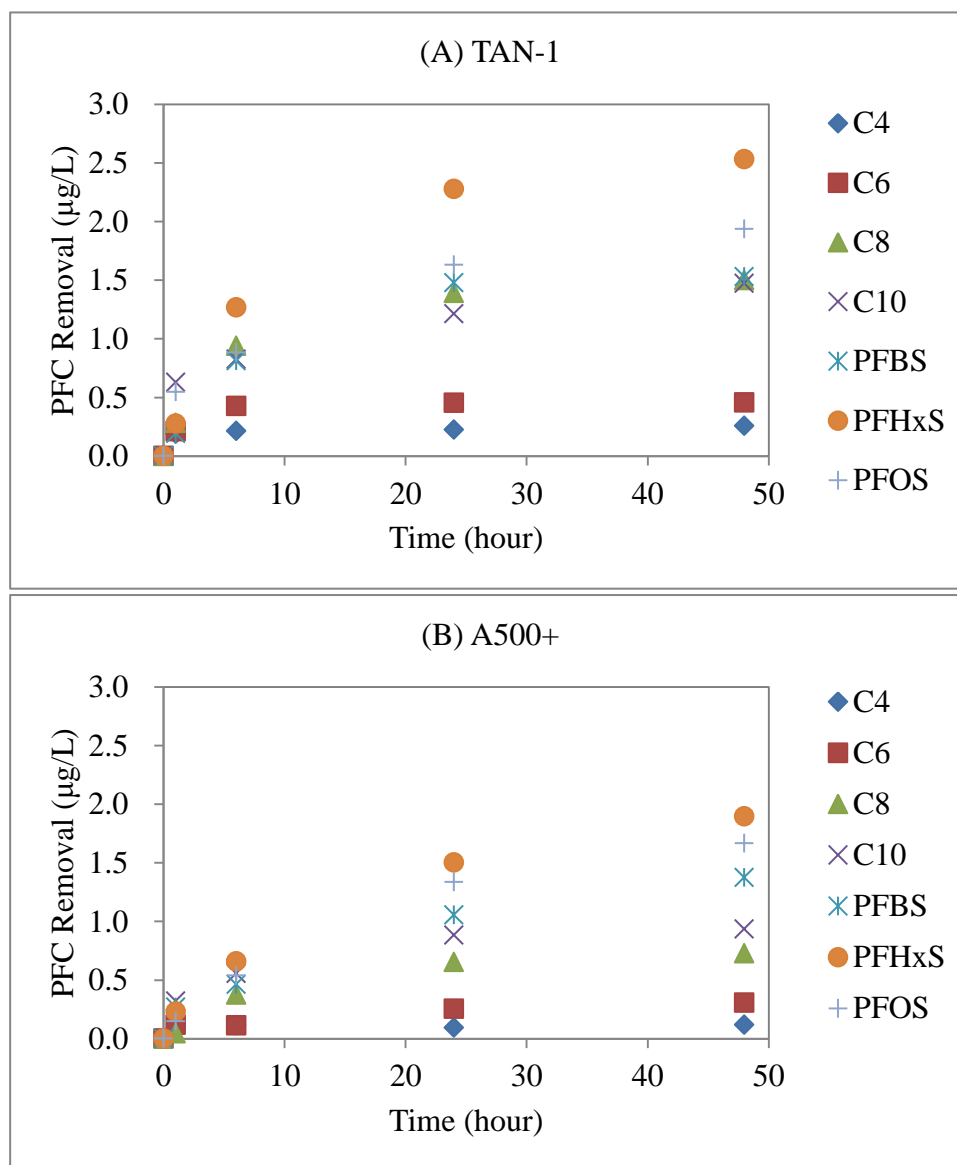


**Figure 4.8** Freundlich isotherms of different PFCs using TAN-1 resins in ultrapure water (resin doses were 50 mg/L, and the contact time was 48 hours)

### 4.3.3 PFCs Removal Kinetics in Surface Water

After the removal kinetics studies in ultrapure water, the five commercially available anion exchange resins were also screened using Grand River water. Two most promising resins (TAN-1 and PFA444) were then tested with Lake Erie water.

#### 4.3.3.1 PFCs removal kinetics in Grand River water





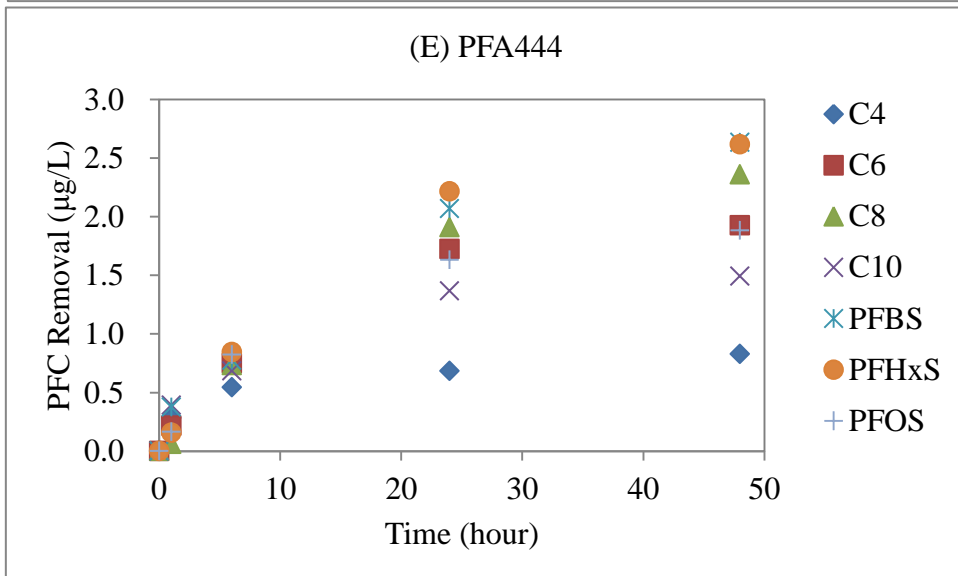
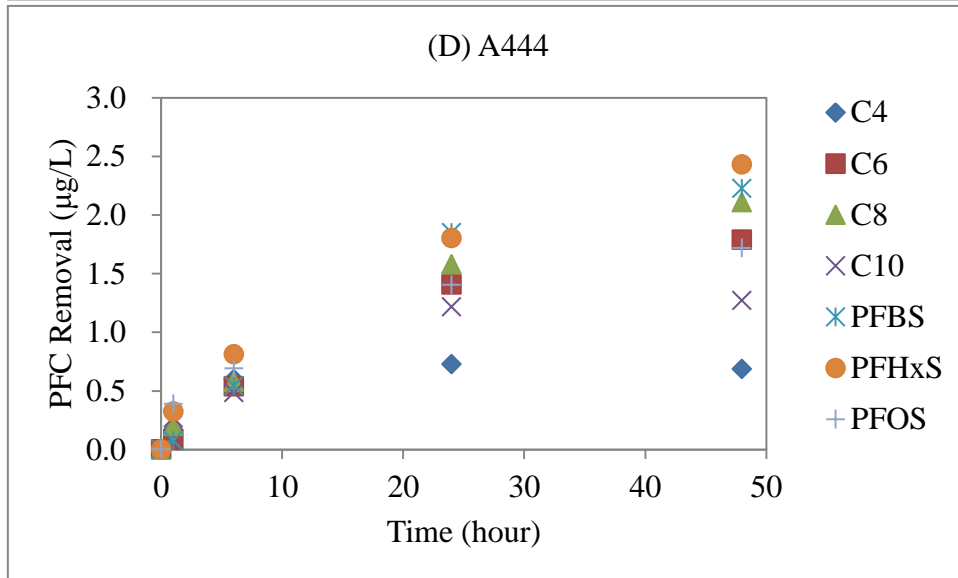
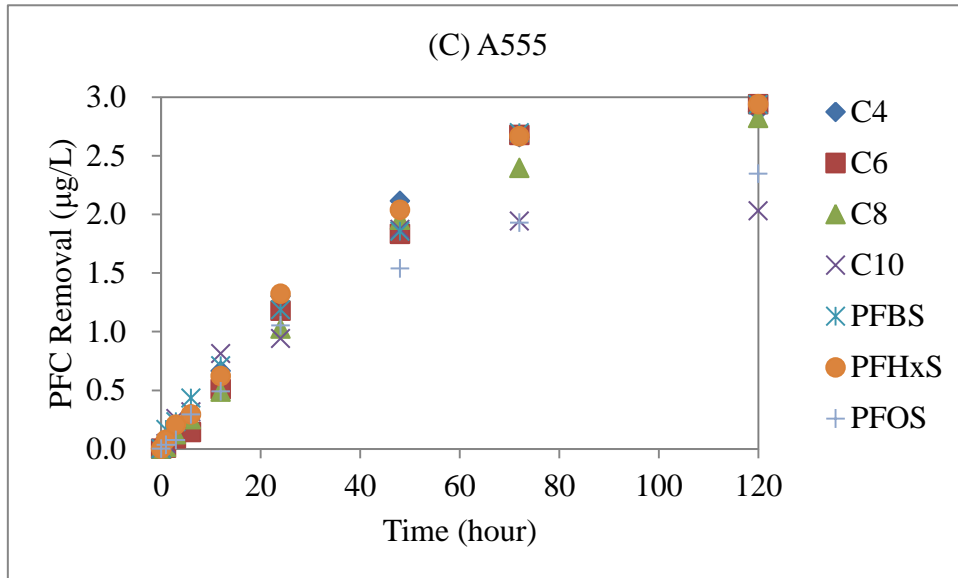


**Figure 4.9 PFCs adsorption kinetics of all five anion exchange resins in Grand River water (initial PFC concentrations were 3 µg/L for each compound; resin doses were 50 mg/L as dry weight): (A) TAN-1; (B) A500+; (C) A555; (D) A444; (E) PFA444.**

The results of PFCs adsorption kinetics in Grand River water using all target resins are shown in Figure 4.9. It can be observed in Figure 4.9 that PFHxS had highest removal (56% to 87%) and PFBA (C4) had lowest removal (5% to 28%) after 48 hours for all five resins in Grand River water. Most of the target PFCs did not reach the equilibrium at 48 hours in Grand River water. The short chain PFCAs tended to reach the equilibrium faster than the other PFCs. Among all the resins, PFA444 had best PFCs removal in Grand River water.

Experimental data of PFCs adsorption kinetics in both Grand River water and Lake Erie water were also simulated using pseudo-second-order model. The kinetics parameters of all target PFCs for all anion exchange resins in Grand River water were calculated and listed in Table 4-6.

**Table 4-6 Pseudo-second-order model parameters of all target PFCs for all anion exchange resins in Grand River water**

Resins	$k_2$ (mg/µg/h)	$q_e$ (ng/mg)	$q_{e, exp}$ (ng/mg)*	Maximum removal (%)	$R^2$
<b>PFBA</b>					
<b>TAN-1</b>	137.8	5.2	5.1	8.6	0.994
<b>A500+</b>	275.8	2.3	2.4	3.9	0.982
<b>A555</b>	121.4	3.2	3.0	4.9	0.999
<b>A444</b>	36.01	14.6	13.7	22.9	0.995
<b>PFA444</b>	16.38	17.3	16.6	27.6	0.991
<b>PFHxA</b>					
<b>TAN-1</b>	127.9	9.3	9.1	15.2	1.000

<b>A500+</b>	20.35	6.9	6.1	10.2	0.960
<b>A555</b>	50.27	6.8	6.4	10.6	0.998
<b>A444</b>	0.53	60.7	35.8	59.6	0.963
<b>PFA444</b>	1.89	47.9	38.5	64.2	0.994
<b>PFOA</b>					
<b>TAN-1</b>	6.55	32.9	30.0	49.9	1.000
<b>A500+</b>	3.29	19.8	14.5	24.2	0.941
<b>A555</b>	4.65	16.0	12.6	21.0	0.973
<b>A444</b>	0.93	57.6	42.2	70.3	0.959
<b>PFA444</b>	0.72	67.9	47.2	78.6	0.996
<b>PFDA</b>					
<b>TAN-1</b>	8.07	31.0	29.5	49.1	0.987
<b>A500+</b>	15.07	20.0	18.7	31.2	0.997
<b>A555</b>	33.82	16.4	15.8	26.4	1.000
<b>A444</b>	4.38	29.8	25.4	42.3	0.973
<b>PFA444</b>	5.31	33.3	29.8	49.7	0.989
<b>PFBS</b>					
<b>TAN-1</b>	3.84	35.9	30.6	51.0	0.995
<b>A500+</b>	2.92	32.5	27.5	45.8	0.957
<b>A555</b>	0.46	51.5	27.2	45.3	0.997
<b>A444</b>	0.64	66.9	44.5	74.2	0.933
<b>PFA444</b>	1.09	66.6	52.6	87.7	0.949
<b>PFHxS</b>					
<b>TAN-1</b>	1.84	60.7	50.6	84.4	0.998
<b>A500+</b>	1.70	47.1	37.9	63.2	0.985
<b>A555</b>	0.97	47.6	33.9	56.5	0.925
<b>A444</b>	1.31	59.7	48.6	81.0	0.969

<b>PFA444</b>	0.58	78.2	52.3	87.2	0.985
<b>PFOS</b>					
<b>TAN-1</b>	3.92	42.7	38.7	64.6	0.986
<b>A500+</b>	1.38	44.5	33.3	55.5	0.991
<b>A555</b>	4.67	31.7	29.0	48.4	0.973
<b>A444</b>	3.30	39.1	34.4	57.3	0.980
<b>PFA444</b>	1.72	47.7	60.0	62.7	0.997

\*  $q_t$  (t=48 hours) values were applied in Table 4-6 as  $q_{e, \text{exp}}$  values, with the assumption that PFCs removed by anion exchange resin reached the equilibrium at 48 hours.

Most of the  $q_{e, \text{exp}}$  values of the target PFCs for all target resins were similar to but slightly lower than their calculated  $q_e$  values, which meant that the adsorption after 48 hours was likely close to the equilibrium; however, there were some exceptions. For example, the  $q_e$  value of PFBS when using A555 resin (51.5 ng/mg) was much larger than its  $q_{e, \text{exp}}$  value of 27.2 ng/mg, which indicated that it took much longer than 48 hours for PFBS to reach equilibrium when using A555 resin. Short chain PFCAs like PFBA (C4) and PFHxA (C6) had higher  $k_2$  values compared to the other PFCs for all the resins. Among all target PFCs, PFHxS had the largest maximum removal of 56.5% to 87.2% and largest  $q_e$  of 47.1 to 78.2 ng/mg. PFSAs had better adsorption performance in Grand River water, compared to PFCAs.

As shown in Appendix D,  $t/q_t$  was plotted with  $t$  to simulate the linear relationship and to calculate the kinetics parameters. The plotting showed good linear relation of the kinetics parameters for all target PFCs in Grand River water, which signified that the PFCs adsorption kinetics data fit the pseudo-second-order model well. The linear regression line of PFBA had largest slope, followed by the PFHxA. All the other PFCs had close slopes. As shown in Equation 4.4, the slope of the curve is  $1/q_e$ ; thus, the large slope revealed a small adsorption capacity. The application of

pseudo-second-order model to the PFCs adsorption data for all the other anion exchange resins showed similar trends as TAN-1 resin.

#### 4.3.3.2 Adsorption kinetics in Lake Erie water

**Table 4-7 Pseudo-second-order model parameters of all target PFCs for TAN-1 and PFA444 resins in Lake Erie water**

Resins	$k_2$ (mg/ $\mu$ g/h)	$q_e$ (ng/mg)	$q_{e, exp}$ (ng/mg) *	Maximum removal (%)	$R^2$
<b>PFBA</b>					
TAN-1	37.29	14.2	13.6	22.7	1.000
PFA444	16.58	24.9	59.5	27.6	0.999
<b>PFHxA</b>					
TAN-1	23.47	23.6	22.6	37.7	1.000
PFA444	3.31	54.7	59.0	64.2	0.982
<b>PFOA</b>					
TAN-1	1.68	52.7	42.2	70.3	0.997
PFA444	0.37	88.9	58.9	78.6	0.961
<b>PFDA</b>					
TAN-1	4.31	52.4	48.8	81.3	0.990
PFA444	2.69	53.5	59.0	49.7	0.941
<b>PFBS</b>					
TAN-1	7.54	49.8	47.6	79.3	0.998
PFA444	3.32	61.7	58.8	87.7	0.987
<b>PFHxS</b>					
TAN-1	1.32	68.4	55.4	92.3	0.959
PFA444	1.14	71.5	58.8	87.2	0.987

PFOS					
TAN-1	1.24	69.4	56.2	93.7	0.935
PFA444	3.50	52.5	59.0	62.7	0.998

\*  $q_t$  (t=48 hours) values were applied in Table 4-6 as  $q_{e, \text{exp}}$  values, with the assumption that PFCs removed by anion exchange resin reached the equilibrium at 48 hours.

The application of the pseudo-second-order model to the adsorption data of all target PFCs onto TAN-1 and PFA444 resins in Lake Erie water as well as the model parameters were shown Table 4-7. The  $q_{e, \text{exp}}$  values of all PFCs were similar to but slightly lower than the calculated  $q_e$  values, which meant that the adsorption after 48 hours was likely close to the equilibrium. The  $R^2$  values were all above 0.93 or even close to 1, which indicated that the pseudo-second-order model fit the data well. Long chain PFCs had larger  $q_e$  values and maximum percentage removals compared to short chain PFCs. When using TAN-1 resin, PFSAAs had larger  $q_e$  values and maximum percentage removals compared to PFCAs. Among all PFCs, PFOS had largest  $q_e$  of 69.4 ng/mg and maximum removal of 93.7%. For PFA444 resin, PFOA had largest  $q_e$  of 88.9 ng/mg.

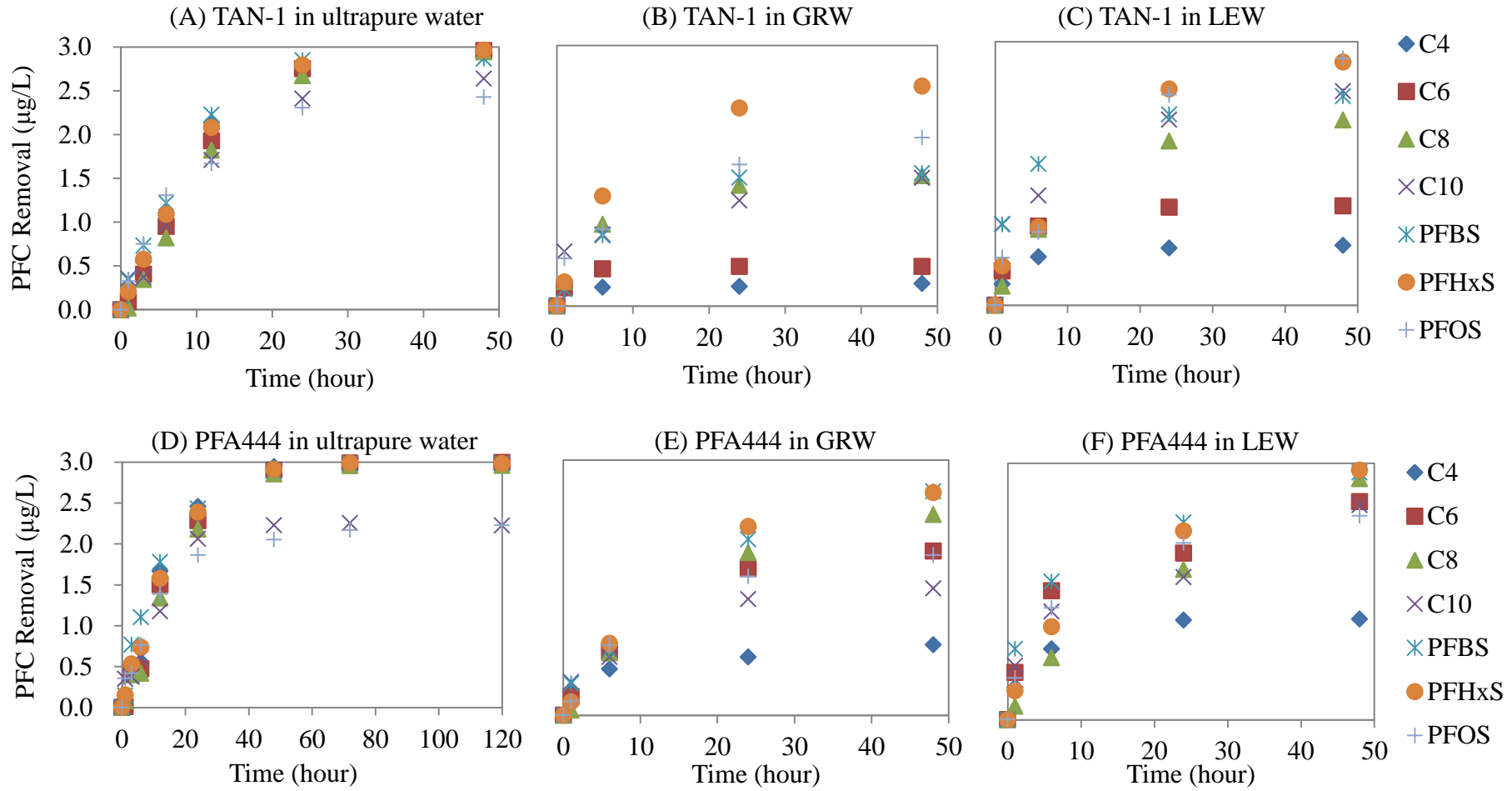


**Figure 4.10 PFCs kinetics using TAN-1 and PFA444 resins in ultrapure water, Grand River water (GRW), and Lake Erie water (LEW) (initial PFC concentrations were 3 µg/L; resin doses were 50 mg/L as dry weight).**

#### **4.3.3.3 Comparison of PFCs removal by anion exchange resins in different waters**

The PFCs kinetics using TAN-1 and PFA444 resins in different water sources were compared in Figure 4.10. In ultrapure water, all PFCs had high percentage removals of more than 80% after 48 hours. In both Grand River water and Lake Erie water, the percentage removals of all target PFCs dramatically decreased compared to ultrapure water. PFC removals decreased more in Grand River water, compared to Lake Erie water. Compared to Grand River water, Lake Erie water has lower concentrations of DOC and inorganic anions as shown in Table 4-2; thus, it has less competition in PFCs adsorption. The equilibrium times of all target PFCs on TAN-1 were around 48 hours in ultrapure water. In both Grand River water and Lake Erie water, equilibrium times of PFBA and PFHxA decreased to a few hours; while the equilibrium times of the other long chain PFCs exceeded 48 hours. These results show that in surface waters, both the adsorption capacities and the adsorption rates decreased. The removals of short chain PFCAs like PFBA and PFHxA significantly decreased to around 10% to 20%. The short chain PFCAs reached the equilibrium much earlier, compared to the results in ultrapure water. In Grand River water, the PFHxS had the largest maximum removal of 84.4% and largest  $q_e$  of ng/mg. PFSAs had better adsorption performance in Grand River water, compared to PFCAs. In surface waters, long chain PFCs experienced a higher removal compared to short chain PFCs, and PFSAs showed better removal compared to PFCAs. These results were caused by the complex impacts of both NOM and inorganic anions in surface water. Among all the anion exchange resins, PFA444 resin showed best PFCs removal performance Grand River water; therefore, it was selected as one of the target anion exchange resins in the studies of adsorption isotherms, impact of inorganic anions, and regeneration batch tests.



#### **4.3.3.4 Factors affecting PFCs removal by anion exchange resins in surface water**

##### (1) Effect of anion exchange resins properties

In surface water, two gel resins showed better PFCs adsorption performance with high maximum removals compared to the macroporous resins. Gel resins were less impacted with NOM and inorganic anions compared to macroporous resins. Among all the anion exchange resins, PFA444 resin performed best PFCs removals. Compared to A444 resin, PFA444 resin had most of their pores in the range of mesopores (2-50 nm). It can be speculated that unlike macroporous resins, gel resins had more pores concentrated in the mesopore range which prevented the large molecular NOMs from being adsorbed. In general, pore volume and surface area did not seem to be key impact factors, probably because all anion exchange resins had small pore volumes compared to activated carbons.

##### (2) Effect of PFC chain length on PFCs removal

Figure 4.11 showed the maximum removal and capacity results of different PFCs using TAN-1 resin in Lake Erie water. It can be seen that with the increase of the carbon chain length, both  $q_e$  and maximum removals of PFCs increased substantially. This meant that the short chain PFCs had more competition with NOM and inorganic anions in surface water; while long chain PFCs with high hydrophobicity were less influenced. Different from the results in ultrapure water, the mechanism of hydrophobic adsorption played a more important role in surface water. As shown in Figure 4.9, all the other resins showed similar trend as TAN-1 resin.

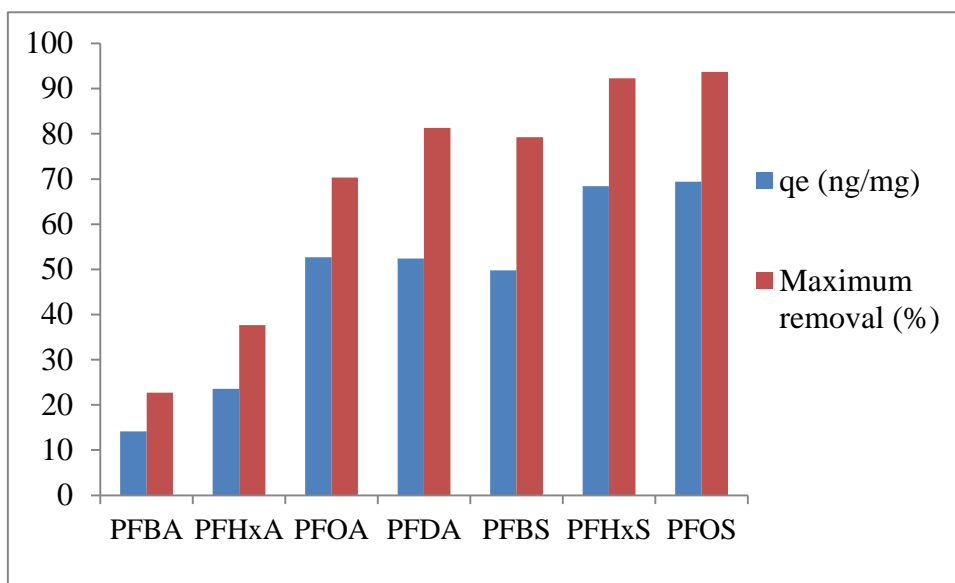


**Figure 4.11 Removal kinetics results of different PFCs using TAN-1 resin in Lake Erie water (initial PFC concentrations were 3  $\mu\text{g/L}$ ; resin doses were 50 mg/L as dry weight).**

### (3) Effect of PFC functional group on PFCs removal

Different from the results in ultrapure water, PFCAs and PFSAs presented obvious differences in adsorption kinetics. From Figure 4.11, it is apparent that PFSAs had much higher maximum removals and  $q_e$  values compared to PFCAs with the corresponding chain length. It indicated that PFSAs with their higher hydrophobicity (as shown in Table 2-1) were less impacted by the competition in surface water.

#### 4.3.4 Effect of Natural Organic Matter on PFC Removal by Anion Exchange

##### Resins

The adsorption kinetics results verified that the PFCs adsorption performance of anion exchange resins observably decreased in surface water, which could be caused by the high concentrations of NOM and inorganic anions. To study the effect of NOM in PFCs adsorption by anion exchange resins, DOC and LC-OCD analyses were conducted for both Grand River water and Lake Erie water. Figure 4.12, 4.13, and

4.14 show the DOC and LC-OCD results in Grand River water as examples to discuss the effect of NOM in PFCs adsorption.

From Figure 4.12, it can be observed that all the anion exchange resins had the ability to remove DOC. The initial DOC of Grand River water was 5.6 mg/L. After 24 hours, TAN-1 resin had the largest DOC removal of 57.8%, and A555 resin had 30.0% DOC removal which was the lowest among all the resins. Compared to the concentrations of PFCs, the concentration of DOC in surface water was several orders of magnitude higher, which would lead to the competition between NOMs and PFCs.

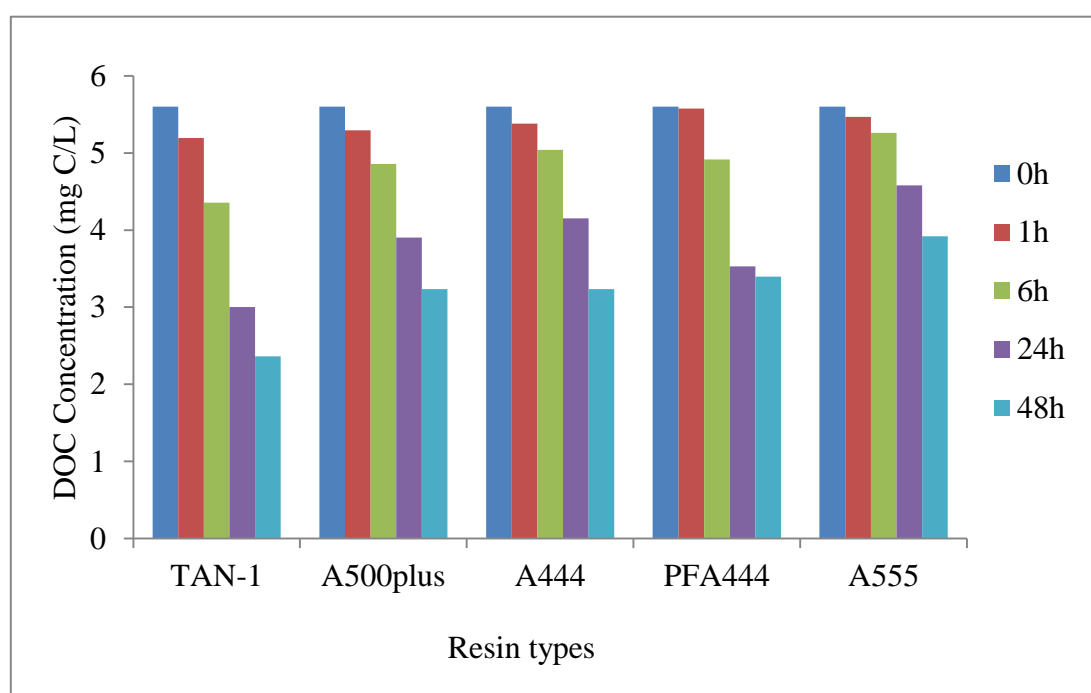


**Figure 4.12 DOC removals by different anion exchange resins in Grand River water**

As a size exclusion instrument, LC-OCD can separate NOM into different fractions including biopolymers, humic substances, building blocks, low molecular weight acids, and low molecular weight neutrals (Huber et al., 2011). As shown in Figure 4.13 and 4.14, the small peaks appeared at 30 min represented the biopolymers; while, the large peak at around 42 min represents the humic substances. The building blocks and low molecular weight acids have retention times of 46 to 53 min, respectively. The LC-OCD results of using all target anion exchange resins after 48 hours in Grand

River water are shown in Figure 4.13, from which it can be found that humic substances could be largely removed by all anion exchange resins; while biopolymers could not. Both building blocks and low molecular weight acids had small amounts of removal by all resins. The LC-OCD results accorded with the findings reported in the literature that the humic substances are the main fraction removed by ion exchange resins (Bazri et al., 2016b). Among all the resins, TAN-1 showed the best NOM removal, and A555 resin had the lowest NOM removal, which further confirmed the DOC results. The other resins showed similar NOM removal. Figure 4.14 showed that the removal of humic substances by TAN-1 resin consistently decreased with increased treatment time. Both building blocks and low molecular weight acids had slight removal only in first a few hours. LC-OCD results showed that humic substances carrying negative charges may be the presentative DOC which competed with PFCs. The results of the other resins and the results in Lake Erie water were similar to the trends shown in Figure 4.14.

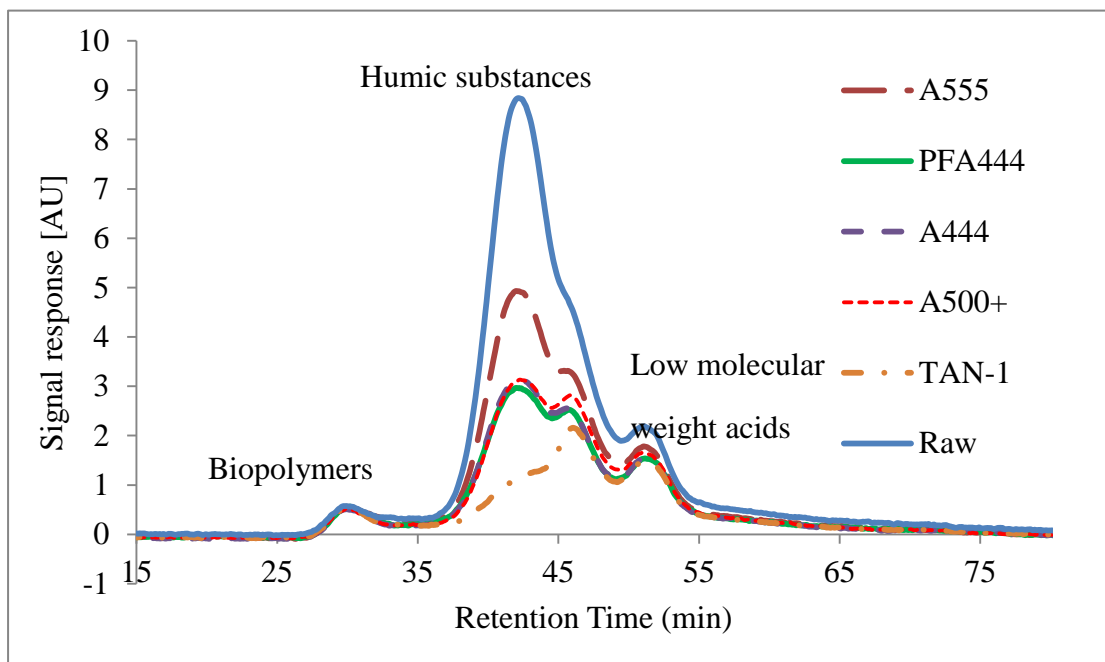


**Figure 4.13 LC-OCD results after 48-hour treatment by anion exchange resins in Grand River water**

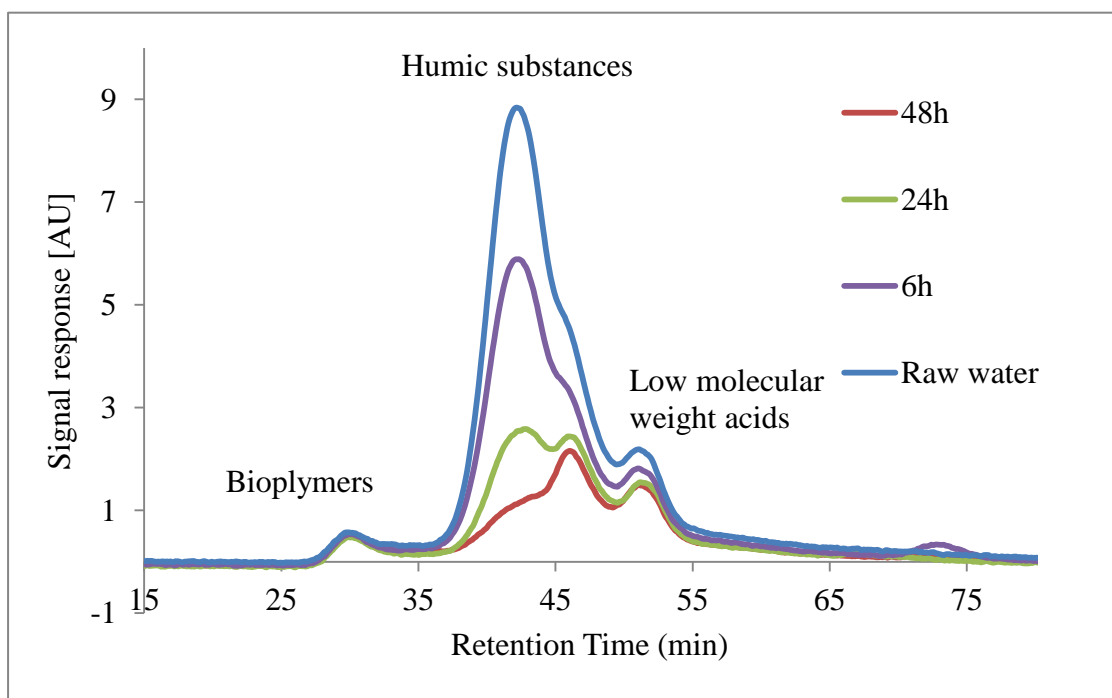


**Figure 4.14 LC-OCD results by TAN-1 resin in different adsorption times in Grand River water**

#### **4.3.5 Effect of Inorganic Anion Competition on PFCs Removal by Anion Exchange Resins**

Besides NOM, inorganic anions existing in surface water were also expected to be an important reason for the reduction of the PFC removal. Take the Grand River water sample as an example, the initial concentrations of chloride, nitrate and sulfate were 1.86, 0.13, 0.57 meq/L (or 66.1, 8.0, and 27.2 mg/L) respectively, which were several orders of magnitude higher than the initial concentrations of the PFCs. Other inorganic anions including nitrite, phosphate, fluoride, and bromide had concentrations lower than 0.5 mg/L; therefore, they were not considered in the inorganic anion competition study. As shown in Figure 4.16, the concentrations of nitrate and sulfate decreased to 0.12 and 0.44 meq/L (7.3 and 20.9 mg/L), and the concentration of chloride increased to 2.25 meq/L (79.7 mg/L) after 48-hour treatment by TAN-1 resin. All target anion exchange resins in this study were contained

chloride as counter ions; as a result, the exchange of anions led to the release of the chloride. After treatment, 23.2% of sulfate and 8.8% of nitrate were removed by TAN-1 resin. After 48 hours, the concentration of chloride released was calculated to be 0.38 meq/L, and the concentrations of nitrate and sulfate removed were 0.012 and 0.13 meq/L respectively. It revealed that besides the ion exchange of nitrate and sulfate, there were 0.24 meq/L anions removed by ion exchange resins after 48 hours, which may be associated with NOM. As shown in Figure 4.12, 3.2 mg C/L NOM was removed after 48 hours by TAN-1 resin. Compared to inorganic anions, only about  $0.5-1.5 \times 10^{-5}$  meq/L of PFCs were removed by TAN-1 resin. Inorganic anion data when using other resins showed similar results. The surface water results indicated that sulfate and nitrate could compete with PFCs in ion exchange process and this was further investigated. The inorganic anions results using other resins and the results in Lake Erie water showed similar trend to the results in Figure 4.15.

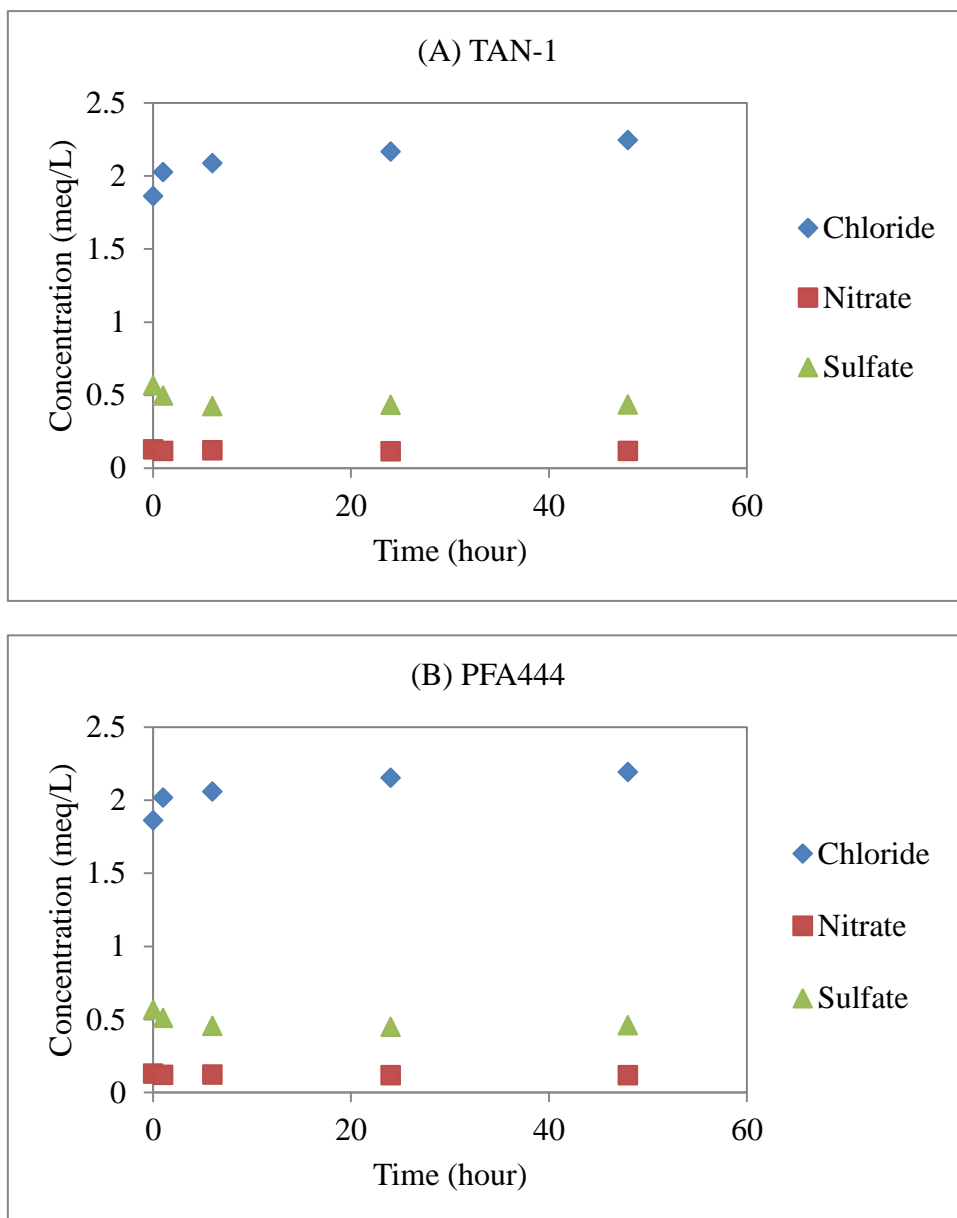


**Figure 4.15 Inorganic anions concentrations after treatment by TAN-1 and PFA444 resins in Grand River water: (A) TAN-1; (B) PFA444.**

#### **4.3.5.1 Influence of sulfate**

As discussed in the removal kinetics studies, both TAN-1 and PFA444 were selected as target anion exchange resins in the effects of inorganic anions studies. Figure 4.16 shows the PFCs adsorption kinetics using both PFA444 and TAN-1 resins in ultrapure water with different sulfate concentrations added. It can be observed that the existence of sulfate would decrease the removal of short chain PFCAs. Discussing

the data using PFA444 resin as an example, at sulfate concentration of 0.21 meq/L (10 mg/L), the removal of PFBA (C4) after 48 hours decreased from 96% to 77%, compared to the control experiments without sulfate. When the concentration of sulfate increased to 0.63 meq/L (30 mg/L), the removal of PFBA when using PFA444 resin further decreased to around 43%, and the removal of PFHxA (C6) started to have a trend to decrease (88% removal). The PFSAs and the long chain PFCAs remained high removals at both sulfate concentrations. TAN-1 resin showed similar results with PFA444 resin. TAN-1 resin had even lower PFBA and PFHxA removals of 16% and 45% respectively at sulfate concentrations of 0.63 meq/L (30 mg/L). It could be explained that the short chain PFCAs such as PFBA and PFHxA are more hydrophilic molecules with high polarity, which have more competition with inorganic anions.

#### **4.3.5.2 Influence of nitrate**

Figure 4.17 showed the PFCs adsorption kinetics using both PFA444 and TAN-1 resins at different nitrate concentrations. At low nitrate concentration of 0.05 meq/L (5 mg/L), all target PFCs remained high percentage removals of more than 97%. When the concentration of nitrate increased to 0.1 meq/L (10 mg/L), the removal of PFBA (C4) when using PFA444 resin had a slight decrease to 92%. The removals of PFSAs and the long chain PFCAs were not influenced by the existence of nitrate at both tested concentrations. TAN-1 resin showed similar results with PFA444 resin. At nitrate concentration of 0.1 meq/L (10 mg/L), TAN-1 had around 70% removal of PFBA. All the other PFCs remained high removals. The concentrations of nitrate and sulfate applied in the tests were in the range of their typical concentrations in surface waters. Comparing with sulfate, nitrate showed less competition with short chain PFCAs at the concentrations similar to in natural waters.



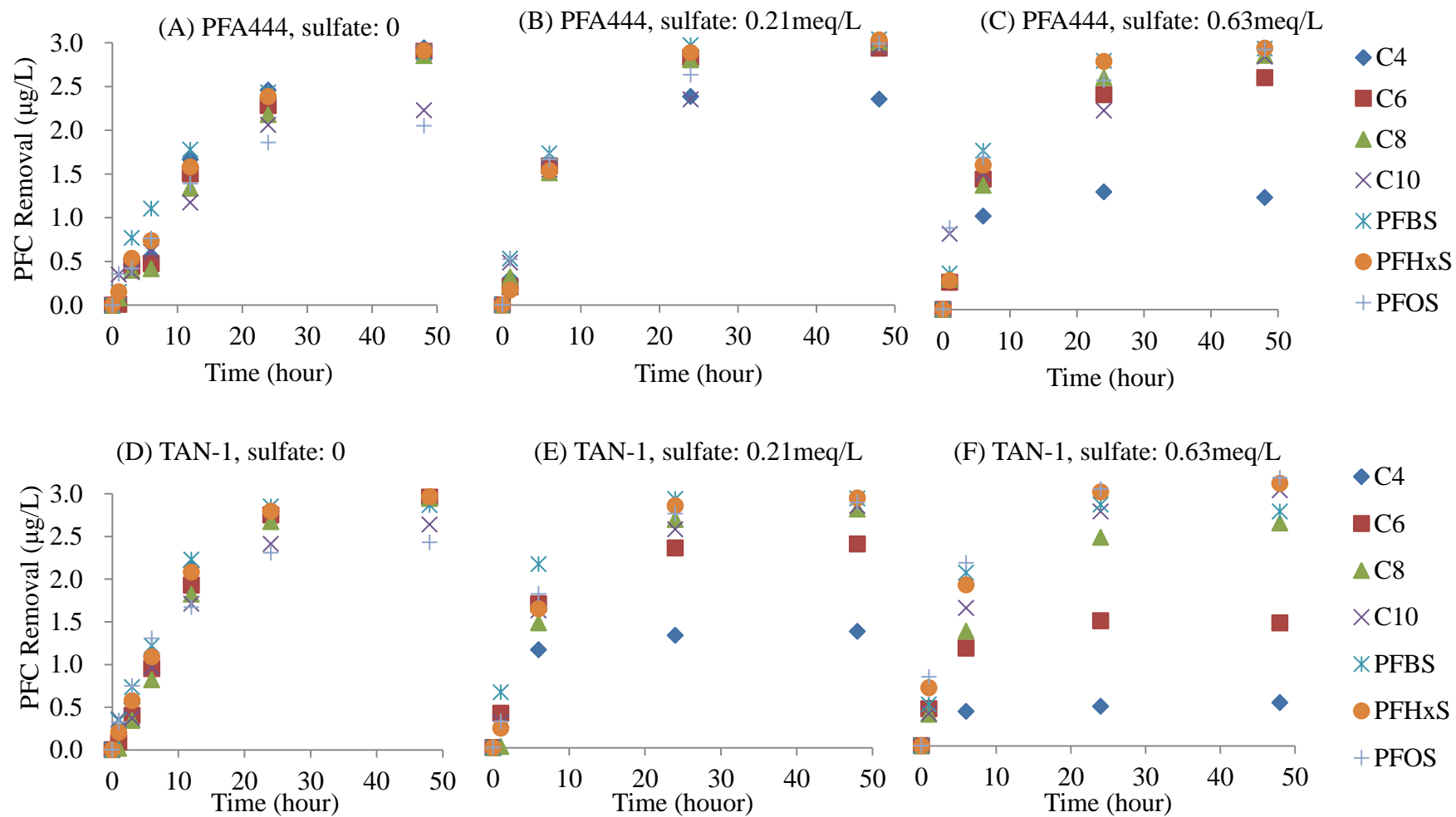
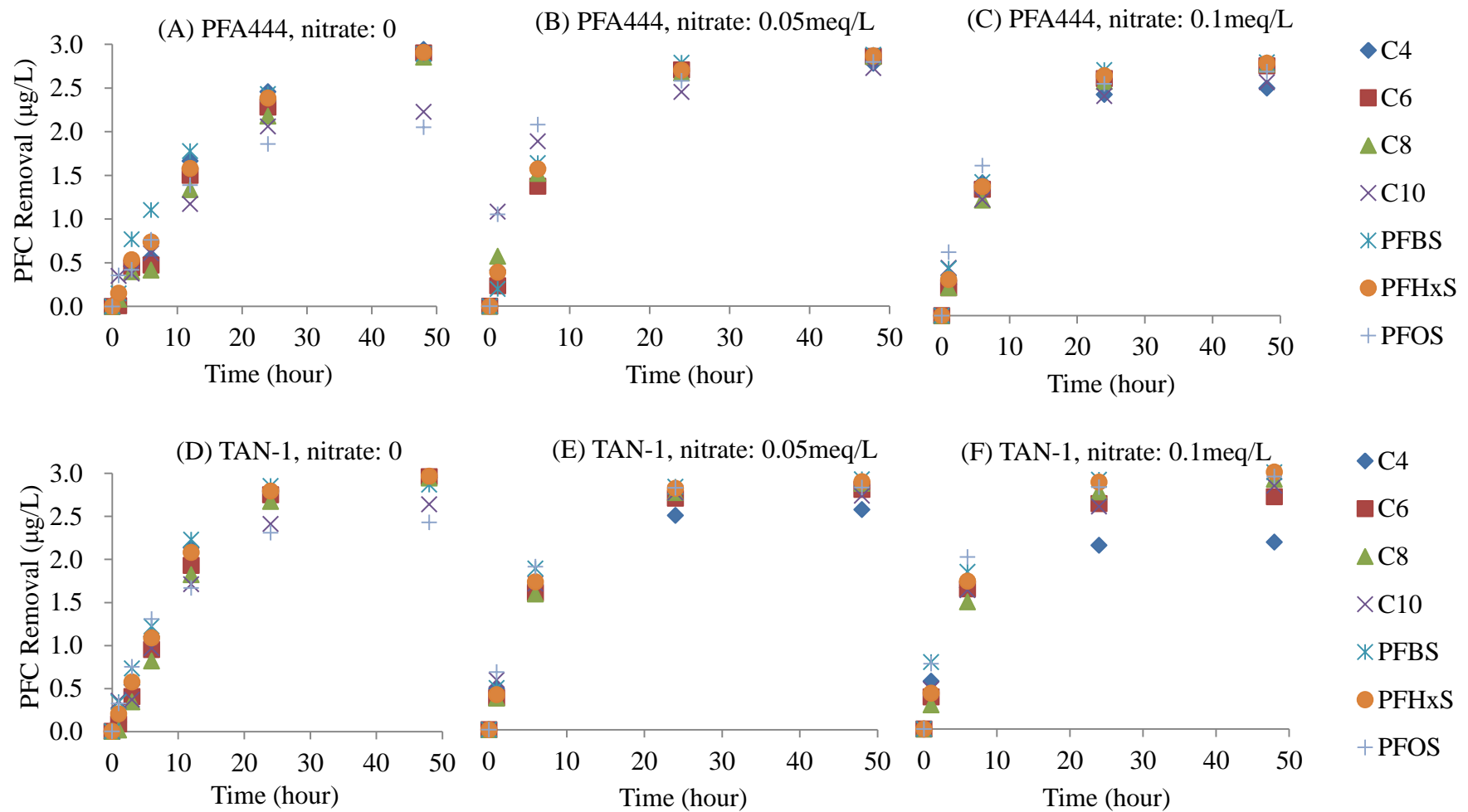


Figure 4.16 Sulfate competitions with PFCs in ultrapure water using both PFA444 and TAN-1 resins



**Figure 4.17 Nitrate competitions with PFCs in ultrapure water using both PFA444 and TAN-1 resins**

#### 4.4 Conclusions

The removal potential of four PFCAs and three PFSAAs by five commercially available anion exchange sorbents were assessed in ultrapure water, a river and a lake waters. The PFCAs were C4 (PFBA), C6 (PFHxA), C8 (PFOA) and C10 (PFDA). The PFSAs included PFBS, PFHxS, and PFOS. Under the conditions tested it was observed that:

(1) In ultrapure water, based on the kinetics experiment results, all anion exchange resins showed good removal of all target PFCs. The anion exchange resin TAN-1 was the best adsorbent. It achieved over 95% removal of all target PFCs in bottle point sorption kinetics experiments within 48 hours. As a Type III anion exchange resin, A555 resin had longest equilibrium time of more than 120 hours.

(2) In ultrapure water, short chain PFCs had high removal of 99% removal for all resins. As long chain PFCs, PFDA and PFOS had more than 67% removal after 48 hours for all resins.

(3) Both the Pseudo-second-order kinetics model and the Freundlich isotherms model had well prediction of the PFCs removal process by anion exchange resins. The adsorption isotherms showed similar results to the kinetics experiments.

(4) In both Grand River and Lake Erie waters, the removal performance of all target PFCs decreased especially for short chain PFCs. PFCAs had lower removal than PFSAs in surface water. All the resins had decreased PFC removal in surface water. As gel resins, PFA444 had relative higher PFCs removal in natural water.

(5) For the influence of resin properties, Type I resins showed higher adsorption rates compared to the Type III resin A555. Pore volume and surface area did not seem to be key impact factors, probably because all anion exchange resins had small pore volumes. In ultrapure water, both gel and macroporous resins showed good PFC removal; while, in surface water, gel resins were less impacted with NOM and inorganic anions compared to macroporous resins.

(6) All the resins had the ability to remove DOC. LC-OCD results showed that humic substances may be the presentative DOC which had competition with PFCs. Among all the

resins, TAN-1 showed the best NOM removal. The decline of the PFC removal may be caused by the competition from both NOM and inorganic anions.

(7) Sulfate concentration could significantly decrease short chain PFCA removal by ion exchange resins; while PFC removal by ion exchange resins could be less influenced by the existence of nitrate.

## Chapter 5

### **PFCAs and PFSA removal during drinking water treatment by ion exchange resins: column tests and regeneration**

#### **Summary**

To examine and optimize the suitable regenerants and operations for regeneration of selected ion exchange resins after PFCs treatment, and also to investigate processes of PFCs removal by ion exchange in column studies and the influence of resin and PFC properties on regeneration, the anion exchange resins regeneration tests and the ion exchange column experiments were conducted in this chapter. In ion exchange column studies, the breakthrough curves of PFCs in anion exchange column were examined. The results of column experiments in Grand River showed that the PFCs started to have complete breakthrough after 35 days or  $1.5 \times 10^5$  bed volumes. In anion exchange regeneration experiments, both batch tests and column tests were conducted. The results from the regeneration batch tests in ultrapure water indicated that the A555 had best regeneration performance. The regeneration batch tests also helped to identify the suitable regenerants for the column tests. In regeneration column tests, the elution curves of different regeneration operations were measured and compared to provide a preferable condition of regeneration.

#### **5.1 Introduction**

Ion exchange has been considered as a promising treatment method for PFCs removal (Deng et al., 2010). Although there have been some studies about using strong anion exchange resins for PFCs removal, they mainly focus on PFCs at high concentrations rather than those typical for source waters used for drinking water production (Deng et al., 2010). Also, the adsorption and regeneration performance of ion exchange resins change a lot

depending on the type of resins. Studies found that PFCs adsorption by certain ion exchange resins was irreversible using conventional regeneration methods (Carter & Farrell, 2010).

Ion exchange resins have been widely used for removing arsenic, metal cations, inorganic anions and NOM in water treatment systems. To decrease the operating cost of the ion exchange process, the regeneration of the ion exchange resins is significant; thus, finding anion exchange resins with good regeneration performance using appropriate regeneration conditions for PFCs removal would help with the application of the PFCs removal by anion exchange process.

Some recent literature studied the regeneration process of ion exchange resins after treating water containing PFCs. Zaggia (2016), Xiao (2012) and Chularueangakorn (2013) investigated the appropriate regeneration conditions for certain ion exchange resins. Zaggia (2016) found that although non hydrophobic resins have lower removal capacity, they are more regenerable compared with highly hydrophobic resins. Cation type of the regenerants is also proved to be an important factor for certain resins (Zaggia et al., 2016). XAD anion exchange resin can be reused eight times with NaOH and methanol without dramatically losing its PFCs removal performance (Xiao et al., 2012). Woodard et al. (2017) applied organic solvent and brine as regenerants for ion exchange regeneration after pilot-scale *ex situ* treatment of PFOA and PFOS. Gao et al. (2017) also used methanol and NaCl/NaOH mixed solution to regenerate IRA67 anion exchange resin after PFCs removal. The limited literature revealed that appropriate regeneration conditions for anion exchange resins after PFCs treatment need to be selected and optimized, and further studies are needed to investigate the influence of resin and PFC properties on regeneration.

As a result, the main objective of this research is to examine the proper regeneration methods for target ion exchange resins. The specific objectives are as follows:

- (1) To examine and optimize suitable regenerants and associated operating conditions for selected ion exchange resins after PFCs treatment.

(2) To investigate the influence of anion exchange resins and PFCs properties on regeneration.

(3) To provide technical support for real PFCs removal applications by testing regeneration conditions and column breakthrough curves. To evaluate one ion exchange resins selected from the batch study, to characterize the PFC breakthrough curves, to evaluate the regeneration efficiency, and to identify the regeneration conditions for pilot- and full-scale design.

In order to achieve the objectives of the study in Chapter 5, anion exchange resins regeneration batch experiments were conducted first to select appropriate resin and regenerant for PFCs removal (the selected resin and regenerant were then applied in the column studies), and to examine the impact factors for regeneration. The anion exchange column tests were then conducted and the breakthrough curves were tested to provide useful information as reference for the design and operation of pilot- and full-scale experiments. As last, the column regeneration experiments were implemented to optimize regeneration conditions and to evaluate the regeneration process after PFCs removal. A schematic diagram of the general experimental procedure of the study in this chapter is shown in Figure 5.1.

As discussed in Chapter 4, TAN-1 resin presented best PFCs removals and shortest equilibrium times in ultrapure water. PFA444 resin showed best PFCs adsorption performance in surface water among all the resin. A555 was the only resin with Type III quaternary ammonium functional group which was designed to reach high regeneration performance. As a result of the considerations discussed above, TAN-1, PFA444, and A555 resins were selected in the anion exchange resins regeneration batch tests. The resin with best regeneration performance in the batch tests, which was the A555 resin, was then applied in both the anion exchange column tests and regeneration column tests.

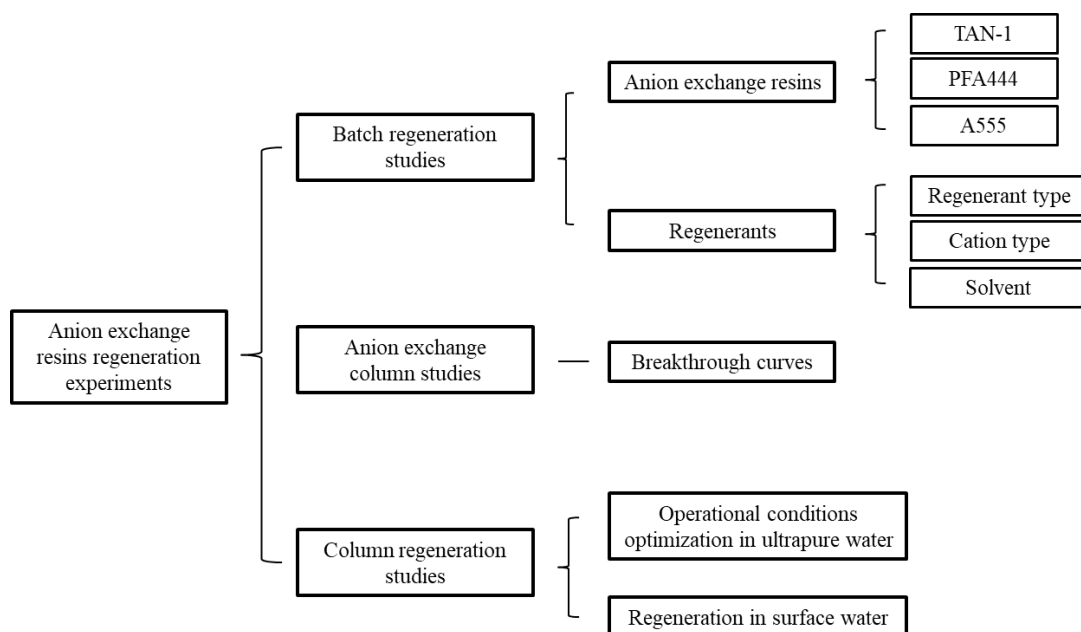


**Figure 5.1 Schematic diagram of the general experimental procedure of the study in Chapter 5.**

## 5.2 Materials and Methods

### 5.2.1 Target Compounds, Water, and Anion Exchange Resins

Four PFCAs and three PFSA s including PFBA, PFH<sub>x</sub>A, PFOA, PFDA, PFBS, PFH<sub>x</sub>S, and PFOS were purchased from Sigma-Aldrich (WI, USA). Their purity and carbon chain length information were listed in Table 4-1. More detailed information about physical and chemical properties of the selected PFCs was provided in Table 2-2 in Chapter 2. Amount of 30 mg of each target PFC was measured and dissolved in 1 L of high purity water to make PFC stock solutions. New solutions were prepared every 6 month, and were stored in polypropylene bottles in the fridge at 4 °C. The concentration of each target PFC spiked in samples was 1.0 mg/L in anion exchange resin regeneration batch tests. The initial concentrations of PFCs spiked in anion exchange column test were 30 µg/L, and the initial concentrations of PFCs spiked in regeneration column test were 60 µg/L.



Ultrapure water was generated from a Millipore Milli-Q<sup>®</sup> UV PLUS water system (MA, USA). Grand River water (GRW) was collected from the raw water intake of the Mannheim Water Treatment Plant (Region of Waterloo, ON, Canada) on August 21st, 2016. Table 5-1 listed the water quality parameters of this batch of Grand River water. No pH adjustment was done for all water samples in the study. Water samples were not filtered prior to the experiments.

**Table 5-1 Grand River water quality parameters**

	<b>pH</b>	<b>Turbidity (NTU)</b>	<b>DOC (mg C/L)</b>	<b>Cl<sup>-</sup> (mg /L)</b>	<b>SO<sub>4</sub><sup>-</sup> (mg/L)</b>	<b>NO<sub>3</sub><sup>-</sup> (mg/L)</b>
GRW	8.2	5.4	9.5	79.4	32.5	5.9

Of all the anion exchange resins tested in Chapter 4, three were selected and used in the regeneration batch tests including Purolite<sup>®</sup> A555 and Purofine<sup>®</sup> PFA444 which were obtained directly from Purolite Corporation (PA, USA), and DOWEX<sup>®</sup> TAN-1 which was purchased from Dow Chemical Company (MI, USA). The properties of target resins are listed in Table 4-3.

### **5.2.2 Regeneration Batch Tests**

The regeneration batch tests were conducted using the bottle point method described in Chapter 4 for resin preloaded with PFCs. The preloading and regeneration conditions were as follows: 100 mg resin was added to a 1 L plastic bottle in contact with a solutions of PFCs with initial concentrations of 1.0 mg/L for each PFC, and the bottle was put on a 150 r/min shaker for 48 hours. After filtering the resin, the concentrations of PFCs in the remaining solution were quantified to verify preloading efficiency for the resin. The preloaded resin was then put in a 1 L bottle with regenerants and the bottle was put back in the shaker for 48h, then the PFCs concentrations were quantified in the regenerants.

The PFC mixture for preloading included four PFCAs (C4, C6, C8, C10) and three PFSAs (PFBS, PFHxS, PFOS). PFC concentrations were 1.0 mg/L for each compound. Ion exchange resin dose (dry weight) was 100 mg/L (50 mg resins in 500 ml water). The contact time was 48h. Based on preliminary results, 48 h preloading would be safe to reach the equilibrium, and reach a more than 98% PFC loading rate (measured for all PFCs using all three target anion exchange resins).

The controlled variables were ion exchange resins and regenerants. Based on the previous kinetics and isotherms results in Chapter 4, three ion exchange resins with good PFCs removal performance were selected for a batch regeneration study. Resins used in this study were A502p, TAN-1, and PFA444. The batch regeneration results will guide the selection of one or two resins for the column study.

For the regenerants, three factors were considered in the fractional factorial experiments: A) regenerant type; B) cation type; C) solvent. The two levels of each factor are shown in Table 5-2:

**Table 5-2 Two-level factors for regenerants**

	<b>A. Regenerant type</b>	<b>B. Cation type</b>	<b>C. Solvent</b>
+	10% chloride salt	Na <sup>+</sup>	H <sub>2</sub> O
-	5% chloride salt and <b>0.5%</b> base	NH <sub>4</sub> <sup>+</sup>	<b>40%</b> Methanol

The factors of the regenerants were selected based on the literature, manufacturer information, and application examples. 5-10% chloride salt and the corresponding base are typical regenerants for strong base resins. In this study, a strong base cation (Na<sup>+</sup>) and a weak base cation (NH<sub>4</sub><sup>+</sup>) were examined for the selected resins. The solutions of water and 80% methanol were studied and compared with 40% in the preliminary experiments. After the preliminary experiments, 40% methanol was then applied as control factor in the regeneration batch studies.

A two-level 2<sup>3</sup> design was conducted for each ion exchange resin. It is shown in table 5-3:

**Table 5-3 Regeneration methods**

	<b>A</b>	<b>B</b>	<b>C</b>	<b>Conditions</b>
<b>1</b>	+	+	+	10% NaCl in H <sub>2</sub> O
<b>2</b>	+	-	-	10% NH <sub>4</sub> Cl in 40% MeOH
<b>3</b>	-	+	-	5% NaCl and 0.5% NaOH in 40% MeOH
<b>4</b>	-	-	+	5% NH <sub>4</sub> Cl and 0.5% NH <sub>4</sub> OH in H <sub>2</sub> O
<b>5</b>	+	+	-	10% NaCl in 40% MeOH
<b>6</b>	+	-	+	10% NH <sub>4</sub> Cl in H <sub>2</sub> O
<b>7</b>	-	+	+	5% NaCl and 0.5% NaOH in H <sub>2</sub> O
<b>8</b>	-	-	-	5% NH <sub>4</sub> Cl and 0.5% NH <sub>4</sub> OH in 40% MeOH

The regeneration efficiency (R) was used in this study to evaluate the regeneration performance of the anion exchange resins in different conditions as mentioned in the factorial design. R is defined and calculated as follows:

$$R = \frac{n_A - n_B}{n_C - n_D} \times 100\% \quad (\text{Equation 5.1})$$

n<sub>A</sub>: initial PFCs concentrations of the loading solution;

n<sub>B</sub>: final PFCs concentrations (after ion exchange) of the loading solution;

n<sub>C</sub>: initial PFCs concentrations of the regenerant;

n<sub>D</sub>: final PFCs concentrations of the regenerant;

For each batch, samples were taken to analyze the n<sub>A</sub>, n<sub>B</sub>, n<sub>C</sub>, and n<sub>D</sub> values.

### 5.2.3 Design of Anion Exchange Column Set-up and Operating Parameters

Two Masterflex<sup>®</sup> peristaltic tubing pump (Model No. 7520-10) (Cole-Parmer Instrument Co., IL, USA) were applied to provide hydraulic loading for the supply water. The columns

used in the anion exchange column tests were Kontes Flex-columns (Internal diameter: 1.5 cm, length: 20 cm, max volume: 36 ml, plastic column) (Kimble, TN, USA).

The setup of the column tests is shown in Figure 5.2. The flow direction is downward. Grand River water spiked with 30  $\mu\text{g/L}$  PFCs was used. The PFCs concentrations in the effluents and spent regenerants were analyzed. The breakthrough curves and elution curves of the column was examined. A parallel column without ion exchange resins was used to check for system losses of the PFCs. When small concentrations of the unwanted ion(s) can be tolerated in the effluent and the exchange in the regeneration step is favorable, cocurrent operation is chosen for regeneration.

The ion exchange resin A555 was selected for the column tests based on its regeneration performance in the batch tests.

Parameters of the column study are summarized in Table 5-4. These were selected based on the following discussions. The column tests were designed to evaluate the regeneration efficiency and to characterize the PFC breakthrough curves. As a result, a small bed volume was used. The empty bed contact time (EBCT) was considered based on the recommended operating conditions and adjusted according to the actual situation. The flow rate and bed volume were also adjusted to shorten the breakthrough time.

Taking the ion exchange resin A555 as a reference, the recommended operating conditions by the manufacture for A555 include the minimum bed depth of 0.8-1m, and the service flow rate of 5-25 m/h (Purolite Corporation, 2015). To shorten the contact time, the hydraulic loading of 5 m/h was applied and the EBCT = 0.24 min was used in the study. Ion exchange resins of 3.54 mL were placed in the column with the column inside diameter of 1.5 cm and bed depth of 2 cm. So the flow rate was 14.7 ml/min.

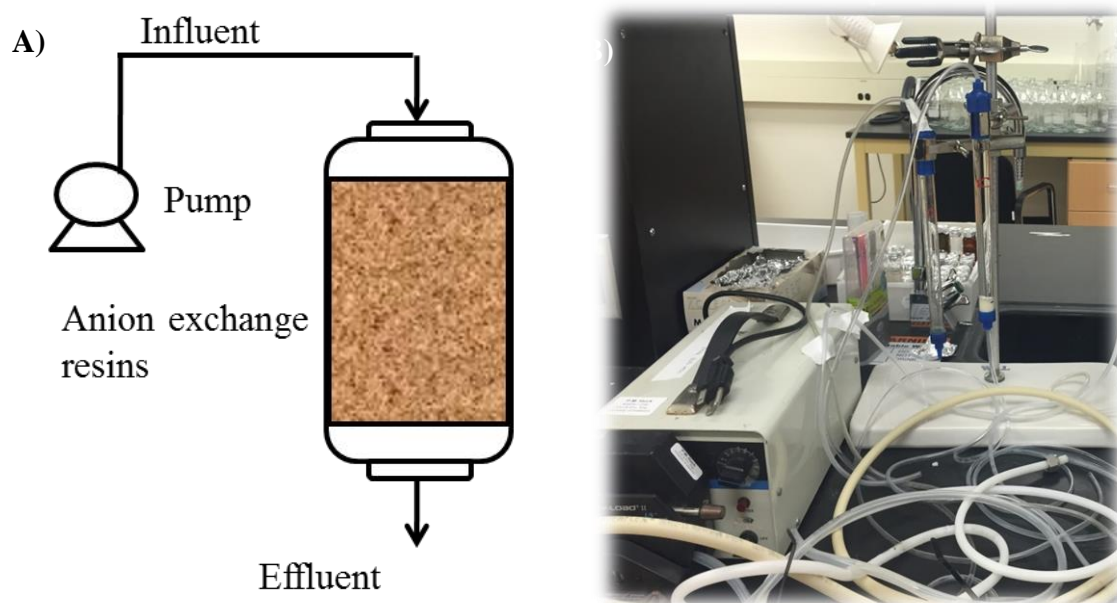


**Figure 5.2 Column test setup for ion exchange resins: A) schematic diagram; B) real setup.**

**Table 5-4 Anion exchange column tests parameters**

Column inside diameter	1.5 cm
Bed depth	2 cm
Bed volume (BV)	3.54 mL
EBCT	0.24 min
Flow rate	14.7 ml/min
Hydraulic loading	5 m/h
Volume/day	21.2 L

The breakthrough (saturation loading) curves were measured in the anion exchange column experiments. Samples of the effluent were collected and analyzed until the effluent concentration of the contaminant of interest equals the influent concentration. The samples were collected every two days according to the estimate breakthrough time of 30 days.

#### 5.2.4 Regeneration Column Tests

In the regeneration column tests, regeneration operational conditions listed in Table 5-5 were optimized in PFCs spiked ultrapure water. The optimized regeneration conditions were then applied in Grand River water. In the regeneration column tests, the loading (breakthrough) curves and the elution curves were measured separately to compare their regeneration performance.

The setup of the regeneration column tests was the same setup as introduced in section 5.2.3. Based on the requirements of the regeneration methods, either cocurrent or countercurrent operation for regeneration could be used in the regeneration column experiments. Considering the easy operation and simple setup for the selected column, the cocurrent operation of downward flow was used for the regeneration.

Controlled variables included water types and regeneration requirements. For water sources, both ultrapure water and natural water spiked with 60 µg/L PFCs were used. For each type of water, the breakthrough curves and elution curves were examined, and the regeneration requirements were optimized through factorial experiments. The type of the regenerants was studied and selected in the batch tests, and the regeneration time was decided by the elution curves. As a result, the regeneration flow rate and regenerant concentration were optimized in the column regeneration study. The experimental design of the regeneration column tests is listed in Table 5-5. The flow rate of 10 ml/min and the NaCl concentration of 10% were proved to be the conditions with good performance, and were repeated to estimate error.

**Table 5-5 Operational conditions need to be optimized for the regeneration column studies**

	A. Flow rate	B. Concentration of the regenerant salt
1	10 ml/min	10%

2	10 ml/min	5%
3	20 ml/min	10%
4	20 ml/min	5%

The breakthrough (saturation loading) curves were tested in the loading experiments. Samples of the effluent were collected and analyzed until the effluent concentration of the contaminant of interest reached equilibrium. The operating parameters of loading process in the regeneration column tests are the same as the anion exchange column tests parameters listed in Table 5-4.

After loading, the regeneration was conducted under the optimized condition in the previous study. A flow rate of 10 ml/min and NaCl concentration of 5% were applied in the natural water regeneration column experiments. The elution curves were detected in this process. Samples of regenerants were collected after it passed through the bed and the concentrations of PFCs were detected. The approximate range of the regeneration volume is around 300 BV. So the samples were collected every 30 BV. For the natural water samples, besides PFC concentrations, DOC, inorganic cations, and LC-OCD results were also monitored.

### 5.2.5 Analyses

All target PFCs were analyzed with a Shimadzu 8030 LC-MS/MS. An SPE process was conducted before the LC-MS/MS analysis. A Poroshell SB C18 column (50 mm × 2.1 mm internal diameter, 1.8 µm packing) (Agilent, CA, USA) was used for separation of the PFCs. Mobile phases were 5 mM ammonium acetate in Milli-Q water and methanol. The established analytical method was described in detail in Chapter 3.

The concentrations of the anions including chloride, sulfate and nitrate were analyzed by Dionex ICS-1100 ion chromatography (IC) system (Thermo Scientific, MA, USA). Dissolved organic carbon (DOC) was determined with Aurora 1030 TOC analyzer (OI

Analytical, TX, USA). Turbidity of all water samples was measured by Hach 2100P Turbidimeter (CO, USA). Water sample pH was monitored using ORION Benchtop 420A pH meter (MA, USA).

Scanning electron microscope (SEM) was conducted using Zeiss Merlin SEM with Gemini II column (Carl Zeiss, Oberkochen, Germany) to characterize the surface properties of the anion exchange resins before and after PFCs treatment in both ultrapure and surface waters. Before analysis, resins were dried at 100 °C for 12 hours and were coated with gold.

## **5.3 Results and Discussion**

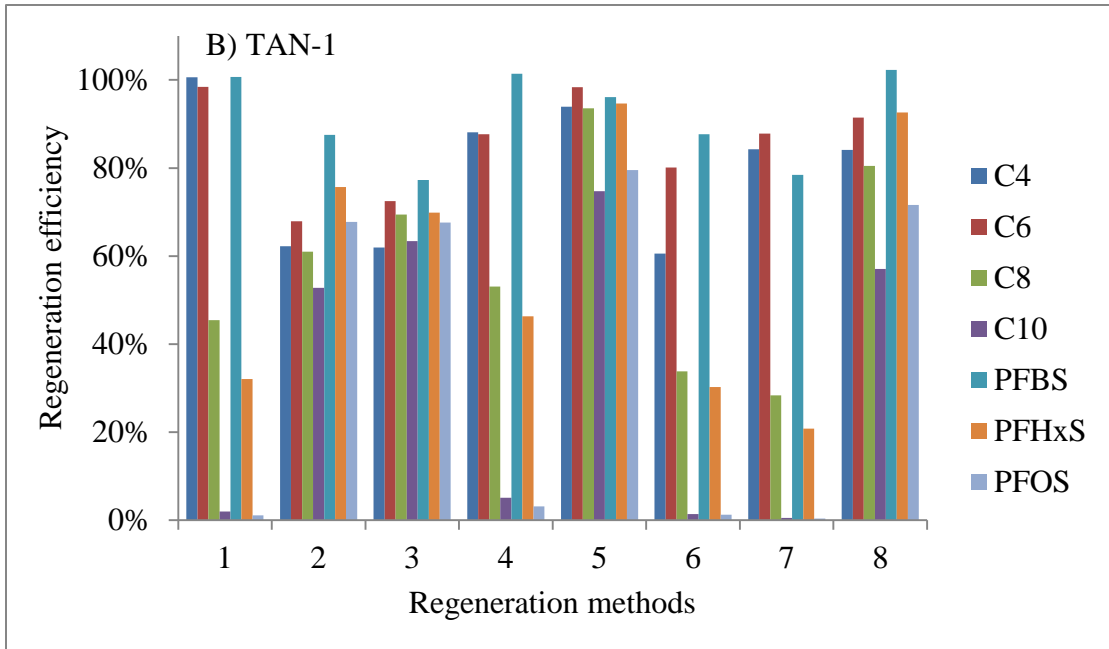
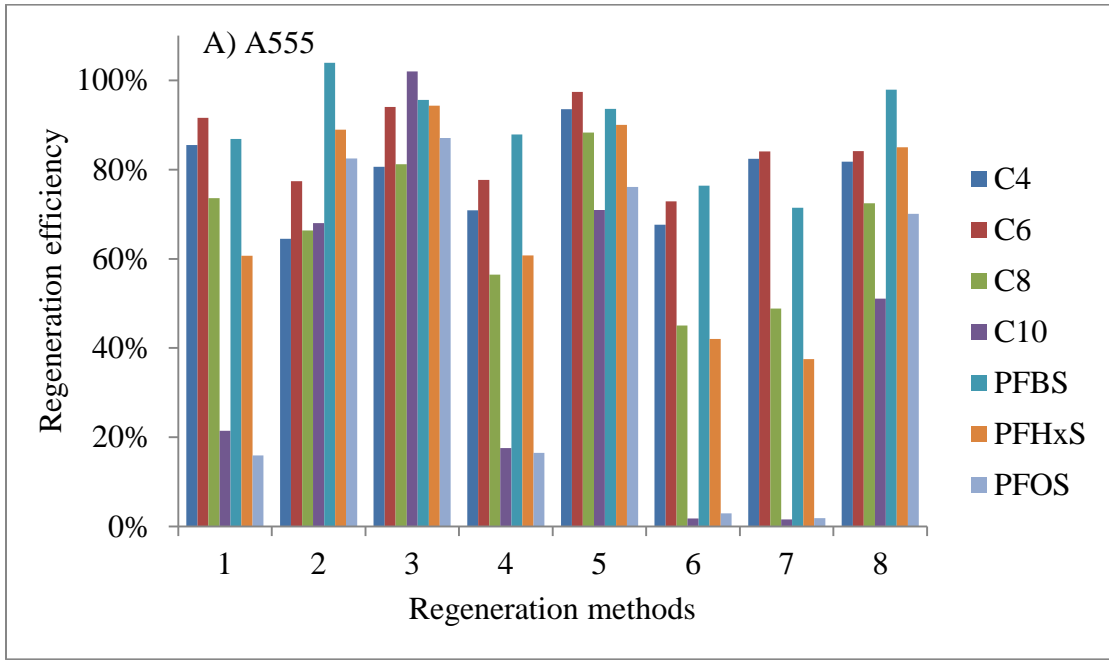
### **5.3.1 Anion Exchange Resins Regeneration Batch Experiments**

The anion exchange resins regeneration batch experiments were conducted to test and select suitable regenerants for 3 selected ion exchange resins, to preliminarily examine if the selected ion exchange resins are regenerable, and to determine the anion exchange resin with the best regeneration performance which was used in the subsequent column studies.

#### **5.3.1.1 Regenerant conditions selection**

As shown in Table 5-3, three impact factors of the regeneration conditions were listed in Table 5-3, including regenerant type, cation type, and solvent type.





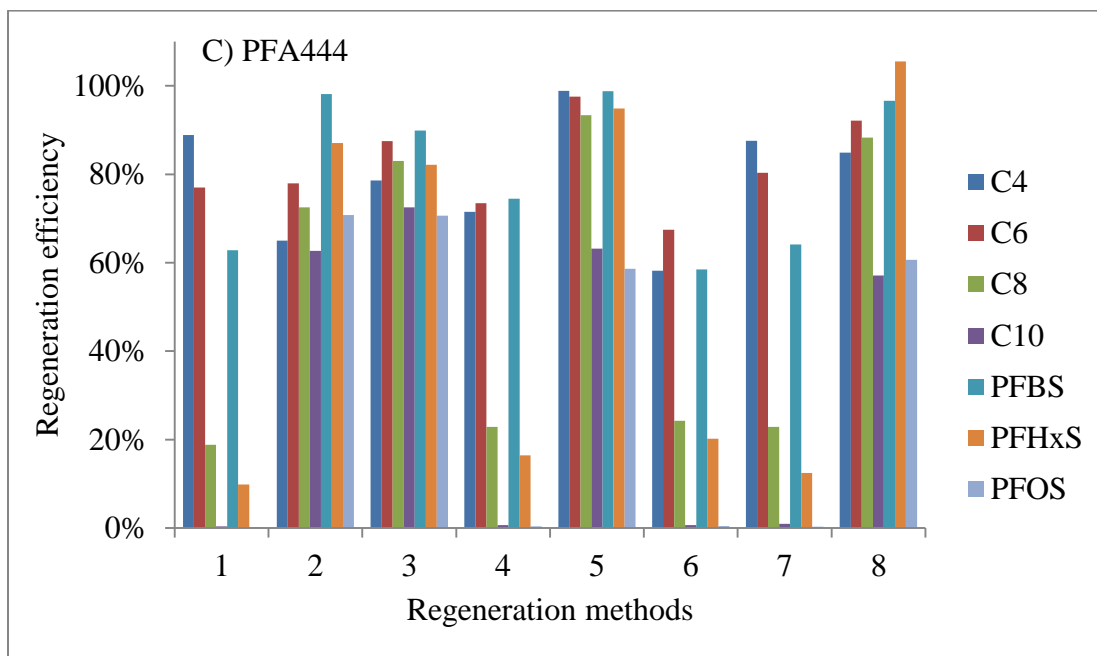


**Figure 5.3 Regeneration efficiencies of target PFCs after regeneration with different methods: A) A555 resin, B) TAN-1 resin, C) PFA444 resin. Regeneration method 1) 10% NaCl in H<sub>2</sub>O; 2) 10% NH<sub>4</sub>Cl in 40% MeOH; 3) 5% NaCl and 0.5% NaOH in 40% MeOH; 4) 5% NH<sub>4</sub>Cl and 0.5% NH<sub>4</sub>OH in H<sub>2</sub>O; 5) 10% NaCl in 40% MeOH; 6) 10% NH<sub>4</sub>Cl in H<sub>2</sub>O; 7) 5% NaCl and 0.5% NaOH in H<sub>2</sub>O; 8) 5% NH<sub>4</sub>Cl and 0.5% NH<sub>4</sub>OH in 40% MeOH (More than 98% uptake of 1 mg/L of each PFC).**

The regeneration efficiency results of the anion exchange resins regeneration batch tests are shown in Figure 5.3. Compared to the regeneration conditions without methanol, the conditions 2, 3, 5, and 8 which included methanol showed much higher PFCs regeneration efficiencies. For the conditions 1, 4, 6, and 8 without organic solvent addition, long chain PFCs performed lower regeneration efficiency than short chain PFCs.

The results showed that short chain PFCs had better regeneration performance than long chain PFCs, and PFCAs had higher regeneration efficiency compared to PFSAs. For the influence of the regenerants, higher concentration of the regenerant salts could help increase the regeneration efficiency. Na<sup>+</sup> ions had better regeneration performance than NH<sub>4</sub><sup>+</sup> ions. It

is probably because that  $\text{NH}_4\text{Cl}$  is an acidic salt, which influenced the regeneration of anions from resins; however,  $\text{NaCl}$  is a neutral salt which is easy to ionize in water and can help with the regeneration. Organic solvents could significantly increase regeneration efficiency of all PFCs especially the long chain PFCs and the PFSAs. It is because that the organic solvents can easily dissolve and remove more hydrophobic compounds such as long chain PFCAs and PFSAs. Among all three selected resins, A555 had higher regeneration efficiencies for most of the PFCs when methanol was not used in the regenerants; thus it was then applied in the column tests.

In the literature, XAD4 and Dow Marathon A resins performed PFOA regeneration efficiencies of 95% and 63% using 5%  $\text{NaCl}$  in methanol as regenerant (Chularueangksorn et al., 2013), which was similar to what was observed in this study. It can be found that, in most of the studies (Woodard et al., 2017; Gao et al., 2017; Xiao et al., 2012), organic solvent was applied to regenerate anion exchange resins after PFCs treatment. As shown in Figure 5.3, A555 resin can reach a high PFOA regeneration efficiency of up to 73.6% in method 1 (10%  $\text{NaCl}$  in  $\text{H}_2\text{O}$ ) without using organic solvent.

As PFCs with a higher polarity, as indicated by their lower mass/charge ration (Table 2.1), short chain PFCAs are more amenable to electrostatic interactions and anion exchange processes, which was speculated to be the reason that short chain PFCAs had better regeneration performance compared to the other PFCs. Electro static interactions played important role in anion exchange process especially for short chain PFCAs. Methanol could increase the regeneration efficiencies of long chain PFCs and PFSAs. This also demonstrated that hydrophobic adsorption was more dominant for long chain PFSAs in anion exchange treatment.

As can be observed in the regeneration conditions selection batch experiments (Figure 5.3), the application of methanol as regenerant can substantially increase the regeneration efficiencies of target PFCs; however, the use of organic solvents will lead to high operational costs because of disposal/treatment requirements for the regenerant waste. Thus, the organic

solvents were not used in the regeneration column experiments. As the resin with best regeneration performance when organic solvents were not used, A555 resin was selected for subsequent column tests. If organic solvents like methanol were to be applied as regenerants, adequate treatment of the regenerant waste as a high concentration chemical oxygen demand wastewater is required before it is discharged.

### **5.3.1.2 Anion exchange resins selection**

As discussed earlier, the regenerants with methanol showed much higher PFCs regenerations. This trend not only showed when using A555 resin, but also when using TAN-1 and PFA 444 resins. When methanol was used in the regenerants, all three resins had extremely high PFCs regeneration performance. However, when there was no organic solvent added in the regenerants, the regeneration performance of the A555 resin was more superior compared to the other two resins, especially when organic solvent was not used. When no methanol was used, PFA444 resin showed lowest regeneration efficiencies for target PFCs compared to the other resins. Among all the three selected resins, A555 resin showed best regeneration performance, especially when organic solvent was not added in the regenerants. Thus, A555 resin was selected to be the one applied in the anion exchange column tests.

## **5.3.2 Anion Exchange Column Tests**

### **5.3.2.1 Breakthrough curves in surface water**

To test the anion exchange performance of PFCs removal and to provide operation reference for the real application, anion exchange column experiments were conducted using A555 resin in both ultrapure water and Grand River water with the initial PFCs concentrations of 30 µg/L and the breakthrough (saturation loading) curves were measured. The column tests in ultrapure water were measured first, and the resulting breakthrough curve is shown in Figure I.1 in Appendix I. The breakthrough curve in ultrapure water showed low initial breakthrough of less than 3% and kept the same trend until the end of the

experiment when the bed volume was 60000. Considering that it would take a very long time to reach complete breakthrough in ultrapure water compared with that in surface water, the column experiment in ultrapure water was ended at bed volume of 60000 without complete breakthroughs. The results of the breakthrough curves of column tests in Grand River water are shown in Figure 5.4. The breakthrough curves ended at the BV of 210000, which was a 35-day experiment.

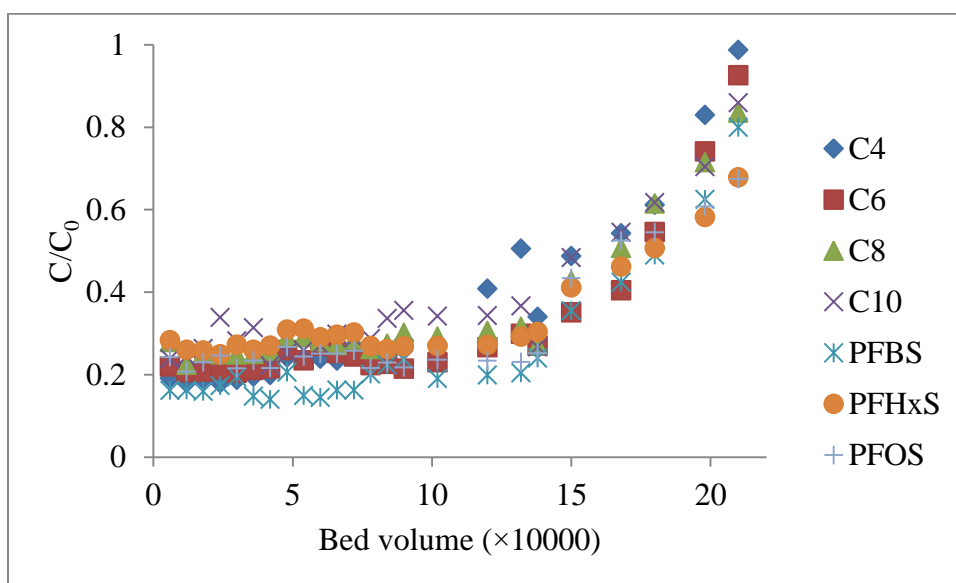


**Figure 5.4 Breakthrough curves of PFCs in anion exchange column tests using Grand River water ( $C_0$  was 30  $\mu\text{g/L}$ )**

From the Figure 5.4, it can be observed that PFCs had breakthrough of around 20% in the first a few collected samples, which indicated that the small ion exchange resin column setup could not removal all PFCs under the designed conditions. The tested breakthrough curves can be separated to two steps. The first step is from 0 to 100000 BV, and the second step is after 100000 BV. In the first step when the BV is below 100000, all selected PFCs showed similar breakthrough of around 20%. PFBS which is the short chain PFSA showed relative lower breakthrough concentrations, and the PFDA which is the long chain PFCA had higher concentrations; while the concentrations of the other PFCs did not show significant

differences. In the second step, the breakthrough curves had gradually increased trend. In this step, PFBA which is the short chain PFCA had higher breakthrough concentrations than the other PFCs. After 210000 BV, PFBA reached nearly 99% breakthroughs.

The phenomenon that there about 20% initial breakthrough and it took a much longer time than might be expected to reach nearly complete breakthroughs in the column tests using GRW may be caused by the following reasons. Firstly, the bed depth was too small to removal all the PFCs during the contact time. To shorten the contact times, the bed depth of the small column was set to be only 2 cm. As discovered in the preliminary experiments, a larger column bed depth could lead to lower initial breakthroughs. Secondly, there could be wall effects in the small column experiments which influenced the ion exchange process. Since it was a small column experiments, the diameter of the column was only 1.5 cm. As the column diameter decreases, the percentage of flow down the walls of the column increases, which increases the wall effects and the initial breakthroughs. Besides, the competition with the NOMs also led to higher initial breakthroughs. As shown in Figure I.1 in the appendix, the column tests using ultrapure water also presented initial breakthroughs, but much lower compared to using GRW.

Perhaps in part due to the initial breakthroughs, the time of the complete breakthroughs was longer than expected, since if material is transported through the column by wall effects it is not really contacting the resin. However the complete reason for the longer than expected breakthrough times is unknown.

Zaggia et al. (2016) also reported that short chain PFCs reached the breakthroughs earlier than long chain PFCs and PFCAs reached the breakthroughs earlier than PFSA by using anion exchange resins, which had the same trend with this study; however, they presented much faster complete breakthroughs at 10000 to 160000 BV. The breakthrough curves results also confirmed the findings of anion exchange resins kinetics experiments in Chapter 4 that short chain PFCAs had lower adsorption capacities in surface water.

The trend of breakthrough curves of target PFCs in column experiments could provide operation reference for the real applications. For the operation of anion exchange treatment to remove PFCs, the treatment should be stopped at the end of the first step when the BV is around 100000 before the breakthroughs occurred, and a regeneration process is needed.

### 5.3.2.2 SEM results

The SEM images of the A555 resin before and after treated (from the column tests in section 5.3.2.1) with PFCs containing water of both ultrapure and surface water are shown in Figure 5.5, 5.6, and 5.7. It showed that PFCs, NOM and even microorganisms can be adsorbed on the surface of the resin and the pore size of the resin decreased after treatment, which could probably explain the decrease of the anion exchange performance after certain time treatment.

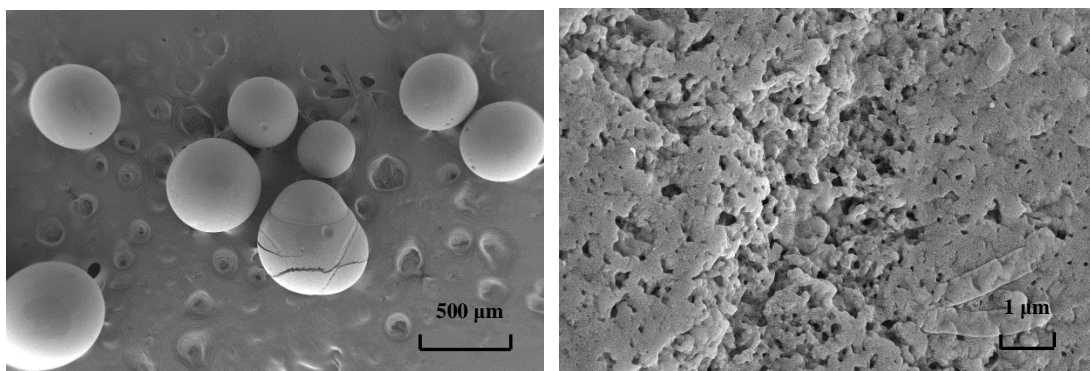


**Figure 5.5 SEM images of unused A555 resin and its surface**

As can be seen in Figure 5.6, after the treatment of the PFCs spiked ultrapure water, the surface of the resin was covered by the substances which were supposed to be largely contributed by PFCs (the PFCs concentrations were 30 μg/L which were close to or even higher than the DOC background in ultrapure water). The pores on the surface of the resins were blocked, so that the effective pore volumes of the resins decreased and the adsorption and ion exchange performance were influenced.

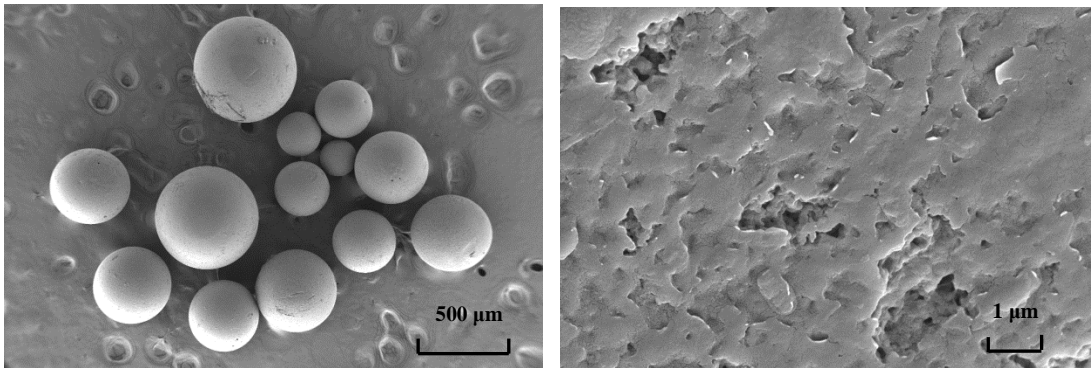


**Figure 5.6 SEM images of A5555 resin and its surface after treating PFCs in ultrapure water.**

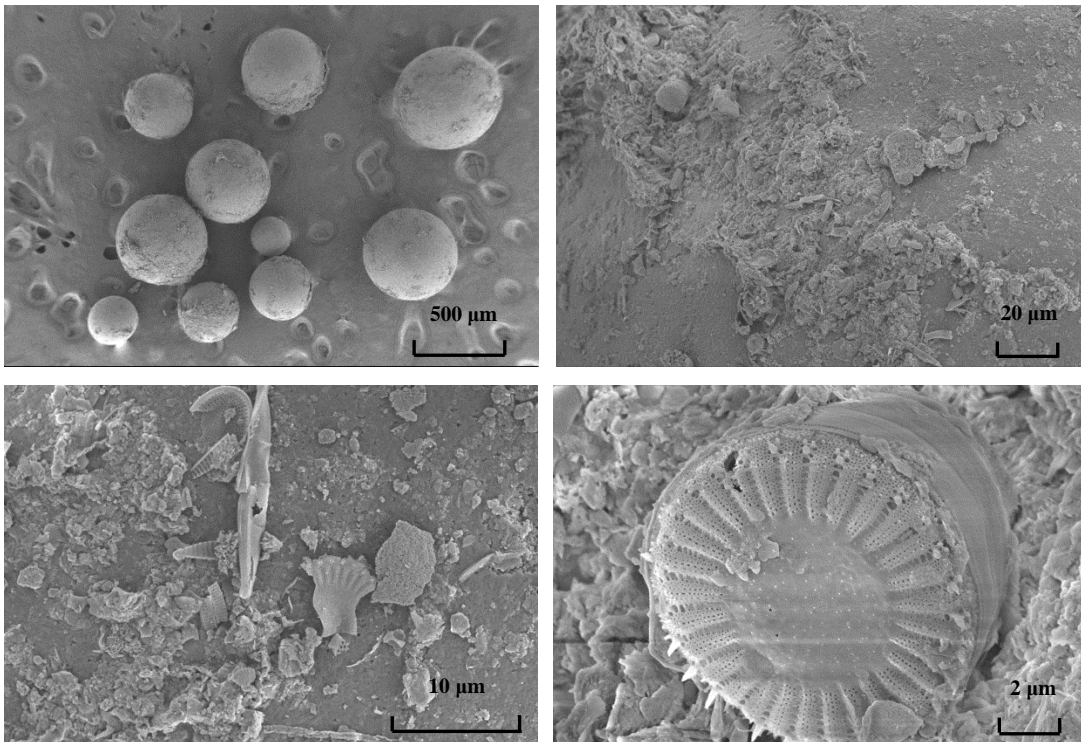


**Figure 5.7 SEM images of A5555 resin and its surface after treated with PFCs in Grand River water.**

In Figure 5.7, the surface of the resin was adsorbed by much more contaminants which were the combinations of the NOM and microorganisms. The microorganism shown in the figure was a typical representative of the diatoms.



### 5.3.3 Anion Exchange Resins Regeneration Method Optimization in Column Experiments

To test the anion exchange resins regeneration in the column experiments, the PFCs spiked ultrapure water was first loaded on the column, and then the column was regenerated using different regeneration methods. The regeneration method with best performance was then applied in the surface water regeneration column experiments. The initial concentration of each PFC spiked in either ultrapure water or Grand River water was kept as 60 µg/L.

#### 5.3.3.1 Column loading using PFCs in ultrapure water

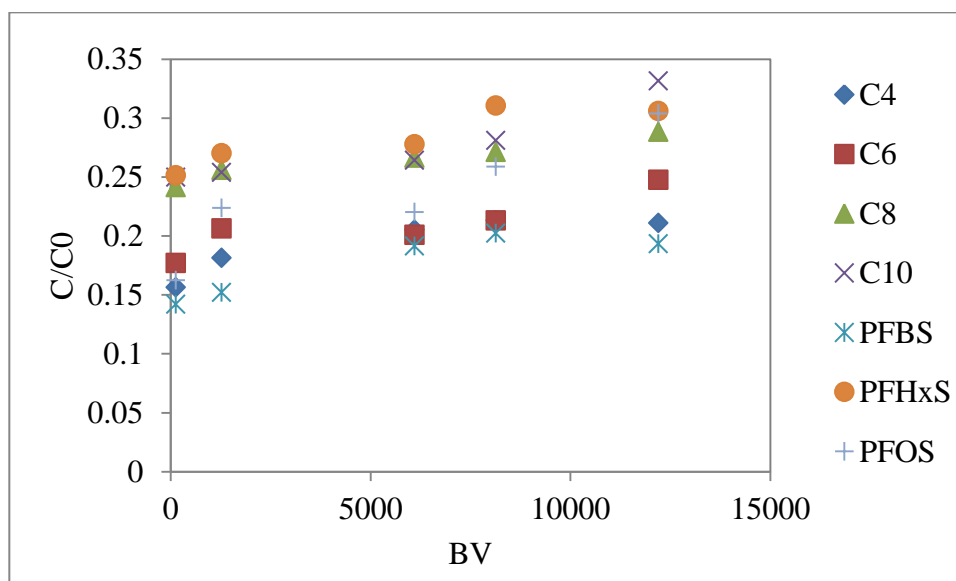


**Figure 5.8 PFCs breakthrough curves for regeneration method optimization ( $C_0$  was 60 µg/L)**

The results of the PFCs breakthrough curves for regeneration method optimization were shown in Figure 5.8. It was an example of the regeneration breakthrough curves. All the other curves were similar to those showing in the Figure 5.8. In the first hour, the effluents were detected to contain 15% to 20% breakthroughs. After 48 hours, the breakthroughs gradually increased to 18% to 32%. The results were similar to the breakthrough results in

the column tests. From the data of Figure 5.8, it can be calculated that the amount of each PFC loaded on the anion exchange resins was from 1.81 to 2.07 mg, which can be transferred to be around 0.512-0.585 mg/ml resin.

### **5.3.3.2 Impact of regeneration conditions**

After loading PFCs spiked ultrapure water, the regeneration conditions were tested and the elution curves were measured and are shown in Figure I.2 in Appendix I. In Figure I.2, the areas surrounded by the elution curves and coordinate axes present the amount of PFCs eluted from the anion exchange column; thus, the regeneration efficiency of each PFC in each condition can be calculated. The results of the regeneration efficiencies are shown in Figure 5.9. Taking PFBA (C4) as an example, the total amounts of PFBA eluted were 1.41, 1.36, 1.00, and 0.92 mg respectively in figures (a), (b), (c), and (d) in Figure I.2. Based on the loaded amount of PFBA in section 5.3.3.1, the regeneration efficiencies of PFBA in the 4 conditions were 77.8%, 75.2%, 55.2%, and 50.8% respectively. It can be observed that in all four conditions, PFBA (C4) showed best regeneration performance, followed with PFHxA (C6). The short chain PFCs had better regeneration performance than long chain PFCs, and PFCAs had better regeneration performance than PFSAs. These data confirmed the results of the regeneration batch tests.

Comparing the regeneration efficiency results in Figure 5.9, a higher concentration of the NaCl (10%) in regenerants had only very slight increase to the regeneration performance compared to 5% NaCl as the calculations in the previous paragraph. A slower regeneration flow rate (10 ml/min) had obvious increased regeneration performance compared to higher flow rate of 20 ml/min. Thus, 5% NaCl and 10 ml/min flow rate was considered to be the best conditions.

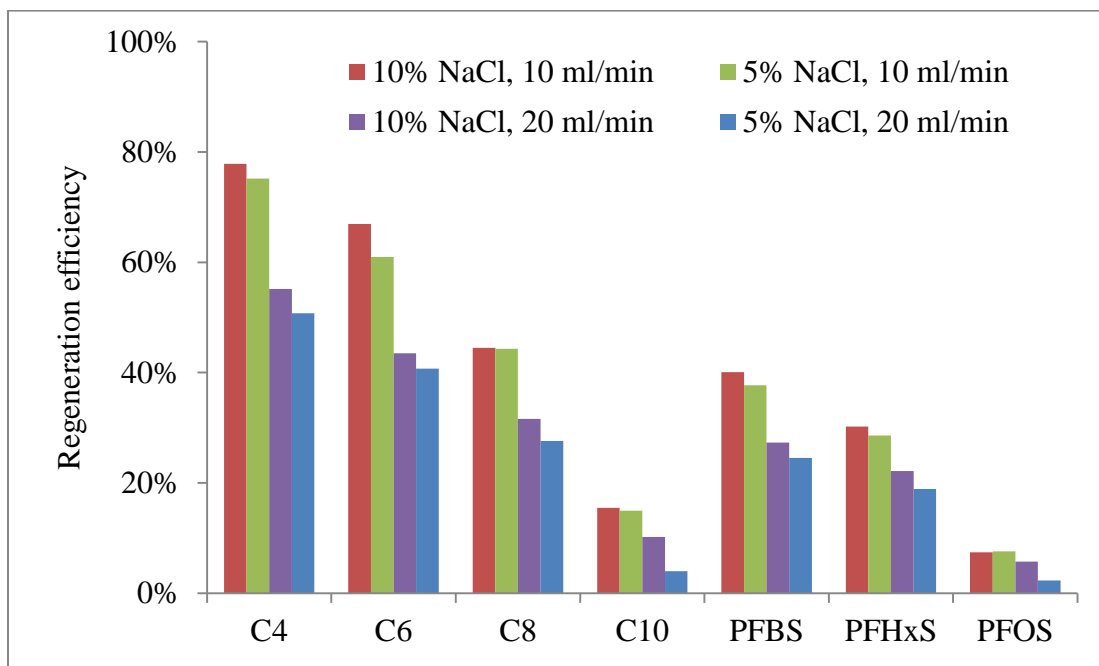


**Figure 5.9** Regeneration efficiencies of target PFCs when using different regeneration operation conditions in ultrapure water.

### 5.3.4 Anion Exchange Resins Regeneration Column Experiments Using Surface Water

#### 5.3.4.1 Loading curves

The loading curve of the DOC is shown in Figure 5.10. The raw GR water had a DOC concentration of 9.3 mg/L. In the first hour, the DOC concentration was already 5.6 mg/L. After 48 hours, it gradually increased to around 8.9 mg/L, which was a 93% breakthrough. After 5 days, the DOC had only very slight increase, which indicated that it was closed to the equilibrium.

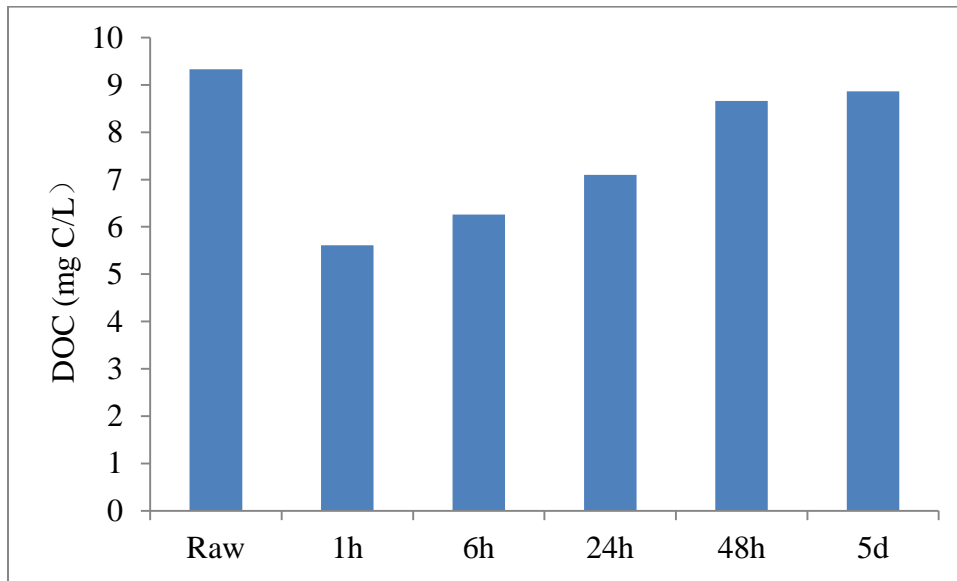


**Figure 5.10 DOC loading curve**

Figure 5.11 presents the loading curves of the inorganic anions. In the first hour, the chloride concentration of the effluent had a sharp increase to 110 mg/L, and concentrations of both nitrate and sulfate had obvious decrease. This was because the sulfate and nitrate in the loading water was exchanged to the anion exchange resins and the chloride was released from the resins. From the first hour to 24 hours, the concentrations of the chloride decreased to near the concentration in raw water, and the concentrations of the nitrate and sulfate also increased to around the concentrations in raw water. After 48 hours, concentrations of all three inorganic ions in the effluent had slight decrease, which may indicate the increase of the PFCs in the effluent.

Considering the DOC and inorganic anions loading results, as well as the PFCs loading curves, the loading time for the regeneration column tests was decided to be 48 hours.

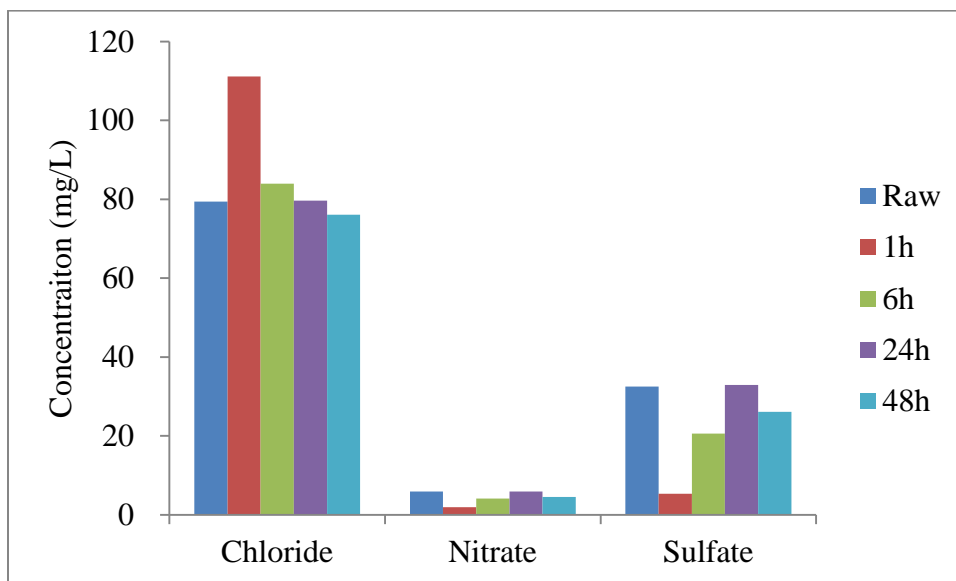


**Figure 5.11 Inorganic anions loading curves**

The loading (breakthrough) curves of PFCs in surface water are shown in Figure 5.12. Unlike the breakthrough curves of PFCs in ultrapure water, it reached the breakthrough much faster in Grand River water. Compared to the results in ultrapure water, the PFCs reached high breakthroughs of 50% to 100% in 48 hours. Compared to the breakthrough curves of anion exchange column experiments in Grand River water, the loading curves in the regeneration column tests reached breakthroughs much faster because the concentrations of PFCs doubled in the regeneration column tests (60 µg/L).

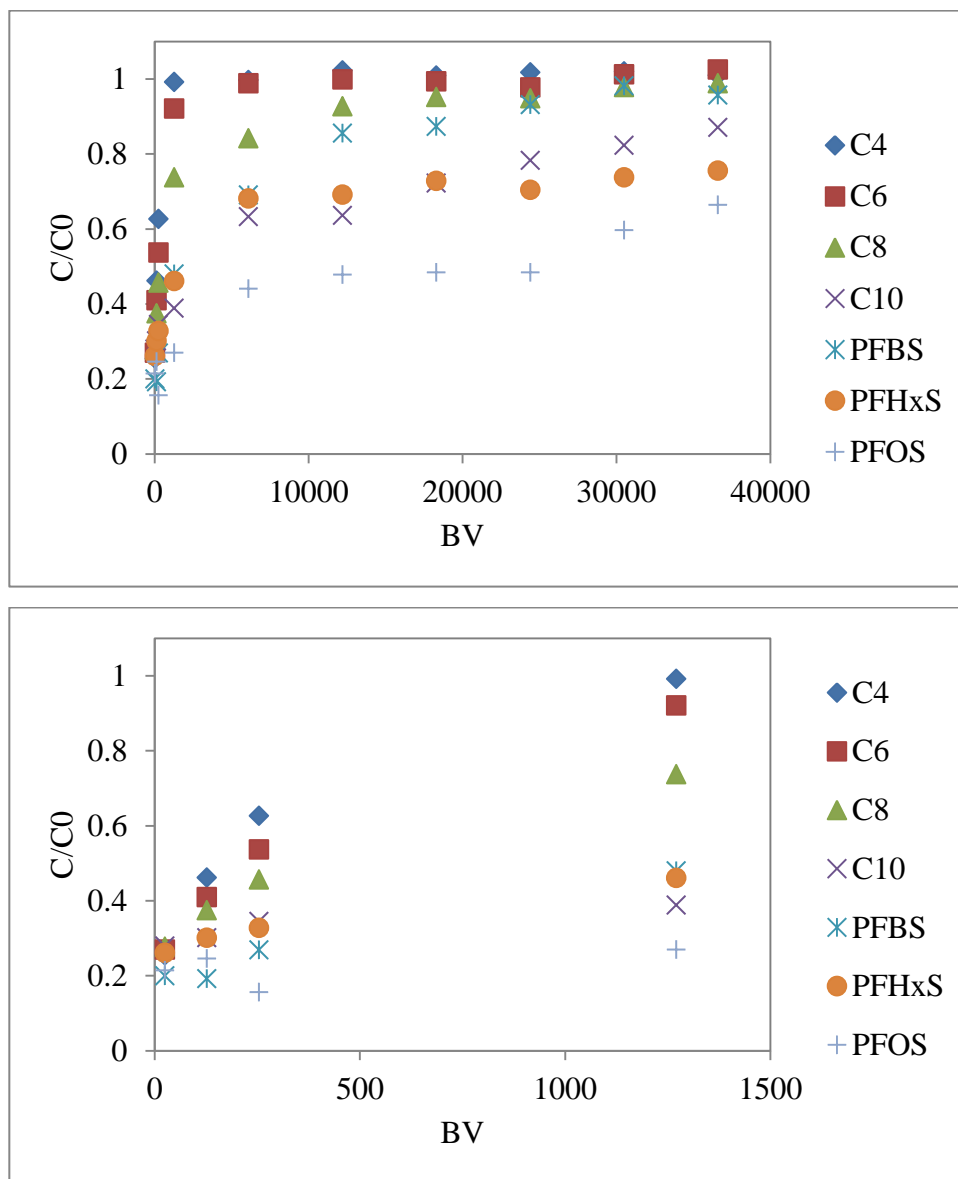


**Figure 5.12 Regeneration loading curves using Grand River water ( $C_0$  was  $60 \mu\text{g/L}$ )**

It can be observed that after 5 hours, PFBA (C4) had already reached near 100% breakthrough. After 24 hours, most PFCs reached the equilibrium. Short chain PFCs and PFCAs showed earlier breakthrough. After 100 hours, PFOS which had an equilibrium of around 50% breakthrough, had concentrations with continued trend to increase.

### 5.3.4.2 Regeneration elution curves

The results of anion exchange resins column regeneration elution curves using Grand River water are shown in Figure 5.13.

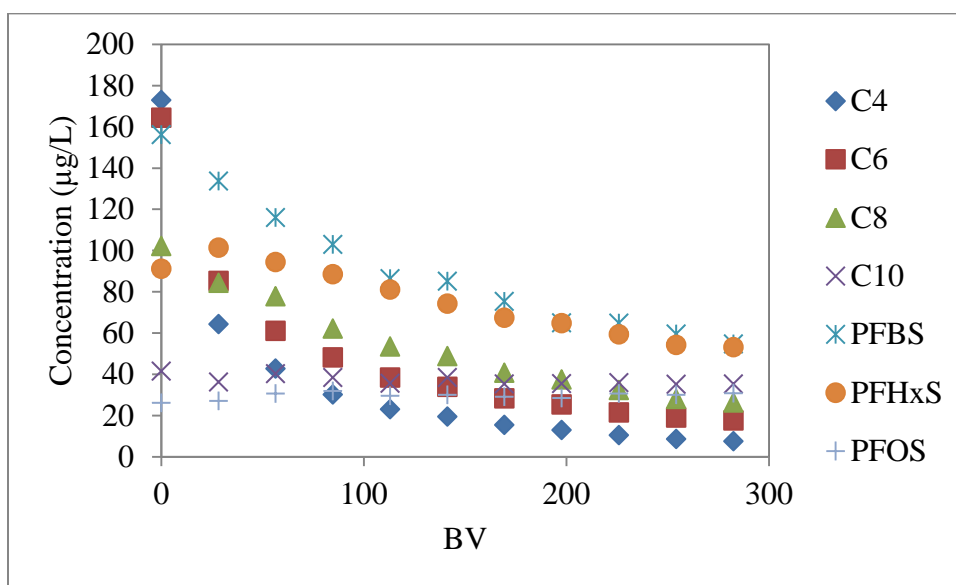


**Figure 5.13 Anion exchange resins column regeneration elution curves using PFCs spiked Grand River water**

Compared to the results of using PFCs spiked ultrapure water in Figure 5.9, all PFCs showed both longer regeneration equilibrium times and lower exchange concentrations. The regeneration efficiencies of target PFCs were calculated to be from 39% to 82%. Different from the results in ultrapure water, short chain PFSA, such as PFBS and PFHxS, showed better regeneration performance. It revealed that PFSA had more competition with NOM and inorganic anions in natural water, so they tended to be regenerated from the anion exchange resins. It also further proofed the experimental results in the batch studies.

## 5.4 Conclusions

In this chapter, three anion exchange resins including A555, PFA444, and TAN-1 were selected and tested in the regeneration batch tests. The results showed that short chain PFCs had better regeneration performance than long chain PFCs, and PFCAs had higher regeneration efficiency compared to PFSAs. For the influence of the regenerants, higher concentration of the regenerant salts could help increase the regeneration efficiency.  $\text{Na}^+$  ions had better regeneration performance than  $\text{NH}_4^+$  ions. Organic solvents could significantly increase regeneration efficiency of all PFCs especially the long chain PFCs and the PFSAs. Among all three selected resins, A555 had the best regeneration ability, especially when regenerants were used without organic solvents, and then applied in the column tests..

A small column test of A555 resin using Grand River water spiked with target PFCs was operated and studied. The breakthrough curves of all PFCs were tested. Before the BV is 100000, all selected PFCs showed similar breakthrough of around 20%. After 100000 BV, the breakthrough concentrations of all PFCs gradually increased and 90% breakthroughs were reached after 220000 BV.

The SEM images of the A555 resin before and after treated with PFCs containing water of both ultrapure and surface water showed that PFCs, NOM and even microorganisms can be adsorbed on the surface of the resin and the pore size of the resin decreased after treatment, which could probably explain the decrease of the anion exchange performance after certain time treatment.

Regeneration column tests showed that a higher concentration of the NaCl (10%) in regenerants had only very slight increase to the regeneration performance compared to 5% NaCl. A slower regeneration flow rate (10 ml/min) had obvious increased regeneration performance compared to higher flow rate of 20 ml/min. Thus, 5% NaCl and 10 ml/min flow rate was considered to be the best conditions. The optimized regeneration methods and operational conditions can be reference for pilot and full-scale designs.



## **Chapter 6**

### **PFCAs and PFSAs removal during drinking water treatment by magnetic nanoparticles**

#### **Summary**

Three magnetic nanoparticles with different polymer coatings were designed and synthesized for PFCs removal. The removal potentials of PFCAs and PFSAs from both ultrapure water and surface water were evaluated using the synthesized magnetic nanoparticles. Bottle point method was applied for adsorption kinetics experiments. PFC concentrations were determined using LC-MS/MS with the method developed in Chapter 3. Pseudo-second-order model was applied to calculate relevant kinetic parameters. The factors impacting PFCs adsorption by magnetic nanoparticles including nanoparticles properties, PFC chain length, and PFC functional groups were investigated based on the experimental data. In ultrapure water, all three designed magnetic nanoparticles had high removals for long chain PFCs and relative low removals for short chain PFCs. PFSAs had better removals compared to PFCAs. Among all target nanoparticles, N1 had the best PFCs removal performance. In surface water, the PFC removals of all three nanoparticles decreased substantially. N1 remained the nanoparticle with best PFC removal performance. The effect of natural organic matters in PFCs adsorption by nanoparticles was studied using LC-OCD and other analysis. LC-OCD results showed that N1 had some removal of biopolymers and humic substances; while N2 and N3 had some removal of low molecular weight acids. As a result, biopolymers and humic substances were hypothesized to be the main competitors for PFC removals using N1, and low molecular acids competed more when using N2 and N3. The effect of inorganic anions, especially sulfate and nitrate, in PFCs adsorption was investigated. All three nanoparticles showed no inorganic anions removal in surface water.

Thus, it is possible that inorganic anions were not the main competitors causing the decrease in PFC removals.

## 6.1 Introduction

In recent adsorption applications, nanoparticles have been novel and promising adsorbents due to their excellent adsorption performance. Nanoparticles can be defined as particles with a size typically ranging from 1 to 100 nm (Banfield and Zhang, 2001). According to the material and component, nanoparticles can be classified into metallic and metal oxide nanoparticles, silica nanoparticles, carbon nanoparticles and some other miscellaneous nanoparticles (Kaur and Gupta, 2009). Among all innovative adsorbents in drinking water treatment, nanoparticles are the most impressive ones. Due to the advantages of high specific surface area, rapid intraparticle diffusion and various modification possibilities, nanoparticles are a kind of promising adsorbents in water and wastewater treatment (Qu et al., 2012).

Some metal oxide nanoadsorbents and carbon nanotubes can be used to adsorb organic contaminants such as naphthalene, benzene, atrazine, trichloroethylene and other trace contaminants (Kaur and Gupta, 2009). Cyanobacterial toxins, e.g. microcystins, are reported to be removed by carbon nanotubes (Upadhyayula et al., 2009) and iron oxide nanoparticles (Lee and Walker, 2010) through adsorption process. The adsorption of arsenic and heavy metal ions using nanoparticles as adsorbents is applied in water and source water treatment (Vunain et al., 2013; Recillas et al., 2010; Singh et al., 2011; Hua et al., 2012). Titanium dioxide nanoparticles with mesoporous hollow sphere structures were synthesized as photocatalysts initially, and then were found to have good dye adsorption capacity (Leshuk et al., 2012; Linley et al., 2013).

In some cases, the adsorption effect of nanoadsorbents is as remarkable as or even better than that of conventional adsorbents (Upadhyayula et al., 2009). The excellent adsorption performance is attributed to the huge specific surface area and active physical and chemical properties of nanoparticles (Kaur & Gupta, 2009). The good adsorption effects provide

possibility for nanoadsorbents to substitute conventional adsorbents. Recently, a new type silica membrane modified  $\text{Fe}_3\text{O}_4$  nanoparticle was studied to remove PFCs and a high removal efficiency of 86.29% is reached (Zhou et al., 2016).

The design of magnetic adsorbents or nanoparticles provides a relatively new approach to remove adsorbents especially nanoadsorbents from water after treatment. Magnetic ion exchange (MIEX) resin is a strong base anion exchange resin with iron oxide incorporated in the core (Lu et al., 2015; Ding L. et al, 2015). The MIEX process was firstly developed to remove DOC by Orica Watercare (Now IXOM Watercare, Australia), Commonwealth Scientific Industrial Research Organization, and South Australian Water Corporation (Fearing et al., 2004; Ding L. et al, 2015). In recent years, it is also reported that MIEX was applied to remove bromate, organic nitrogen, and some other organic contaminants (Ding L. et al, 2015; Nguyen et al., 2011; Tang et al., 2014; Lu et al., 2015).

In the literature review, no magnetic or polymer modified nanoparticles have been studied for PFCs removal; however, some of them have been applied for metals removal (Lofrano et al., 2016; Huang et al., 2016) and for organic compounds removal (Mahmoodi et al., 2016; Ou et al., 2016; Tang et al., 2016; Huang et al., 2016; Tao et al., 2017). Magnetic nanoparticle adsorbents which composed of a maghemite core and a silica mesoporous layer were proved to have ability to simultaneously remove polycyclic aromatic hydrocarbons (PAHs) and  $\text{Cd}^{2+}$  in the concentrations of 1 mg/L (Huang et al., 2016). Cobalt ferrite nanoparticles modified with polyoxometalate were synthesized and applied as magnetic catalyst for photocatalytic dye degradation (Mahmoodi et al., 2016). Polyoxometalates nanoparticles were modified with amino functionalized  $\text{Fe}_3\text{O}_4$  to have magnetic property and they exhibited high tetracycline removal performance (Ou et al., 2016).

As the reviewed studies revealed, magnetic adsorbents or nanoparticles show a potential for their application in drinking water treatment because they can be magnetically separated. To study surface modified magnetic nanoparticles and their adsorption performance for PFCs removal is the main objective of the study in this chapter. To achieve better PFCs removal

performance, the magnetic nanoparticles were custom designed and synthesized. The magnetic core allows for separation/removal from the water after treatment and the outer layers were modified to resemble anion exchange sites.

In this study, three magnetic nanoparticles with different polymers were synthesized and their PFC removals were studied in batch experiments. The PFCs removal kinetics were tested using the synthesized nanoparticles in both ultrapure water and natural water. The influence of water quality, nanoparticle property, and PFC properties on PFC removals was studied.

## **6.2 Materials and Methods**

### **6.2.1 Magnetic Nanoparticles**

In this chapter, the design of the magnetic nanoparticles was conducted together by the NSERC Chair in Water Treatment group at the University of Waterloo and the Dr. Frank Gu's group in Department of Chemical Engineering at University of Waterloo. The synthesis of the nanoparticles and the characterization of the nanoparticles including TEM, zeta potential, and dynamic light scattering analysis were conducted and relevant data were generated by Perry Everett who was a student from Dr. Frank Gu's group at the time. All the other work in this chapter including the PFCs removal kinetics experiments, the PFCs measurements, the LC-OCD and inorganic anion analysis, all related data analysis, writing and interpretation were performed by the author.

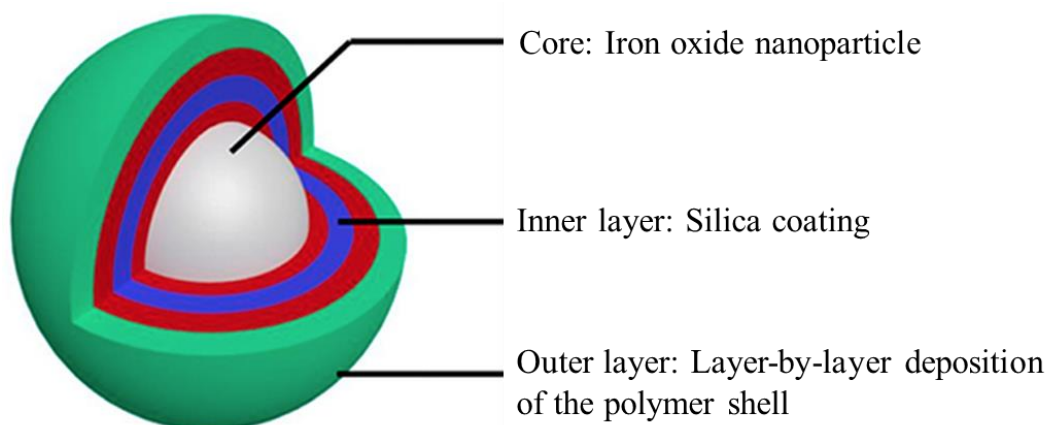


**Figure 6.1 Schematic of the synthesized nanoparticles**

As shown in Figure 6.1, the core of the nanoparticle was superparamagnetic iron oxide nanoparticle (SPION). It is only magnetic when exposed to a magnetic field. The diameter of the controlled SPION aggregate (CSA) is around 250 nm. Silica coating was then modified on the CSA to prevent oxidation. The coprecipitation method used was hydrothermal reaction of ferric salts under basic/reducing conditions which is the most common method for iron oxide nanoparticles. Layer-by-layer (LbL) method was applied for the desposition of the polymer shells. Based on electrostatic attraction between oppositely charged polymer layers, two types of polymers were alternately attached to the surface of the nanoparticles. Poly (sodium 4-styrenesulfonate) (PSS) were used for all nanoparticles as the anionic layer. For the cationic polymers, three different polymers were selected and used to make three different nanoparticles to test their PFCs removal performance.

Three cationic polymers were selected in this study as designed coatings for PFCs removal including poly [dimethyl diallyl ammonium chloride] (pDADMAC, N1 is used to represent the nanoparticle modified by this polymer), poly [bis (2-chloroethyl) ether-alt-1,3-bis [3-(dimethyl amino) propyl] urea] quaternized (polyBEP, N2 is used to represent the nanoparticle modified by this polymer), and poly (acrylamide-co-diallyl dimethyl ammonium chloride) (pAA-co-DADMAC, N3 is used to represent the nanoparticle modified by this polymer). The structures of the three polymers are shown in Figure 6.2. Since anion

exchange resins performed well the PFC removal studies described in Chapter 4 and 5, the functional groups of the anion exchange resins are also considered in the design of the nanoparticles. As can be observed, all three selected polymers have quaternary ammonium functional groups which are similar to anion exchange resins. These three polymeric cations modified on the nanoparticles were expected to increase the PFCs removal performance. The basal layers for all nanoparticles were 8 coatings of pDADMAC/PSS. The adsorption layers were 2 coatings of (cationic polyelectrolyte)/PSS.

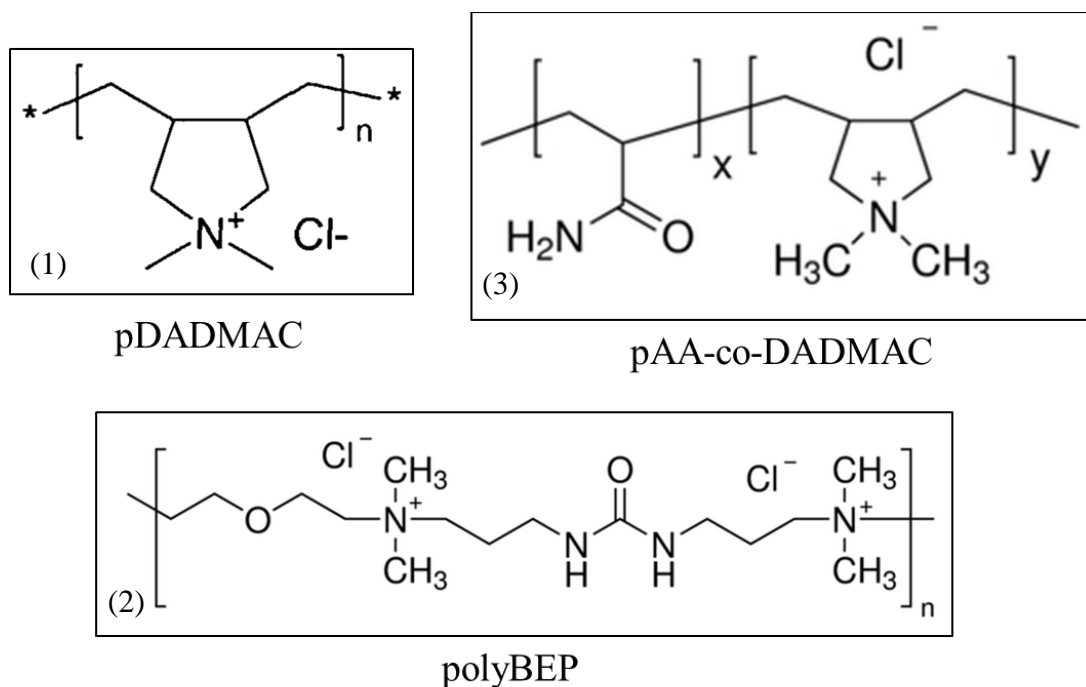


**Figure 6.2 Structures of three selected polymers modified on the magnetic nanoparticles: (1) N1: pDADMAC; (2) N2: polyBEP; (3) N3: pAA-co-DADMAC.**

For the coating procedures, pH was adjusted to neutral first if needed. Nanoparticles were then added to a polymer solution. Polymer concentration was kept at 10 g/L. The concentration of the silicate coated iron nanoparticles was 5.8 g/L. Salt concentration was 200 mM. Polymer solution was stirred for 1 hour. The particles were then washed with

ultrapure water. Any chemicals used in this chapter without specific illustration were purchased from Sigma Aldrich (USA).

### 6.2.2 Target Compounds and Water

Four PFCAs and three PFSA's including PFBA, PFHxA, PFOA, PFDA, PFBS, PFHxS, and PFOS were purchased from Sigma-Aldrich (WI, USA). Their purity and carbon chain length information are listed in Table 4-1. More detailed information about physical and chemical properties of the selected PFCs is provided in Table 2-2 in Chapter 2. Amount of 30 mg of each target PFC was measured and dissolved in 1 L of high purity water to make PFC stock solutions. New solutions were prepared every 6 month, and were stored in polypropylene bottles in the fridge at 4 °C. The concentration of each target PFC spiked in samples was 3.0 µg/L in all magnetic nanoparticles batch tests.

Ultrapure water was generated from a Millipore Milli-Q® UV PLUS water system (MA, USA). Batches of surface water from the Grand River was collected from the raw water stream of the Mannheim Water Treatment Plant (Region of Waterloo, ON, Canada). Grand River water was collected twice, on July 25<sup>th</sup>, 2015 and on October 18<sup>th</sup>, 2015. The first batch of water sample was used for the PFCs kinetics studies of N1 nanoparticles, and the second batch of water was used for the studies of N2 and N3. Table 6-1 lists the water quality parameters of these batches of waters from Grand River. No pH adjustment was done for all water samples in the study.

**Table 6-1 Grand River water quality parameters**

<b>Date</b>	<b>pH</b>	<b>Turbidity (NTU)</b>	<b>DOC (mg C/L)</b>	<b>Cl<sup>-</sup> (mg /L)</b>	<b>SO<sub>4</sub><sup>-</sup> (mg/L)</b>	<b>NO<sub>3</sub><sup>-</sup> (mg/L)</b>
July 25 <sup>th</sup> , 2015	7.6	1.8	6.7	57.3	24.2	8.1
Oct. 18 <sup>th</sup> , 2015	7.9	4.6	7.4	63.3	26.2	7.3

### 6.2.3 Kinetic Tests

The bottle point technique was used for PFCs adsorption kinetics of all three nanoparticles. Briefly, polypropylene opaque bottles (VWR, PA, USA) filled with 1 L PFC samples and nanoparticles were placed on an orbital shaker with a speed of 150 rotations per minute at room temperature. Mixtures of PFCs were spiked at concentration of 3.0  $\mu\text{g/L}$  for each PFC in each sample. A separate bottle was needed for each data point i.e. for different contact times or adsorbent dosages. After a preset contact time, the bottle was taken off the shaker and the sample was then analyzed.

To ensure that the PFC concentrations and the pH were uniform in all bottles of the same batch, a large polypropylene container was used to prepare a batch of PFC solution which was then distributed into individual bottles. Ultrapure water or filtered natural water which was enough for a whole batch of experiments was filled in the large container. Calculated amount of mixture PFCs were then spiked in the water to reach the nominal PFC concentration of 3.0  $\mu\text{g/L}$  for each solute. After the PFC containing solution was stirred and well-mixed, the accurate initial concentrations of the PFCs were measured.

For adsorption kinetics experiments, a screening study of three magnetic nanoparticles (N1, N2, and N3) was conducted in both ultrapure water and Grand River water to test their PFC adsorption performance. An aliquot of nanoparticles equivalent to 50 mg (calculated as dry weight) were measured and added to the 1 L bottles in all kinetics experiments. Seven target PFCs were spiked as a mixture at concentration of 3.0  $\mu\text{g/L}$  for each PFC in each sample. The contact times for N1 samples were 1, 3, 6, 12, 24, and 48 hours. The contact times for N2 and N3 samples were 1, 6, 12, and 24 hours. The samples were taken off and analyzed at the listed contact times. Before analysis, samples were put on a magnet to let the nanoparticles precipitate to the bottom of the bottle. The liquid supernatant samples were then taken and filtered using 0.45  $\mu\text{m}$  nylon filters (Pall Corporation, NY, USA) to make sure that all nanoparticles were removed. The effect of magnetic separation is shown in the Figure F.1 in Appendix F.



#### **6.2.4 Analyses**

All target PFCs were analyzed with a Shimadzu 8030 LC-MS/MS. An SPE process was conducted before the LC-MS/MS analysis. A Poroshell SB C18 column (50 mm × 2.1 mm internal diameter, 1.8 µm packing) (Agilent, CA, USA) was used for separation of the PFCs. Mobile phases were 5 mM ammonium acetate in Milli-Q water and methanol. The established analytical method was described in detail in Chapter 3.

The concentrations of the anions including chloride, sulfate and nitrate were analyzed by Dionex ICS-1100 ion chromatography (IC) system (Thermo Scientific, MA, USA) with Dionex ASRS<sup>TM</sup> 300 column (4 × 250mm). Dissolved organic carbon (DOC) was determined with Aurora 1030 TOC analyzer (OI Analytical, TX, USA). Turbidity of all water samples was measured by Hach 2100P Turbidimeter (CO, USA). Water sample pH was monitored using ORION Benchtop 420A pH meter (MA, USA).

### **6.3 Results and Discussion**

#### **6.3.1 Nano Adsorbents Properties**

The work of nanoparticles properties analysis in this section including transmission electron microscope (TEM), zeta potential, and dynamic light scattering (shown in Figure 6.3, 6.4, and 6.5) were done by Perry Everett.

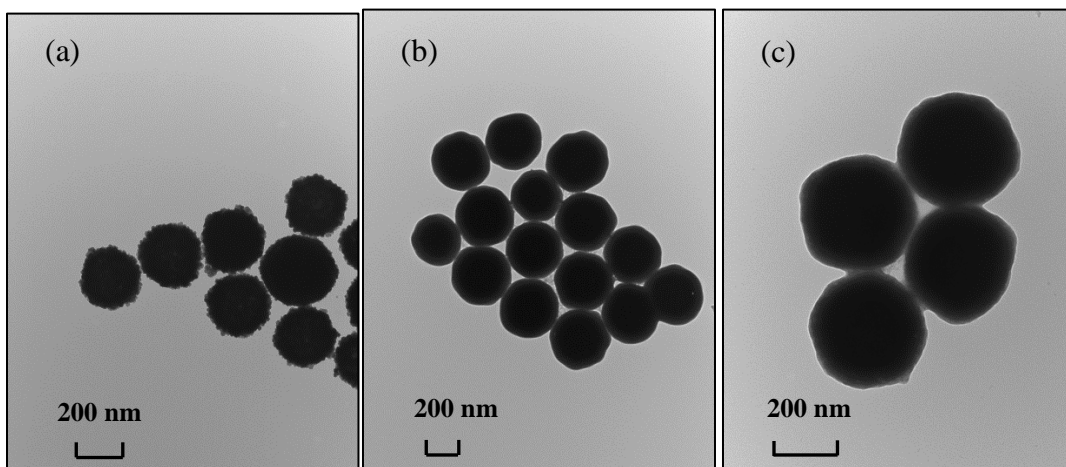


**Figure 6.3 TEM images of synthesized nanoparticles: (a) bare CSA Particles; (b) SiO<sub>2</sub> coated CSA particles; (c) LbL coated SiO<sub>2</sub>/CSA particles.**

The TEM results of synthesized nanoparticles are shown in Figure 6.3. The synthesized nanoparticles were spherical particles of uniform size and shape. The bare CSA particles had irregular rough edges with diameters around 200 to 300 nm. The SiO<sub>2</sub> coated CSA particles were similar or slightly larger in size (around 300 nm) compared to the bare CSA particles but had much smoother edges. After the polymer coating using the LbL method, the diameter of nanoparticle was around 300 to 400 nm.

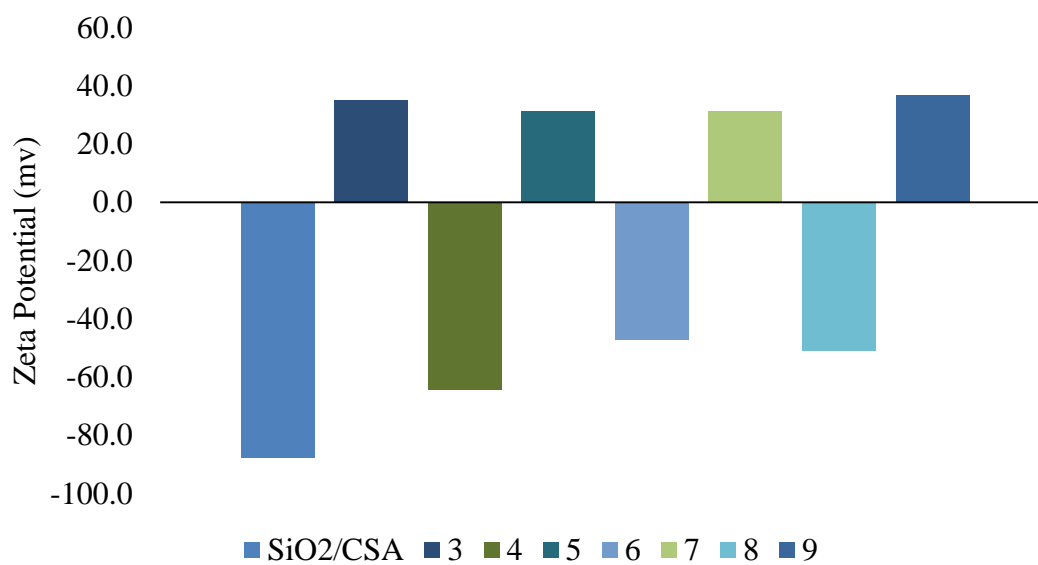


**Figure 6.4 Zeta potential variation during the nanoparticle coating procedure**

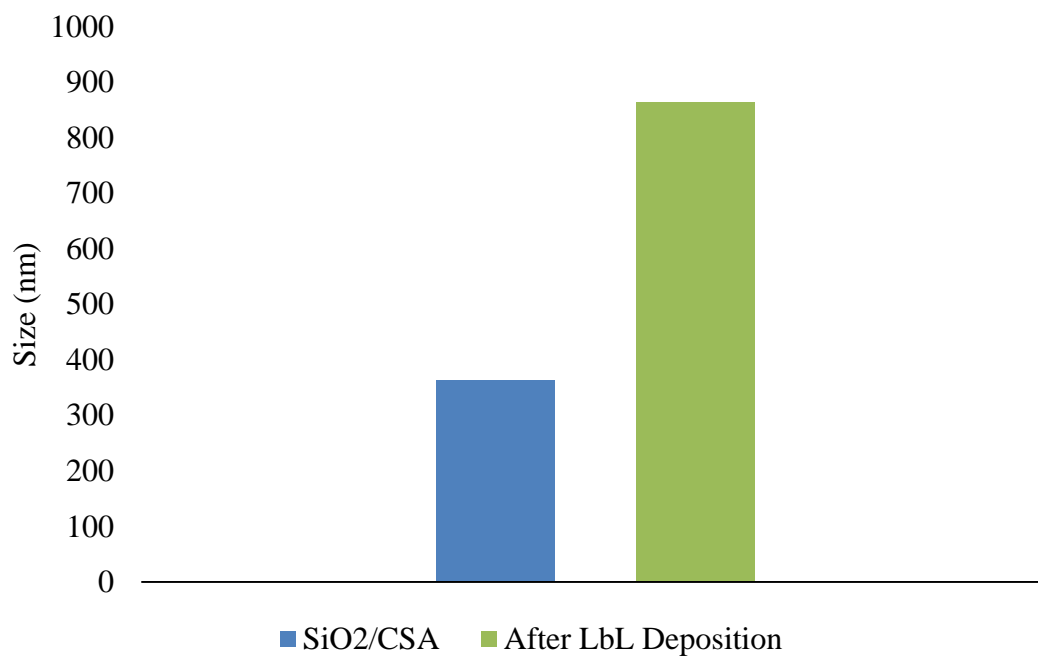


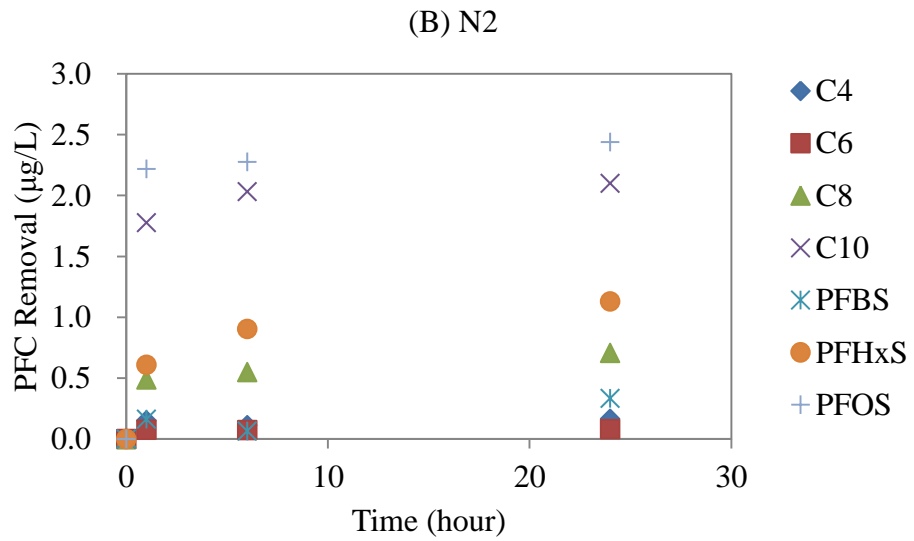
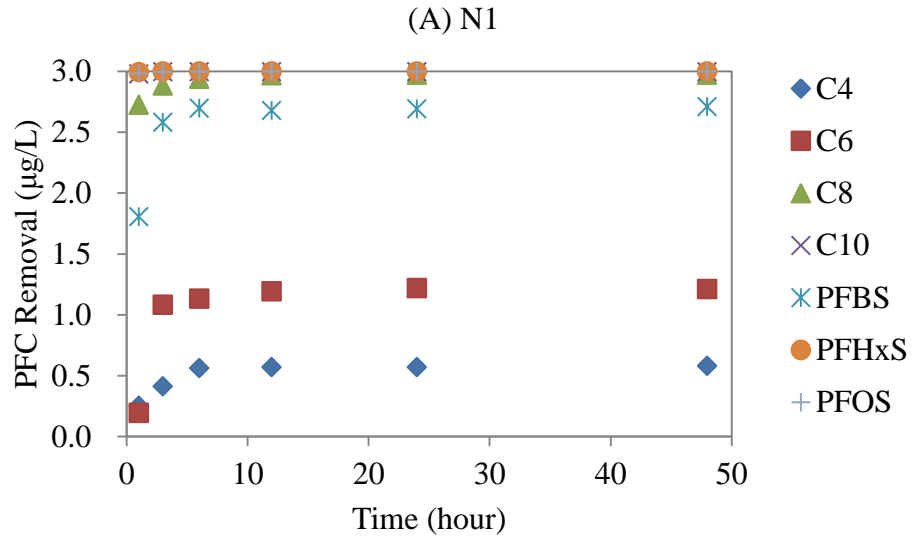
**Figure 6.5 Dynamic light scattering results of nanoparticles before and after LbL deposition**

The zeta potential and dynamic light scattering results of the synthesized nanoparticles are shown in Figure 6.4 and 6.5. In the zeta potential data, the alternate coating of pDADMAC and PSS lead to the positive and negative change of the zeta potential. After around 9 coatings, the absolute value of the zeta potential displayed a positive surface charge of around + 36.8 mv, which meant that the nanoparticles had relevant stability.

In the dynamic light scattering results, it showed that after LbL deposition, the particle size reached 800 nm, which was much higher than in the SEM results. The cohesion of several nanoparticles likely lead to higher particle size measurements in the dynamic light scattering compared with the SEM results. In Figure 6.3 (c), it can be seen that several nanoparticles seem to be attached to each other.

### **6.3.2 Adsorption Kinetics and Capacities in Ultrapure Water**

The results of PFCs adsorption of all three nanoparticles in ultrapure water shown in Figure 6.6 indicated that all the nanoparticles could reach at least some removal of PFCs in ultrapure water at equilibrium. For N1 nanoparticles, short chain PFCAs like PFBA (C4) and PFHxA (C6) had only 20% and 40% equilibrium removal respectively. As short chain PFSA, PFBS had 90% equilibrium removal. All the other PFCs had high removal of more than 99%. Compared to N1, nanoparticles N2 and N3 with different polymers showed similar but decreased PFC removal. PFSAs were better removed than PFCAs. Long chain PFCs were better removed compared to short chain ones. As long chain PFCs, PFDA and PFOS reached maximum removals of more than 90% for N1 and 40% to 80% for N2 and N3. Because there were no sufficient nanoparticles left to follow up with isotherms for capacity determination, percentage removal was used here instead.



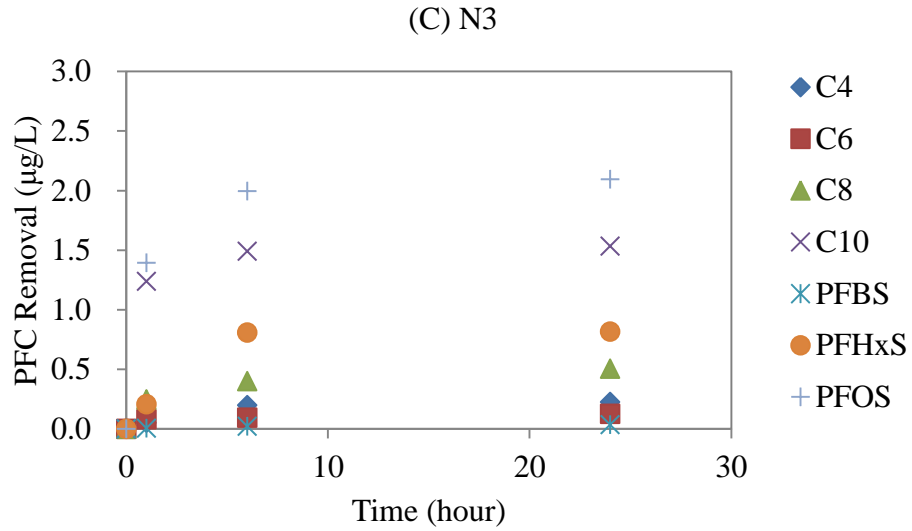


**Figure 6.6 PFCs adsorption kinetics of all three nanoparticles in ultrapure water (initial PFC concentrations were 3 µg/L each; adsorbent doses were 50 mg/L as dry weight): (A) N1: pDADMAC; (B) N2: polyBEP; (C) N3: PAA-co-DADMAC.**

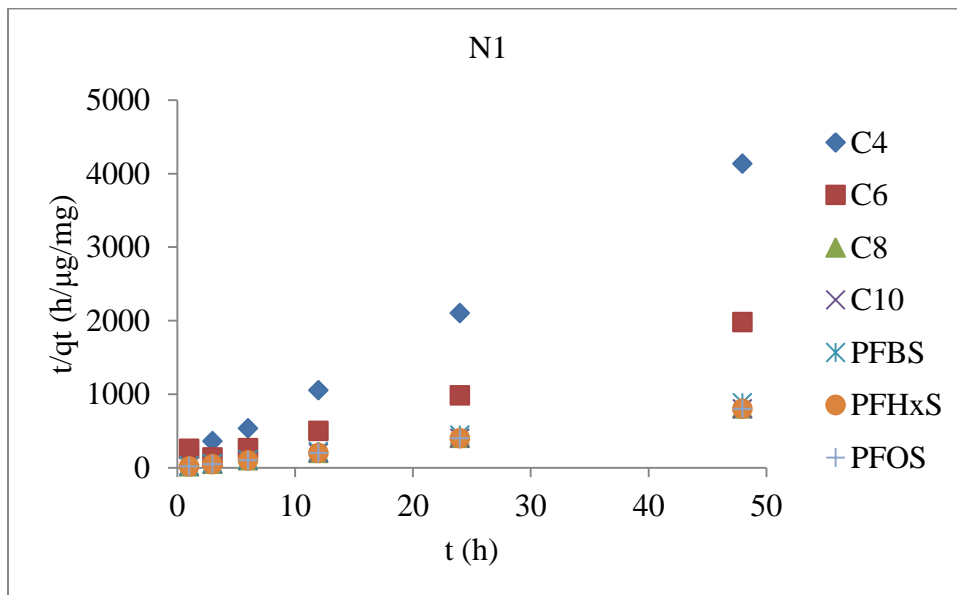


**Figure 6.7 Application of the pseudo-second-order model to the adsorption data of all target PFCs onto N1 particle in ultrapure water (initial PFC concentrations were 3 µg/L; adsorbent doses were 50 mg/L as dry weight).**

Pseudo-second-order model was applied for calculating kinetics parameters of PFCs adsorption using nanoparticles. Figure 6.7 shows the plot of the pseudo-second-order model application for PFC removals by N1 in ultrapure water. The plot showed good linearity, which suggested that the PFCs adsorption kinetics data fit the pseudo-second-order model well. The kinetics data plots of PFBA and PFHxA had larger slopes than the other PFCs. The kinetics data plotted for all the other PFCs were quite close and could not be well separated, which indicated that all the other PFCs had similar pseudo-second-order model parameters. The plots of the pseudo-second-order model applied to the PFCs adsorption data for N2 and N3 nanoparticles showed similar trends as N1 and are presented in the Appendix G Figures G.1.

**Table 6-2 Pseudo-second-order model parameters of all target PFCs for all nanoparticles in ultrapure water**

N1							
Kinetics parameters	PFBA	PFHxA	PFOA	PFDA	PFBS	PFHxS	PFOS
$q_e$ (ng/mg)	11.9	25.6	59.6	60.0	54.5	60.0	60.0
$q_{e, exp}$ (ng/mg)	11.6	24.2	59.4	59.9	54.2	60.0	60.0
$k_2$ (mg/µg/h)	92.5	19.9	222	4980	72.5	28000	3840
$R^2$	0.999	0.988	1.000	1.000	1.000	1.000	1.000
Maximum removal (%)	19.3	40.3	99.1	99.9	90.3	100	100
N2							
Kinetics parameters	PFBA	PFHxA	PFOA	PFDA	PFBS	PFHxS	PFOS

<b>q<sub>e</sub> (ng/mg)</b>	3.5	1.6	14.7	42.4	8.6	23.8	49.3
<b>q<sub>e, exp</sub> (ng/mg)</b>	3.3	1.6	14.1	42.0	6.7	22.6	48.8
<b>k<sub>2</sub> (mg/μg/h)</b>	187	1510	56.8	107	15.2	30.8	73.1
<b>R<sup>2</sup></b>	0.982	0.999	0.996	1.000	0.968	0.998	1.000
<b>Maximum removal (%)</b>	5.53	2.68	23.6	70.0	11.1	37.7	81.3
<b>N3</b>							
<b>Kinetics parameters</b>	<b>PFBA</b>	<b>PFHxA</b>	<b>PFOA</b>	<b>PFDA</b>	<b>PFBS</b>	<b>PFHxS</b>	<b>PFOS</b>
<b>q<sub>e</sub> (ng/mg)</b>	5.1	2.7	10.7	31.0	0.9	18.0	42.7
<b>q<sub>e, exp</sub> (ng/mg)</b>	4.5	2.5	10.1	30.7	0.7	16.3	41.9
<b>k<sub>2</sub> (mg/μg/h)</b>	66.1	251.	61.6	134	167	25.3	48.1
<b>R<sup>2</sup></b>	0.992	0.994	0.999	1.000	0.997	0.987	1.000
<b>Maximum removal (%)</b>	7.50	4.22	16.8	51.1	1.18	27.2	69.8

Table 6-2 shows Pseudo-second-order model parameters of all target PFCs for all nanoparticles in ultrapure water. In Table 6-2, Pseudo-second-order model parameters including  $k_2$ ,  $q_e$ , and  $R^2$  were summarized as well as the experimental  $q_e$  ( $q_{e,exp}$ ) and maximum percentage removal. All the PFCs adsorption kinetics using all three nanoparticles in ultrapure water reached high  $R^2$  values greater than 0.96, which meant that the adsorption kinetics data fit the pseudo second-order model well.

Among all the nanoparticles, N1 had high  $k_2$  (19.9-33800 mg/μg/h) values for all target PFCs. The high  $k_2$  values revealed that N1 had high adsorption rates for all target PFCs, which is also evident in Figure 6.6. Compared to N1, N2 and N3 had lower  $k_2$  values especially for long chain PFCs. This indicated that N1 had superior adsorption rates for long chain PFCs. N2 had slightly higher  $k_2$  values than N3, especially for short chain PFCs. N3 showed the lowest  $k_2$  values for all target PFCs. For  $q_e$  and  $q_{e,exp}$  values, N1 had highest



values among all nanoparticles. The  $q_e$  and  $q_{e,exp}$  values for all nanoparticles were close, which indicated that the adsorption kinetics data were well simulated by the model. Short chain PFCAs like PFBA and PFHxA had low  $q_e$  values and maximum percentage removals. These results showed that nanoparticles had same equilibrium times but larger maximum removals for long chain PFCs rather than short chain ones in ultrapure water.

Compared to the PFCs adsorption kinetics results of anion exchange resins, magnetic nanoparticles had much higher  $k_2$  values which indicated that they had short equilibrium times. Nanoparticles especially N2 and N3 had much lower  $q_e$  values for all PFCs especially short chain ones compared to anion exchange resins (47-114 ng/mg).

Magnetic nanoparticles had short equilibrium times for PFC adsorption. In the first few hours (about 10 hours), all PFCs could reach equilibrium. As presented in Chapter 4, the investigated anion exchange resins showed much higher equilibrium times of 48 to 120 hours for the target PFCs. It can be observed that nanoparticles adsorbed PFCAs faster compared to anion exchange resins. The reason for the fast kinetics of nanoparticles could be that nanoparticles had much smaller particle size and the PFCs were easy to be transferred to the surface of the nanoparticles. Anion exchange resin had no obvious selectivity for PFCAs in ultrapure water; while nanoparticles preferred to remove long chain PFCAs. Similar trends could be observed for the PFSAs. This may point to hydrophobic interactions as the main mechanism influencing PFC removals by nanoparticles in ultrapure water. Among all nanoparticles, N1 had the best adsorption performance in ultrapure water with the shortest equilibrium time and excellent PFC removals.

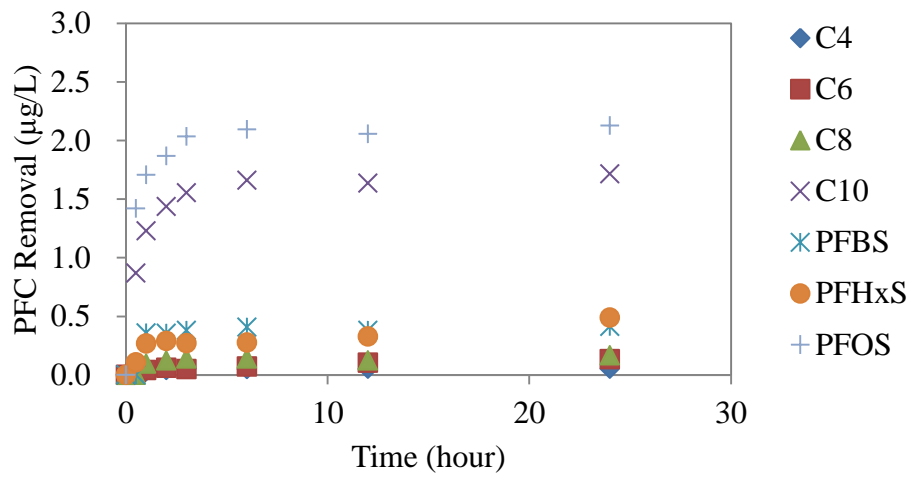
Ou et al. (2016) reported that amino functionalized  $Fe_3O_4$  modified polyoxometalates nanoparticles had  $q_e$  of 186.18 mg/g for tetracycline removal calculated by the pseudo-second-order model. Iron nanoparticle-doped magnetic carbons were tested to reach an equilibrium capacity of 311 mg/g and  $k_2$  of  $0.0058 \text{ min}^{-1}$  for the adsorption of bisphenol A (Tang et al., 2016). A few research papers also presented high adsorption capacity of nanoparticles for organic compounds treatment; however, most of these studies were for

wastewater treatment and the concentrations of target compounds were in the range of mg/L, so it is difficult to directly compare the adsorption kinetics results of the magnetic nanoparticles with the reported values in the literature.

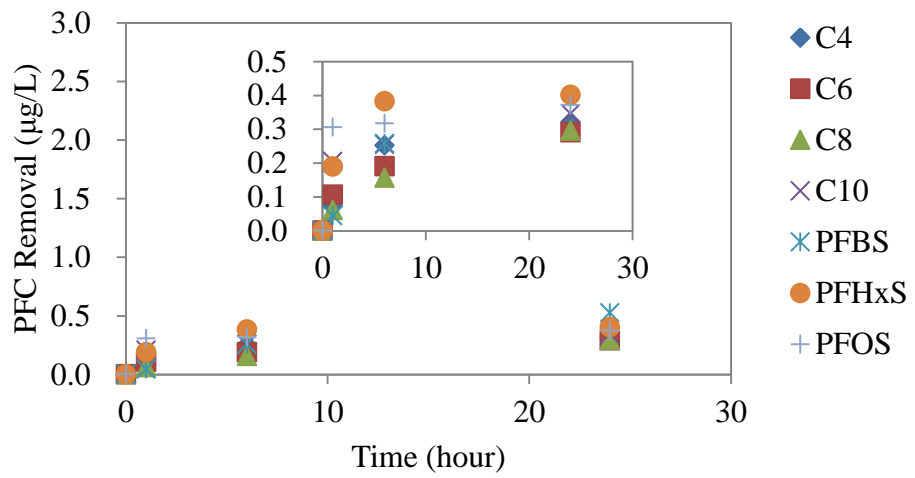
### **6.3.3 Adsorption Kinetics and Capacities in Surface Water**

The results of PFCs adsorption kinetics in Grand River water using different nanoparticles are shown in Figure 6.8 and Table 6-3. In ultrapure water, long chain PFCs had high percentage removals of more than 60% after 24 hours. In Grand River water, the percentage removals of all target PFCs decreased dramatically. PFCs removals decreased more when using N2 and N3, compared with N1. The equilibrium times of all target PFCs were around 10 hours in ultrapure water. In GRW, equilibrium times of all target PFCs decreased to a few hours. This phenomenon states that in surface waters, the adsorption rates of all target PFCs would significantly decrease. Among all the nanoparticles, N1 showed best PFCs removal performance Grand River water. For N1 nanoparticles, long chain PFCs seemed to have better removal performance compared to short chain PFCs, and PFSA showed better adsorption performance compared to PFCAs in Grand River water. As long chain PFSA, PFOS had 71% removal after 24 hour. PFDA which is the long chain PFCA had 57% removal after 24 hours. All the other PFCs showed less than 20% removal. For N2 and N3 nanoparticles, all target PFCs had very low percentage removal of less than 20% and 10% respectively. These results are likely linked to complex impacts of both NOM and inorganic anions present in surface water.

(A) N1



(B) N2



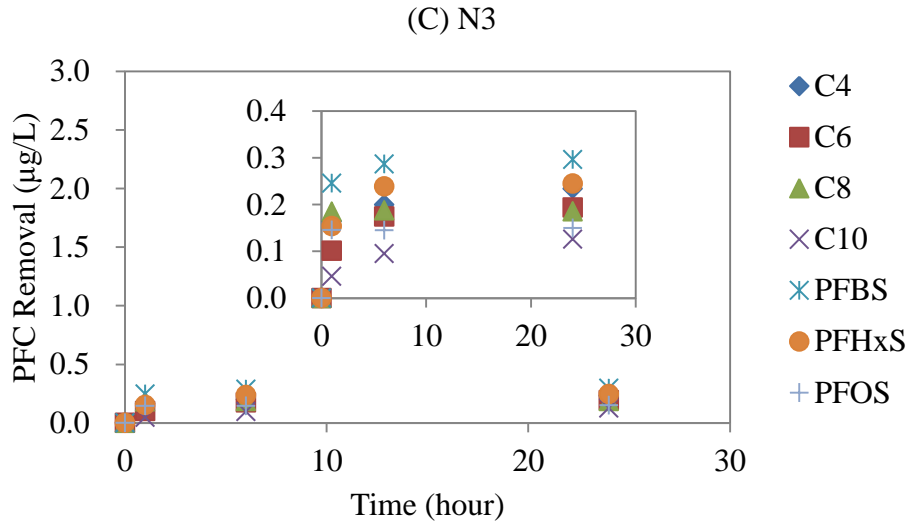


**Figure 6.8 PFCs adsorption kinetics of all three nanoparticles in Grand River water (initial PFC concentrations were 3 µg/L each; adsorbent doses were 50 mg/L as dry weight): (A) N1: pDADMAC; (B) N2: polyBEP; (C) N3: PAA-co-DADMAC.**

Experimental data of PFCs adsorption kinetics using three magnetic nanoparticles in Grand River water were also simulated using pseudo-second-order model similar to the PFCs adsorption kinetics in ultrapure water. The detailed pseudo second-order model parameters for all nanoparticles in Grand River water are listed in Table 6-3. The  $k_2$  values of different magnetic nanoparticles did not show obvious trends for the target PFCs. It seems that the nanoparticles had very high PFCs removal kinetics, so that the  $k_2$  values were difficult to determine and with more uncertainty. Also, N2 and N3 each had only 3 data points for the fitting which is not very reliable and the results are therefore associated with a high uncertainty.

For N1 nanoparticles, PFOS had the largest maximum removal of 70.9% and largest  $q_e$  of 42.8 ng/mg. PFSAs had better adsorption performance in Grand River water, compared to PFCAs. The existence of NOM could largely decrease the removal of short chain PFCs when

using nanoparticles. For N2 nanoparticles, all target PFCs had low maximum removal of 9.7% to 17.5%. Among all PFCs, PFBS which is the short chain PFSA showed highest maximum percentage removal and  $q_e$  values, which could be the results of the competition with NOMs in natural water. For N3 nanoparticles, all target PFCs had low maximum removal of less than 10% as well as low  $q_e$  values of less than 6 ng/mg. From the  $k_2$ ,  $q_e$ , and maximum percentage removal data, it can be observed that N1 nanoparticles performed is more selective in surface water compared to N2 and N3. N1 preferred to adsorb long chain PFCs; while, N2 and N3 had higher removal and shorter equilibrium times for short chain PFCs which is different from the results in ultrapure water.

**Table 6-3 Pseudo-second-order model parameters of all target PFCs for all nanoparticles in Grand River water**

N1							
Kinetics parameters	PFBA	PFHxA	PFOA	PFDA	PFBS	PFHxS	PFOS
$q_e$ (ng/mg)	1.05	3.07	3.33	34.7	8.27	10.1	42.8
$q_{e, exp}$ (ng/mg)	1.03	2.66	3.34	34.32	8.27	9.78	42.54
$k_2$ (mg/ $\mu$ g/h)	2770	69.3	253	69.3	377	34.6	94.2
$R^2$	0.999	0.964	0.973	1.000	0.998	0.933	1.000
Maximum removal (%)	1.71	4.43	5.57	57.2	13.8	16.3	70.9
N2							
Kinetics parameters	PFBA	PFHxA	PFOA	PFDA	PFBS	PFHxS	PFOS
$q_e$ (ng/mg)	7.42	6.48	7.40	7.31	18.7	8.35	7.58
$q_{e, exp}$ (ng/mg)	6.42	5.81	5.91	6.92	10.5	8.02	7.41
$k_2$ (mg/ $\mu$ g/h)	37.5	51.2	21.0	85.8	2.9	131	203
$R^2$	0.997	0.992	0.983	0.994	0.965	0.999	0.998
Maximum	10.7	9.69	9.85	11.5	17.5	13.4	12.4

removal (%)							
<b>N3</b>							
<b>Kinetics parameters</b>	<b>PFBA</b>	<b>PFHxA</b>	<b>PFOA</b>	<b>PFDA</b>	<b>PFBS</b>	<b>PFHxS</b>	<b>PFOS</b>
<b>q<sub>e</sub> (ng/mg)</b>	4.81	4.03	3.78	2.74	5.99	5.01	3.00
<b>q<sub>e, exp</sub> (ng/mg)</b>	4.68	3.88	3.71	2.51	5.93	4.90	2.99
<b>k<sub>2</sub> (mg/μg/h)</b>	259	256	6860	162	695	418	3170
<b>R<sup>2</sup></b>	0.999	1.000	1.000	0.999	1.000	1.000	1.000
<b>Maximum removal (%)</b>	7.79	6.46	6.18	4.19	9.88	8.17	4.99

To comparing the removal kinetics results for nanoparticles in Grand River water with the anion exchange resins results shown in Chapter 4, nanoparticles had obvious high  $k_2$  values and lower  $q_e$  values. Zhou et al. (2016) reported silica membrane modified  $Fe_3O_4$  nanoparticles had  $q_e$  values of 2.92-11.11 mg/g and  $k_2$  values of 1.64-40.57 mg/g/min for target PFCs removal in surface water calculated by pseudo-second-order model. Comparing to the literature results, designed nanoparticles in this study had similar  $k_2$  values and lower  $q_e$  values; however, the concentrations of PFCs and nanoparticle doses in this study were both lower than it was reported in the literature.

In Figure 6.9, taking N1 data as an example,  $t/q_t$  was plotted with  $t$  to simulate the linear relationship and to calculate the kinetics parameters. The plotting showed good linear relation of the kinetics parameters for all target PFCs in Grand River water, which signified that the PFCs adsorption kinetics data fit the pseudo-second-order model well. The linear regression line of PFBA (C4) had largest slope, followed by the PFHxA (C6) and PFOS (C8). All the other PFCs had close slopes. The large slope revealed a small adsorption capacity. Application data of the pseudo-second-order model for N2 and N3 (there were 3 data points for each particle) showed similar trends to N1, and are shown in Figure G.2 in Appendix G.

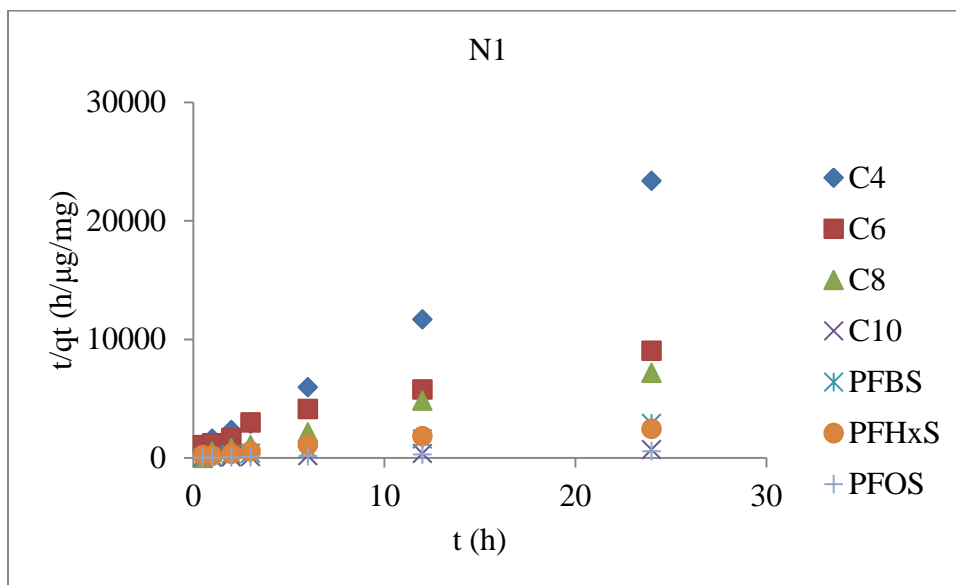


**Figure 6.9** Application of the pseudo-second-order model to the adsorption data of all target PFCs onto N1 particle in Grand River water (initial PFC concentrations were 3  $\mu\text{g/L}$ ; adsorbent doses were 50 mg/L as dry weight).

### 6.3.4 Factors Affecting PFC Removal by Magnetic Nanoparticles

#### 6.3.4.1 Effect of PFC properties

The adsorption kinetics results of different PFCs using N1 particle in ultrapure water are shown in Figure 6.10. The PFC properties are mainly influenced by the carbon chain length and functional groups. Both  $q_e$  and maximum removal were compared for different PFCs. It is obvious that the short chain PFCAs PFBA and PFHxA had much lower  $q_e$  and maximum removal values compared to the long chain PFCs in ultrapure water. As summarized in Table 2-1, long chain PFCs have higher hydrophobicity than short chain PFCs, and PFSAAs are more hydrophobic than PFCAs. The results of PFCs adsorption in ultrapure water indicate that the designed magnetic nanoparticles preferred to adsorb PFCs with high hydrophobicity. It can be postulated that in ultrapure water, without the competition of NOM, the

hydrophobic interactions between nanoparticles and PFCs played a more important role than the electrostatic interactions. All three nanoparticles showed similar PFCs adsorption selectivity in ultrapure water.

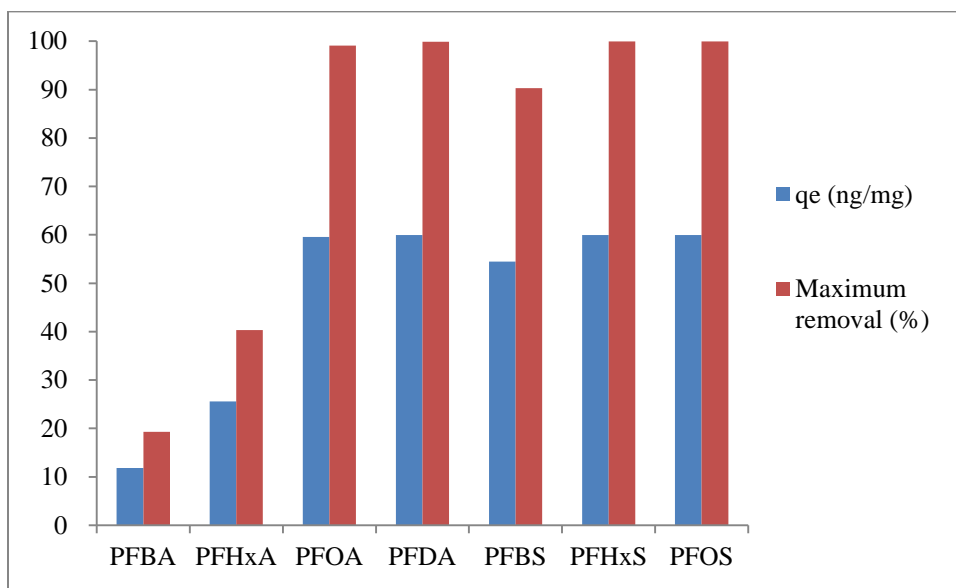


**Figure 6.10 Adsorption results of different PFCs using N1 particle in ultrapure water**

### 6.3.4.2 Effect of nanoparticle properties

The three magnetic nanoparticles were synthesized using the same method and the same iron oxide core with silica coating. The only difference is that they were modified by different cationic polymer coatings. N1 was modified using pDADMAC which had the simplest monomer in structure. N2 was modified by polyBEP and N3 was coated with pAA-co-DADMAC. Both pDADMAC and pAA-co-DADMAC had dimethyl diallyl ammonium functional group in their monomers.

The results of  $q_e$  values of different PFCs using all three nanoparticles in ultrapure water and in surface water are demonstrated in Figure 6.11 and 6.12 respectively. In ultrapure water, N1 had much higher  $q_e$  values for all target PFCs compared to N2 and N3



nanoparticles. Compared to N3, N2 particles had higher  $q_e$  values for long chain PFCs such as PFDA and PFOS; while, they had lower  $q_e$  values for short chain PFCs like PFBA and PFHxA. It is speculated that the diallyl ammonium functional group (N3) is more likely to attract short chain PFCs compared to propyl ammonium functional group (N2), probably because that the propyl ammonium functional group was more likely to adsorb hydrophobic compounds. Compared to N1, the polymers of N2 and N3 had monomers with more complicated functional groups and structures which did not help with the PFCs removal.

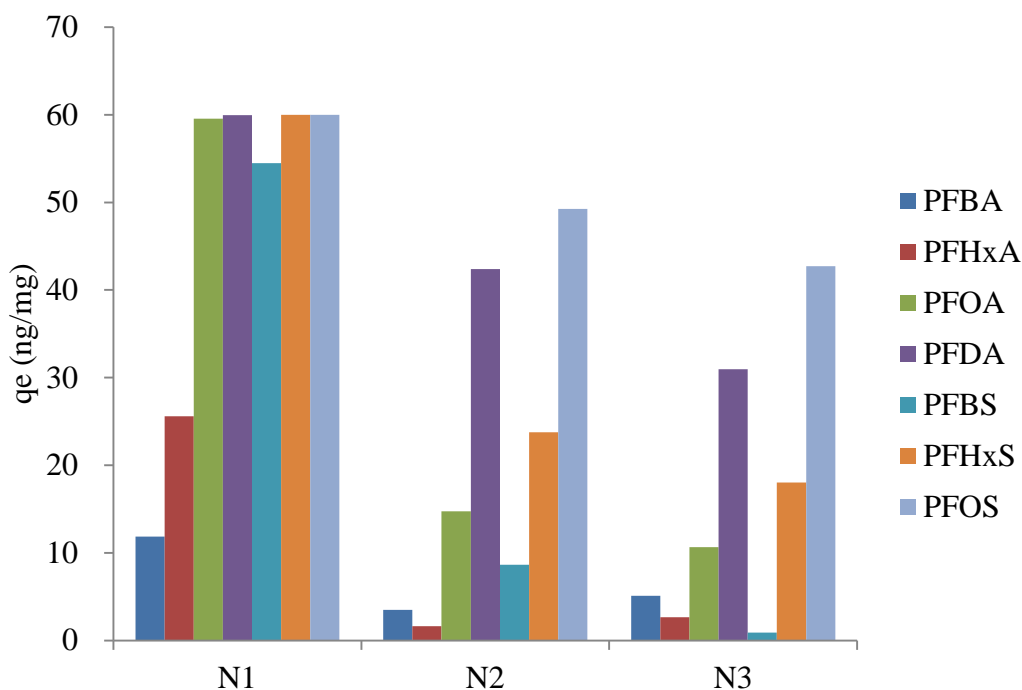


**Figure 6.11 Results of  $q_e$  of different PFCs using all three nanoparticles in ultrapure water**

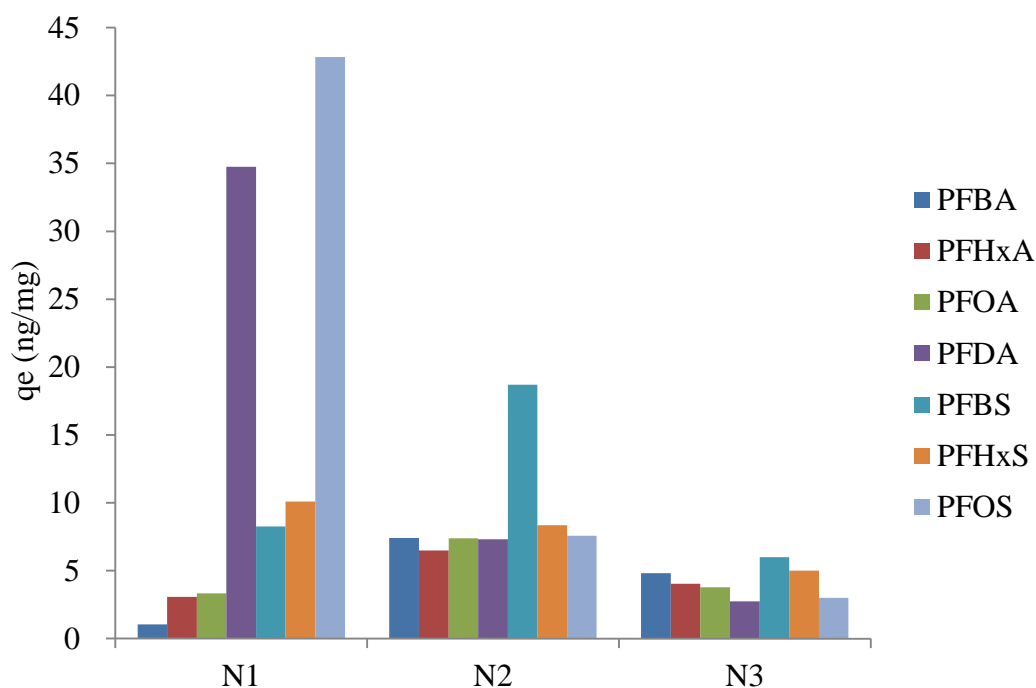


**Figure 6.12 Results of  $q_e$  of different PFCs using all three nanoparticles in Grand River water**

In surface water, the  $q_e$  values of PFCAAS for all three nanoparticles greatly decreased in most cases; however, different nanoparticles had different selectivity for target PFCs. N1 showed a similar trend as in ultrapure water which was that PFSAs had better removal compared to PFCAs and long chain PFCs had better removal compared to short chain ones. For N3 nanoparticles, short chain PFCs had higher  $q_e$  values. For N2, PFBS had higher  $q_e$  values than the other PFCs. Among all the synthesized nanoparticles, N1 showed best PFCs adsorption performance, followed with N2 and N3.

### 6.3.5 Effect of NOM competition in PFCs adsorption by magnetic nanoparticles

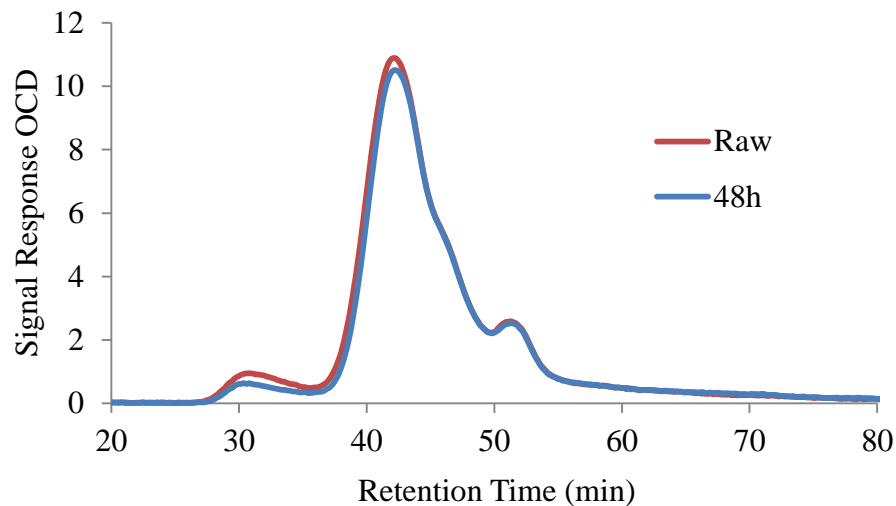


**Figure 6.13 LC-OCD results of raw water and after 48 hours using N1**

The adsorption kinetics results verified that the PFCs adsorption performance by magnetic nanoparticles would dramatically decrease in surface water, which could be caused by the high concentrations of NOM and inorganic anions. To verify the effect of NOM and inorganic anions in PFCs adsorption by magnetic nanoparticles, LC-OCD, DOC, and IC analyses were conducted for Grand River water. Figure 6.13, 6.14, and 6.15 showed the LC-OCD, DOC and inorganic anions results in Grand River water as examples to discuss the effect of NOM on PFCs adsorption in surface water.

As a size exclusion instrument, LC-OCD can separate NOM into different fractions including biopolymers, humic substances, building blocks, low molecular weight acids, and low molecular weight neutrals (Huber et al., 2011). As shown in Figure 6.13, the removed organic compounds included both the biopolymers (the small peaks appeared at 30 min) and humic substances (the large peaks appeared at around 42 min) after 48 hours using N1. The biopolymers had 33.6% removal; while only 3.6% of humic substances were removed after 48 hours. The building blocks and low molecular weight acids (appeared in the retention time

of 45 to 55 min) had no removal by N1 nanoparticles. The LC-OCD results for N2 and N3 are shown in Appendix H Figure H.1. The results showed that N2 and N3 had barely biopolymers and humic substances removal (less than 0.5% removals); while 11.5% removal of low molecular weight acids was observed for both N2 and N3. It is worth noting that both N2 and N3 had an additional peak showing with a retention time of 65 min after the experiments ran for 24 hours which might be caused by leaching of shorter chain organics from the nanoparticles and are supported by the DOC results for N2 and N3 in Figure 6.14. The LC-OCD results showed that biopolymers and small amount of humic substances and may be the representative portion of the DOC which competed with PFCs when using N1 nanoparticles; while, low molecular weight acids may be the portion of the DOC competing with PFCs when using N2 and N3. High concentrations of humic substances were proved to be no significant competition with silica membrane coated on  $\text{Fe}_3\text{O}_4$  nanoparticles for PFCs removal (Zhou et al., 2016), which matched with the LC-OCD results of designed nanoparticles for PFCs removal in this study.

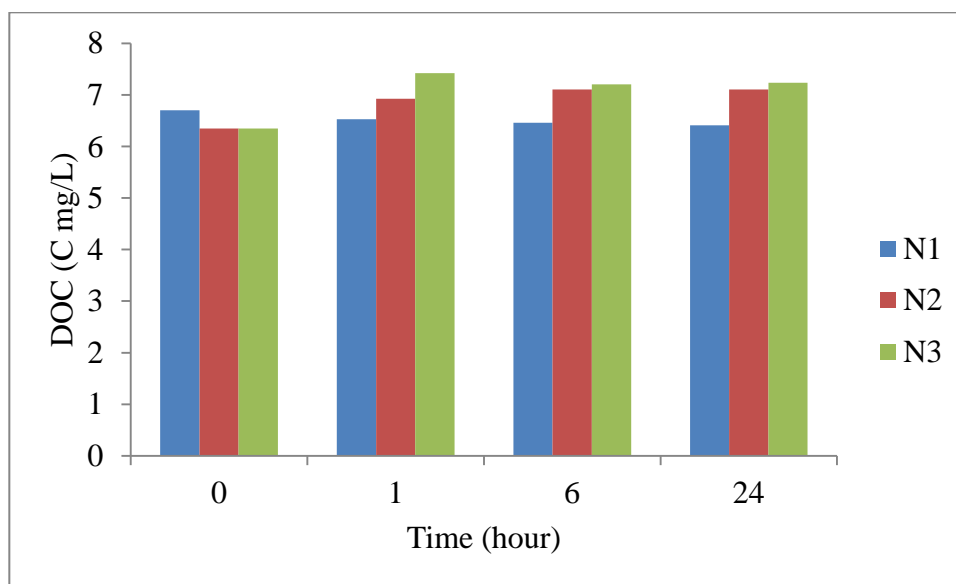


**Figure 6.14 NOM results for three magnetic nanoparticles N1, N2 and N3 in Grand River water**

From Figure 6.14, it can be observed that none of three nanoparticles had good DOC removal. For N1, the initial DOC was 6.7 mg/L and about 0.3 mg/L DOC was removed by N1 after 48 hours. For N2 and N3, the DOC values increased after treatment. The initial DOC of Grand River water was 6.3 mg/L. After 24 hours, N2 and N3 had the similar DOC concentration of 6.7 mg/L. As discussed for the LC-OCD results, the increase of the DOC was probably caused by the leaching of organics from the N2 and N3 nanoparticles. Compared to the concentrations of PFCs, the concentration of DOC in surface water was several orders of magnitude higher, which would lead to the competition between NOMs and PFCs.

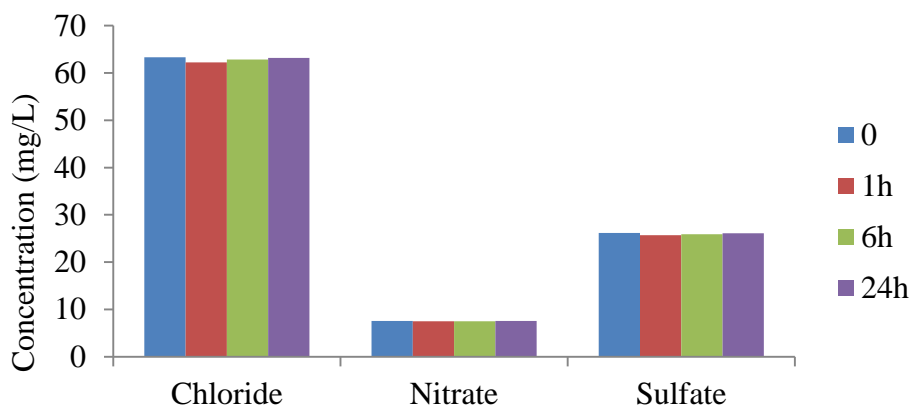


**Figure 6.15 Anion concentrations using N2 in Grand River water**

Figure 6.15 showed the variation of inorganic anions concentrations during the PFCs adsorption process using N2 nanoparticles in Grand River water. The results showed that N2 had no inorganic anions removal during the contact time of 24 hours. N1 and N3 also showed no inorganic anions removal. It implied that none of the synthesized nanoparticles had inorganic anions uptake and inorganic anions may not be the key impact factor for the decrease of the PFCs adsorption performance in surface water. The hydrophobic interactions mechanism influenced the PFCs removal process more when there was no NOM competition; while the influence of the electro static interactions mechanism did not interfered much.

As discussed previously in this chapter, custom designed magnetic nanoparticles performed higher adsorption rates and lower adsorption capacities for target PFCs comparing with anion exchange resins and other nanoparticles reported in the literature. Further studies are needed to design nanoparticles with better adsorption performance especially in surface water and to test their regeneration feasibility.

## 6.4 Conclusions

The major findings in this study are summarized as follows.

(1) Novel magnetic nanoparticles with three different polymers (N1, N2, N3) for PFCs removal were designed and synthesized. They were then applied in PFCs removal kinetics experiments in both ultrapure and surface water.

(2) In ultrapure water, all three designed magnetic nanoparticles had high removals for long chain PFCs and relative low removals for short chain PFCs. PFSAs had better removals compared to PFCAs. Among all target nanoparticles, N1 had the best PFCs removal performance. It reached 20% and 40% removal for PFBA and PFHxA respectively. All the other PFCs reached more than 90% removal after 48 hours.

(3) In surface water, the PFCs removal of all three nanoparticles largely decreased. N1 remained the nanoparticle with best PFCs removal performance. N2 and N3 had less 20% removal for all target PFCs in surface water after 48 hours.

(4) LC-OCD results showed that N1 had some removal of biopolymers and humic substances; while N2 and N3 had some removal of low molecular acids. As a result, biopolymers and humic substances were hypothesized to be the main competitors for N1, and low molecular acids competed more with N2 and N3.

(5) All three nanoparticles showed no inorganic anions removal in surface water. Thus, it is possible that inorganic anions may not be the main competitor causing the decrease in PFC removals.

(6) Comparing with anion exchange resins and other nanoparticles in literature, three designed nanoparticles exhibited much faster PFCs removal kinetics but lower PFCs adsorption capacities, especially in surface water.

(7) Further studies are needed to design and synthesize nanoparticles with better PFCs removal performance based on the presented results in this study, and to test their regeneration performance.

## Chapter 7

### Conclusions and recommendations

#### 7.1 Summaries and Conclusions

The overall goal of the research introduced in this thesis was to investigate the behavior of PFCs during the ion exchange treatment and the magnetic nanoparticles adsorption processes, to examine more efficient approaches compared to conventional water treatment processes to remove PFCs by ion exchange and adsorption processes in drinking water treatment, and to investigate the factors influencing these processes. Firstly, several classes of PFCs were selected to be the target compounds which were identified as commonly detected PFCs in drinking water sources and potential contaminants. PFCAs, PFSAs, and PFPAs were selected as the target PFC classes in the development of the analytical method. PFCAs and PFSAs were then chosen to be the target PFCs in the study of ion exchange and magnetic nanoparticles adsorption processes. Secondly, an LC-MS/MS analytical method suitable for the analysis of all 13 types from 3 classes of target PFCs at trace concentration levels in water was established. After the LC-MS/MS method was developed, four PFCAs including PFBA (C4), PFHxA (C6), PFOA (C8), and PFDA (C10), and three PFSAs including PFBS, PFHxS, and PFOS were ultimately selected as target compounds for the drinking water treatment studies. Five commercially available anion exchange resins with different properties were chosen to test their PFCs removal kinetics in both ultrapure water and Grand River water in batch studies. Based on the kinetics results, TAN-1 and PFA444 were selected as target anion exchange resins for the removal kinetics study in Lake Erie water, the isotherms study in ultrapure water, and the study of inorganic anion effects. The influence of NOM and inorganic anions on PFCs removal in the anion exchange process was examined in these studies for the selected resins. Then, the regeneration performance of TAN-1, PFA444, and A555 resins for PFCs removal in different conditions was examined in batch studies. As



the resin with best regeneration performance, A555 was chosen to be used in the column experiments. Based on the batch studies of PFCs removal in the anion exchange process, an anion exchange column experiment was designed and the breakthrough curves using both ultrapure water and surface water were measured to provide useful information about operational conditions for the real application. The regeneration column studies were then conducted to test suitable regeneration conditions for PFCs removal. At last, magnetic nanoparticles with three different polymer coatings were designed and synthesized for PFCs removal. The PFCs adsorption kinetics of the synthesized nanoparticles in both ultrapure water and Grand River water were investigated.

The major conclusions drawn from the research are as follows:

#### **7.1.1 Development of an LC-MS/MS Analytical Method for Target PFCs**

(1) An LC-MS/MS method for seven PFCAs (C4-C10), three PFSA (PFBS, PFHxS, PFOS), and three PFPA (PFHxPA, PFOPA, PFDPA) was successfully established.

(2) The target PFCs can be analyzed in both ultrapure water and surface water at trace concentrations. With the SPE process, the MDLs of the PFCAs and PFSA ranged from 0.1 ng/L to 1.0 ng/L, and the MDLs of PFPA ranged from 5.0 to 5.1 ng/L.

(3) The results of method recoveries, repeatability, and calibration curves confirmed the reliability of the LC-MS/MS method for the target PFCs.

#### **7.1.2 PFCs Removal Performance of Selected Anion Exchange Resins**

(1) In ultrapure water, all anion exchange resins showed good removal of all target PFCs. The anion exchange resin TAN-1 was the best adsorbent. It achieved over 95% removal of all target PFCs in bottle point sorption kinetics experiments within 48 hours. A555 resin had longest equilibrium time of more than 120 hours.

(2) In ultrapure water, all PFCs reached very high removal of more than 80%. Long chain PFCs such as PFDA and PFOS were less removed than the other PFCs.

(3) Isotherms results in ultrapure water showed that at lower equilibrium aqueous concentrations, short chain PFCs had larger equilibrium carbon capacities than the long chain ones; vice versa.

(4) In surface water, all the anion exchange resins had decreased PFC removal in surface water. Short chain PFCs were less removed than long chain ones. PFCAs had lower removal than PFSAs. Among the resins studied PFA444 had the highest PFCs removal and fastest kinetics in natural water. The decline of the PFC removal in natural water may be caused by the competition from both NOM and inorganic anions.

(5) For the influence of resin properties, Type I resins showed higher adsorption rates compared to the Type III resin A555. In surface water, gel resins were less impacted with NOM and inorganic anions compared to macroporous resins; while, in ultrapure water, both gel and macroporous resins showed good PFC removal. Pore volume and surface area did not seem to be key impact factors, probably because all anion exchange resins had small pore volumes compared to activated carbons.

(6) All the resins had the ability to remove DOC. LC-OCD results showed that humic substances may be the portion of the DOC which competed with PFCs. Among all the resins, TAN-1 showed the best NOM removal.

(7) Sulfate concentration could substantially decrease short chain PFCA removal by ion exchange resins; while PFC removal by ion exchange resins was less influenced by the presence of nitrate.

### 7.1.3 Anion Exchange Resins Regeneration Performance for PFCs Removal and Column Experiments

(1) The batch experiments results showed that short chain PFCs had better regeneration performance than long chain PFCs, and PFCAs had higher regeneration rates compared to PFSAs.

(2) For the influence of the regenerants, higher concentration of the regenerant salts could help increase the regeneration efficiency.  $\text{Na}^+$  ions had better regeneration performance than  $\text{NH}_4^+$  ions. Methanol could significantly increase regeneration rates of all PFCs especially the long chain PFCs and the PFSAs. Without organic solvent, the regeneration performance of the selected anion exchange resins for long chain PFCs and PFSAs decreased.

(3) Among all three selected resins, A555 had best PFCs regeneration performance, and was then applied in the column tests.

(4) In the anion exchange column experiments, the breakthrough curves of all PFCs were tested in both ultrapure water and Grand River water. The ultrapure water results did not show trend of breakthrough at the end of the batch when the BV was 200000. The Grand River water results showed that before the BV is 100000, all selected PFCs showed similar breakthrough of around 20%. After 100000 BV, the breakthrough concentrations of all PFCs gradually increased and 90% breakthroughs were reached after 220000 BV. These results provided useful information about operational conditions for pilot and full-scale designs.

(5) The SEM images of the A555 resin before and after treated with PFCs containing water of both ultrapure and surface water showed that NOM (PFCs were also supposed to be contributed to be covered on the surface of the resins in the ultrapure water treatment) and even microorganisms can be adsorbed on the surface of the resin and the pores of the resins were blocked, which could probably explain the decrease of the anion exchange performance after certain time treatment.

(6) Regeneration column tests showed that a higher concentration of the NaCl (10%) in regenerants had only very slight increase to the regeneration performance compared to 5% NaCl. A slower regeneration flow rate (10 ml/min) had obvious increased regeneration performance compared to higher flow rate of 20 ml/min. Thus, 5% NaCl and 10 ml/min flow rate were considered to be the best conditions.

#### **7.1.4 PFCs Removal Performance of Synthesized Magnetic Nanoparticles**

(1) In ultrapure water, all three designed magnetic nanoparticles had high removals for long chain PFCs and relative low removals for short chain PFCs. PFSAAs had better PFCs removal compared to PFCAs. Among all target nanoparticles, N1 had best PFCs removal performance. It reached 20% and 40% removal for PFBA and PFHxA respectively. All the other PFCs reached more than 90% removal after 48 hours.

(2) In surface water, the PFCs removal of all three nanoparticles largely decreased. N1 remained the nanoparticle with best PFCs removal performance. N2 and N3 had less 20% removal for all target PFCs in surface water after 48 hours.

(3) LC-OCD results showed that N1 had some removal of biopolymers and humic substances; while N2 and N3 had some removal of low molecular acids. As a result, biopolymers and humic substances were hypothesized to be the main competitors for N1, and low molecular acids competed more with N2 and N3.

(4) All three nanoparticles showed no inorganic anions removal in surface water. Thus, it is possible that inorganic anions may not be the main competitor causing the decrease in PFC removals.

#### **7.1.5 Contributions to Knowledge**

The contributions to knowledge in this thesis include:

(1) The analysis of three types of PFCs including PFCAs, PFSAs, and PFPAs was applied in one LC-MS/MS method with short retention times and low MDLs.

(2) The influence of resin characteristics, PFCs properties, and water qualities on PFCs removal and the mechanisms of the influence were thoroughly investigated. Five resins, seven PFCs, and three water types were systematically studied to test their influence. The results would help to understand the ion exchange process for PFCs removal and help select suitable anion exchange resins for PFCs removal.

(3) The regeneration conditions of anion exchange resins after PFCs removal were tested and optimized. The impact factors to regeneration including resin properties, PFC properties, water qualities, regenerant types, and operational conditions were investigated as well as the mechanisms.

(4) The anion exchange column experiments provided useful information about operational conditions for pilot and full-scale designs.

(5) New types of adsorbents, magnetic nanoparticles for PFCs removal, were designed in collaboration with colleagues in the Dept. of Chemical Engineering. These novel adsorbents were synthesized by the partners from Dept. of Chemical Engineering, and their PFCs removal performance and impact factors were investigated by the author. It was a new attempt of using novel adsorbent for PFCs removal, and provided new knowledge for designing more feasible nanoparticles for PFCs removal.

## **7.2 Recommendations for Future Research**

Several research issues which will be of interest to water treatment were noted over the course of this study. The following suggestions should be considered in further studies.

(1) As newly detected PFCs in natural water, PFPAs were included in the development of the LC-MS/MS analytical method. The behavior and fate of PFPAs during adsorption and ion exchange processes need to be investigated.

(2) Bottle point experiments and bench scale column studies were conducted for anion exchange process to investigate the PFCs removal and regeneration performance. In future studies, pilot and full scale column experiments should be investigated to validate the trend observed in bench studies.

(3) The primary mechanism of PFCs removal by anion exchange resins was discussed in this study which could be a synergistic effect of both adsorption and ion exchange mechanisms; however, how to select and design suitable anion exchange resins and nanoparticles for PFCs removal based on these mechanisms will need more investigations.

(4) To further understand the competition of NOM fractions with PFCs in ion exchange and adsorption processes, future study should investigate the effects of isolated fractions of NOM on PFCs removal separately.

(5) The regeneration performance of selected anion exchange resins for long chain PFCs without using organic solvent was found to be unsatisfactory in both batch and column studies. New types of anion exchange resins and new regeneration conditions which can increase the regeneration rates for long chain PFCs need to be investigated in future studies.

(6) The synthesized magnetic nanoparticles in this study were proved to have very high adsorption rates for the investigated PFCs. Further studies will need to improve the modification of the nanoparticles to increase their stability and their PFCs adsorption performance especially in surface water.

(7) The study of using magnetic nanoparticles for PFCs removal was a proof of concept experiment to test its feasibility. The separation of the magnetic nanoparticles and the design of the application need further investigation. The regeneration of the nanoparticles will also need to be studied.

(8) The PFCs removal studies in this research were observed in ultrapure water and two surface waters (one river water and one lake water). In future studies, groundwater can be used as source water to study the effect of different waters on PFCs removal.

## References

- Ahrens, L., Harner, T., Shoeib, M., Lane, D. A., Murphy, J. G. (2012) Improved characterization of gas-particle partitioning for per- and polyfluoroalkyl substances in the atmosphere using annular diffusion denuder samplers. *Environmental Science & Technology*, 46(13), 7199-7206.
- Agency for Toxic Substance and Disease Registry (ATSDR). (2009) Draft toxicological profile for perfluoroalkyls. ATSDR, Atlanta, US.
- Alexander B. H., Olsen G. W., Burriss J. M., Mandel J. H., Mandel J. S. (2003) Mortality of employees of a perfluorooctanesulphonyl fluoride manufacturing facility. *Occupational and Environmental Medicine*, 60, 722-729.
- Ali I., Asim M., & Khan T. A. (2012) Low cost adsorbents for the removal of organic pollutants from wastewater. *Journal of Environmental Management*, 113, 170-183.
- Anumol T., Merel S., Clarke B. O., & Snyder S. A. (2013) Ultra high performance liquid chromatography tandem mass spectrometry for rapid analysis of trace organic contaminants in water. *Chemistry Central Journal*, 7 (104), 1-14.
- American Public Health Association (APHA). (2012) Standard methods for the examination of water and wastewater. American Public Health Association, American Water Works Association, and Water Pollution Control Federation, 22<sup>nd</sup> edition, Washington, D.C., US.
- Awad, E., Zhang, X., Bhavsar, S.P., Petro, S., Crozier, P.W., Reiner, E.J., Fletcher, R., Tittmier, S.A., & Braekevelt, E. (2011) Long-term environmental fate of perfluorinated compounds after accidental release at Toronto Airport. *Environ. Sci. Technol.* 45 (19), 8081-8089.



Banfield J. & Zhang H. (2001) Nanoparticles in the environment. *Reviews in Mineralogy and Geochemistry*, 44 (1), 1-58.

Barbaro P. & Liguori F. (2009) Ion exchange resins: catalyst recovery and recycle. *Chemical Reviews*, 109 (2), 515-529.

Bartolome M., Gallego-Pico A., Huetos O., Lucena M., Castario A. (2016) A fast method for analyzing six perfluoroalkyl substances in human serum by solid-phase extraction on-line coupled to liquid chromatography tandem mass spectrometry. *Analytical Bioanalytical Chemistry*, 408 (8), 2159-2170.

Bazri M. M., Barbeau B., & Mohseni M. (2016a) Evaluation of weak and strong basic anion exchange resins for NOM removal. *Journal of Environmental Engineering*, 142 (10), 04016044.

Bazri M. M., Martijn B., Kroesbergen J., & Mohseni M. (2016b) Impact of anionic ion exchange resins on NOM fractions: effect on N-DBPs and C-DBPs precursors. *Chemosphere*, 144, 1988-1995.

Berger U., Kaiser M., Karrman A., Barber J., Leeuwen S. (2011) Recent developments in trace analysis of poly- and perfluoroalkyl substances. *Analytical Bioanalytical Chemistry*, 400 (6), 1625-1635.

Bhatnagar A., Hogland W., Marques M. & Sillanpaa M. (2013) An overview of the modification methods of activated carbon for its water treatment applications. *Chemical Engineering Journal*, 219, 499-511.

Brooke, D., Fotitt, A. & Nwaogu, T.A. (2004) Environmental risk evaluation report: perfluorooctane sulfonate (PFOS). Report Produced by Environment Agency's Science Group. Environment Agency, UK.

Carter K. & Farrell J. (2010) Removal of perfluorooctane and perfluorobutane sulfonate from water via carbon adsorption and ion exchange. *Separation Science and Technology*, 45, 762-767.

Chang Y., Chen W., Bai F., Chen P., Wang G. & Chen C. (2012) Determination of perfluorinated chemicals in food and drinking water using high-flow solid-phase extraction and ultra-high performance liquid chromatography tandem mass spectrometry. *Anal Bioanal Chem.*, 402, 1315-1325.

Chen X., Xia X., Wang X., Qiao J. & Chen H. (2011) A comparative study on sorption of perfluorooctane sulfonate (PFOS) by chars, ash and carbon nanotubes. *Chemosphere*, 83, 1313–1319.

Cheng W., Dastgheib S. A. & Karanfil T. (2005) Adsorption of dissolved natural organic matter by modified activated carbons. *Water Research*, 39, 2281-2290.

Chowdhury Z. et al. (2013) Activated carbon solutions for improving water quality. American Water Works Association, Denver, US.

Chularueangaksorn P., Tanaka S., Fujii S. & Kunacheva C. (2013) Regeneration and reusability of anion exchange resin used in perfluorooctane sulfonate removal by batch experiments. *J. Appl. Polym. Sci.*, 884-890.

Corwin C. J. and Summers R. S. (2010) Scaling trace organic contaminant adsorption capacity by granular activated carbon. *Environ. Sci. Technol.*, 44, 5403-5408.

Demirbas A. (2008) Heavy metal adsorption onto agro-based waste materials: A review. *Journal of Hazardous Materials*, 157, 220-229.

Demirbas A. (2009) Agricultural based activated carbons for the removal of dyes from aqueous solutions: A review. *Journal of Hazardous Materials*, 167, 1-9.

Deng S., Yu Q., Huang J. & Yu G. (2010) Removal of perfluorooctane sulfonate from wastewater by anion exchange resins: Effects of resin properties and solution chemistry. *Water Research*, 44 (18), 5188-5195.

Deng S., Yu Q., Huang J. & Yu G. (2010) Removal of perfluorooctane sulfonate from wastewater by anion exchange resins: Effects of resin properties and solution chemistry. *Water Research*, 44 (18), 5188-5195.

Deng S., Zhang Q., Nie Y. et al. (2012) Sorption mechanisms of perfluorinated compounds on carbon nanotubes. *Environmental Pollution*, 168,138-144.

D'eon J. C., Crozier P. W., Furdui V. I., et al. (2009) Perfluorinated phosphonic acids in Canadian surface waters and wastewater treatment plant effluent-- Discovery of a new class of perfluorinated acids. *Environmental Toxicology and Chemistry*, 28 (10), 2101-2107.

De Ridder D. J., Verliefde A. R. D., Heijman S. G. J. et al. (2011) Influence of natural organic matter on equilibrium adsorption of neutral and charged pharmaceuticals onto activated carbon. *Water Science & Technology*, 63 (3), 416-423.

De Silva A. O., Allard, C. N., Spencer C., et al. (2012) Phosphorus-containing fluorinated organics-- polyfluoroalkyl phosphoric acid diesters (diPAPs), perfluorophosphonates (PFPAAs), and perfluorophosphinates (PFPIAs) in residential indoor dust. *Environ. Sci. Technol.*, 46 (22), 12575-12582.

Ding H., Peng H., Yang M. & Hu J. (2012) Simultaneous determination of mono- and disubstituted polyfluoroalkyl phosphates in drinking water by liquid chromatography–electrospray tandem mass spectrometry. *Journal of Chromatography A*, 1227, 245- 252.

Ding L., Marinas B. J., Schideman L. C. & Snoeyink V. L. (2006) Competitive effects of natural organic matter: parametrization and verification of the three-component adsorption model COMPSORB. *Environ. Sci. Technol.*, 40 (1), 350-356.

- Ding L., Du B., Luo G., & Deng H. (2015) Adsorption of bromate from emergently polluted raw water using MIEX resin: equilibrium, kinetic, and thermodynamic modeling studies. *Desalination and Water Treatment*, 56, 2193–2205.
- Dudley L. A. M. B. (2012) Removal of perfluorinated compounds by powdered activated carbon, superfine powdered activated carbon, and anion exchange resins. Thesis submitted to the Graduate Faculty of the North Carolina State University, (US).
- Eriksen K. T. Sorenen M., Mclaughlin J. K. et al. (2009) Perfluorooctanoate and perfluorooctanesulfonate plasma levels and risk of cancer in the general Danish population. *Journal of National Cancer Institute*, 101 (8), 605-609.
- European Food Safety Authority (EFSA). (2008) Perfluorooctane sulfonate (PFOS), perfluorooctanoic acid (PFOA) and their salts. *The EFSA Journal*, 6 (53), 1-131.
- Eschauzier C., Beerendonk E., Scholte-Veenendaal P. & De Voogt P. (2012) Impact of treatment processes on the removal of perfluoroalkyl acids from the drinking water production chain. *Environ. Sci. Technol.*, 46 (3), 1708–1715.
- Esparza X., Moyano E., de Boer J., Galceran M. T. & van Leeuwen S. P. J. (2011) Analysis of perfluorinated phosphonic acids and perfluorooctane sulfonic acid in water, sludge and sediment by LC–MSMS. *Talanta*, 86, 329-336.
- Fearing D. A., Banks J., Guyetand S. et al., (2004) Combination of ferric and MIEXs for the treatment of a humic rich water. *Water Research*, 38 (10), 2551-2558.
- Flores C., Ventura F., Martin-Alonso J. & Caixach J. (2013) Occurrence of perfluorooctane sulfonate (PFOS) and perfluorooctanoate (PFOA) in N.E. Spanish surface waters and their removal in a drinking water treatment plant that combines conventional and advanced treatments in parallel lines. *Science of the Total Environment*, 461-462, 618-626.

Fujii Y., Harada K. H., and Koizumi A. (2012) Analysis of perfluoroalkyl carboxylic acids in composite dietary samples by gas chromatography/mass spectrometry with electron capture negative ionization. *Environmental Science & Technology*, 46, 11235-11242.

Gao Y., Deng S., Du Z., Liu K., & Yu G. (2017) Adsorptive removal of emerging polyfluoroalkyl substances F-53B and PFOS by anion-exchange resin: A comparative study. *Journal of Hazardous Materials*, 323, 550-557.

Gosetti F., Chiuminatto U., Zampieri D., et al. (2010) Determination of perfluorochemicals in biological, environmental and food samples by an automated on-line solid phase extraction ultra high performance liquid chromatography tandem mass spectrometry method. *Journal of Chromatography A*, 1217 (50), 7864-7872.

Guo R., Reiner E. J., Bhavsar S. P. et al. (2012) Determination of polyfluoroalkyl phosphoric acid diesters, perfluoroalkyl phosphonic acids, perfluoroalkyl phosphinic acids, perfluoroalkyl carboxylic acids, and perfluoroalkane sulfonic acids in lake trout from the Great Lakes region. *Anal Bioanal Chem*, 404 (9), 2699-2709.

Gutierrez L., Li X., Wang J. et al. (2009). Adsorption of rotavirus and bacteriophage MS2 using glass fiber coated with hematite nanoparticles. *Water Research*, 43 (20), 5198-5208.

Hansen M., Borresen M. H., Schlabach M. & Cornelissen G. (2010) Sorption of perfluorinated compounds from contaminated water to activated carbon. *J Soils Sediments*, 10 (2), 179-185.

Harris, D. C. (2007) *Quantitative chemical analysis*. New York W. H. Freeman & Company, New York.

Health Canada, 2016a. Perfluorooctanoic acid (PFOA) in drinking water. Retrieved January 11, 2017 from <https://www.healthycanadians.gc.ca/health-system-systeme-sante/consultations/acide-perfluorooctanoic-acid/alt/perfluorooctanoic-eng.pdf>.

Health Canada, 2016b. Perfluorooctane sulfonate (PFOS) in drinking water. Retrieved January 11, 2017 from <https://www.healthycanadians.gc.ca/health-system-systeme-sante/consultations/perfluorooctane-sulfonated-eng.pdf>.

Hlouskova V., Hradkova P., Poustka J. et al. (2013) Occurrence of perfluoroalkyl substances (PFASs) in various food items of animal origin collected in four European countries. *Food Additives & Contaminants: Part A*, 30 (11), 1918-1932.

Ho Y. & McKay G. (1999) Pseudo-second order model for sorption processes. *Process Biochemistry*, 34, 451-465.

Hua M., Zhang S., Pan B., Zhang W., Lv L. & Zhang Q. (2012). Heavy metal removal from water/wastewater by nanosized metal oxides: A review. *Journal of Hazardous Materials* 211, 317-331.

Huang Y., Fulton A. N., & Keller A. A. (2016) Simultaneous removal of PAHs and metal contaminants from water using magnetic nanoparticle adsorbents. *Science of the Total Environment*, 571, 1029-1036.

Huber S., Balz A., Abert M. & Pronk W. (2011) Characterisation of aquatic humic and non-humic matter with size-exclusion chromatography - organic carbon detection - organic nitrogen detection (LC-OCD-OND). *Water Research*, 45 (2), 879-885.

Jensen, A.A., Poulsen, P.B. & Bossi, R. (2008) Survey and environmental/health assessment of fluorinated substances in impregnated consumer products and impregnating agents. No. 99. Danish Environmental Protection Agency, Copenhagen, Denmark.

Kaiser, M.A., Barton, C.A., Botelho, M., et al. (2006) Understanding the transport of anthropogenic fluorinated compounds in the environment. *Organohalogen Compd.*, 68, 675-678.

Kaur A. & Gupta U. (2009). A review on applications of nanoparticles for the preconcentration of environmental pollutants. *Journal of Materials Chemistry*, 19, 8279-8289.

Lacina O., Hradkova P., Pulkrabova J. & Hajslova J. (2011) Simple, high throughput ultra-high performance liquid chromatography-tandem mass spectrometry trace analysis of perfluorinated alkylated substances in food of animal origin Milk and fish. *Journal of Chromatography A.*, 1218 (28), 4312-4321.

Lagergren, S. (1898). About the theory of so-called adsorption of soluble substances. *Kungliga Svenska Vetenskapsakademiens. Handlingar*, 24 (4), 1-39.

Lampert D., Frisch M., & Speitel G. D. (2007) Removal of perfluorooctanoic acid and perfluorooctane sulfonate from wastewater by ion exchange. *Practice Periodical of Hazardous, Toxic, and Radioactive Waste Management*, 11(1), 60-68.

Lankova D., Lacina O., Pulkrabova J. & Hajslova J. (2013) The determination of perfluoroalkyl substances, brominated flame retardants and their metabolites in human breast milk and infant formula. *Talanta*, 177, 318-325.

Lau C. (2012) Perfluoroalkyl acids: Recent research highlights. *Reproductive Toxicology*, 33 (4), 405-409.

Lee J. & Walker H. (2011). Adsorption of microcystin-Lr onto iron oxide nanoparticles. *Colloids and Surfaces A: Physicochemical and Engineering Aspects*, 373, 94-100.

Lee S. & Ahn K. (2004) Monitoring of COD as an organic indicator in waste water and treated effluent by fluorescence excitation-emission (FEEM) matrix characterization. *Water Science and Technology*, 50(8), 57-63.

Leshuk T., Linley S., Baxter G., & Gu F. (2012) Mesoporous hollow sphere titanium dioxide photocatalysts through hydrothermal silica etching. *Appl. Mater. Interfaces*, 4, 6062-6070.

Li Q. L., Snoeyink V. L., Marinas B. J. & Campos C. (2003) Pore blockage effect of NOM on atrazine adsorption kinetics of PAC: the roles of PAC pore size distribution and NOM molecular weight. *Water Research*, 37, 4863-4872.

Lian F., Xing B. & Zhu L. (2011) Comparative study on composition, structure, and adsorption behavior of activated carbons derived from different synthetic waste polymers. *Journal of Colloid and Interface Science*, 360, 725-730.

Linley S., Leshuk T., & Gu F. (2013) Synthesis of magnetic rattle-type nanostructures for use in water treatment. *Appl. Mater. Interfaces*, 5, 2540-2548.

Liu R., Ruan T., Wang T. et al. (2013) Trace analysis of mono-, di-, tri-substituted polyfluoroalkyl phosphates and perfluorinated phosphonic acids in sewage sludge by high performance liquid chromatography tandem mass spectrometry. *Talanta*, 111, 170-177.

Lofrano G., Carotenuto M., Libralato G. et al., (2016) Polymer functionalized nanocomposites for metals removal from water and wastewater: An overview. *Water Research*, 92, 22-37.

Loos R., Tavazzi S., Paracchini B., Canuti E. & Weissteiner C. (2013) Analysis of polar organic contaminants in surface water of the northern Adriatic Sea by SPE followed by UPLC-QTRAP MS using a hybrid triple-quadrupole linear ion trap instrument. *Anal Bioanal Chem.*, 405 (18), 5875-5885.

López de la Torre M. & Guijarro M. (2010) Covalent bonds on activated carbon. *Eur. J. Org. Chem.* 27, 5147-5154.

Lu X., Shao Y., Gao N., & Ding L. (2015) Equilibrium, thermodynamic, and kinetic studies of the adsorption of 2,4-dichlorophenoxyacetic acid from aqueous solution by MIEX resin. *Journal of Chemical and Engineering Data*, 60 (5), 1259-1269.



Martin, J. W., Kannan, K., Berger, U., Voogt, P. D., Field, J., et al. (2004) Analytical challenges hamper perfluoroalkyl research. *Environmental Science & Technology*, 38(13), 248-255.

Mahmoodi N. M., Rezvani M. A., Oveisi M., Valipour A., & Asli M. A. (2016) Immobilized polyoxometalate onto the modified magnetic nanoparticle as a photocatalyst for dye degradation. *Materials Research Bulletin*, 84, 422-428.

Mathworks. (2016) Curve fitting toolbox documentation. Retrieved November 26, 2016 from <https://www.mathworks.com/help/curvefit>.

Matsui Y., Fukuda Y. Inoue T. & Matsushita T. (2003) Effect of natural organic matter on powdered activated carbon adsorption of trace contaminants: characteristics and mechanism of competitive adsorption. *Water Research*, 37 (18), 4413-4424.

Montgomery Watson Harza (MWH), (2005) *Water treatment: principle and design*, Second edition. John Wiley & Sons, Inc., Hoboken, US.

Najm I. N., Snoeyink V. L. & Richard Y. (1991) Effect of initial concentration of a SOC in natural-water on its adsorption by activated carbon. *J Am Water Works Assoc*, 83, 57-63.

Nguyen T. V., Zhang R., Vigneswaran S. et al., (2011) Removal of organic matter from effluents by Magnetic Ion Exchange (MIEX®). *Desalination*, 276 (1), 96-102.

Ochoa-Herrera V. & Sierra-Alvarez R. (2008) Removal of perfluorinated surfactants by sorption onto granular activated carbon, zeolite and sludge. *Chemosphere*, 72, 1588-1593.

Onghena M., Moliner-Martinez Y., Pico Y. & Campins-Falco P. (2012) Analysis of 18 perfluorinated compounds in river waters: Comparison of high performance liquid chromatography-tandem mass spectrometry, ultra-high-performance liquid chromatography-tandem mass spectrometry and capillary liquid chromatography–mass spectrometry. *Journal of Chromatography A*, 1244, 88-97.

Ou J., Mei M., & Xu X. (2016) Magnetic adsorbent constructed from the loading of amino functionalized Fe<sub>3</sub>O<sub>4</sub> on coordination complex modified polyoxometalates nanoparticle and its tetracycline adsorption removal property study. *Journal of Solid State Chemistry*, 238, 182-188.

Peiris R., Halle C., Budman H., Moresoli C., Peldszus S., Huck P. M. & Legge R. L. (2010) Identifying fouling events in a membrane-based drinking water treatment process using principal component analysis of fluorescence excitation-emission matrices. *Water Research*, 44, 185-194.

Pelekani C. and Snoeyink V. L. (1999) Competitive adsorption in natural water: role of activated carbon pore size. *Water Research*, 33(5), 1209-1219.

Post G., Cohn P. D. & Cooper K. R. (2012) Perfluorooctanoic acid (PFOA), an emerging drinking water contaminant: A critical review of recent literature. *Environmental Research*, 116, 93-117.

Punyapalakul P., Suksomboon K., Prarat P. & Khaodhiar S. (2013) Effects of Surface Functional Groups and Porous Structures on Adsorption and Recovery of Perfluorinated Compounds by Inorganic Porous Silicas. *Separation Science and Technology*, 48, 775-788.

Qu X., Brame J., Li Q. & Alvarez P. J. J. (2012). Nanotechnology for a safe and sustainable water supply: enabling integrated water treatment and reuse. *Accounts of Chemical Research*, 46(3), 834-843.

Rahman M., Peldszus S. & Anderson W. (2014) Behaviour and fate of perfluoroalkyl and polyfluoroalkyl substances (PFASs) in drinking water treatment: a review. *Water Research*, 50, 318-340.

Rahman M. (2014) Removal of perfluorinated compounds form ultrapure and surface waters by adsorption and ion exchange. PhD thesis. Department of Civil & Environmental Engineering. University of Waterloo.

Rahmani S. & Mohseni M. (2017) The Role of Hydrophobic properties in ion exchange removal of organic compounds from water. *The Canadian Journal of Chemical Engineering*, 95, 1449-1455.

Recillas S., Colon J., Casals E., Gonzalez E. & Puentes V. (2010) Chromium VI adsorption on cerium oxide nanoparticles and morphology changes during the process. *Journal of Hazardous Materials*, 184, 425-431.

Rivera-Utrilla J., Sanchez-Polo M., Gomez-Serrano V. et al. (2011) Activated carbon modifications to enhance its water treatment applications. An overview. *Journal of Hazardous Materials*, 187 (1-3), 1–23.

Rumsby P., McLaughlin C. L. & Hall T. (2009) Perfluorooctane sulphonate and perfluorooctanoic acid in drinking and environmental waters. *Philosophical Transactions: Mathematical, Physical and Engineering Sciences*, 367 (1904), 4119-4136.

Schuricht F., Borovinskaya E. S., & Reschetilowski W. (2017) Removal of perfluorinated surfactants from wastewater by adsorption and ion exchange - Influence of material properties, sorption mechanism and modeling. *Journal of Environmental Sciences*, 54, 160-170.

Sinclair E. & Kannan K. (2006) Mass loading and fate of perfluoroalkyl surfactants in wastewater treatment plants. *Environ. Sci. Technol.*, 40 (5), 1408-1414.

Sindik O., Orata F. Weber R. & Osibanjo O. (2013) Per- and polyfluoroalkyl substances in selected sewage sludge in Nigeria. *Chemosphere*, 92 (3), 329-335.

Singh S., Barik K. & Bahadur D. (2011) Surface engineered magnetic nanoparticles for removal of toxic metal ions and bacterial pathogens. *Journal of Hazardous Materials*, 192, 1539-1547.

Suffet I. & McGuire M. (1980) Activated carbon adsorption of organics from the aqueous phase. *Ann Arbor Science*, Ann Arbor, US.

Summers, R.S. (1986) Activated carbon adsorption of humic substances: Effect of molecular size and heterodispersity. PhD thesis, Department of Civil Engineering, Stanford University.

Takagi S., Adachi F., Miyano K. et al. (2011) Fate of perfluorooctanesulfonate and perfluorooctanoate in drinking water treatment processes. *Water Research*, 45 (13), 3925-3932.

Taniyasu, S., Kannan K., So M. et al. (2005) Analysis of fluorotelomer alcohols, fluorotelomer acids, and short- and long-chain perfluorinated acids in water and biota. *Journal of Chromatography A*. 1093(1), 89-97.

Taniyasu S., Kannan K., Yeung L. W. Y et al. (2008) Analysis of trifluoroacetic acid and other short-chain perfluorinated acids (C2–C4) in precipitation by liquid chromatography–tandem mass spectrometry: Comparison to patterns of long-chain perfluorinated acids (C5–C18). *Anal. Chim. Acta.*, 619 (2), 221-230.

Tang Y., Li S., Zhang Y., Yu S., & Martikka M. (2014) Sorption of tetrabromobisphenol A from solution onto MIEX resin: batch and column test. *Journal of the Taiwan Institute of Chemical Engineers.*, 45 (5) 2411-2417.

Tang L., Xie Z., Zeng G. et al. (2016) Removal of bisphenol A by iron nanoparticle-doped magnetic ordered mesoporous carbon. *Royal Society of Chemistry Advances*, 6 (31), 25724-25732.

Tao J., Xiong J., Jiao C., Zhang D., Lin H., & Chen Y. (2017) Cellulose/polymer/silica composite cotton fiber based on a hyperbranch-mesostructure system as versatile adsorbent for water treatment. *Carbohydrate Polymers*, 166, 271-280.

Treguer R., Couvert A., Wolbert D. Suty H. & Randon G. (2006) Influence of porosity and surface chemistry of commercially available powdered activated carbons for the removal of dissolved organic carbon. *Water Science & Technology: Water Supply*, 6(3), 27-34.

Trier X., Granby K. & Christensen J. H. (2011) Tools to discover anionic and nonionic polyfluorinated alkyl surfactants by liquid chromatography electrospray ionisation mass spectrometry. *Journal of Chromatography A*, 1218 (40), 7094-7104.

Tseng R., Wu F., & Juang R. (2010) Characteristics and applications of the Lagergren's first-order equation for adsorption kinetics. *Journal of the Taiwan Institute of Chemical Engineers*, 41, 661-669.

Ullah S., Alsberg T., Vestergren R. & Berger U. (2012) Determination of perfluoroalkyl carboxylic, sulfonic, and phosphonic acids in food. *Anal Bioanal Chem.*, 404 (8), 2193-2201.

Upadhyayula V. K. K., Deng S., Mitchell M. C. & Smith G. B. (2009). Application of carbon nanotube technology for removal of contaminants in drinking water: A review. *Science of the Total Environment*, 408, 1-13.

United States Environmental Protection Agency (USEPA) (2009a) Drinking water contaminant candidate List 3 (CCL 3) and regulatory determination. Retrieved on July 28, 2016 from <https://www.epa.gov/ccl>

USEPA (2009b) Method 537. Determination of selected perfluorinated alkyl acids in drinking water by solid phase extraction and liquid chromatography/tandem mass spectrometry (LC/MS/MS). EPA, Washington, D.C., US.

USEPA (2011a) Regulatory determinations for the third drinking water contaminant candidate list. EPA, Washington D.C., US.

USEPA (2011b) Revisions to the unregulated contaminants monitoring regulations (UCMR3) for public water systems. 76 (42), 11713-11737.

USEPA (2013) Emerging contaminants – perfluorooctane sulfonate (PFOS) and perfluorooctanoic acid (PFOA). Emerging contaminants fact sheet – PFOS and PFOA. EPA, Washington, DC, US.

USEPA (2016a) Drinking water health advisory for perfluorooctanoic acid (PFOA). Retrieved July 28, 2016 from [https://www.epa.gov/sites/production/files/2016-05/documents/pfoa\\_health\\_advisory\\_final\\_508.pdf](https://www.epa.gov/sites/production/files/2016-05/documents/pfoa_health_advisory_final_508.pdf)

USEPA (2016b) Drinking water health advisory for perfluorooctane sulfonate (PFOS). Retrieved July 28, 2016 from [https://www.epa.gov/sites/production/files/2016-05/documents/pfos\\_health\\_advisory\\_final\\_508.pdf](https://www.epa.gov/sites/production/files/2016-05/documents/pfos_health_advisory_final_508.pdf).

USEPA (2016c) Drinking water contaminant candidate List 4 (CCL 4) and regulatory determination. Retrieved on Jan. 1, 2017 from <https://www.epa.gov/ccl>.

Velten S., Knappe D. R. U., Traber J. et al. (2011) Characterization of natural organic matter adsorption in granular activated carbon adsorbers. *Water Research*, 45 (13), 3951-3959.

Vunain E., Mishra A. K. & Krause R. W. (2013) Fabrication, Characterization and Application of Polymer Nanocomposites for Arsenic(III) Removal from Water. *J Inorg Organomet Polym*, 23, 293-305.

Wang, Z., MacLeod, M., Cousins, I. T., Scheringer, M., Hungerbuehler, K. (2011) Using COSMOtherm to predict physicochemical properties of poly- and perfluorinated alkyl substances (PFASs). *Environmental Chemistry*, 8(4), 389-398.

White S. S. Stanko J. P., Kato K. et al. (2011) Gestational and chronic low-dose PFOA exposures and mammary gland growth and differentiation in three generations of CD-Mice. *Environmental Health Perspect*, 119 (8), 1070-1076.

Woodard S., Berry J., & Newman B. (2017) Ion exchange resin for PFAS removal and pilot test comparison to GAC. *Remediation*, 27, 19-27.

Xiao F., Davidsavor K. J., Park S., Nakayama M., Phillips B. R. (2012) Batch and column study: Sorption of perfluorinated surfactants from water and cosolvent systems by Amberlite XAD resins. *Journal of Colloid and Interface Science*, 368 (1), 505–511.

Yan Z., Cai Y., Zhu G. et al. (2013) Synthesis of 3-fluorobenzoyl chloride functionalized magnetic sorbent for highly efficient enrichment of perfluorinated compounds from river water samples. *Journal of Chromatography A*, 1321, 21-29.

Yang L., Yu W., Yan X. & Deng C. (2012) Decyl-perfluorinated magnetic mesoporous microspheres for extraction and analysis perfluorinated compounds in water using ultrahigh-performance liquid chromatography-mass spectrometry. *J. Sep. Sci.*, 35 (19), 2629-2636.

Yao Y., Volchek K., Brown C. E., Robinson A., & Obal T. (2014) Comparative study on adsorption of perfluorooctane sulfonate (PFOS) and perfluorooctanoate (PFOA) by different adsorbents in water. *Water Science & Technology*, 70 (12), 1983-1991.

Yu Z., Peldszus S. & Huck P. M. (2009) Adsorption of Selected Pharmaceuticals and an Endocrine Disrupting Compound by Granular Activated Carbon. 1. Adsorption Capacity and Kinetics. *ES&T*, 43 (5), 1467-1473.

Yu J., & Hu J. (2011) Adsorption of perfluorinated compounds onto activated carbon and activated sludge. *Journal of Environmental Engineering*, 137 (10), 945-951.

Zaggia, A., Conte L., Falletti L., Fant M., Chiorboli A. (2016) Use of strong anion exchange resins for the removal of perfluoroalkylated substances from contaminated drinking water in batch and continuous pilot plants. *Water Research*, 90, 137-146.

Zareitalabad P., Siemens J., Hamer M. & Amelung W. (2013) Perfluorooctanoic acid (PFOA) and perfluorooctanesulfonic acid (PFOS) in surface waters, sediments, soils and wastewater – A review on concentrations and distribution coefficients. *Chemosphere*, 91 (6), 725-732.

Zhou Y., He Z., Tao Y. et al., (2016) Preparation of a functional silica membrane coated on Fe<sub>3</sub>O<sub>4</sub> nanoparticle for rapid and selective removal of perfluorinated compounds from surface water sample. *Chemical Engineering Journal*, 303, 156-166.

## Appendix A

### LC-MS/MS Method Repeatability for PFCs Analysis

The method repeatability results were summarized in Table 1. From the coefficient of variation (RSD) results shown in Table 1, it was obvious that PFDA, PFBS, as well as three PFPAs had somewhat higher RSDs, which means that these compounds would have more uncertainty during the analytical method. The uncertainty may be caused by any operations in the process, including sample preparation, SPE, instrument analysis, and so on. The coefficients of variation for all PFCs ranged from 6.7% to 12.4%, which were satisfactory results.

**Table A-1 Method repeatability results for analyzing selected PFCs**

<b>PFCs</b>	<b>Peak area average</b>	<b>Standard deviation</b>	<b>Coefficient of variation</b>
<b>PFBA</b>	76766	6685	8.71%
<b>PFPeA</b>	64292	4841	7.53%
<b>PFHxA</b>	55991	5642	10.08%
<b>PFHpA</b>	95343	8789	9.22%
<b>PFOA</b>	93837	7134	7.60%
<b>PFNA</b>	76816	5124	6.67%
<b>PFDA</b>	121386	14135	11.64%
<b>PFBS</b>	1721	180	10.44%
<b>PFHxS</b>	34679	2544	7.34%
<b>PFOS</b>	27401	2405	8.78%
<b>PFHxPA</b>	2037	216	10.59%
<b>PFOPA</b>	2189	272	12.43%
<b>PFDPA</b>	1782	200	11.24%



## Appendix B

### Adsorption Kinetics Using GAC (F400) and Purolite A502p Resin for PFCs Removal

(1) Adsorption kinetics using F400 in ultrapure water (Carbon dose: 10 mg/L)

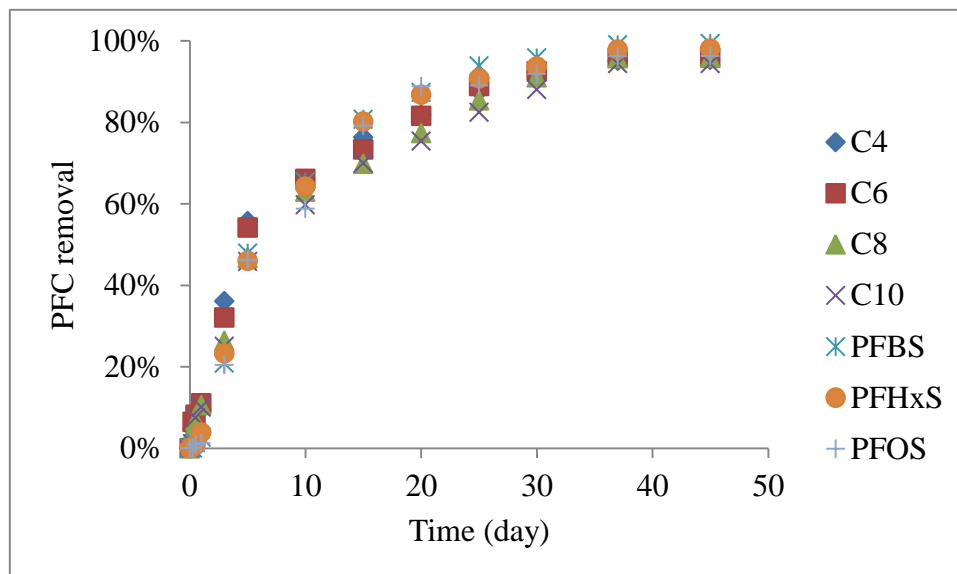


Figure B.1 Percentage removal of target PFCs using F400 in ultrapure water

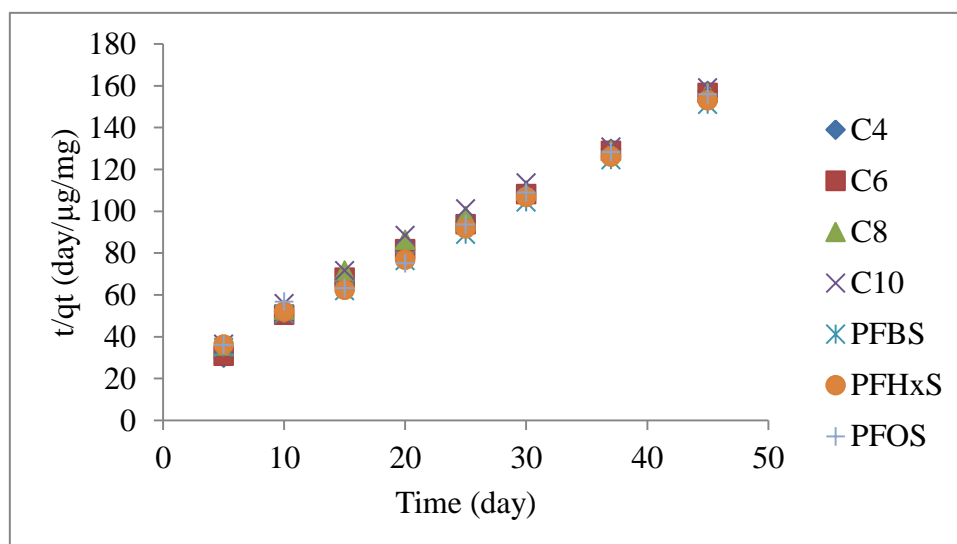
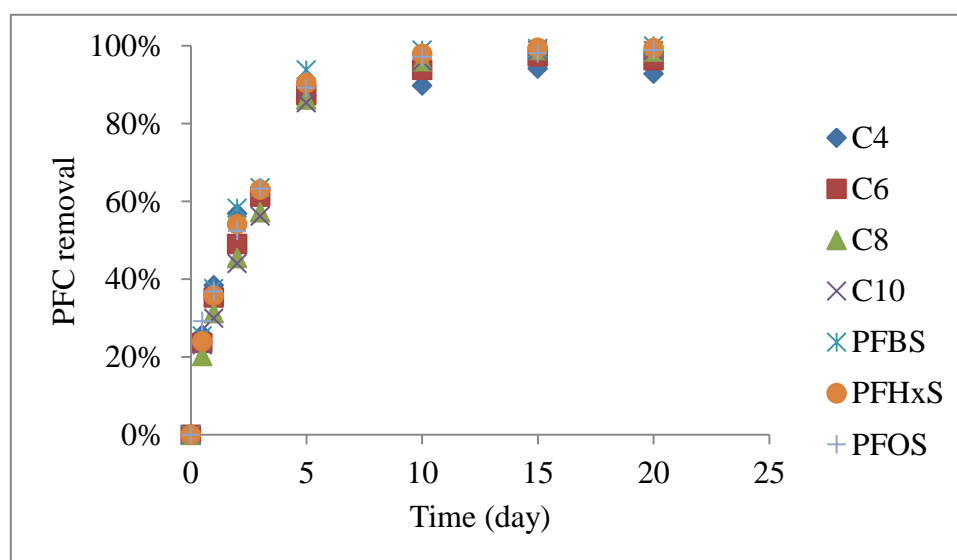


Figure B.2 Application of the pseudo-second-order model to data of Figure B.1.

**Table B-1 Pseudo-second-order model and kinetics parameters for F400 adsorption**

	C4	C6	C8	C10	PFBS	PFHxS	PFOS
$q_e$ ( $\mu\text{g}/\text{mg}$ )	0.325	0.331	0.344	0.340	0.351	0.347	0.343
$k_2$ ( $\text{mg}/\mu\text{g}/\text{day}$ )	0.534	0.476	0.344	0.337	0.407	0.399	0.396
$R^2$	0.998	0.997	0.995	0.995	0.998	0.998	0.993
$v$ ( $\mu\text{g}/\text{mg}/\text{day}$ )	0.0562	0.0522	0.0408	0.0389	0.0501	0.0481	0.0465
<b>Maximum removal (%)</b>	95.30	95.83	95.88	94.37	99.33	98.08	96.23

(2) Adsorption kinetics using Purolite A502p resin in ultrapure water (resin dose: 10 mg/L)



**Figure B.3 Percentage removal of target PFCs using A502p resin in ultrapure water**

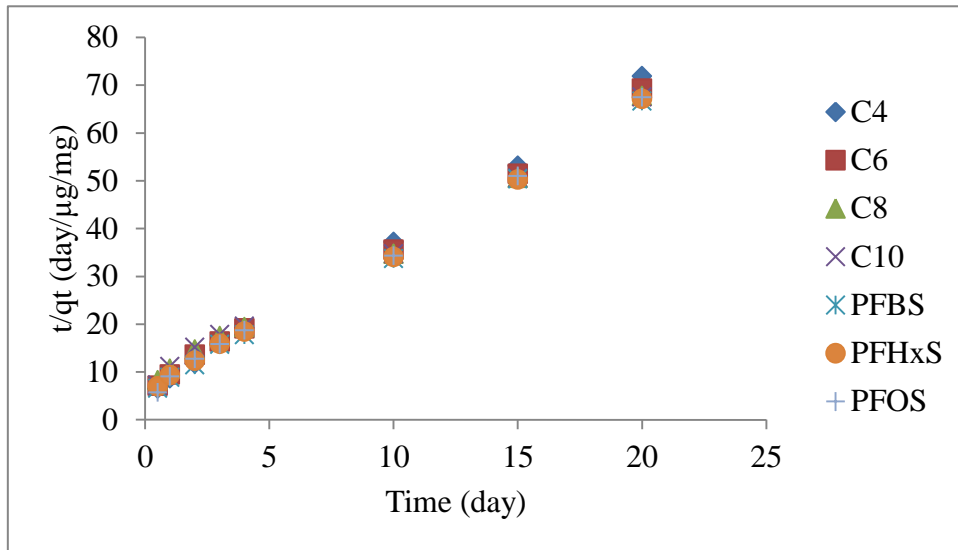


**Figure B.4 Application of the pseudo-second-order model to adsorption data of Figure B.3**

**Table B-2 Pseudo-second-order model and kinetics parameters using A502p**

	<b>C4</b>	<b>C6</b>	<b>C8</b>	<b>C10</b>	<b>PFBS</b>	<b>PFHxS</b>	<b>PFOS</b>
<b>q<sub>e</sub> (µg/mg)</b>	0.306	0.325	0.342	0.342	0.332	0.334	0.329
<b>k<sub>2</sub> (mg/µg/day)</b>	2.023	1.482	1.123	1.110	1.645	1.491	1.615
<b>R<sup>2</sup></b>	0.999	0.998	0.996	0.995	0.998	0.998	0.997
<b>v (µg/mg/day)</b>	0.189	0.157	0.131	0.130	0.182	0.166	0.175
<b>Maximum removal (%)</b>	94.09	97.26	98.92	98.84	99.33	99.48	98.10

**(3) Adsorption kinetics using Purolite A502p resin in Grand River water (resin dose: 100 mg/L)**

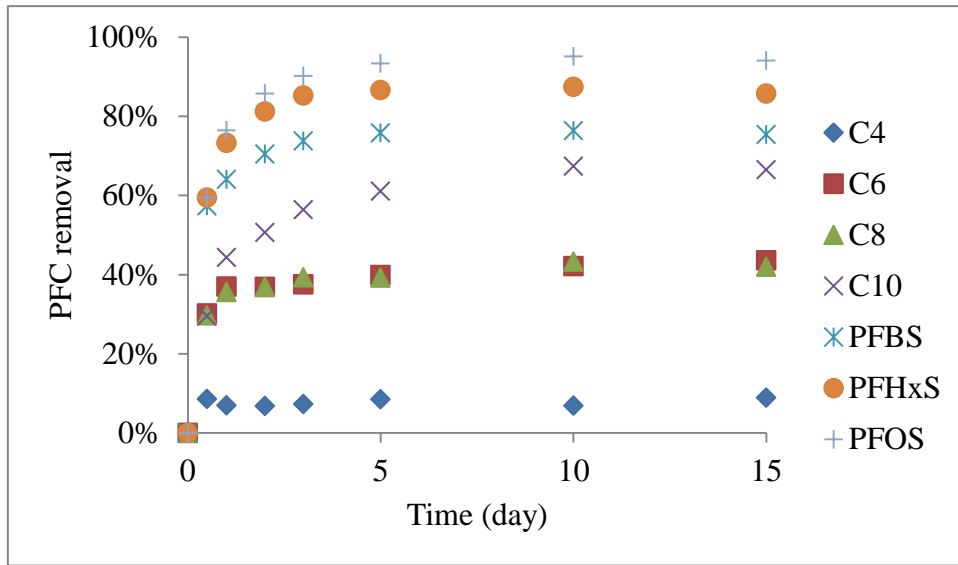


**Figure B.5 Percentage removal of target PFCs using A502p resin in Grand River water**

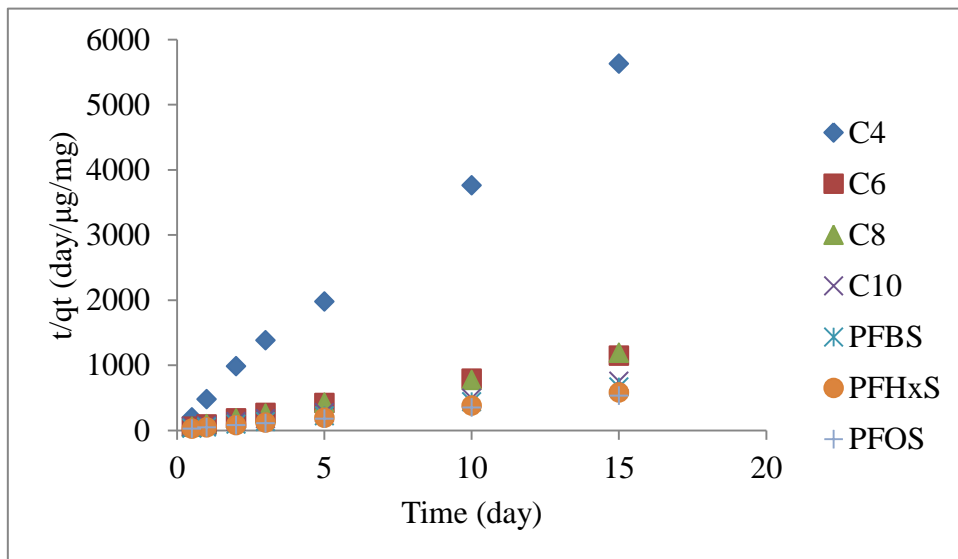


**Figure B.6 Application of the pseudo-second-order model to adsorption data of Figure B.5**

**Table B-3 Pseudo-second-order model and kinetics parameters using A502p**

	<b>C4</b>	<b>C6</b>	<b>C8</b>	<b>C10</b>	<b>PFBS</b>	<b>PFHxS</b>	<b>PFOS</b>
<b>q<sub>e</sub> (µg/mg)</b>	0.003	0.013	0.013	0.021	0.023	0.026	0.029
<b>k<sub>2</sub> (mg/µg/day)</b>	856.520	201.293	279.207	70.102	315.286	286.189	151.106
<b>R<sup>2</sup></b>	0.998	0.999	0.999	0.999	1.000	1.000	1.000
<b>v (µg/mg/day)</b>	0.0064	0.0354	0.0467	0.0310	0.1663	0.1962	0.1258
<b>Maximum removal (%)</b>	8.89	43.56	41.99	66.50	75.37	85.73	94.07

## Appendix C

### PFCs Isotherms Using GAC (F400) and A502p Resin

#### (1) PFCs mixture isotherms using GAC (F400)

Seven PFCs including PFBA, PFH<sub>x</sub>A, PFOA, PFDA, PFBS, PFH<sub>x</sub>S, and PFOS were spiked as a mixture in ultrapure water with a concentration of 3 µg/L for each compound. The doses of F400 (dry weight) were 0, 2, 4, 6, 8, 10, 12 mg/L respectively. The contact time for all samples was 20 days.

**Table C-1 Freundlich isotherms parameters of PFCs spiked as a mixture in ultrapure water using F400**

PFCs	Freundlich intensity factor 1/n (dimensionless)	Freundlich capacity factor K <sub>f</sub> [(ng/mg)(L/ng) <sup>1/n</sup> ]	R <sup>2</sup>
PFBA	0.467	9.02	0.877
PFH <sub>x</sub> A	0.407	12.12	0.833
PFOA	0.529	4.47	0.879
PFDA	0.649	1.79	0.829
PFBS	0.298	26.56	0.795
PFH <sub>x</sub> S	0.316	22.84	0.769
PFOS	0.382	13.78	0.733

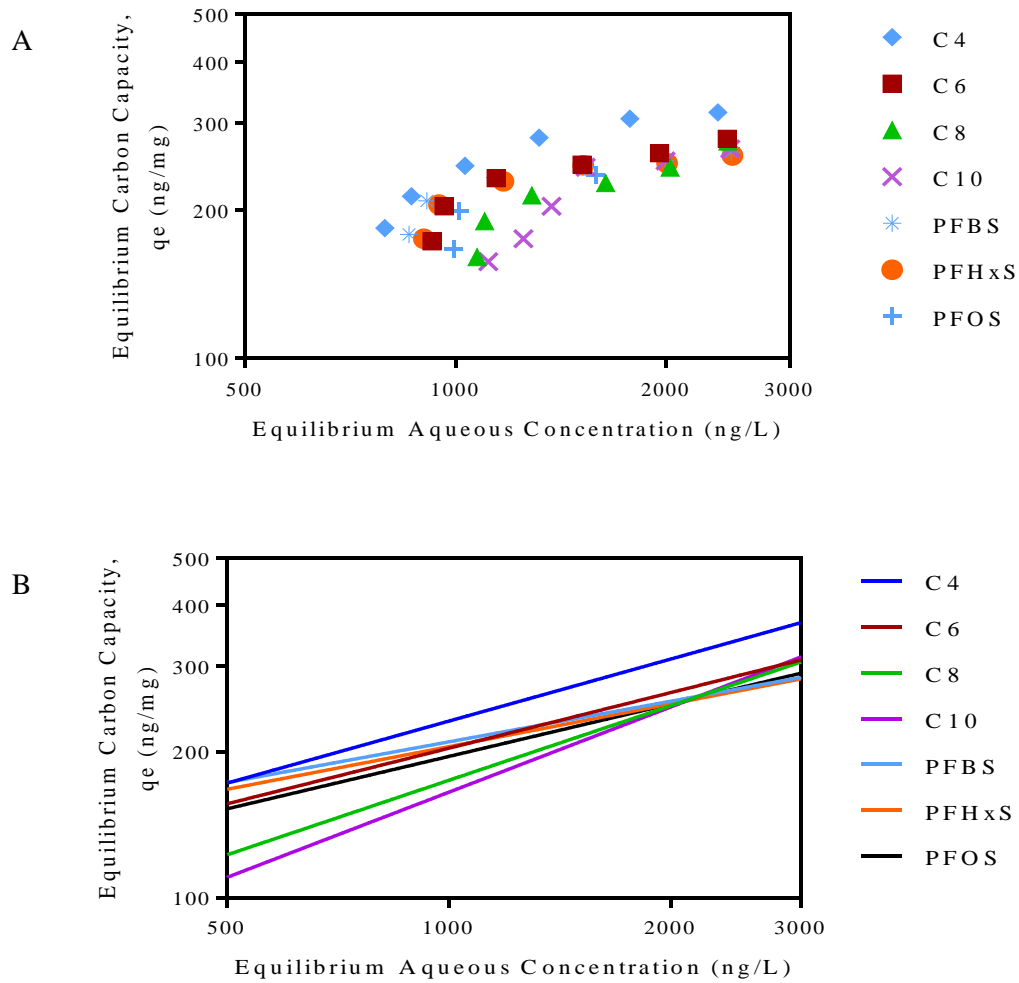


**Figure C.1 Freundlich isotherms of PFCs spiked as a mixture in ultrapure water using F400: A) experimental data of Freundlich isotherms; B) trend lines of isotherms.**

## (2) Single compound PFC isotherms using GAC (F400)

Two PFCs including PFBS and PFOS were spiked separately in ultrapure water with a concentration of 3  $\mu\text{g/L}$  for each compound. The doses of F400 (dry weight) were 0, 2, 4, 6, 8, 10, 12, 14 mg/L respectively. The contact time for all samples was 45 days.

**Table C-2 Freundlich isotherms parameters of PFBS and PFOS in ultrapure water using GAC (F400)**

	Number of data points	Freundlich intensity factor $1/n$ (dimensionless)	Freundlich capacity factor $K_f$ [(ng/mg)(L/ng) <sup>1/n</sup> ]	$R^2$
PFBS	6	0.334	105.81	0.883
PFOS	7	0.784	7.72	0.935

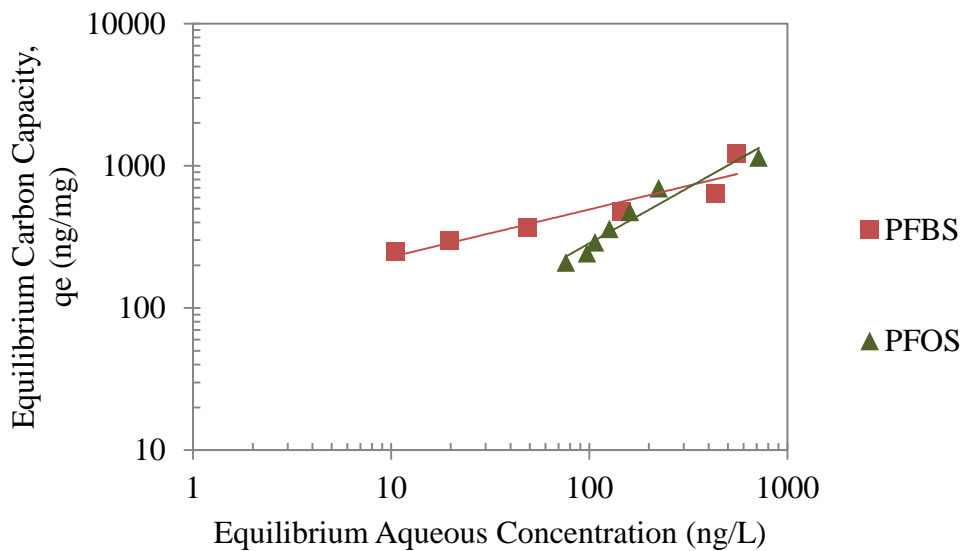


**Figure C.2 Freundlich isotherms of PFBS and PFOS in ultrapure water using F400**

**(3) Single compound PFC isotherms using A502p resin**

Two PFCs including PFBS and PFOS were spiked separately in ultrapure water with a concentration of 3  $\mu\text{g/L}$  for each compound. The doses of A502p resin (dry weight) were 0, 2, 4, 6, 8, 10, 12, 14 mg/L respectively. The contact time for all samples was 15 days.



**Table C-3 Freundlich isotherms parameters of PFBS and PFOS in ultrapure water using A502p resin**

	Number of data points	Freundlich intensity factor $1/n$ (dimensionless)	Freundlich capacity factor $K_f$ [(ng/mg)(L/ng) <sup>1/n</sup> ]	$R^2$
<b>PFBS</b>	3	0.254	335.99	0.969
<b>PFOS</b>	7	0.692	19.50	0.964

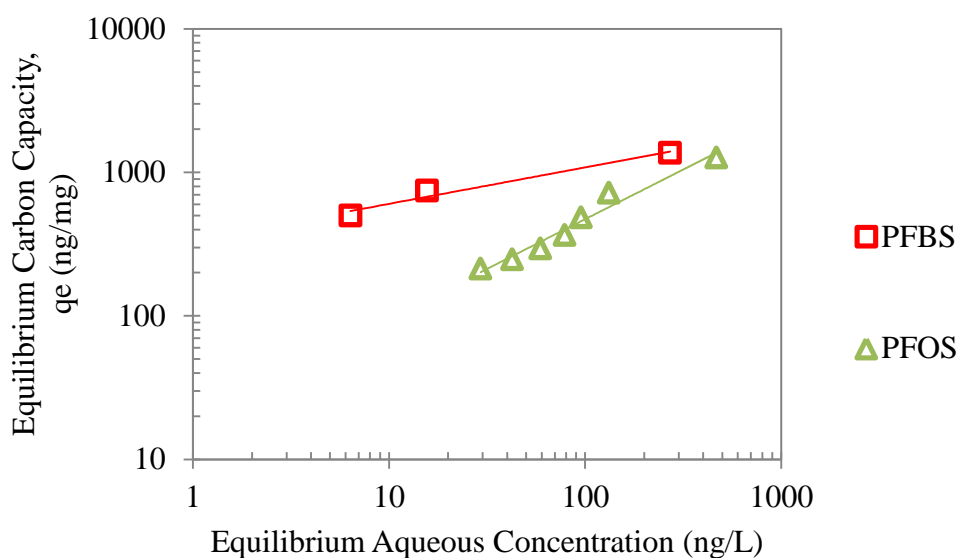


**Figure C.3 Freundlich isotherms of PFBS and PFOS in ultrapure water using A502p resin**

**(4) Comparison of PFSA isotherms for two different types of adsorbents: F400 and A502p**

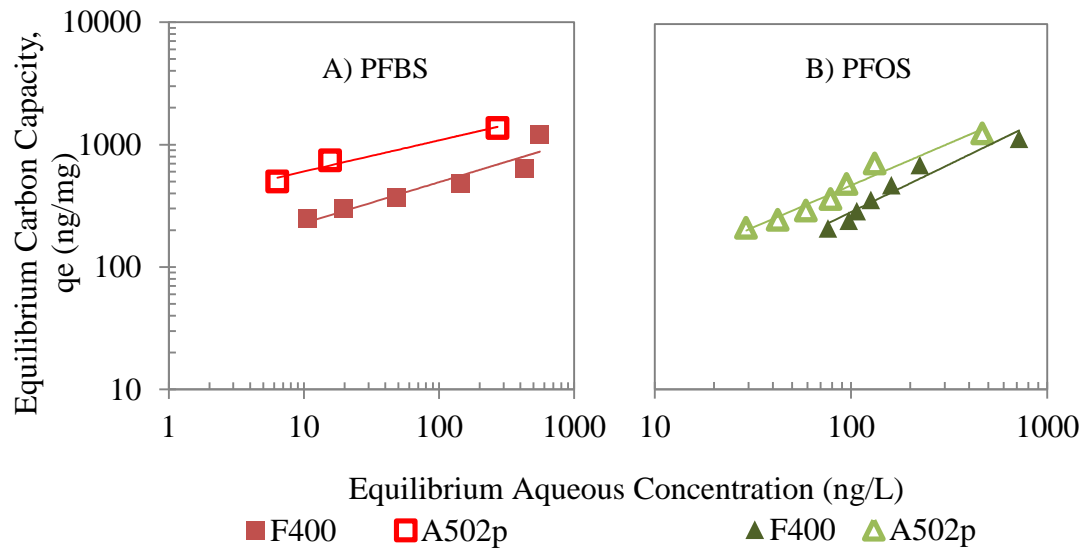


**Figure C.4 Comparison of Freundlich isotherms of PFBS and PFOS in ultrapure water using F400 and A502p**

## Appendix D

### Application of the Pseudo-Second-Order Model to the Adsorption Data of All Target PFCs onto TAN-1 Resin in Different Surface Waters

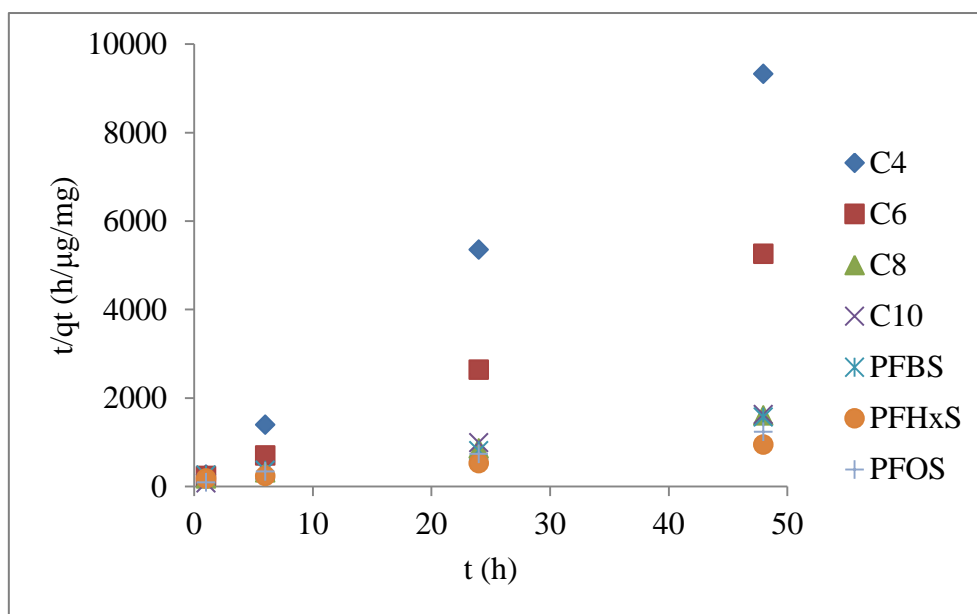


Figure D.1 Application of the pseudo-second-order model to the adsorption data of all target PFCs onto TAN-1 resin in Grand River water (initial PFC concentrations were 3  $\mu\text{g}/\text{L}$ ; resin doses were 50 mg/L as dry weight).

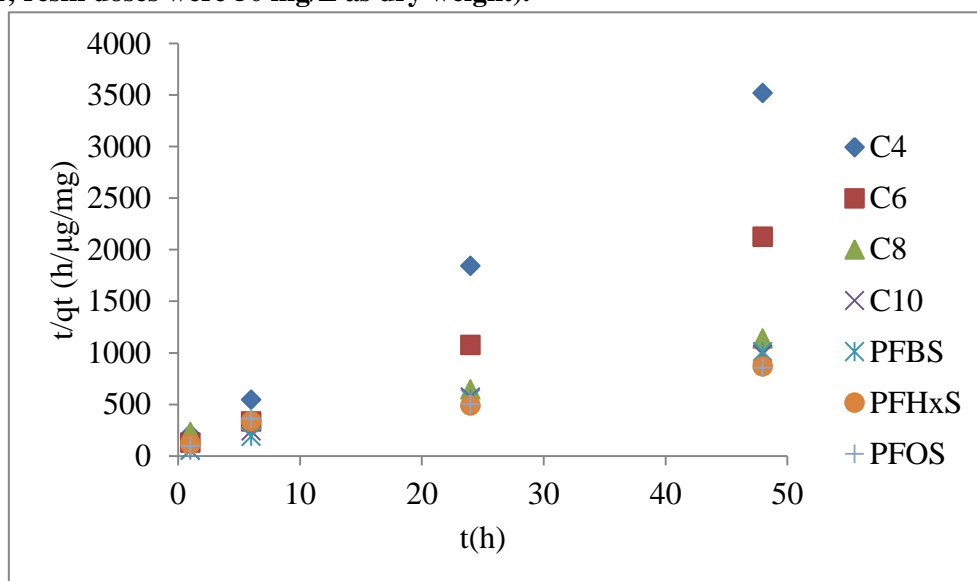
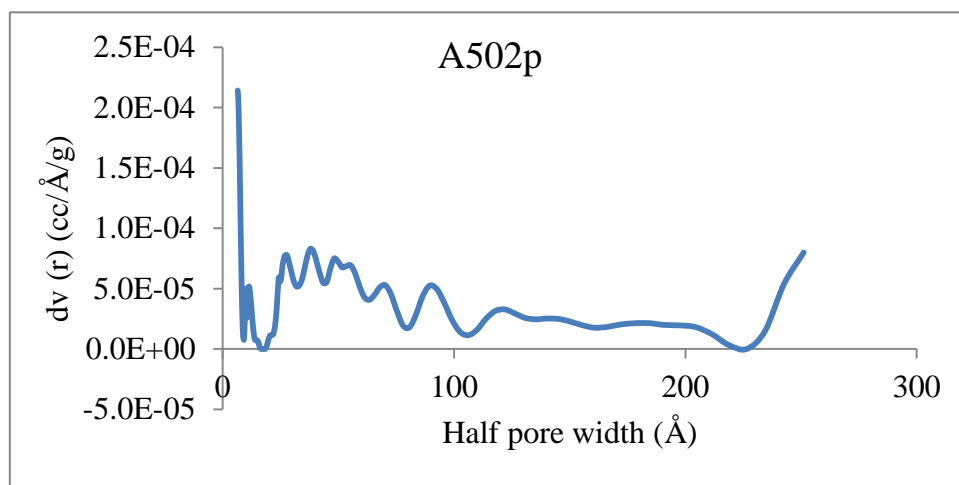
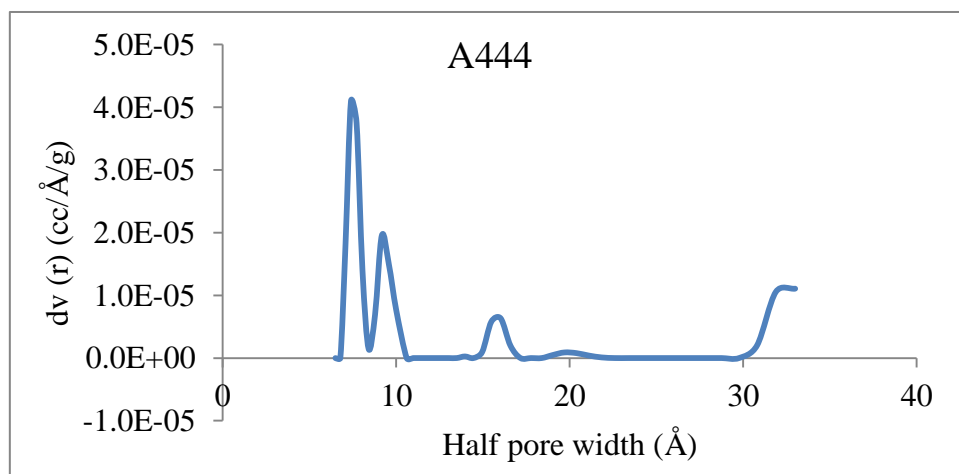
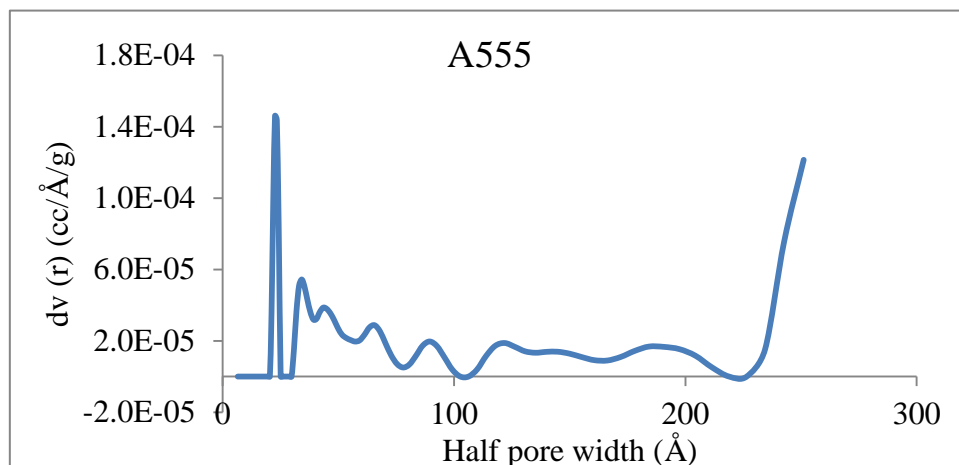
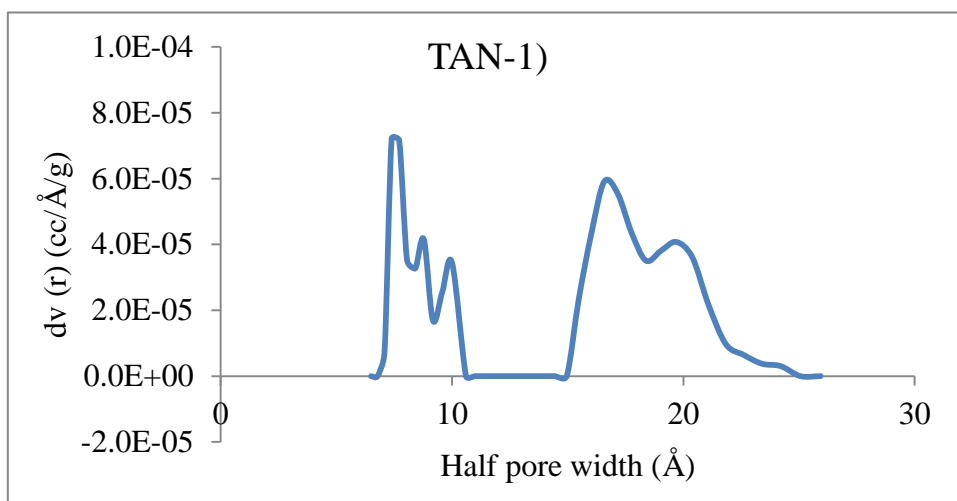
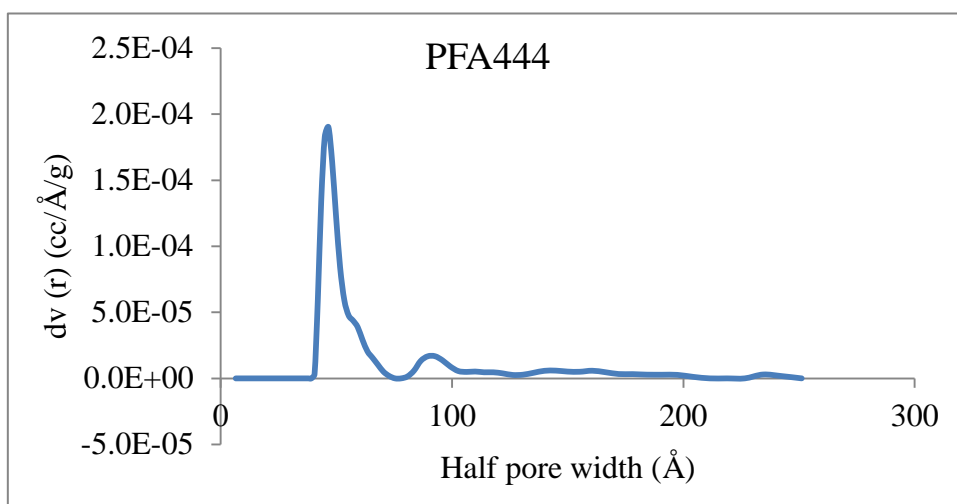
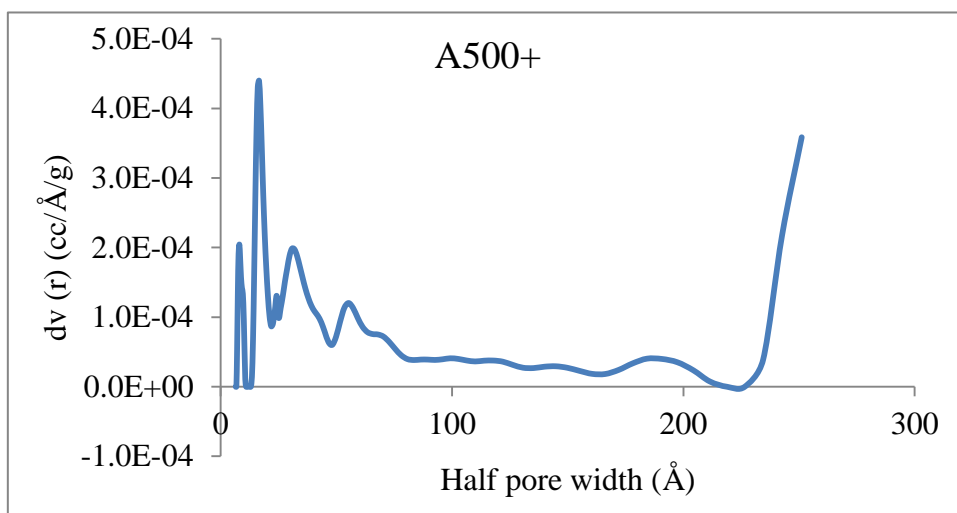


Figure D.2 Application of the pseudo-second-order model to the adsorption data of all target PFCs onto TAN-1 resin in Lake Erie water (initial PFC concentrations were 3  $\mu\text{g}/\text{L}$ ; resin doses were 50 mg/L as dry weight).

## Appendix E

### Pore Size Distribution Results for Anion Exchange Resins





**Figure E.1 Pore volume distribution for all anion exchange resins**

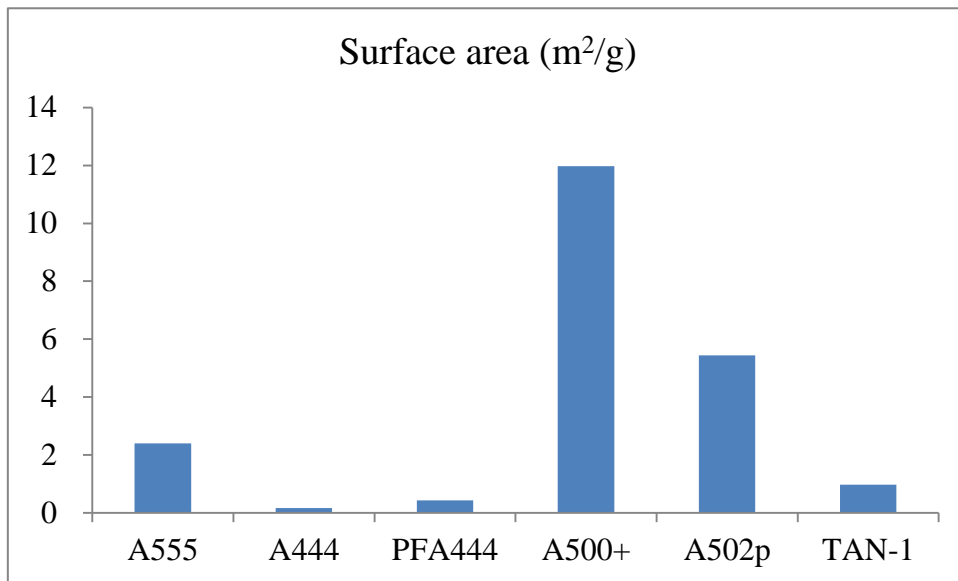


**Figure E.2 Surface areas for all anion exchange resins**

## Appendix F

### The Effect of Magnetic Separation for Nanoparticles

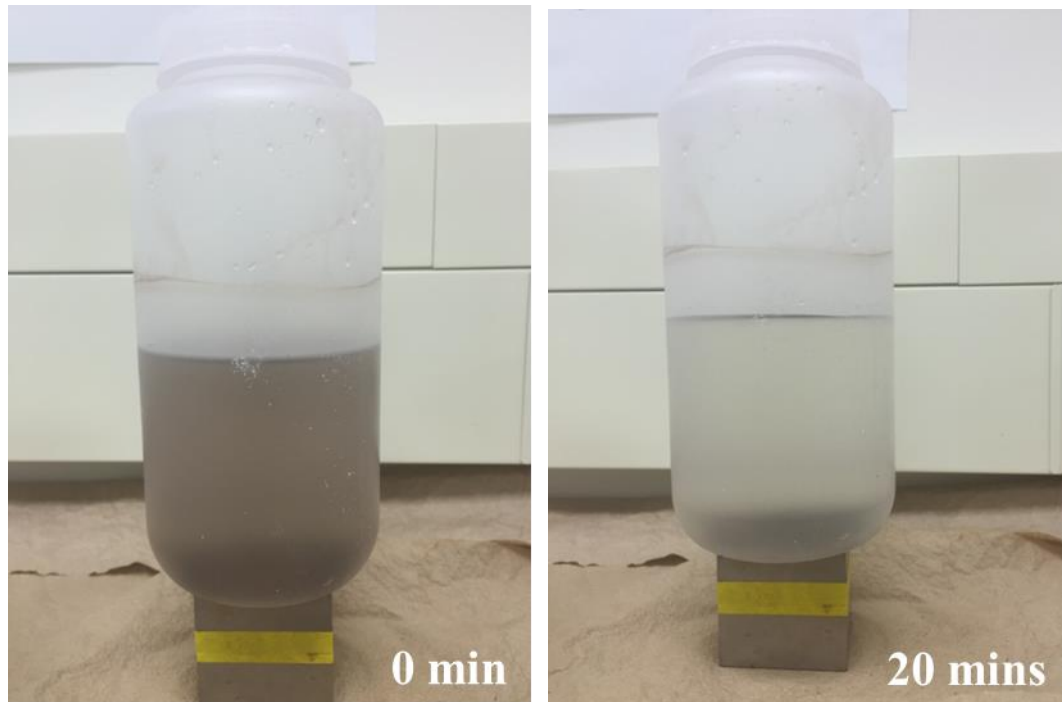


**Figure F.1** The effect of magnetic separation for nanoparticles

## Appendix G

### Pseudo-Second-Order Model for N2 and N3

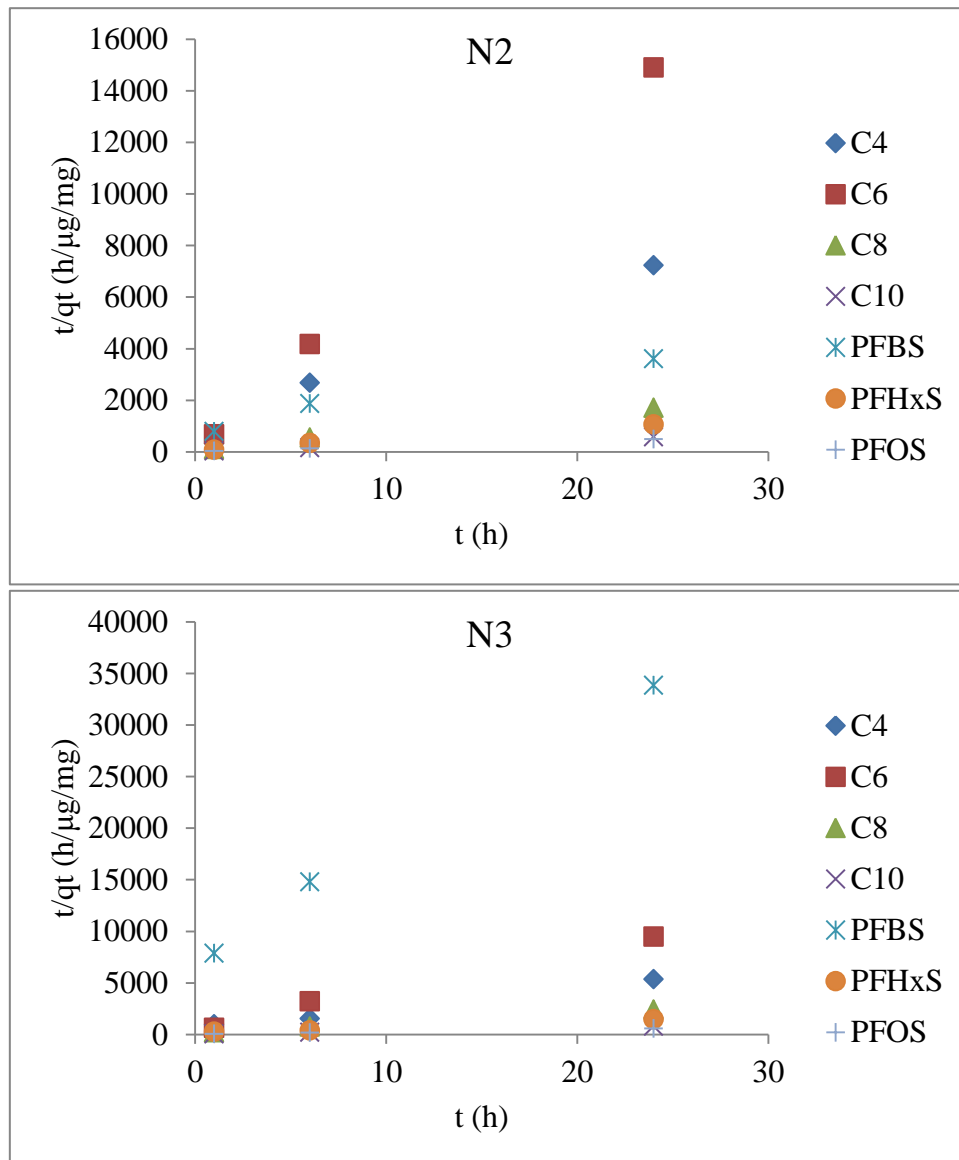


**Figure G.1 Application of the pseudo-second-order model to the adsorption data of all target PFCs onto N2 and N3 particles in ultrapure water (initial PFC concentrations were 3 μg/L; adsorbent doses were 50 mg/L as dry weight).**



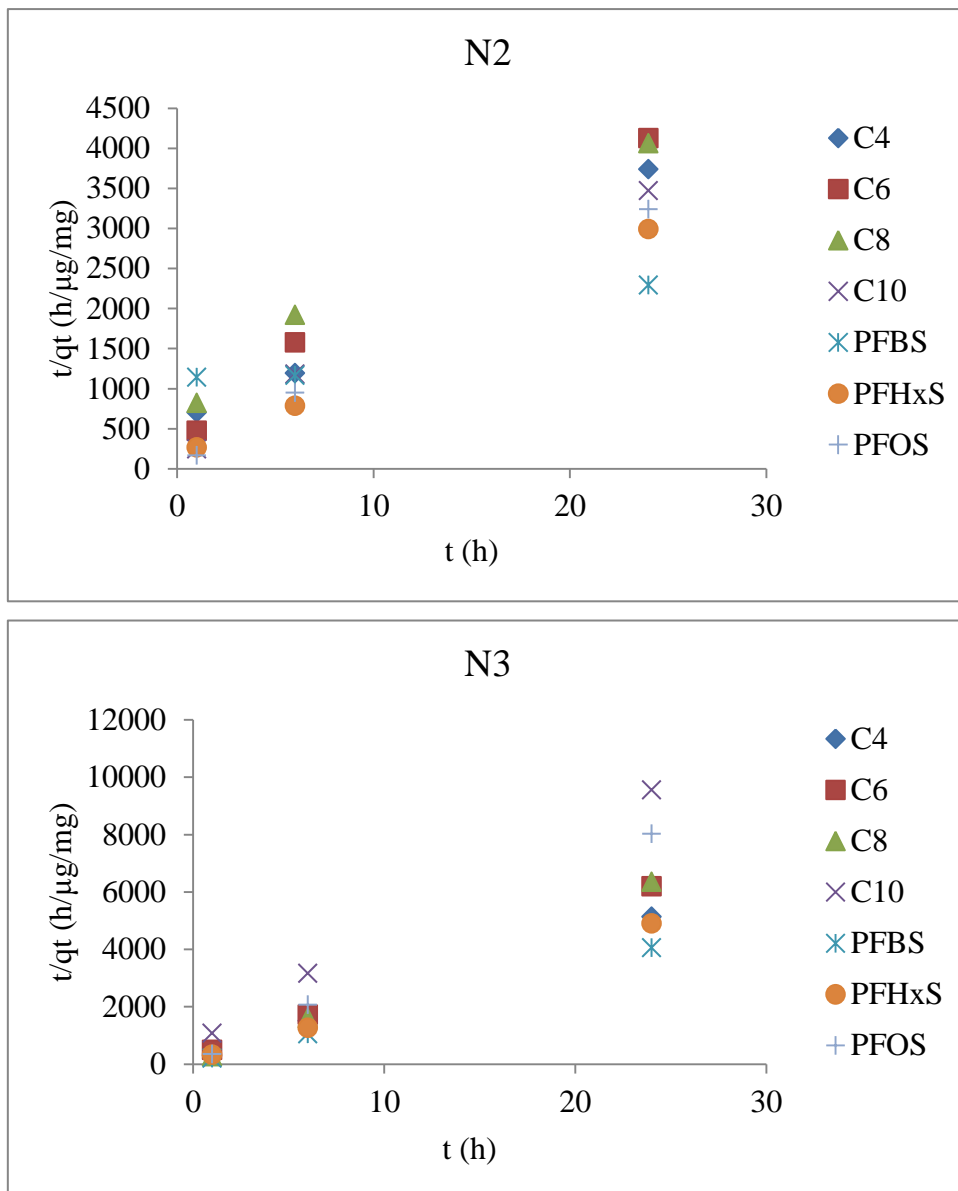


**Figure G.2 Application of the pseudo-second-order model to the adsorption data of all target PFCs onto N2 and N3 particles in Grand River water (initial PFC concentrations were 3  $\mu\text{g}/\text{L}$ ; adsorbent doses were 50  $\text{mg}/\text{L}$  as dry weight).**

## Appendix H

### LC-OCD Results of Grand River Raw Water and after 24 Hours

#### Treatment Using N2 and N3

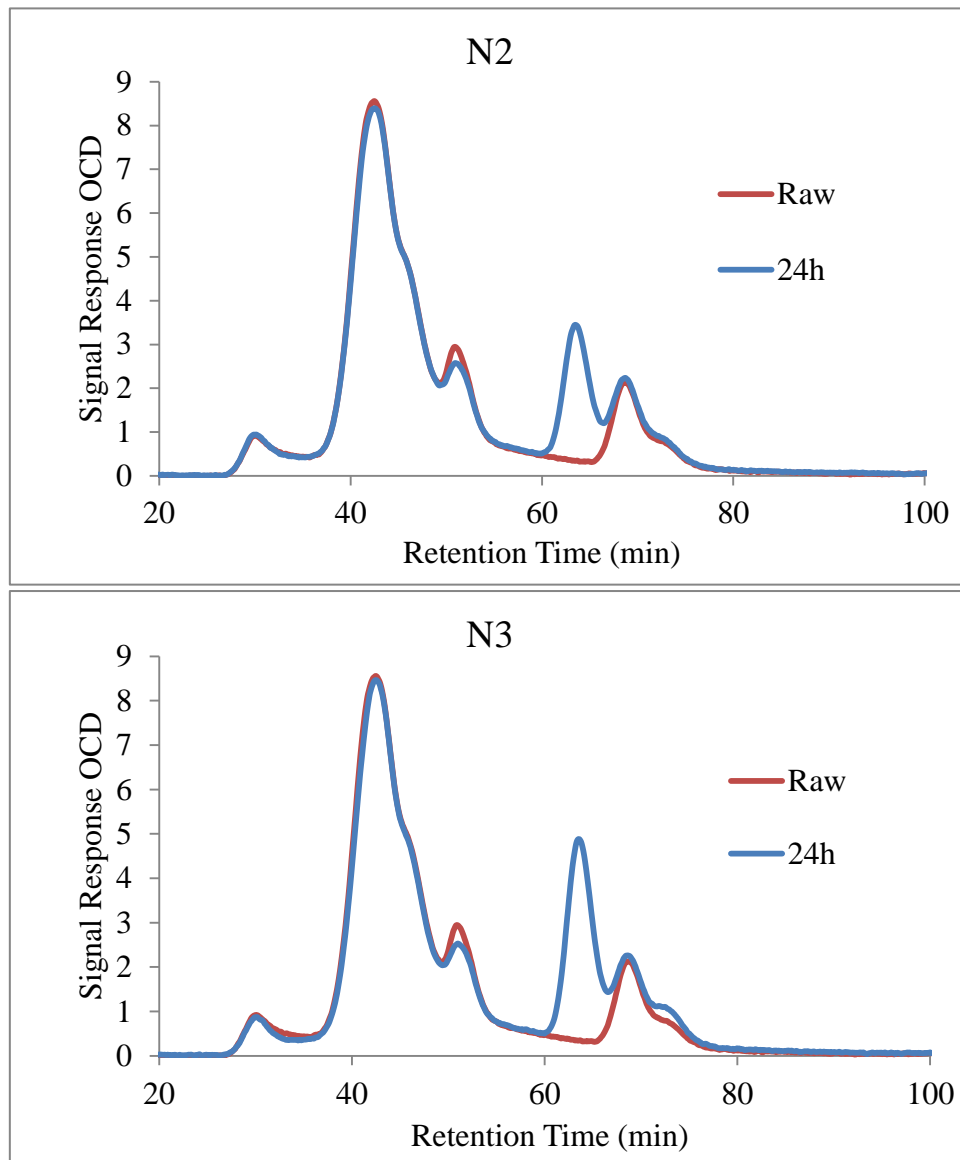


**Figure H.1 LC-OCD results of raw water and after 24 hours treatment using N2 and N3.**

## Appendix I

### Supporting Documents for Column Experiments

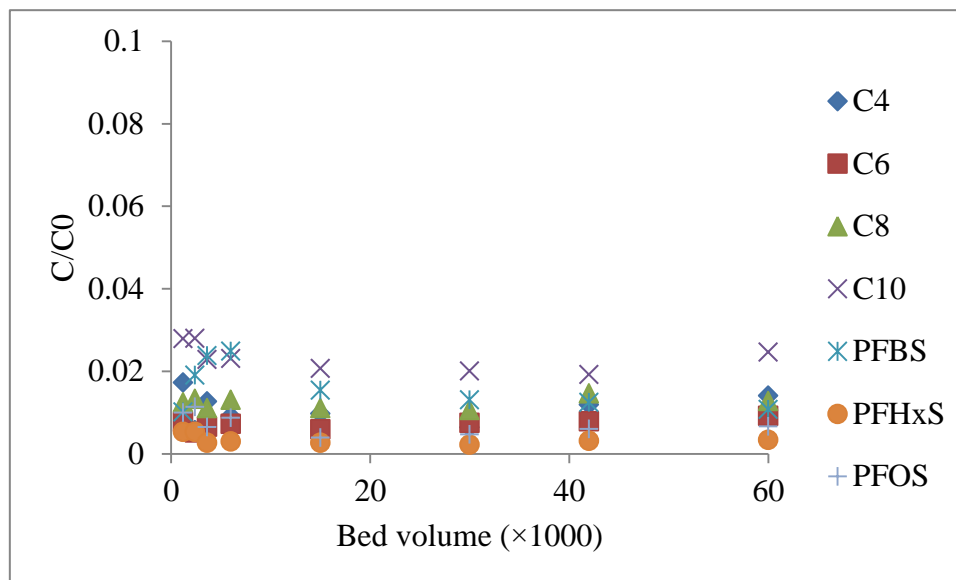


**Figure I.1 Breakthrough curves of PFCs in anion exchange column tests in ultrapure water ( $C_0$  was 30  $\mu\text{g/L}$ ).**

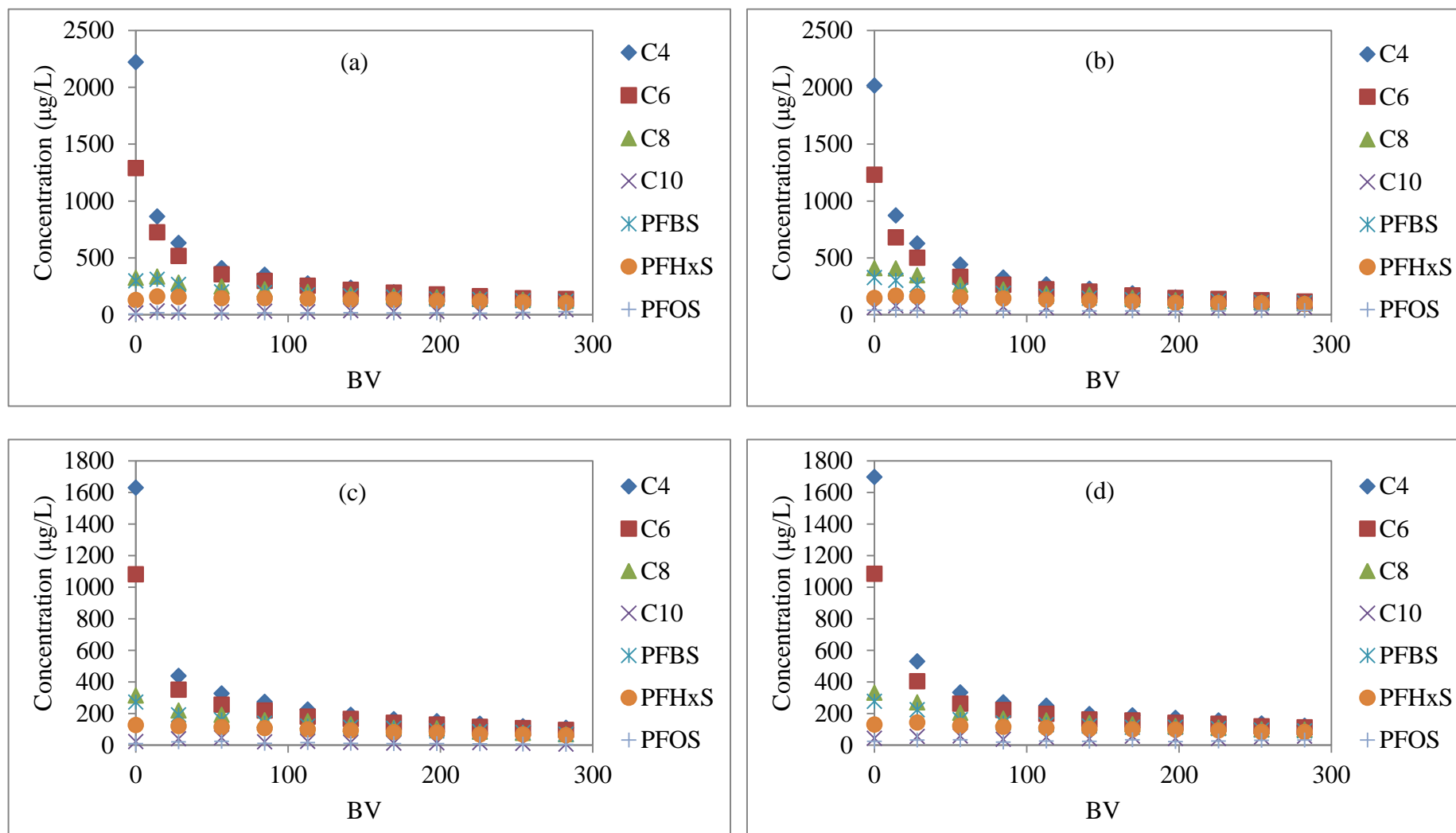


**Figure I.2 Elution curves of different regeneration operation conditions in ultrapure water: (a) 10% NaCl, flow rate: 10 ml/min; (b) 5% NaCl, flow rate: 10 ml/min; (c) 10% NaCl, flow rate: 20 ml/min; (d) 5% NaCl, flow rate: 20 ml/min.**